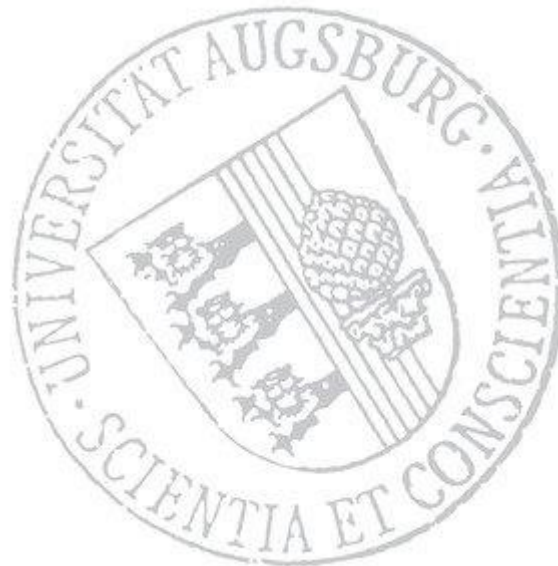# Universität Augsburg University

Health-Relevant, Compound Ozone and Temperature Burden in Europe:
Statistical Modeling and Climate Change Projections

Cumulative Doctoral Thesis for the Award of a Scientific Doctoral Degree (Dr. rer. nat) at the University of Augsburg (Faculty of Applied Computer Science)

Kumulative Dissertation (Inaugural-Dissertation) zur Erlangung des Grades Doktor der Naturwissenschaften (Dr. rer. nat.) der Universität Augsburg (Fakultät für Angewandte Informatik)

submitted by

Sally Ann Jahn

Date of Submission: December 14, 2022
Date of Oral Exam: August 02, 2023

Affidavit

I hereby declare that my doctoral thesis entitled "Health-Relevant, Compound Ozone and Temperature Burden in Europe: Statistical Modeling and Climate Change Projections" is the result of my own work. I did not receive any help or support from commercial consultants. All sources and/or materials applied are listed and specified in the thesis. Furthermore, I verify that this thesis has not yet been submitted as part of another examination process neither in identical nor similar form.

Augsburg, August 2023

_____
Sally Ann Jahn

Eidesstattliche Erklärung

Hiermit erkläre ich an Eides statt, die Dissertation "Health-Relevant, Compound Ozone and Temperature Burden in Europe: Statistical Modeling and Climate Change Projections" eigenständig, d.h. insbesondere selbstständig und ohne Hilfe eines kommerziellen Promotionsberaters, angefertigt und keine anderen als die von mir angegebenen Quellen und Hilfsmittel verwendet zu haben. Ich erkläre außerdem, dass die Dissertation weder in gleicher noch in ähnlicher Form bereits in einem anderen Prüfungsverfahren vorgelegen hat.

Augsburg, August 2023

_____
Sally Ann Jahn

Foreword

Having reached the end of my exciting and occasionally also challenging, but primarily educative and instructive road to my PhD and now finally finding myself on the verge of completing my doctoral degree, I would like to express my gratitude to a variety of important persons who accompanied me during my time as a PhD student.

First, I would like to thank my supervisor Prof. Dr. Elke Hertig for all her persistent and helpful support, the very constructive working relationship as well as her always attentive and courteous manner. She always took the time to discuss my research and provided guidance and scientific input. She also gave valuable and critical comments, advice, and recommendations to prepare, but also encourage me as a researcher, especially as a female scientist, to opt for a hopefully long and fruitful career in science and academia.
I would also like to thank all further colleagues of my working group at the Professorship of Regional Climate Change and Health who supported me during my doctorate in one way or another, with my specific thanks directed to my colleague Irena Kaspar-Ott.

Second, and particularly, I would like to express my sincere gratitude to Prof. Dr. Harald Kunstmann and his entire working group at the Chair of Regional Climate and Hydrology, specifically including, but not limited to my colleagues: Jan Bliefernicht, Maximilian Graf, Barbara Haese, Manuel Lorenz, Thomas Rummler und Andreas Wagner. Thank you for my instant integration in your working group, for your academic but also general support and your always immediate and helpful advice.
Furthermore, I would like to address and emphasize the general friendly, supportive, and collegial atmosphere and great community at the Faculty of Applied Computer Science, in particular the Institute of Geography. I want to specifically mention and thank my colleagues and friends Selina Thanheiser and Reiner Schwandt, as well as all further members of my "Success Team" (German: "Erfolgsteam"), namely, Christian Röger und Erik Petersen in this regard. I really enjoyed our inspiring and regular discussions at our monthly meetings.

Superior and sincere thanks are especially owed to my family, particularly my mom and dad. I want to thank them for their support and guidance throughout my whole life. Without them, I would have never achieved as much in life, and I am so grateful for their lifelong strong, unforgettable, and unconditional support.
My last and greatest thanks go to my long-time companion Peter. Thank you for your advice and support to improve my programming skills, your open ears and constant encouragement as well as your motivational speeches and unceasing confidence in me during my entire PhD journey. Without you my doctorate would have never been such a pleasant and amazing experience.

To conclude, I enjoyed working on this dissertation very much. Thank you all for helping me to become the scientist, and person, I am today.

Executive Summary

Air pollution is nowadays the number one environmental health risk worldwide with tropospheric, surface, ground-level ozone representing one major air pollutant being associated with numerous serious health outcomes. Climate change presents as well one of the most challenging threats to human wellbeing affecting the lives of billions of people around the world. In the discussion about ongoing climate change, one central topic of environmental health science and projection research is the projected increase in thermal load as rising surface air temperatures may lead to the intensification of future heat-related health burden. But climate change is not only expected to alter air temperatures, but also, e.g., various meteorological and synoptic conditions on different spatial scales, influencing again the occurrence of heat and thermal load. Furthermore, changes in the climate system, including meteorology and synoptic conditions, will also play an essential role in future ozone pollution, leading to a possible worsening of the by ground-level ozone induced health burden until the end of the 21st century. Concurrent occurrences of health-relevant ozone pollution and air temperature levels under current and future climatic conditions are of particular interest, as there is evidence that synergistic effects of compound occurrences result in an even intensified human health risk beyond the sum of the individual impacts of each single health stressor alone. Consequently, understanding the mechanisms of main meteorological and synoptic drivers and the impacts of climate change on health-relevant compound surface ozone and air temperature occurrences is crucial also with regard to upcoming climate change mitigation and adaption strategies focusing on the protection of human health.

Therefore, this dissertation focuses on the analysis of the relationship between ground-level ozone and surface air temperature as well as on the role of synoptic and meteorological conditions on compound occurrences of both health stressors, with the European domain as the regional focus. The analysis provides a spatial characterization of the varying linkages between surface ozone and air temperature. Furthermore, the most important key drivers of compound ozone-temperature events are assessed. With these newly gained insights this work sets out to evaluate not just recent but also projected future region- and site-specific health burden induced by ground-level ozone alone or in combination with heat. In this regard, an additional focus is set on the evaluation of the impact and changes of precursor emissions, beside climatic changes, on future local, ground-level ozone. The results presented in this thesis will be particularly of interest for the development of current and future warning systems and protection strategies focusing on the interplay between air quality, heat, and human health in Europe.

At first, a statistical downscaling model and projection framework to evaluate the role of large-scale meteorological conditions and prevailing air pollution levels on compound ozone-temperature events and to assess current and future event occurrences is developed. The evaluation is based on processed observational monitoring data of selected station pairs with different air quality settings and site characteristics (i.e., station types). An ozone-temperature season from April to September showing a strong linkage between and elevated levels of both target variables is defined and focused on. Logistic regression, one of the two tested main modeling approaches, shows a superior performance to model and hence later project the occurrence of compound ozone-temperature events. Large-scale mean air temperature conditions and ozone persistence represent the key dominant factor influencing compound occurrences in southeastern and northwestern parts of the study domain, respectively. The projected changes in the frequency of compound events under future climate change scenarios until the end of the 21st century reveal a general increase in event occurrences over central Europe, with south- to central-eastern parts of the study domain turning out to be hotspot regions of strongest frequency shifts. But no clear station type dependences of model and projection results become evident. Additionally, in this first analysis, in comparison to

central Europe, weak correlations between both target variables in northern and southern parts of the study domain become already apparent.

Secondly, the classification of the whole European domain into regions with homogeneous, coherent ground-level ozone and air temperature characteristics and patterns allows a more regional and site-specific analysis of the relationship between both target variables as well as of current and future compound event occurrences in the defined ozone-temperature season. The regionalization based on both variables, surface ozone and air temperature, lead to six robust, geographically, and environmentally meaningful European ozone-temperature regions. The results confirm a strong and direct correlation and linkage between both target variables in central, but not to the same extent in northern and southern parts of the European study domain. In order to identify region-specific main meteorological and synoptic drivers of compound ozone-temperature events, statistical downscaling models for representative stations of varying site characteristics and hence alternating air quality settings per region are developed. Climate change projections to assess potential frequency shifts show substantial increases of health-relevant compound ozone-temperature events until the end of the 21st century across all central European regions. The results based on the regionalization, modeling, and projection approach show primary regional, not station-type dependences, and underline the minor role of pollution regimes, in this context. Most importantly, it becomes apparent that the applied study framework is to a large extent only suitable for all central European regions and further research with revised and adapted approaches needs to be conducted for northern and southern parts of Europe.

Finally, future local ground-level ozone in the European area based on a statistical downscaling modeling and projection framework using information on climate as well as emission changes until the end of the 21st century is assessed. Therefore, beside meteorological variables, processed monthly O_3 time series data that reflect the larger-scale total changes of ozone resulting from climate and precursor emission changes based on reanalysis and climate model data are used. A sensitivity analysis evaluates the impact of different statistical downscaling model choices, mainly differing in terms of the predictor variables used, to quantify more detailed the influence of specific predictors and predictor sets on modeled and projected local surface ozone. Results show that even if the two large-scale predictors mean air temperature and solar radiation can explain already a large fraction of the daily ozone variability, statistical models based on a thermal-radiative forcing are in general only well-performing and decisive for central parts of Europe, while for southern, western, and north-western European stations further predictors are desirable. The main model choice using station-specific predictor optimums by additionally always including total changes of ozone as emission-related predictor reveals a substantial contribution of the large-scale predictors mean air temperature and solar radiation on surface ozone in most parts of southern and central Europe, while especially in northern parts of the study domain the total large-scale monthly ozone predictor plays an important role in ground-level ozone pollution. Regionally and in sign and magnitude varying projection results based on climate model, predictor configuration, and scenario considered are assessed based on all chosen and evaluated varying statistical downscaling model choices. Following the main model choice with site-specific models based on optimum predictor sets by always adding emission-related information, multi-model results reveal in general European-wide reductions in local ground-level ozone under a moderate middle of the road scenario but increases across Europe under a more pessimistic one with enhanced regional rivalry.

Zusammenfassung

Luftverschmutzung stellt heutzutage weltweit das größte umweltbedingte Gesundheitsrisiko dar. Troposphärisches, bodennahes Ozon gilt als einer der schädlichsten Luftschadstoffe, der mit zahlreichen schwerwiegenden gesundheitlichen Folgen in Verbindung gebracht wird. Der Klimawandel ist ebenfalls eine der größten Bedrohungen für das menschliche Wohlergehen, welcher das Leben von Milliarden von Menschen auf der ganzen Welt beeinträchtigt. Die Umwelt- und Gesundheitsforschung setzt im Rahmen des fortwährenden Klimawandels einen zentralen Fokus auf die projizierte Zunahme der Wärmebelastung, da steigende bodennahe Lufttemperaturen zu einer Intensivierung der künftigen hitzebedingten Gesundheitslast führen können. Der Klimawandel wird sich jedoch voraussichtlich nicht nur auf Lufttemperatur, sondern auch auf weitere meteorologische und synoptische Bedingungen unterschiedlicher räumlicher Auflösung auswirken, die wiederum selbst das Auftreten von Hitze und thermischer Belastung beeinflussen. Darüber hinaus spielen Änderungen des Klimas, einschließlich der Meteorologie und Synoptik, ebenfalls einen wesentlichen Faktor bei der zukünftigen Ozonbelastung. Eine Verschlechterung der ozonbedingten Gesundheitsbelastung bis zum Ende des 21. Jahrhundert kann hierdurch resultieren. Beim zeitgleichen Auftreten thermischer und ozonbedingter Belastungssituationen unter den gegenwärtigen und zukünftigen klimatischen Bedingungen können synergistische Effekte zu einem deutlich erhöhten Risiko führen, welches über die Summe der Einzelwirkung jedes Gesundheitsfaktors hinausgeht. Folglich ist das Verständnis des Wirkungszusammenhangs zwischen den wichtigsten meteorologischen und synoptischen Schlüsselfaktoren, den klimatischen Veränderungen, und den gesundheitsrelevanten Temperatur-Ozon-Ereignissen, auch im Hinblick auf künftige Abschwächungs- und Anpassungsstrategien im Rahmen des Klimawandels zum Schutz der menschlichen Gesundheit von entscheidender Bedeutung.

Die Doktorarbeit legt deshalb den Schwerpunkt auf die Analyse des Zusammenhangs zwischen bodennahmen Ozon und oberflächennaher Lufttemperatur und des Einflusses von meteorologischen und synoptischen Bedingungen auf das kombinierte Auftreten beider Gesundheitsfaktoren. Der europäische Raum stellt den regionalen Fokus dar. Die Analyse liefert eine räumliche Charakterisierung der variierenden Zusammenhänge zwischen Ozon und Lufttemperatur. Darüber hinaus werden die wichtigsten Schlüsselfaktoren kombinierter Ozon-Temperatur-Ereignisse erfasst. Mit den damit verbundenen neu gewonnenen Erkenntnissen werden nicht nur die gegenwärtigen, sondern auch die zukünftigen projizierten regions- und standortspezifischen gesundheitsrelevanten Belastungen durch Ozon allein oder in Kombination mit Hitze analysiert. Ein zusätzlicher Schwerpunkt wird diesbezüglich, neben dem klimatischen Wandel, auf die Bewertung der Auswirkungen von Vorläuferemissionen und deren Veränderungen auf zukünftiges lokales, bodennahes Ozon gelegt. Die in dieser Arbeit vorgestellten Ergebnisse zielen insbesondere auf die Entwicklung aktueller und zukünftiger Warnsysteme und Schutzstrategien ab, die sich auf das Zusammenspiel von Luftqualität, Hitze und menschlicher Gesundheit in Europa konzentrieren.

Zunächst wird ein statistischer Downscaling-Modell- und Projektionsansatz entwickelt, um die Rolle großräumiger meteorologischer Bedingungen und vorherrschender Luftverschmutzung auf kombinierte Ozon-Temperatur-Ereignisse zu bewerten und deren jetziges als auch zukünftiges Auftreten zu beurteilen. Die Analyse basiert auf den prozessierten Beobachtungsdaten ausgewählter Stationspaare mit unterschiedlichen Luftqualität- und Standortmerkmalen (d.h. Stationstypen). Eine Ozon-Temperatur-Saison von April bis September, die erhöhte Werte beider Zielvariablen und eine starke Verknüpfung dieser aufweist, wird definiert und bildet den Fokus der Analyse. Logistische Regression, eine der beiden gewählten Modellierungsansätze, erweist sich als besonders geeignet für die Modellierung und somit anschließende Projektion kombinierter Ozon-Temperatur-Ereignisse. Großräumige mittlere Lufttemperaturbedingungen in südöstlichen als auch Ozonpersistenz in

nordwestlichen Teilen des Untersuchungsgebiets sind die jeweils dominanten Faktoren, die das Auftreten dieser Ereignisse beeinflussen. Die projizierten Veränderungen unter zukünftigen Klimawandelszenarien bis zum Ende des 21. Jahrhunderts zeigen eine allgemeine Zunahme in deren Auftreten, wobei sich die süd- bis zentralöstlichen Gebiete als Hotspot-Regionen mit stärksten Häufigkeitszunahmen darstellen. Es werden jedoch keine eindeutigen Abhängigkeiten zwischen den Modell- und Projektionsergebnissen und den einzelnen zugrundeliegenden Stationstypen ersichtlich. Zudem zeigen sich bereits in dieser ersten Analyse, im Vergleich zu Zentraleuropa, nur schwache Korrelationen zwischen den beiden Zielvariablen in nördlichen und südlichen europäischen Stationslagen.

Zweitens ermöglicht eine Gliederung des gesamteuropäischen Raums in Regionen mit einheitlichen Ausprägungen und Mustern von Ozon und Lufttemperatur in der definierten Ozon-Temperatur-Saison eine regional- und standortspezifischere Analyse deren Beziehung sowie des rezenten und zukünftigen Auftretens deren kombinierter Ereignisse. Die Regionalisierung auf Basis beider Zielvariablen führt zu sechs robusten, geografisch und umweltwissenschaftlich sinnhaften europäischen Ozon-Temperatur-Regionen. Starke, direkte Korrelationen und Verknüpfungen beider Variablen werden in den zentralen, aber nicht im gleichen Maße in den nördlichen und südlichen Regionen ersichtlich. Um regionsspezifische meteorologische und synoptische Schlüsselfaktoren kombinierter Ozon-Temperatur-Ereignisse zu ermitteln, werden pro Region für ausgewählte repräsentative Stationen mit unterschiedlichen Luftqualitäts- und Standortmerkmalen statistische Downscaling-Modelle entwickelt. Projektionen im Rahmen des Klimawandels ergeben eine erhebliche Zunahme der Häufigkeiten gesundheitsrelevanter kombinierter Ozon-Temperatur-Ereignisse bis zum Ende des 21. Jahrhunderts in allen zentraleuropäischen Regionen. Die auf dem gewählten Ansatz basierenden Ergebnisse zeigen primär regionale, nicht stationsbezogene Abhängigkeiten und unterstreichen somit die diesbezüglich geringe Bedeutung von lufthygienischen Regimen. Es wird vor allem ersichtlich, dass das angewandte Rahmenkonzept der Studie weitgehend nur für alle zentraleuropäischen Regionen geeignet ist und überarbeitete und angepasste Ansätze für die nördlichen und südlichen Teile Europas entwickelt werden müssen.

Schließlich wird die künftige, lokale bodennahe Ozonbelastung im europäischen Raum auf Basis eines statistischen Downscaling-Modellierungs- und Projektionsansatzes bewertet, der sowohl Informationen über Klima- als auch Emissionsänderungen bis zum Ende des 21. Jahrhunderts beinhaltet. Neben meteorologischen Variablen wird hierbei auch die monatliche Ozonbelastung auf der Grundlage von Reanalyse- und Klimamodelldaten berücksichtigt. Diese spiegelt großräumige Ozonveränderungen wider, die sich aus Änderungen des Klimas und der Vorläuferemissionen ergeben. Eine Sensitivitätsanalyse bewertet die Auswirkungen verschiedener Modelloptionen, die sich primär in Bezug auf die zugrundeliegende Wahl von Prädiktoren und Prädiktorsets unterscheiden, um deren Einfluss auf Modell- und Projektionsergebnis zu quantifizieren. Die Ergebnisse zeigen, dass zwei großräumige Prädiktoren, mittlere Lufttemperatur und Solarstrahlung, bereits einen erheblichen Teil der täglichen Ozonvariabilität erklären. Aber die rein auf einem thermisch-radiativen Antrieb basierende Modelloption liefert im Allgemeinen nur belastbare Ergebnisse für Zentraleuropa. Für süd-, west- und nordwesteuropäische Stationen sind weitere Prädiktoren wünschenswert. Die hauptsächlich betrachtete Modelloption, die neben den ermittelten stationsspezifischen Prädiktoren zusätzlich den emissionsbezogenen Ozon-Prädiktor berücksichtigt, identifiziert als wichtigste Einflussfaktoren der Ozonbelastung großräumige mittlere Lufttemperatur und Sonneneinstrahlung in den meisten südlichen und zentralen, aber monatliches Ozon in den nördlichen Teilen Europas. Die regional und in Vorzeichen und Stärke variierenden Projektionsergebnisse basieren auf den gewählten Klimamodellen, Prädiktorkonfigurationen und den betrachteten Szenarien und werden auf Basis aller gewählter Modelloptionen bewertet. Die Multi-Modell-Ergebnisse der Hauptmodelloption zeigen über Europa insgesamt eine Verringerung der lokalen bodennahen Ozonbelastung unter einem moderaten mittleren, aber einen Anstieg bei einem pessimistischeren Szenario mit verstärkter regionaler Rivalität.

Contents

List of Figures

List of Tables

1. Chapter 1 - Introduction

1.1 Background

1.1.1 Air and Ozone Pollution

Air pollution is the number one environmental health risk worldwide, leading to about 7 million deaths attributable to the joint effects of ambient and household air pollution according to estimates of the World Health Organization (WHO; please refer to Appendix A to get an overview of used abbreviations, and acronyms) (WHO, 2021). In Europe, air pollution also represents the biggest environmental health risk and has significant and multiple impacts on the health of the European population, leading to e.g., respiratory, cardiovascular, and cerebrovascular diseases (EEA, 2021). Exposure to key air pollutants may thus lead to a variety of physical but also mental diseases and cause the loss of healthy years of life and premature death, especially due to higher levels of exposure or among vulnerable subgroups with increased susceptibility to air pollution (WHO, 2021). These risk groups include, but are not limited to e.g., children, people with pre-existing conditions like asthma, pregnant women, or the elderly. The WHO published new health-relevant global Air Quality Guidelines (WHO-AQG) in 2021 to assess the impacts of air pollution on human health (WHO, 2021). The European Union (EU) defined standards for all pollutants in their Ambient Air Quality Directive (EU-AQD) in 2008 (EEA, 2021), which are less strict than the WHO guidelines. But, as corollary of the European Green Deal, the EU plans according to their Action Plan: "Towards a Zero Pollution for Air, Water and Soil" and their zero pollution vision for 2050 (European Comission, 2021) to align their air quality standards more closely to the WHO recommendation levels, as adverse health effects have already become evident to occur by violating these stricter WHO guidelines.

Tropospheric, so-called surface or ground-level ozone O_3 (hereinafter also simplified referred to as ozone or O_3) is colorless and invisible gas and represents one of the major, health-relevant air pollutants. The worldwide rates of adverse health effects triggered by exposure to ozone related air pollution have increased in the recent past with regard to a very high confidence level according to the Intergovernmental Panel on Climate Change (IPCC) (IPCC, 2022). Ozone occurs naturally in the troposphere mostly due to downward mixing from the stratosphere, with (pre-industrial) ground-level concentrations being generally about 10-20 ppb (about 20-40 µg/m^3; please refer to Appendix A for details on O_3 units) in the absence of far-reaching anthropogenic influences (Sillman, 2014). But because of human activities, background ozone concentrations have amounted to far higher levels in the Northern Hemisphere following the industrial era, with e.g., northern Europe measuring ozone levels above 80 ppb (160 µg/m^3) on approximately 30-60 days per year (Sillman, 2014). The main source of ground-level ozone is nowadays photochemical production in a polluted atmosphere based on a complex and sunlight-driven sequence of reactions following emissions from anthropogenic as well as natural sources. The WHO-AQG target value (WHO, 2021, WHO, 2006) for short-term exposure of 100 µg/m^3 (WHO-100) and the long-term objective EU target value (EEA, 2019) of 120 µg/m^3 (EU-120) were both defined for the protection of human health and are based on daily maximum 8-hour running ozone means (hereinafter referred to as MDA8O3). According to the European Environment Agency's (EEA) 2020 report (EEA, 2020), both target values, WHO-100 and EU-120, were surpassed by 96% and 87% of all reporting European stations fulfilling the underlying quality standards (minimum data coverage of 75%) in 2018, respectively.

Ground-level O_3 is generally referred to as a secondary pollutant, as it is not directly emitted but photochemically produced, with its formation enhanced by rising air temperatures and solar radiation. Ozone often occurs with more visible species (e.g., sulfate aerosols) during pollution events and represents, e.g., the primary ingredient of photochemical smog (Sillman, 2014).

The formation of O_3 is overall based on a nonlinear and temperature-dependent chemistry that is influenced and determined by the general ambient conditions, the general photochemical state of the system and accompanying precursor emissions (Pusede et al., 2015). There exist two main precursors of ozone both being emitted by natural and anthropogenic sources, namely: (1) hydrocarbons, more generally volatile organic compounds VOCs, and (2) oxides of nitrogen NO_x, more precisely nitrogen oxide NO and nitrogen dioxide NO_2. VOCs and NO_x thus represent the major origins of O_3 that react in the atmosphere and highly determine ozone formation and pollution. Typical natural sources of these precursors include, for instance, e.g., biogenic emissions from vegetation, microbes, and animals but also abiotic emissions from biomass burning and lightning. Anthropogenic sources are based on e.g., industrial, or commercial emissions, traffic, or chemical solvents. During pollution events, while relevant NO_x emissions are generally based on anthropogenic sources (e.g., motorized vehicles or coal-fired power plants), emissions of VOCs can be the result of human activities (mostly petroleum fuel or petroleum products-based sources) as well as natural occurring (primarily emissions from oaks, conifers and other deciduous trees) (Sillman, 2003). Zhao et al. (2022) demonstrated e.g., for a peak O_3 event in September 2010 in Los Angeles, that, among NO_x sources, on-road gasoline, on-road diesel, off-road diesel, and soil NO_x accounted for over 60% of the observed ground level O_3 concentrations. Among VOC sources, upwind boundary conditions and biogenic sources accounted for approximately 90% of the formed ground-level O_3. However, in addition to precursor substances, meteorology, and synoptic conditions as well as other various factors, including interacting ones, generally impact ozone formation and transport processes and determine regional and site-specific concentration levels. These factors include, but are not limited to: the duration and intensity of solar radiation, the ratio of VOCs and NO_x, the amount and specific chemical composition of VOCs, the cycle and supply of odd hydrogen radicals like the hydroxyl OH and hydroperoxyl HO_2 radicals (based also on e.g., the availability of water vapor) as well as their dominant radical sinks (e.g., nitric acid HNO_3, peroxides or peroxyacetyl nitrate PAN) (Sillman, 2003, Sillman, 1999).

Based on these two major precursor sources of ground-level ozone, a distinction is generally made between two main photochemical regimes determining O_3 formation and concentrations: (1) a NO_x-sensitive (-limited) or (2) a VOC-sensitive (-limited) regime. The regimes are primary based on the relation between O_3 and its two major precursor classes and are strongly influenced by e.g., the VOC/NO_x-ratio or photochemical aging (Sillman, 1999). Although it is challenging to identify the major contributors to specific observed ozone concentrations due to the complex formation of O_3 from precursor emissions, it is essential to extract the dominant sources of each precursor in the respective regime, i.e., the dominant sources of NO_x in the VOC-limited regime or the dominant VOC sources in the NO_x-limited regime, in order to design effective emission control strategies to reduce ozone pollution (Zhao et al., 2022). This is especially true as there is evidence that the major sources of O_3 are not equally regulable, as e.g., most of the VOC emissions contributing to O_3 formation are often biogenic and thus not easily controllable. Biogenic VOC emissions not only mainly contributed, as described above, in Los Angeles to the peak ozone pollution event in 2010 (Zhao et al., 2022), but have also represented, e.g., the dominant VOC source across Austria since the early 2000s (Mayer et al., 2022). As a result, anthropogenic NO_x emissions controls often provide the best approach to mitigate and lower O_3 pollution. In general, NO_x-sensitive regimes are typical in continental, rural and suburban areas. These regimes show comparably low NO_x and high VOC concentrations, and ozone increases with rising NO_x, but is rather insensitive to increasing VOC conditions (Sillman, 2003, Sillman, 2014). In VOC-sensitive regimes O_3 concentrations are generally reduced by increasing NO_x and rise with increasing levels of VOCs. These conditions are often observed in urban areas much closer to emission sources (Sillman, 2003, Sillman, 2014). As an air mass moves away from an urban centre and hence from emission sources, its VOC/NO_x ratio changes due to further photochemical reactions, meteorological processes and the occurrence of fresh emissions, with VOC-sensitive conditions being more

and more replaced by NO_x-sensitive ones (EEA, 2016). But those relations need to be seen as a rule of thumb and regimes at various locations may also shift over time as a result of progressively installed control and reduction strategies regarding anthropogenic precursor emissions. For example, Mayer et al. (2022) found in their study of Austrian summertime surface ozone concentrations that ozone production was predominantly NO_x-sensitive in rural and VOC-sensitive in urban environments, but over time a shift in the ozone chemical regime towards NO_x limitation at suburban sites was identified.

To measure ozone concentrations and other air pollutants, monitoring stations have been installed at numerous locations across Europe. Their measurements and processed monitoring data form generally the basis to evaluate the defined EU and WHO standards and guidelines (EEA, 2020). The locations of the fixed sampling points are typically chosen with varying ambient conditions across Europe in order to account for macro- and micro-scale site-specific characteristics. Monitoring sites can primarily be classified based on predominant emissions sources and the distribution and density of buildings. The common definition of the area surrounding the specific station divides the database into urban and suburban stations in continuously and largely built-up urban areas, respectively, and rural stations in all other ones (EEA, 2020). Considering the direct classification of station sites, the distinction is as follows: traffic or industrial stations are near single major roads or an industrial area/source, respectively. Background stations are generally installed to monitor background concentration levels of ozone. These background levels are considered to be representative for a given region and are regarded as the average exposure of the general population (EEA, 2020). Based on this monitoring site classification, varying station and site characteristics with different ozone sensitivities can be included and distinguished in ozone pollution studies. Consequently, in respective analysis, it can also be accounted for the presence of different regimes, as e.g., as described above, rural stations are often NO_x-sensitive and more polluted urbanized stations tend to be more VOC-sensitive (Sillman, 2003).

1.1.2 Health-relevant Compound Occurrences

Natural hazards or multiple drivers can jointly occur resulting in complex risks leading or contributing to negative societal or environmental effects. These simultaneous occurrences that may cause or worsen the impacts that are induced by one independent variable alone can be defined as compound (extreme) events (Zscheischler et al., 2020). The co-occurrence of heatwaves and droughts represents e.g., one typical example of a compound event. According to the IPCC (2021), due to human activities, the chance of these events generally have likely increased since the 1950s. Ground-level ozone as well as surface air temperature (hereinafter often simply referred to as temperature) are often correlated and health-relevant levels repeatedly co-occur, leading to a severe and intensified human health burden, as outlined below. Consequently, concurrent occurrences of both health stressors can be defined as compound ozone-temperature (o-t-) events.

Ozone can be defined as a natural hazard as exposure to O_3, occurring almost exclusively by inhalation, can lead to various harmful human health effects and thus increased morbidity and mortality (Nuvolone et al., 2018, WHO, 2021). The severity and extent of symptoms is influenced by a wide range of factors and is highly determined via the duration and intensity of the exposure, causing adverse acute, short-term, and chronic, long-term health outcomes. To list a few of these various negative health impacts: irritating effects on eyes, mucous membranes, and airways as well as inflammatory responses, lung damage, and changes in lung tissue and airways (WHO, 2008, WHO, 2013, WHO, 2006). In addition, exposure to ozone is also repeatedly associated with cardiac health risks e.g., life-threatening arrhythmias, myocardial infarction, and heart failure (Eis et al., 2010). A good overview on short- and long-term health effects of O_3 alongside a description of recent health impact estimates regarding mortality and morbidity is given in Nuvolone et al. (2018). There exists a significant variability of individual responses to the exposure to O_3. This leads to the identification of vulnerable

subgroups that are specifically susceptible to ozone pollution and normally show a higher morbidity and mortality risk e.g., the elderly or people with pre-existing medical conditions (Eis et al., 2010, WHO, 2013). In 2019,16.800 and 19.070 premature deaths were related to ozone exposure in 27 reporting member states of the European Union and across 41 reporting European countries, respectively (EEA, 2021).

Temperature also represents a severe health stressor as single day or prolonged episodes of elevated levels, e.g., heatwave periods, negatively affect human health based on induced thermal load. Enhanced mortality just represents the tip of the iceberg of possible health effects, as thermal load may also cause or worsen e.g., severe dehydration, heat exhaustion, thrombogenesis, heat rush, and life-threatening heat strokes. In this regard, good overviews of heat-related health risks are provided by Ebi et al. (2021) and McGregor (2015). In accordance with ozone, also the level of exposure, including duration, severity, and frequency, as well as the population exposed and its susceptibility, influence the health impacts caused by temperature (Matthies et al., 2008). Various specifically vulnerable subgroups with an increased risk regarding thermal load exist e.g., people of advanced age or with pre-existing conditions like cardiovascular or respiratory diseases (Ebi et al., 2021).

Based on the above presented O_3 formation and further associated, underlying processes, surface air temperatures are often strongly correlated with ground-level ozone concentrations and elevated levels of both environmental variables repeatedly co-occur (e.g., Schnell and Prather, 2017, Hertig, 2020). As exposure to ozone pollution as well as thermal load both affect human health independently, the compound occurrence of both health stressors represents a particular severe human health burden. There is evidence that concurrent health-relevant levels of ozone and temperature pose an even intensified threat to human life due to synergistic effects resulting in a risk beyond the sum of their individual impacts (WHO, 2008, Analitis et al., 2008). It became apparent that e.g., heatwaves can increase the by air pollution induced mortality risk (IPCC, 2022), with particularly ozone pollution leading to an enhanced human health burden on hot days (Pattenden et al., 2010) and with prolonged concurrent episodes of heat and ozone pollution resulting in higher mortality (Hertig et al., 2020, Analitis et al., 2014). In 2018, an increment in attributable deaths of 20% for 41 reporting European countries was found due to the effect of the observed high temperatures of that year which favored the photochemical formation of O_3, leading to elevated concentrations and hence resulting in overall stronger health impacts (EEA, 2019). Consequently, compound o-t-events combining two natural hazards and composing a substantial health risk for the general population are of specific interest for and should be the focus of further environmental health science and projection studies.

1.2 Motivation and Problem Description

1.2.1 Linkage and Regionalization

There exists a strong and complex relationship between ozone and temperature, with the o-t-linkage being determined by various direct and indirect causalities. For example, to name one example for each, a direct and indirect causality, respectively: (direct) the sequence of reactions determining O_3 formation are enhanced by warm temperatures; (indirect) the sunlight-driven and photochemical ozone formation is based on high solar radiation which is usually also leading to elevated temperature levels. Since the link between ozone and temperature is very complex, previous research was conducted regarding various altering ambient conditions in different sites and regions, including the spatial and temporal evaluation of their joint occurrence and relationship as well as the identification of main drivers (e.g., Porter and Heald, 2019, Abdullah et al., 2017, Kerr et al., 2019, Varotsos et al., 2019, Bloomer et al., 2009). Meteorological and synoptic mechanisms mainly determining ozone concentrations alone (Carro-Calvo et al., 2017, Otero et al., 2016) or in combination with temperature levels (Hertig, 2020, Hertig et al., 2020) were analyzed. It became evident that

the correlation and linkage between both health stressors as well as their respective main drivers varied not only with the location of site and season but were also only valid under certain ambient conditions and tended to deviate or break under extreme circumstances. Please note that in the reminder of this chapter as well as in Chapter 5 - Summary and Synthesis and Chapter 6 - Conclusion and Outlook, in the context of the o-t-relationship, the term direct solely refers to the strong linkage between ozone and temperature with a large positive response of ozone on increasing temperature levels. Hence, it is used independently of the various above mentioned direct and indirect causalities determining the o-t-relationship. The relationship between ozone and temperature hence needs to be evaluated over a broad range of temperatures, as the strong and direct linkage between both variables can only be assumed under moderate temperature conditions. On the one hand, elevated ozone concentrations, showing a strong dependence on temperature particularly in polluted regions, show in general a strong response and association with temperature levels surpassing 20°C (Sillman, 2003), so a clear o-t-linkage is not expected under cooler temperature conditions. On the other hand, there is evidence that extremely high air temperatures result in a break of the strong and direct linkage between both variables observed under moderate temperature conditions. Even if in some regions an approximately linear increase of ozone with rising temperature levels became evident for a wide range of moderate summer air temperatures, this positive o-t-slope might change or even reverse under extremely high temperatures, like found by Steiner et al. (2010) in their study of four Californian air basins. Correspondingly, Shen et al. (2016) detected ozone suppression with significant decreases in the found direct o-t-slopes in their chosen season from May to September at very hot conditions with daily maximum temperatures surpassing their 95th percentiles at about a fifth of all examined sites in northeastern, southwestern, and deep southern parts of the United States. In accordance, considering previous European heatwave episodes, in which higher O_3 concentrations were in general accompanied by higher air temperatures, a break of the o-t-relationship in the higher percentiles of both variables was observed during the 2003 heatwave (Varotsos et al., 2019). These alterations of the direct link between both variables under extreme heat are in general often primarily the result of emission changes from e.g., biogenic sources under very high air temperature levels. But, next to accompanying and strongly affecting emissions, also meteorological and synoptic conditions spatiotemporally determine the o-t-linkage. Porter and Heald (2019) found that meteorological phenomena played an important role regarding the summertime o-t-relationship in Europe. Otero et al. (2016) identified meteorology as the most important driver of maximum daily ozone and its extreme values in central, but not to the same extent in southern and northern parts of their European study domain which were comparably high influenced by ozone persistence and hence precursor emissions. The deviation of the most important meteorological, synoptic as well as further drivers of ozone and temperature, considered alone or in combination, from one region to another or within an extended area has also been identified by further previous and recent studies (e.g., Hertig et al., 2020, Kerr et al., 2019, Rasmussen et al., 2012). As ambient temperature conditions vary throughout the year and across the European domain, a spatiotemporal variation of the o-t-correlation and linkage can be assumed over Europe. Furthermore, identified main drivers of single and joint occurrences of health-relevant ozone concentrations and air temperature levels may additionally vary temporally and regionally across Europe.

Consequently, European-wide variations regarding ozone concentration and air temperature levels, health-relevant compound conditions as well as the o-t-relationship need to be addressed by a region-wise analysis. A regionalization based on both target variables with the classification of Europe into distinct ozone-temperature regions showing similar spatiotemporal patterns and characteristics is essential in this regard. As a result, the region-specific linkage and correlation between ozone and temperature as well as the respective main drivers of health-relevant single and compound occurrences can hence be evaluated. Regionalizations were already conducted by previous studies based on ozone (Carro-Calvo et al., 2017, Boleti

et al., 2020, Lehman et al., 2004, Lyapina et al., 2016, Varotsos et al., 2013) or temperature (Bador et al., 2015, Chidean et al., 2015, Scotto et al., 2011), but have so far been still missed with regard to a joint consideration of both variables in Europe. Consequently, even if there exists research work in which the main drivers, linkage and health-relevant occurrences of ozone and temperature were investigated, often just one variable was considered or specific selected study areas of smaller dimension or regions and domains outside of Europe built the spatial focus. Various previous studies were based on domains where it is, at least nowadays, well known that elevated summer ozone concentrations usually coincide with moderate to high temperatures and missed to clarify the comparability with or the transferability of the results to further regions with deviant ambient conditions. Literature review and the current presented evaluation show that the lack of previous research focusing on both target variables, ozone, and temperature, and specifically highlighting environment-related and regional variations in their joint occurrence, linkage and main driving mechanisms is especially true for Europe. As a result, questions remain regarding how the o-t-correlation and relationship and underlying main drivers of compound occurrences change from one region to another across the European domain.

1.2.2 Future Ozone and Air Temperature

Long-term changes in ozone pollution and air temperatures arising from climate change represent one major research focus of previous and ongoing environmental health science and projection studies. In recent research, future projections have been in general based on different scenarios of the last two generations of the Coupled Model Intercomparison Project Phase 5 (CMIP5) (Taylor et al., 2012) and Phase 6 (CMIP6) (Eyring et al., 2016) (please also refer to Appendix A for a short overview of related scenarios). Hot days or heatwaves become almost certain more intense or frequent in the future (IPCC, 2021), also over a wide range of Europe (Schoetter et al., 2014, Meehl and Tebaldi, 2004). Considering O_3 under climate change, the ozone-climate penalty was defined. The term refers to increased ozone concentrations due to global warming and hence rising air temperatures that might negate and jeopardize emission controls and pollution mitigation strategies (Colette et al., 2015, Wu et al., 2008). There is evidence that summer ozone concentrations are prone to increase in future European climate if anthropogenic mitigation strategies and emission controls are not taken into account (Katragkou et al., 2011, Colette et al., 2015). Shen et al. (2016) reported for large parts of the United States, keeping anthropogenic emissions at present-day levels, and following the RCP4.5 scenario assumptions, substantial increases in ozone episodes from 2000 to 2050. Schnell et al. (2016) found increases and decreases in summertime mean and high-percentile O_3 in polluted and clean environments, respectively. This is in accordance with recent results assessed for the observational period 2000-15 in Europe, with daily mean ozone concentrations decreasing at rural and stabilizing or increasing in suburban and urban sites (Boleti et al., 2020). These results also highlight the importance to take varying station site characteristics (e.g., urban, suburban, or rural) in ozone pollution and projection studies into account. A major challenge is to project future ozone concentrations during single or prolonged episodes of heat, also complicating the assessment of the by ozone pollution in combination with thermal load induced health burden under climate change (IPCC, 2022). Meehl et al. (2018) found for most areas in the world with regard to RCP6.0 emission scenarios a decline in ozone concentrations on even intensifying future heat wave days compared to non-heat wave days in the 21st century, but an increase by keeping anthropogenic precursor emissions constant at 2005 levels. Hertig (2020) assessed a strong increase in concurrent ozone pollution and thermal load event frequencies under RCP8.5 scenario assumptions in her southern German study area in Bavaria.

Considering environmental health science and projection studies, two main modeling approaches are generally selected: 1) dynamical or 2) statistical. Projections of future ground-level ozone are generally based on the usage of a dynamical modeling approach, e.g., on the

application of chemical transport models. Future assessments rely on the inclusion and integration of general circulation models (GCM) and regional climate models (RCM). Dynamical models are usually computationally expensive and so, there exists only a limited number of models and model runs. Statistical models are in comparison to dynamical models computationally less expensive. In statistical downscaling, empirical links between large-scale and local-scale climate are identified and applied to output from climate models. Perfect Prognosis (PP) statistical downscaling is based on an, on observed data calibrated, statistical model that links large-scale predictors to local-scale predictands and that is later applied to large-scale predictors generated by climate model output (Maraun and Widmann, 2018). In the context of future ozone pollution alone or in combination with heat days or episodes, site-specific and station-based ozone and temperature data often form the basis of the selected predictand. Meteorological variables and synoptic conditions that are usually extracted from reanalysis-based variables are used as predictors. In the PP statistical downscaling and projection approach, projections are done by replacing the meteorological and synoptic predictor data with the corresponding and usually preprocessed respective climate model data. Several studies exist and were already mentioned above using a statistical modeling approach to evaluate the relationship between meteorological and synoptic conditions and ozone pollution alone or in combination with temperature, also by including projections based on Earth System Model (ESM) output (e.g., Hertig, 2020, Hertig et al., 2020, Otero et al., 2016). But the number of studies is limited and often, especially if future projections were also considered, a focus on environmental predictors was set and hence only the relationship between meteorological and synoptic conditions and ozone concentrations considered. So, the impact and changes of precursor emissions or the influence of ozone persistence were not included in statistical analysis. Consequently, if the generated statistical models were or might be used to assess changes under future climatic conditions throughout the 21st century, e.g., also in follow-up research, the incorporation of emission changes and their impacts on ozone in future pollution projections was or would be impossible. But in the future, e.g., decarbonization of both the transport sector and the power sector along with a decreasing trend of NO_x emissions, acting as limiting factor for ozone production at various sites, might be expected at the European level, especially in the context of the specified or intended climate neutrality goals or zero pollution visions. So, in comparison to the historical period, with e.g., extensive NO_x emissions occurring from traffic in urban areas and by fossil fuel burning from industries and power plants outside these areas, future precursor emission reductions might strongly determine ozone concentration levels and hence need to be included in environmental health science and projection studies. For example for Europe, an increase as well as a reduction of the health burden induced by ground-level ozone in 2050 (RCP4.5) was assessed by Orru et al. (2019), by considering climate change alone or in combination with reductions of ozone precursor emissions, respectively. Furthermore, most already published research studies still relied on the ESM output of CMIP5 regarding climate change projections in the context of future ozone pollution.

CMIP6's multi-model climate change projections based on alternative scenarios of future emissions and land use changes (O'Neill et al., 2016) have been used for the latest assessments of the IPCC (e.g., IPCC, 2021, IPCC, 2022) and should generally form the basis of most recent and future projection studies. According to the IPCC (2021), global surface ozone pollution is with a high confidence projected to range from strong reduction (e.g., SSP1-2.6) to no improvement or degradation (e.g., SSP3-7.0). There is a high confidence in the projection of ozone pollution to worsen over all continental aeras throughout the 21st under SSP3-7.0 scenario assumptions, incorporating no climate change mitigation and only weak air pollution control strategies (IPCC, 2021). Even in scenario assumption SSP5-8.5 including stringent air pollution control, it is highly confident that ongoing climate change and high methane CH_4 levels negate substantially ozone pollution reductions until at least 2080 (IPCC, 2021). Research studies integrating climate change projections from e.g., CMIP6 rely on the

information provided by the output from ESM. But merely a small number of CMIP6's ESM have O_3 information output available and if so, then only with a monthly resolution. These few models include ozone based on two options: (1) prescribed from a by CMIP6 provided dataset and (2) interactively computed. All ESM that do not have an interactive chemistry model themselves and are dependant on the inclusion of the fixed ozone dataset provide identical O_3 information. The monthly ozone time series data extracted from ESM output reflect the larger-scale total changes of O_3 resulting from climate and precursor emission changes under different scenario assumptions. So, even if information on ozone precursors themselves are not provided, information on their change and impact on future surface ozone can be extracted directly from these by specific ESM modeled monthly ozone data. Consequently, ozone pollution and projection studies using this monthly O_3 information are hence able to consider the impact and changes of precursor emissions in their assessments of future estimations of ground-level ozone.

In summary, further research complementing existing work on recent and future ozone pollution by using PP statistical downscaling models and projections is essential. In general, only a small number of studies exists analyzing concurrent elevated ozone concentration and air temperature levels under recent and future climatic conditions. So especially, further research with a specific focus on the future occurrence of compound o-t-events in Europe is required. Updated and adjusted ESM data and respective scenario assumptions of CMIP6 need to be integrated in upcoming assessments of future O_3 pollution and compound o-t-event occurrences. Ozone information provided by some CMIP6's ESM should be evaluated in this regard in order to subsequently integrate respective, processed, and prepared, pollution output in future environmental health science and projection studies. As a result, the influence and changes of precursor emissions can hence be incorporated and taken into account in forthcoming ground-level ozone projections.

1.3 Research Objectives and Structure

1.3.1 Research Areas and Questions

As outlined above, air pollution represents the major environmental health threat in Europe, with exposure to surface ozone posing a major risk to the European population. Until the end of the 21st century, the health burden induced by ground-level ozone is expected to worsen due to ongoing climate change. Compound occurrences of health-relevant surface ozone and air temperature levels are of particular interest to environmental health science and projection studies, as there is evidence of an even intensified resulting health risk when both stressors occur at the same time. The overall aim of this dissertation is hence to improve our current understanding and knowledge regarding recent and future health-relevant occurrences of ground-level ozone alone or alongside surface air temperature in Europe. The following four primary research areas (RA) with several main research questions (RQ) summarize the main objectives of this dissertation. Three individually written and prepared peer-reviewed scientific research articles (Research Articles 1-3) investigate these research questions in detail. Methodologically, evaluations are primarily based on PP statistical downscaling models and projections.

RA1: European O-t-Associations and Main Drivers
(Research Article 1)

> **RA1-RQ1:** Is there an association between day-to-day variation in surface ozone and air temperature levels in Europe?

> **RA1-RQ2:** How do statistical regression-based downscaling models represent the influence of main drivers based on meteorological variables and prevailing ozone persistence on health-relevant compound o-t-events in central Europe?

RA2: Region-specific Relationships and Compound O-t-Event Occurrences
(Research Article 2)

RA2-RQ1: How is the European domain dividable into regions based on the regional phenomena of surface ozone and air temperature?

RA2-RQ2: How do statistical downscaling models incorporating meteorological variables and synoptic conditions capture region-specific compound o-t-events?

RA3: Future Compound Ozone and Temperature Burden under Climate Change
(Research Article 1 and 2)

RA3-RQ1: What are the expected changes in future health burden induced by compound o-t-events until the end of the 21st century under central European climate change projections?

RA3-RQ2: To what extent are the proposed projection frameworks suitable across the whole European domain?

RA4: Future Local, Ground level O$_3$ under Climate and Emission Changes
(Research Article 3)

RA4-RQ1: How are local, ground-level O$_3$ concentrations modeled, and future changes projected by a statistical downscaling framework including information on climate and precursor emission changes under different scenario assumptions in the European area?

RA4-RQ2: How does the variation of the chosen statistical downscaling models, mainly differing in terms of the predictor variables used, impact model and projection results?

1.3.2 Thesis Outline

This thesis consists of six chapters, starting with an introductory chapter (Chapter 1) that has outlined so far, the background, motivation, and problem of the research work at hand. The overall objectives of the dissertation have been presented, including the main underlying research areas alongside all within raised research questions. Finally, this last subchapter of Chapter 1 outlines the general structure of this thesis. The remainder of the dissertation is divided into three main chapters (Chapters 2-4), dealing with the topics, and answering the research questions formulated in the previous section. These chapters comprise the three individually written and prepared peer-reviewed scientific research articles. Each of these articles consists of a largely independent study following the typical structure and standards of high-quality journal publications. A general, summarizing discussion and synthesis of the results and central contents of the publications are outlined in Chapter 5. All raised research questions regarding the four research areas presented above are addressed and respective work and results presented. Chapter 6 contains concluding remarks, recapitulating the main contributions and findings as well as evaluating them with respect to their general significance as well as the current scientific knowledge and state of the art. Furthermore, an outlook on issues that remain open and may be investigated in future studies is given. Furthermore, ongoing, and possible applications of the results and contributions of the presented dissertation in current and future research projects are highlighted.

In Appendix A an overview of all in Chapters 1, 5 and 6 used units, abbreviations and acronyms is provided. Appendix B lists all publications and conference contributions of the author realized or pursued till the submission and publication date of the dissertation. Appendix C outlines the contributions of the author to the different scientific journal articles presented in Chapters 2, 3, and 4. Appendix D-F list all Supplementary Information originally submitted and later provided with the original research articles.

Chapter 2 - Research Article 1: The research article titled "Modeling and projecting health-relevant combined ozone and temperature events in present and future Central European climate" addresses RQ1 and RQ2 of RA1 as well as RQ1 and RQ2 of RA3.

The research article presented in Chapter 2 evaluates the relationship between compound ozone-temperature events, defined based on concurrent health-relevant elevated levels of MDA8O3 and daily maximum temperature values, and large-scale meteorological conditions as well as prevailing air pollution levels. Central Europe and the peak ozone-temperature season from April to September, 1993-2012, represent the regional and temporal focus, respectively. Two main statistical regression-based modeling approaches are evaluated to identify main drivers of combined ozone-temperature events. In a preliminary screening process using reanalysis and output data of seven models of the CMIP5, suitable predictors to assess and project compound o-t-events are selected. Statistical downscaling projections until the end of the 21st century are generated under CMIP5's RCP4.5 and RCP8.5 scenario assumptions and potential frequency shifts in compound o-t-event occurrences considering mid- and end-century central European climatic conditions evaluated. A holistic focus on central Europe is chosen across the whole modeling and projection process. Please note, in Chapter 2 - Research Article 1 presented results are still based on ESM output and related scenario assumptions from CMIP5 (instead of the up-to-date phase CMIP6) due to the start date of the respective, underlying research work.

Chapter 3 - Research Article 2: The research article titled "Using Clustering, Statistical Modeling, and Climate Change Projections to Analyze Recent and Future Region-Specific Compound Ozone and Temperature Burden Over Europe" addresses RQ1 and RQ2 of RA2 as well as RQ1 and RQ2 of RA3.

The research article comprised in Chapter 3 presents a regionalization approach based on surface ozone and air temperature to highlight the regional phenomena of o-t-characteristics, patterns, and variabilities and to account for spatiotemporally varying environmental and climatic conditions across Europe. The o-t-season from April to September, 2004-2018, is considered in this regard. The regionalization forms the basis of the presented work, dividing the European domain into six distinct ozone-temperature regions. The division allows the specification and comparison of region-specific variations in observed o-t-relationships across Europe. The main objective is to model and project current and future compound o-t-events, taking region-specific differences based on the identified o-t-regions into account. Statistical downscaling models evaluating the region-specific relationships between distinct meteorological variables and synoptic conditions and health-relevant compound o-t-events are generated for selected representative stations per o-t-region and later used in respect of climate change projections until the end of the 21st century. Potential frequency shifts considering mid-, and end-century European climatic conditions of compound o-t-events are assessed based on eight ESM from CMIP6 considering SSP2-4.5 and SSP3-7.0 scenario assumptions. As a result, regionally varying recent and future by compound o-t-events induced health burden over Europe is evaluated.

Chapter 4 - Research Article 3: The research article titled "Future Local Ground-level Ozone in the European area from Statistical Downscaling Projections Considering Climate and Emission Changes" addresses RQ1 and RQ2 of RA4.

The research article presented in Chapter 4 assesses future local ground-level ozone in the European area from statistical downscaling projections by considering not only climate but also emission changes. A statistical downscaling model and projection framework using information on meteorology as well as precursor emissions is applied. Precursor emissions are included by the incorporation of monthly O_3 time series data that reflect the larger-scale total changes of O_3 as emission-related predictor. So even if the changes of precursor emissions are not directly included in models and projections, the information about their change and impact on ozone is nevertheless considered. In this regard, for projections, output is derived from suitable

CMIP6's ESM for SSP2-4.5 and SSP3-7.0 scenario assumptions. Results based on ESM with an interactive computation of the atmospheric chemistry versus ESM with prescribed O_3 changes based on a fixed dataset is compared. A sensitivity analysis evaluates the impact of different statistical downscaling model choices, mainly differing in terms of the predictor variables used, to quantify the influence of specific predictors and predictor sets on model and projection results. The impact of varying climate models, predictor configurations, and scenarios on the assessment of current and future local O_3 occurrences can hence be assessed, with a special focus set in this regard on the evaluation of the influence of emissions, beside solely climate change information, on anticipated O_3 changes.

Please note, the research articles presented in Chapters 2, 3 and 4 are adapted and adjusted to meet layout and style of this written thesis but are still treated as closed entities and individual publications. No further adjustments in design and structure are hence incorporated, including e.g., headings and chapter numbers. Regarding the tables and figures of each publication, layout and numbers are altered to meet the style and to be integrated in the general structure of this manuscript. The final bibliography of this thesis is composed of all used references, including the ones of all submitted and published research articles.

2. Chapter 2 - Research Article 1

Modeling and projecting health-relevant combined ozone and temperature events in present and future Central European climate

Publication:

This chapter contains one original research article submitted to the hybrid, multidisciplinary journal *Air Quality, Atmosphere & Health* published by Springer Nature and received in May 2020. The article was accepted in October 2020 and published online in November 2020. The printed version was published in Volume 14, issue 4, in April 2021:

JAHN, S.* & HERTIG, E. 2021. Modeling and projecting health-relevant combined ozone and temperature events in present and future Central European climate. *Air Quality, Atmosphere & Health*, 14, 563-580. https://doi.org/10.1007/s11869-020-00961-0

*Sally Jahn is first and corresponding author.

The layout of the original, online published article, including the used citation style as well as figure and table designs, numbers, and captions, was adapted and adjusted to be consistent with the rest of the manuscript. No changes in spelling, including e.g., used abbreviations and acronyms, were made and the main text of this chapter is still in this regard in accordance with the published version. The Supplementary Material (Online Resources 1-3) is available online alongside the original article and is added to this dissertation without further adjustments as Appendix D.

Individual author contributions (as in Appendix C):

The main topic of this study was formulated by Elke Hertig. The specific study design was developed by Sally Jahn and Elke Hertig. Statistical downscaling modeling and projection approaches were designed by Sally Jahn in discussion with Elke Hertig, who also provided the idea and support for the integration of ozone persistence into the projection process. Literature review, data download and processing, all computations including statistical downscaling model and projection development and implementation, the final analysis, and preparation of figures were performed by Sally Jahn. Discussions and interpretation of the main results were done during the evaluation meetings with Elke Hertig. Sally Jahn prepared the manuscript, which was improved with the aid and contributions of Elke Hertig. The authors thank Irena Kaspar-Ott for the final proof-reading of the manuscript.

Modeling and projecting health-relevant combined ozone and temperature events in present and future Central European climate

Sally Jahn[1] & Elke Hertig[2]

[1]Regional Climate Change and Health, Institute of Geography and Faculty of Medicine, University of Augsburg, Alter Postweg 118, 86159 Augsburg, Germany

[2]Regional Climate Change and Health, Faculty of Medicine, University of Augsburg, Alter Postweg 118, 86159 Augsburg, Germany

Abstract

Statistical models to evaluate the relationships between large-scale meteorological conditions, prevailing air pollution levels and combined ozone and temperature events, were developed during the 1993-2012 period with Central Europe as regional focus. Combined ozone and temperature events were defined based on the high frequency of coinciding, health-relevant elevated levels of daily maximum tropospheric ozone concentrations (based on running 8-h means) and daily maximum temperature values in the peak ozone and temperature season from April to September. By applying two different modeling approaches based on lasso, logistic regression, and multiple linear regression mean air temperatures at 850 hPa, ozone persistence, surface thermal radiation, geopotential heights at 850 hPa, meridional winds at 500 hPa, and relative humidity at 500 hPa were identified as main drivers of combined ozone and temperature events. Statistical downscaling projections until the end of the twenty-first century were assessed by using the output of seven models of the Coupled Model Intercomparison Project Phase 5 (CMIP5). Potential frequency shifts were evaluated by comparing the mid- (2031-2050) and late-century (2081-2100) time windows to the base period (1993-2012). A sharp increase of ozone-temperature events was projected under RCP4.5 and RCP8.5 scenario assumptions with respective multi-model mean changes of 8.94% and 16.84% as well as 13.33% and 37.52% for mid- and late-century European climate.

Introduction

Air pollution poses the single largest environmental risk to human health in Europe resulting in a substantial public health burden for the European population (EEA, 2019). Tropospheric ozone (O_3), representing one major air pollutant, is not directly emitted to the atmosphere, but produced by a photochemical chain reaction in the presence of solar radiation. It is formed by the reaction of precursor gases such as volatile organic compounds (VOC), carbon monoxide (CO), or nitrogen oxides (NO_x) that is enhanced by rising air temperatures and solar radiation. Elevated levels of O_3 cause a variety of human health effects primary affecting the cardio-pulmonary system (Nuvolone et al., 2018, Srebot et al., 2009, WHO, 2006, WHO, 2013). The severity and extent of symptoms are highly determined via duration and intensity of the exposure to the reactive and oxidative O_3 gas. Elevated concentrations have irritating effects on eyes, mucous membranes, and airways. Lung inflammation and tissue damage, asthma, a reduction of the self-cleaning mechanism of the bronchi, cardiac arrhythmia, heart attacks, and heart failure are possible resulting respiratory or cardiovascular diseases (Eis et al., 2010, Srebot et al., 2009, WHO, 2006). Elevated mortality levels were linked to tropospheric O_3, while

potentially susceptible people with, e.g., corresponding previous illnesses show a higher disease and mortality risk (Eis et al., 2010, WHO, 2013). The Ambient Air Quality Directive (AQD) of the European Union suggests 120 µg/m^3 (daily maximum 8-h mean) as a target value for protecting human health from O$_3$ (EEA, 2019). The WHO even recommended the use of 100 µg/m^3 in their Air Quality Guidelines (AQG), admitting that even under this threshold, some sensitive individuals may suffer from negative health effects (WHO, 2006). The WHO (2013) assumed that the implemented target values to protect humans from ozone pollution are all in all too high. Hertig et al. (2019) analyzed the relationship between daily maximum 1-h ozone concentrations and myocardial infarction (MI) frequencies. The city of Augsburg (Bavaria, Germany) was the regional focus. In conclusion, they argued that the existing AQD target value is only suitable to a limited extent as enhanced MI risks already occurred at median to moderately high ozone pollution levels. A maximum risk was found at approximately the 75th percentile with the value referring to 116 µg/m^3.

Elevated air temperature levels (Baccini et al., 2008, Hajat and Kosatky, 2010, Song et al., 2017) and heatwave episodes (Anderson and Bell, 2011, Gasparrini and Armstrong, 2011, Guo et al., 2017, Robine et al., 2012) can negatively affect human health and were associated with increased mortality. A higher cardiovascular, cerebrovascular, or respiratory mortality rate just represents the final extreme end of a variety of adverse impacts on human health. Increasing thermal load can lead to or worsen health effects, for example, severe dehydration, heat exhaustion, cramps, syncope, oedema, thrombogenesis, heat rush, and life-threatening heatstrokes (McGregor, 2015). Health impacts are determined by the level of exposure with respect to duration, severity, and frequency as well as the exposed population and its sensitivity (Matthies et al., 2008). There exist a vast number of worldwide as well as national-based indicators and target values to describe extreme temperatures and periods of excessive heat (e.g., DWD, 2020, ETCCDI, 2009).

As indicated, due to the specific characteristics of ozone formation and further underlying processes, high ozone concentrations often co-occur with elevated air temperature levels (Fiore et al., 2015). As exposure to poor air quality as well as thermal load both already affect human health independently, their combined occurrence poses an even intensified threat to human life, especially as synergistic effects lead to a risk beyond the sum of their individual effects (Katsouyanni and Analitis, 2009, WHO, 2008). Thus, for example, ozone pollution is an enhanced threat to human health on hot days (Pattenden et al., 2010), while with prolonged periods of heat associated mortality is higher during ozone pollution events (Analitis et al., 2014).

The occurrence of high temperatures and elevated levels of ozone are substantially influenced by meteorological and air pollution conditions. As both health stressors are apparently target variables to assess health burden occasions for the European population and are dependent on recent and future climatic conditions, a variety of assessments exist, investigating separately air temperature or O$_3$ levels in Europe. Future changes of these health stressors are additionally analyzed in terms of anthropogenic induced global climate change. Recent studies found that precursor emissions show a substantial impact on the relationship between the strongly correlated ozone and temperature target variables (Bloomer et al., 2009, Coates et al., 2016, Sillman and Samson, 1995). Meteorological and synoptic conditions influencing O$_3$ pollution (Carro-Calvo et al., 2017, Otero et al., 2016) or elevated air temperatures on single or consecutive days (Black et al., 2004, Krueger et al., 2015) were evaluated for Europe. Various studies analyzed future health outcomes related to air pollution (Fang et al., 2013, Hendriks et al., 2016) or heat events (Gasparrini et al., 2017, Takahashi et al., 2007) under twenty-first century climate change. A growing number of days with temperature extremes and heat waves were identified in Europe (Jacob et al., 2014, Meehl and Tebaldi, 2004, Schoetter et al., 2014). By not considering future anthropogenic mitigation strategies and emission policies, an increase of surface ozone concentrations over Europe in summer was found (Katragkou et al., 2011), largely for high-percentile O$_3$ levels and polluted environments

(Schnell and Prather, 2017). Even if future-projected ozone concentration levels are highly determined by changing precursor emission levels, there is growing evidence that the increasing effect of a warming climate could negate recent and future pollution mitigation strategies and policies (Colette et al., 2015, Hendriks et al., 2016). Even with a strong reduction of precursor emissions, ozone standards may still be violated in the future at individual stations or regions (Moghani and Archer, 2020).

Only a rare number of studies investigated concurrent elevated temperature and O_3 levels under recent and future climatic conditions. Hertig (2020) assessed the relationship between large-scale meteorological mechanisms and elevated levels of daily maximum ground-level temperature and ozone concentrations for Bavarian cities. Furthermore, combined threshold exceedances of both target variables were analyzed. Projections under RCP8.5 were provided to illustrate changes of these health stressors under future climate change. A strong frequency increase of co-occurring O_3 pollution and thermal load events was identified. A recent study by Meehl et al. (2018) investigated the relationship between heat waves and surface ozone concentrations around the world under RCP6.0 emission scenarios in the twenty-first century. For most areas, a decline was found in ozone concentrations on even intensifying future heat wave days compared to non-heat wave days. In contrast, an increase was assessed for most areas by keeping anthropogenic precursor emissions strongly influencing O_3 pollution levels constant at 2005 levels.

In summary, merely a few assessments exist analyzing the co-occurrence of combined elevated temperature and O_3 levels representing a relevant threat for human health in Europe. Enhanced attention should be paid to the possible impacts of future climate change on these harmful occasions. Thus, the motivation for this study is to assess the relationships between meteorological conditions and the joint occurrence of elevated tropospheric ozone concentrations and air temperature values over Central Europe. Co-occurring high levels of the two variables are considered to define combined ozone and temperature events (hereafter "o-t-events"; please refer to Table S1 in the Supplementary Material (Online Resource 1) to get an overview of all used abbreviations and acronyms). The response of the o-t-events to meteorological factors as well as prevailing atmospheric and O_3 pollution conditions is investigated to better understand the main drivers of these highly health-relevant events. Projections providing an integration of climate change scenario assumptions until the end of the twenty-first century are presented based on seven models of the fifth phase of the Coupled Model Intercomparison Project (CMIP5) (Taylor et al., 2012). Thus, potential frequency shifts of such health burden occurrences under future climate conditions are assessed.

This paper is organized as follows. The "Data" section presents the initial selection and preprocessing of predictand and predictors by additionally referring to their underlying respective datasets (e.g., reanalyses and earth system model (ESM) output). The "Methods" section introduces all applied statistical model techniques and approaches, the framework of their implementation, the metrics to evaluate their performance to assess the occurrence of combined o-t-events, and the employment of the subsequent projections. The "Results" section presents the results of all statistical modeling and projecting processes. Finally, the discussion and concluding remarks can be found in the "Discussion" and "Conclusion" sections.

Data

Predictand data

Since the main drivers of concurrent elevated air temperature and O_3 levels as well as possible future frequency shifts are assessed, the o-t-events represent the target variable for the statistical downscaling models and subsequent projections. Accordingly, stations with measurement data on surface daily maximum ozone and air temperature in Europe were selected to define these combined events.

Station-based air quality and temperature data

Station-based ozone data were retrieved from the European air quality database data product AirBase version 8 maintained by the European Environment Agency (EEA) (EEA, 2014). Data collected within the subsequent Air Quality e- Reporting starting from 2013 based on new rules for reciprocal exchange of information and reporting were disregarded to assess homogenously submitted and prepared air quality monitoring data and information sets. Valid daily maximum ozone values (selected by EEA's predefined quality flags indicating the quality of the data) based on running 8-h means (henceforth named "MDA8O3") calculated from the corresponding hourly data were retrieved. An observational base period of 20 years from 1993 to 2012 was chosen as temporal focus. Beside the large-scale prevailing meteorological and climatic conditions, location-specific ozone concentrations are influenced by various station environment characteristics. To guarantee the best possible homogeneity of the database, the impact of factors other than meteorological variables, e.g., altitudinal vegetation change, crucially influencing ozone concentrations was minimized for all selected stations. Thus, only ozone stations located primarily in the planar up to the colline zone with an altitude height under 700 m were considered.

Station-based daily maximum surface air temperature (hereafter "TX") observations based on adjusted, homogenized blended temperature series were obtained from the European Climate Assessment & Dataset project (ECA&D) (Klein Tank et al., 2002). Only valid TX observations (selected by ECA&D's predefined quality code) in the country-based blended series of the ECA&D dataset were considered. Only temperature stations in the spatial vicinity of the ozone stations were selected. In order to reproduce the respective temperature as accurately as possible, merely temperature stations located at a distance of at most 10 km and with a maximum altitude difference of 200 m to the corresponding ozone station were chosen.

Station selection

Based on the respective database, all possible station pairs were evaluated to select suitable matches. To minimize the influence of missing values, each ozone and temperature station was required to have at least 75% of valid daily data (valid data for MDA8O3 and TX as defined above). Spearman rank correlation coefficients calculated between the daily and monthly MDA8O3 and TX time series of each station pair show primarily a strong relationship between both variables in spring to late summer. Thus, all analyses are based on the months from April to September, herein after referred to as the ozone-temperature season (hereafter "o-t-season"). Only station pairs with an on average monthly correlation coefficient of at least 0.5 in the o-t-season were selected, leading to an exclusion of eight ozone stations. All of these stations but two (located in Greece) were spread over Northern Europe (namely Great Britain, Finland, and Sweden), showing a weaker correlation between both target variables probably due to the overall, high latitude-based lower solar radiation durations, and intensities. Temperature time series were directly assigned to the paired ozone station to create a combined time series per location. Only station pairs with at least 75% of valid season-specific data across all years, based on their combined time series, were selected.

As a result, 85 station pairs in Central Europe build the regional focus of the study. The mean distance and the mean altitude difference between all paired stations is 4.72 km (min 0.2, max 9.91, median 4.64) and 31.54 m (min 0, max 146, median 10), respectively. These location differences between TX and MDA8O3 are not further referred to throughout the paper but should always be kept in mind. Hereafter, "station" is used to refer to these linked ozone and temperature station pairs, with all spatial station information being represented for the respective ozone station. An overview of all finally chosen ozone stations with more detailed station metadata and station pair characteristics is given in Table S2 in the Supplementary Material (Online Resource 1).

To assess the different air quality settings of each location, the finally selected stations are categorized in five station classes based on EEA's predefined types of station and area as follows: urban traffic ("ut", 13 stations), urban background ("ub", 37 stations), suburban background ("sb", 27 stations), rural industrial ("ri", 2 stations), and rural background ("rb", 6 stations). The selected stations are spread across five different countries in Central Europe, namely Austria, Belgium, Germany, The Netherlands, and Switzerland. Throughout the remaining sections, the term "Central Europe" is used to refer to this set of countries. The specific location of each analyzed station together with its respective class, highlighted by shape and color, is shown in Figure 2.1. On this and all following maps showing spatial distributions and locations, x- and y-axis represent longitude and latitude. Apart from that, hereafter, only the shape of the stations indicates the class of each station.
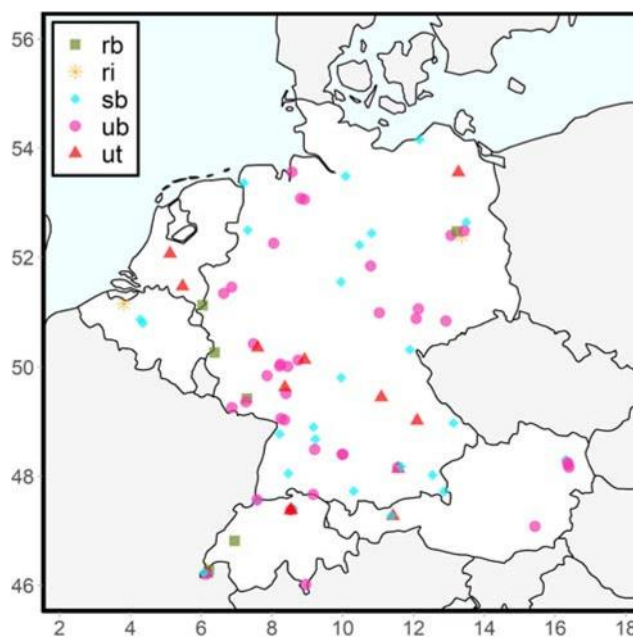
Fig. 2.1 Location of all 85 selected stations in Central Europe
Color and shape of points indicate the class of each station. Classes are specified as follows: rb = rural background, ri = rural industrial, sb = suburban background, ub = urban background, ut = urban traffic.

Combined events

Health-relevant, co-occurring high levels of MDA8O3 and TX were used to define o-t-events. Based on a 31-day window, the 75th percentiles for both target variables were calculated with respect to daily mean averages across all years in the base period. As a result, fixed daily values to define threshold exceedances for each variable and day in the o-t-season for all subsequent analysis in the observation, historical, and future projection period were generated. The selection of the 75th percentile was determined by the results of previous health-related studies presented and outlined in the "Introduction" section as well as the actual respective ozone and temperature values the percentiles amounted to taking into account all analyzed stations in Central Europe. More details on this will be given in the "Results" section. Temperature levels as well as ozone concentrations need to exceed these percentile-based thresholds. Additionally, ozone pollution levels surpassing a threshold of 100 µg/m^3 were also considered as a health-relevant ozone event in accordance with the WHO AQG. Thus, days with thermal load or TX exceedances were observed if TX values rose above the 75th percentile-based thresholds, while MDA8O3 exceedances were defined for days with ozone pollution levels beyond the respective 75th percentile-based or 100 µg/m^3 thresholds. If not otherwise specified, herein after TX and MDA8O3 exceedances refer to these definitions.

On combined event days, mean and median MDA8O3 and TX levels in the o-t-season amounted to 121.55 µg/m^3 (min 39.75 µg/m^3, max 262.73 µg/m^3) and 119.15 µg/m^3 as well as

27.5 °C (min 12.4 °C, max 40.2 °C) and 27.9 °C, respectively. Frequency analyses in the base period revealed a higher amount of event days from April to September compared to the remaining months, confirming the defined o-t-season based on spearman rank correlation coefficients.

Predictor data and selection

Predictor metrics belonged to two different types. The first type was considered as "meteorological". Suitable predictors to assess and project o-t-events were chosen and preselected based on a preliminary screening process using reanalysis and ESM data. The second type was considered as "persistence-based" and comprised only O_3 pollution persistence metrics.

The initial selection of predictor variables was determined by literature review (Carro-Calvo et al., 2017, Hertig, 2020, Krueger et al., 2015, Otero et al., 2016), data availability in the chosen ERA5 reanalysis (from the European Centre for Medium-Range Weather Forecasts (ECMWF); Hersbach and Dee, 2016), and earth system models (ESMs) as well as own analysis. The following large-scale meteorological variables formed the initial database: geopotential heights at the 850 hPa and 500 hPa levels (GH850, GH500), mean sea level pressure (MSLP), mean air temperatures at 850 hPa, 500 hPa, and 2 m (MT850, MT500, and MT2m), relative humidity at 850 hPa and 500 hPa (RH850, RH500), surface solar radiation downwards (SSRD), surface thermal radiation downwards (STRD), total cloud cover (TCC), and zonal and meridional winds at 850 hPa and 500 hPa (UWind850, UWind500, and VWind850, VWind500). Predictor data was retrieved with a 0.75° × 0.75° resolution. Matching predictor data for projections under scenarios historical, RCP4.5, and RCP8.5 (CMIP5 label: historical, rcp45, rcp85) were extracted from seven CMIP5-ESMs listed in Table 2.1. RCP4.5 and RCP8.5 represent one intermediate and the highest representative concentration pathway with a radiative forcing stabilized at approximately 4.5 W/m^2 by or still rising, greater than 8.5 W/m^2 after 2100, respectively (for detail, refer to IPCC, 2013).

The first run of the available ensemble was chosen for all variables. Thus, differences arising from the use of different ESMs were considered, whereas uncertainties from different initial conditions were not regarded. In accordance with the periods considered in the statistical downscaling models and projections, historical runs from 1993 to 2005 and scenario runs from 2006 to 2100 were used. Model data was regridded by nearest neighbor remapping to match the ERA5 resolution. Based on the geographic coordinates of each of the 85 stations, the mean of the nine grid boxes covering the area over and around the respective station location was calculated for all predictor variables.

The chosen statistical downscaling approach uses only observational data for both predictand and predictors (reanalysis) to train the statistical models. The models are later applied to ESM output assuming that the ESMs provide large-scale fields similar to the observed atmospheric variability. A simple linear scaling bias correction technique, used, e.g., by Gohar et al. (2017) and Teutschbein and Seibert (2012), was chosen and adapted to remove the monthly mean bias between reanalysis and climate model data.

The monthly mean difference between reanalysis and climate model data from 1993 to 2005 was used to bias-correct the respective ESM data from 1993 to 2100. Brands et al. (2013) assess the ESM performance to reproduce observed climatology not just on the basis of analyzing mean differences (bias), but also by examining distributional differences between reanalysis (ERA-Interim) and ESMs. Accordingly, to compare the distributional similarity between ERA5 reanalysis and ESM data, the two-sample Kolmogorov-Smirnov test (KS test) was applied. The used monthly time series were centered to have zero mean by subtracting the specific mean of the o-t-season from each timestep. Distribution differences were tested on the 95% significance level. To ensure a high consistency between ERA5 and ESM predictor data, all variables for which significant distributional differences remained for at least one

station across all respective ERA5-ESM pairs were rejected. As a result, RH850, TCC, and UWind500 as well as UWind850 were hereafter neglected.

Indicated by previous research work, persisting pollution levels represent one of the most important drivers of ozone concentrations for specific locations in (Hertig et al., 2019) and across Europe (Otero et al., 2016). Thus, to account for prevailing pollution episodes, six MDA8O3 persistence metrics were added to the initial model input predictor set of each station. Persistence metrics were calculated by averaging the MDA8O3 concentrations of one to up to six preceding days.

Table 2.1 CMIP5 Earth System Models considered in this study

ESM	Institution	Atmospheric Grid Resolution
ACCESS1-0	Commonwealth Scientific and Industrial Research Organization (CSIRO) and Bureau of Meteorology (BOM), Australia	1.25° x 1.88°
CanESM2	Canadian Centre for Climate Modelling and Analysis, Canada	2.79° x 2.80°
CMCC-CMS	Centro Euro-Mediterraneo per I Cambiamenti Climatici, Italy	3.71° x 3.75°
CNRM-CM5	Centre National de Recherches Météorologiques/Centre Européen de Recherche et Formation Avancée en Calcul Scientifique, France	1.40° x 1.41°
IPSL-CM5-MR	Institut Pierre-Simon Laplace, France	1.27° x 2.50°
MIROC-ESM	Japan Agency for Marine-Earth Science and Technology, Atmosphere and Ocean Research Institute (The University of Tokyo), and National Institute for Environmental Studies, Japan	2.79° x 2.81°
MPI-ESM-MR	Max Planck Institute for Meteorology, Germany	1.87° x 1.88°

Methods

Statistical downscaling models

Main drivers of o-t-events from April to September were analyzed by station-based statistical models representing the final results of two multistep modeling approaches. Initially, logistic regression (LR) was used to directly assess the probability of combined o-t-events. For comparison, multiple linear regression (MLR) was applied to assess at first separately the drivers of MDA8O3 concentrations and of TX values (henceforth named "MDA8O3-MLR" and "TX-MLR", respectively). Subsequently, the occurrence of o-t-events was deduced based on a combination of each single modeling result. According to the holistic European focus, a final European-wide predictor set was defined within both modeling processes. This set was then used across all stations to generate final station-based downscaling models. The importance of a predictor at each location is primarily expressed by its respective regression coefficient. Projections of o-t-events until the end of the twenty-first century were generated for each specific station based on these statistical downscaling models. To analyze health-relevant o-t-events under current but also future climatic conditions, the final predictor set should desirable meet the following criteria:

- contain at least one circulation dynamic, thermal, radiation, and humidity-based predictor as well as an ozone persistence metric to cover each climate change-relevant information content

- include only those predictors which carry physically meaningful and substantially relevant information of the predictand

- be based on unique, outstanding predictors, i.e., predictors of almost same information contents are eliminated to avoid overfitting the final station models

Standardized time series of all predictors entered the statistical models. Standardization based on respective means and standard deviations was done to ease interpretability of regression coefficients and thus the identification of main drivers. In order to achieve consistent and comparable results from the downscaling process, identical predictors were used for all predictands and modeling approaches, with the exception that no pollution persistence metrics entered the TX-MLR modeling process. Regression was performed within the free software environment for statistical computing R.

Logistic regression

Logistic regression (Peng et al., 2010, Wilks, 2006) representing a common technique for probability forecasts was used to model the likelihood of o-t-events. For this approach, o-t-events were coded as binary time series with values of 0 (non-event) and 1 (event). LR is based on a logit transformation with the response not having to follow a normal distribution. To analyze the relationship between all predictors and the predictand variable and to identify the main drivers of o-t-events, lasso (lasso, least absolute shrinkage and selection) regression (Hastie et al., 2009, Hastie et al., 2015, Tibshirani, 1996, Tibshirani, 2011) was used and embedded in a tenfold cross-validation process. Lasso regression tries to enhance prediction accuracy by shrinking or setting some coefficients to 0. Thus, lasso performs a variable selection leading to a subset of predictors showing the strongest impact on the predictand, accounting for multicollinearity of predictors. Hence, it is favored to ease interpretability of the statistical models. Within lasso, a tenfold cross-validation was used to determine tuning parameter t. The parameter t controls the amount of shrinkage applied to the estimates. Due to the highly imbalanced data sets, resulting from low numbers of exceedance days with mean and median non-event to event ratios of 5.3 (min 4.5, max 8.0) and 5.2, a stratified resampling method was embedded in the modeling process. Applying the SMOTE algorithm (Chawla et al., 2002) for unbalanced classification problems, an equally distributed dataset was generated (using R's DMwR package). The package glmnet was used for lasso regression. Predictors chosen in at least 90% of all cross-validation training models entered the final predictor set to build a lasso regression model per station based on all observations. As a result of the screening process, an optimized predictor set for every station was extracted. A final, unified European-wide predictor set was created by choosing only predictors selected by more than half of the station-specific LR models. Since predictors which carry the same information, but occur on different pressure levels (e.g., VWind500 and VWind850), entered the model building process, the variable with the higher mean absolute standardized regression coefficient across all models was finally chosen to limit similar information contents. Final station-based LR models were built based on the generated uniform, for whole Europe standardized final predictor set and later used for projections.

Multiple linear regression

MLR is considered as an effective tool to study the impact of predictors on the mean of the response variable. Thus, MDA8O3 concentrations and TX values were predicted separately and the results subsequently combined to assess the occurrence of o-t-events. The performance of this approach to model o-t-events was evaluated and compared to the LR model results. In accordance to the previously described approach, a similar multistep predictor selection process was used and adapted within the MLR model building process. The selection of predictors to create a specific optimum for each station was conducted through a

backward regression procedure starting with models including all potential predictors. Step by step, the least important variables were sequentially removed from the regression equation according to the Akaike Information Criterion (AIC, Akaike, 1974). To account for multicollinearity, variables with a variance inflation factor (VIF) larger than 10 were excluded from the equation (James et al., 2013). The two separate final European-based predictor sets for the MDA8O3-MLR as well as TX-MLR models were created analogously to the LR approach.

Model performance

Typical evaluation metrics as accuracy and error rate are not suitable for highly imbalanced data sets when the primary goal is the identification of rare events (Branco et al., 2016). Performance of the LR statistical downscaling models was thus evaluated using various typical performance metrics for two-class situations and imbalanced datasets. The common and most often applied metrics especially in machine learning with imbalanced data sets are precision, recall and the F1-score (He and Ma, 2013). Recall also named true positive rate (TPR) is used to measure the fraction of actual observed events that are correctly predicted, whereas the true negative rate (TNR) measured the fraction of actual observed non-events that are correctly predicted. Precision is used to measure the fraction of the predicted events that did actually occur. Precision and recall range from 0 to 1 with a perfect score of 1. The F1-score is based on precision and recall and gives equal weight to both measures. Besides these, various other metrics were used for model evaluation and are given in Table S3 in the Supplementary Material (Online Resource 2). For the MLR models, additionally, the coefficient of determination R^2 is used to determine the model performance. The performance evaluation of the final LR and MLR station models was also embedded in a tenfold cross-validation procedure.

Projections

Statistical projections of o-t-events and thus potential frequency shifts of these health-relevant occurrences until the end of the twenty-first century were assessed by comparing time slice differences under RCP4.5 and RCP8.5 scenario conditions. Therefore, 20-year periods in mid-century (2031-2050) and late-century (2081-2100) climate were compared to the base period (1993-2012). Twenty-year periods are suitable time slices because they are expected to be long enough to average out internal variability. Thus, air quality and temperature impacts representing the consequence of changes in forcing can be reliably assessed. Projections were conducted by exchanging the ERA5 predictor data used for modeling building with the corresponding ESM data. As a consequence of the carried out performance evaluation, the LR models were chosen for projections. More details on this will be given later in the "Statistical model performance and predictors" section. As ozone persistence predictor data with a daily resolution is not provided by the chosen ESMs, MDA8O3-MLR models were used to project the ozone pollution concentrations under future climate conditions. As previous day ozone concentrations represent a predictor in the MLR models themselves, a proxy calculated by averaging all daily-based observations across all years in the base period for March 30th was used as a start value. The approach is accompanied by the fundamental assumption that future MDA8O3 concentrations in spring are similar to recently observed values. Several advantages exist by using an observation-forced proxy as start value. The accumulation of possible uncertainties and error sources based on the underlying model equations and simplifications are reduced by integrating an annual constant initial start value. Projecting the remaining MDA8O3 concentration levels in the o-t-season using ESM data also guarantees that the statistical relationships, their linked underlying processes, and causal relations regarding the predictors themselves as well as between predictors and predictand are accounted for. Projections of o-t-events could thus be interpreted against the background of stabilized ozone persistence conditions, with daily and monthly fluctuations presented in future ozone

concentration predictor data. To evaluate the goodness of this approach, statistically modeled ozone values were used. Thus, MLR models based on only original predictor data and models including the start dummy are compared to each other. The results show a strong agreement across all models with a mean and median monthly correlation of 0.83 (min 0.35, max 0.98) and 0.86. Only seven stations (DEBB021, DEBE027, DEBE034, DEBE051, DEMV003, DEMV007, NL00639) showed significant distributional differences between both time series (α = 0.05). Thus, MDA8O3 concentrations were projected by using the proxy as initial yearly start value across all 85 stations and seven ESMs as well as under both, RCP4.5 and RCP8.5, scenario conditions.

Results

Co-occurrence of health-relevant levels

The seasonal median value of TX was 21.07 °C with 25% and 75% of data being below 17.27 °C and 24.88 °C, respectively. All values were calculated as means over all 85 stations by only considering the months in the underlying o-t-season. According seasonal median MDA8O3 concentrations were 82.02 µg/m^3 with 25% and 75% of data being below 65.68 µg/m^3 and 101.34 µg/m^3, respectively. For each station, mean TX and MDA8O3 values from April to September over the years are shown in Table S2 (Online Resource 1). The mean TX and MDA8O3 concentration level over Central Europe in the o-t-season was 20.97 °C and 84.85 µg/m^3, respectively. Considering station characteristics, the upper 25% of MDA8O3 data exceeded on average the WHO AQG across all stations for all but two classes (ri and ut), highlighting the utility of the applied 75th percentile-based and 100 µg/m^3 thresholds to define o-t-events.
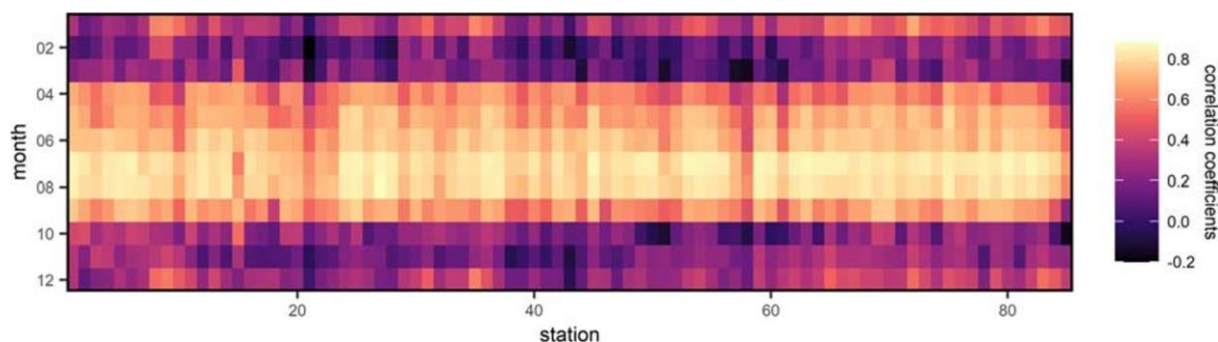
Fig. 2.2 Spearman rank correlation coefficients between observed MDA8O3 concentrations and TX values for each station in Central Europe during the 1993-2012 period
Station numbers depicted on the x-axis are in accordance with Table S2 in the Supplementary Material (Online Resource 1).

The strong observation-based relationship between MDA8O3 concentrations and TX values in the o-t-season is shown in Figure 2.2. Significant (α = 0.05), high monthly correlations from April to September become visible for all 85 stations. A high frequency of co-occurring values of MDA8O3 and TX exceeding the 75th thresholds in the base period became apparent. Elevated TX values were often accompanied by high MDA8O3 pollution levels; on average, 66% of days with elevated thermal load also showed MDA8O3 values surpassing the 75th threshold (min 50, max 74, median 68). Thus, thermal load occurrences were associated with coinciding O$_3$ pollution. Averaged across all 85 stations, on 592 days (min 380, max 671) in the base period (approx. 16% of all days in the o-t-season), combined 75th threshold exceedances of both target variables were observed with a median of 602 days. The spatial distribution over Central Europe, shown in Figure 2.3, revealed a higher absolute and relative amount of these occasions especially in central to northern parts of the study region.
Taking the additional threshold of 100 µg/m^3 used to define combined o-t-events into account, the occurrence of thermal load was connected with co-occurring MDA8O3 exceedances on

average on 75% of days (min 50, max 88, median 75). A total of 670 days (ca. 18% of all days in the o-t-season) with o-t-events (min 381, max 802, median 674) were overserved on average per station. As may be expected in accordance with the "Introduction" section presented analysis (e.g., EEA, 2019) and the described ozone formation in the presence of solar radiation, the spatial distribution (not shown) revealed that especially stations in southern Central Europe show a higher proportion of heat days with MDA8O3 exceedances and a higher frequency of o-t-events. Thus, at these stations, MDA8O3 concentrations exceeded more often the WHO AQG.
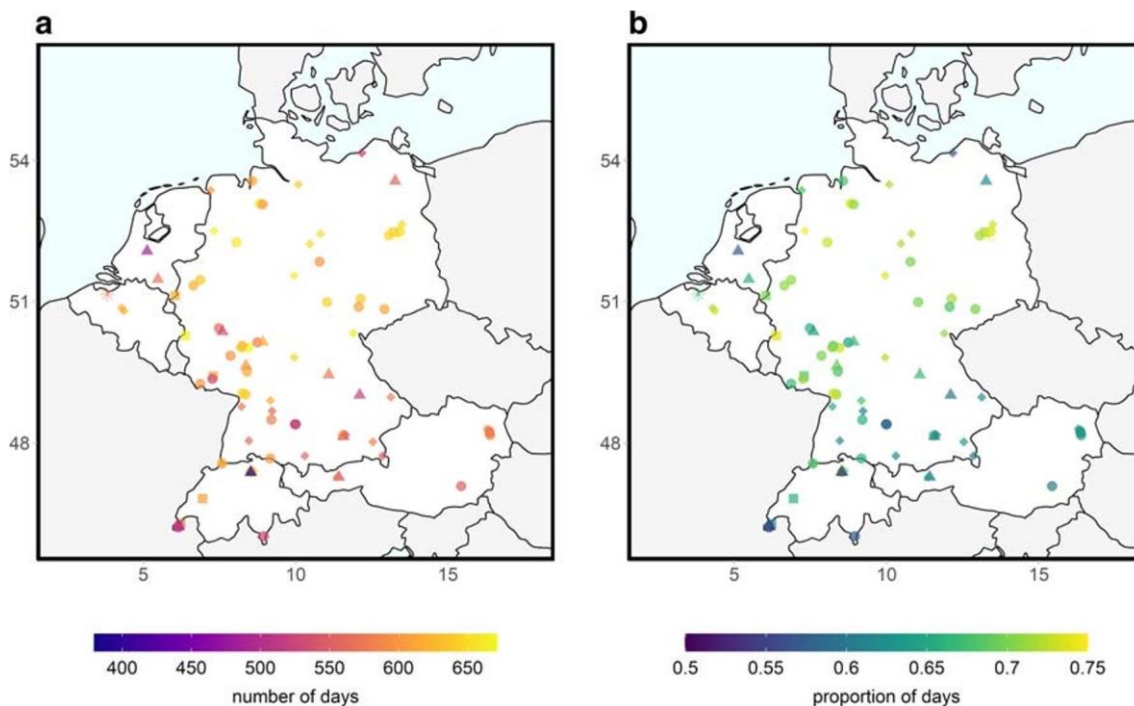
Fig. 2.3 Spatial distribution of the number of days with observed combined exceedances of MDA8O3 and TX values
Results are shown for exceedances over the 75th threshold (a) and the proportion of these event days to the total number of days with thermal load (b)

Statistical model performance and predictors

The final predictor set of the LR models subsequently used for projections contained the following meteorological variables: GH850, MT850, RH500, STRD, and VWind500. Beside these meteorological variables, only ozone pollution levels of the first previous day of all initial chosen persistence metrics were identified as one main driver of o-t-events, henceforth named "LagO3". Thus, the final predictor set contained at least one circulation dynamic, thermal, radiation, and humidity-based predictor as well as an ozone persistence metric, all identified to have a strong effect on the probability of occur-ring o-t-events. Regarding statistical model performance, the mean and median F1-score of the LR model results across all stations was 0.63 (min 0.49, max 0.74). Thus, the models showed in general an acceptable performance to predict o-t-events. The TPR and TNR means and medians amounted to 0.83 (min 0.74, max 0.89) and 0.84 as well as 0.81 (min 0.75, max 0.85), respectively. Hence, a similar, balanced performance of the models was achieved to identify known events and non-events. Additional results concerning LR model performance analysis and evaluation can be found in Table S3 in the Supplementary Material (Online Resource 2). In comparison, the second model approach based on the combination of results of the two separate MLR models showed considerably less performance to model o-t-events. These final predictor sets for the MLR models sets were both composed of RH500, SSRD, and VWind500. For MDA8O3-MLR models, LagO3 was additionally selected within the predictor screening process. The cross-

validated mean and median F1-score amounted to 0.36 (min 0.25, max 0.45) across all stations. As the respective MLR models aimed to assess the mean of the TX and MDA8O3 response, not surprisingly, on average, TNR values with a mean and median of 0.94 (min 0.85, max 0.97) were accompanied by low TPR values with a mean and median of 0.28 (min 0.17, max 0.37) and 0.27. As might be expected, the high TNR in comparison to the low TPR values indicated in general the inability of the models to assess elevated levels of both target variables. Since the LR models clearly outperformed the combined MLR models in capturing o-t-events, only the first model approach was used to analyze and project future frequency shifts in these combined events. As the MDA8O3-MLR models were applied to generate the LagO3 predictor for subsequent statistical projections, their ability to assess the mean of the surface daily maximum ozone response was additionally evaluated. The coefficient of determination R^2 ranged between 0.43 and 0.73 with mean and median values of 0.58 across Central Europe. The spatial distribution of the F1-score for LR models and R^2 for MDA8O3-MLR models is shown in Figure 2.4. Although model performances were satisfactory in general over Central Europe to reliably project future MDA8O3 concentrations and frequency shifts in o- t-events, station-specific findings should always be treated with caution and be evaluated against the background of the respective individual model quality.
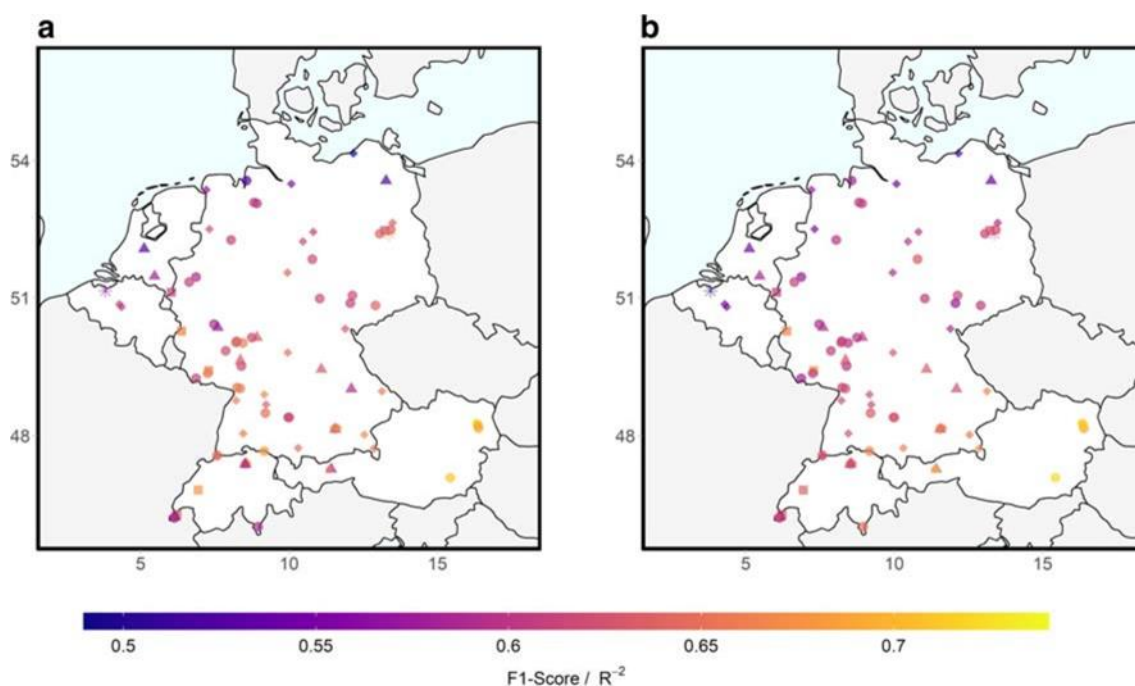
Fig. 2.4 Spatial distribution of the F1-score for LR (a) and of R^2 for MDA8O3-MLR (b)

As MDA8O3-MLR models are used for projecting MDA8O3 concentrations and LR models to assess future frequency shifts in the occurrence of o-t-events, the two model approaches build the focus of the following sections.

Main Drivers

Drivers of MDA8O3

The strength and kind of a relationship between a predictor and a respective target variable can be interpreted in terms of the magnitude and the sign of the predictor's standardized regression coefficient. Consequently, LagO3 was identified as the most important driver (MID) of MDA8O3 concentrations not just on average across Central Europe with a mean standardized coefficient of 17.23 (min 11.93, max 26.66, median 16.95), but also as the most important driver at each single station. The respective mean coefficient for SSRD was 4.37 (min 1.74, max 10.88, median 3.91) representing the second most important driver ("SMID")

across Central Europe. The predictors VWind500 and RH with values of -2.43 [min -8.55, max 1.70, median -2.65) and -1.79 (min -3.16, max 1.09, median -1.92) showed in general a smaller and negative influence. Thus, for example, rising relative humidity levels reduce in general MDA8O3 concentrations. Since tropospheric ozone is formed in the presence of sunlight based on the reaction of precursor gases showing an increased reactivity by rising air temperatures and solar radiation, the statistical model equations capture the underlying physical processes of O_3 formation. As air temperature can mostly be regarded as a proxy for solar radiation in the o-t-season, the identification of SSRD as one of the most important drivers within the study region highlights and confirms previous findings identifying the strong relationship between temperature and ozone (Coates et al., 2016, Jacob and Winner, 2009, Oswald et al., 2015). The overall found impact of VWind500 is in good agreement with earlier studies showing that wind speed and direction influence ozone concentrations (Dueñas et al., 2002, Gardner and Dorling, 2000, Husar and Renard, 1998). Elevated relative humidity values indicate increased instability and cloudiness and thus reduced incoming solar radiation. The negative impact of RH on O_3 concentrations was also specified in previous studies (Camalier et al., 2007, Demuzere et al., 2009, Dueñas et al., 2002). The spatial distribution of the SMID and TMID reflect the importance of different MDA8O3 governing mechanisms. In the western parts of Europe, VWind500 plays a major role, indicating that inflow from remote sources is important for MDA8O3 concentrations, while in the eastern parts of Europe, in situ radiation-related predictors are primarily related with spring and summertime ozone concentrations.

The identification of main drivers in general concurs well with Otero et al. (2016). By examining the influence of synoptic and local meteorological conditions on MDA8O3 concentrations over Europe, the authors found evidence that next to ozone persistence also some meteorological parameters play an important role in explaining most of the observed ozone variance, e.g., maximum temperature, relative humidity, and solar radiation. Figure 2.5 shows the spatial distribution of the identified second and third most important driver ("TMID") of MDA8O3 concentrations in Central Europe.
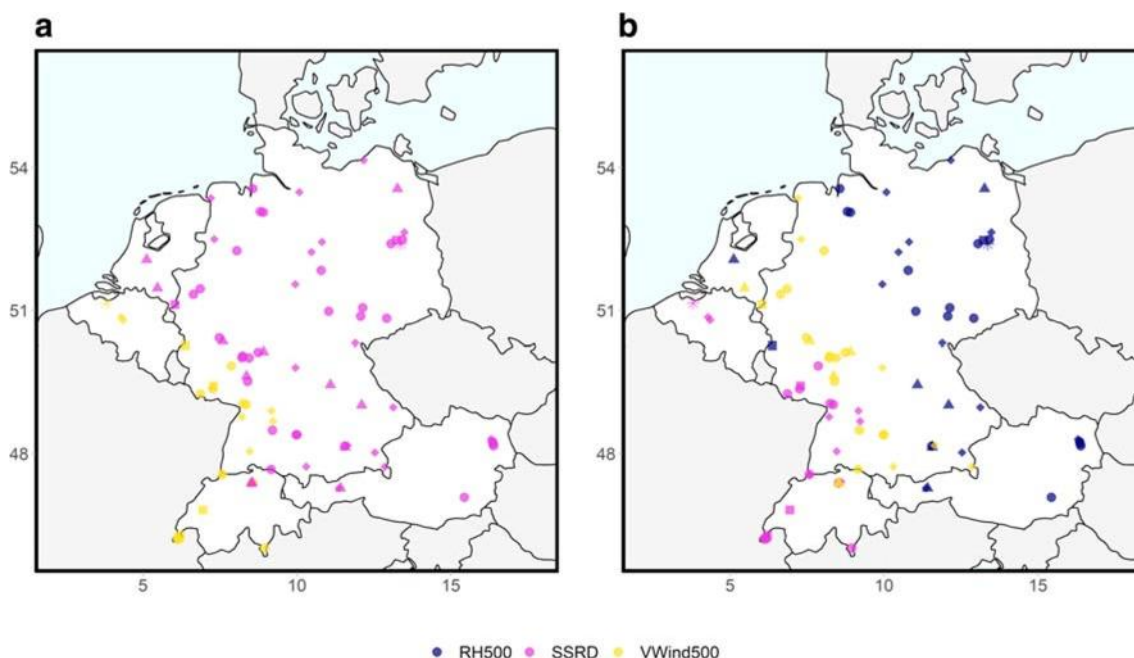
Fig. 2.5 Spatial distribution of the second most important (a) and third most important driver (b) of MDA8O3 in MLR
The shape of the legend symbols has no meaning.

Drivers of combined events

Table 2.2 gives an overview of the averaged standardized regression coefficients over Central Europe for the LR models. The results emphasize the physical validity of the models as MT850

and LagO3 were in general identified as the strongest influencing factors of o-t-events. The spatial distribution of main drivers in Central Europe, grouped by the most (a), second most (b), and third most important drivers (c), is shown in Figure 2.6. The respective odds ratio (OR) is depicted for each driver (d-f) representing the odds that an o-t-event will occur given the presence of the specific main driver, compared to the odds of the event occurring in the absence of that predictor. Thus, OR above 1 indicate higher odds of an o-t-event to appear. Respectively, OR below one lower the odds of an o-t-event.

Table 2.2 Standardized regression coefficients in LR for each predictor variable
Numbers are the mean and median across all stations, minimum and maximum values are shown in brackets.

Predictor	Mean	Median
GH850	0.64 [0.13, 1.15]	0.69
LagO3	1.21 [0.82, 1.68]	1.22
MT850	1.78 [0.12, 4.86]	1.57
RH500	-0.24 [-0.65, 0.15]	-0.24
STRD	-1.30 [-2.91, -0.30]	-1.24
VWind500	-0.34 [-0.98, 0.43]	-0.35

It became apparent that LagO3 was the MID in northwestern Central Europe. Hence, the persistence of ozone pollution, i.e., prevailing high pollution levels due to an incomplete degradation of previous day concentrations of O_3, may play a substantial role in driving MDA8O3 concentrations in these regions. Persistence can cause long-lasting or day-to-day increases of high concentration levels leading to persistently elevated ozone levels on subsequent days. MT850 represented the MID for the majority of stations in southern to eastern Central Europe with some predictors showing occasional elevated to extremely high OR (d). At these stations, it became evident that o-t-events could mainly be explained by mean temperature levels above the boundary layer at the 850 hPa level.

STRD was in general the third most important impactor factor (Table 2.2) in Central Europe, with low radiation values favoring the occurrence of o-t-events. This is also supported by the low OR < 1 (Figure 2.6e and f) shown for stations selecting STRD as the second and third most important driver. STRD is mainly controlled by water vapor and aerosols such as cloud water droplets as well as mainly determined by the shallow layer close to the surface. Hence, it may be a proxy for high specific, thermal radiation-relevant trace element loadings and pollution events as well as moist and humid conditions. Thus, days with lower STRD favored the occurrence of o-t-events. VWind500 is an indicator of airflow conditions, with positive values representing wind from southern directions. GH850 represents a circulation dynamic predictor with low values also being considered as indicator for cold, moist, and humid conditions. VWind500 was only selected twice as TMID and GH850 were occasionally selected as SMID and TMID at stations in the northwestern part of Central Europe with, according to the OR, low wind levels, and high geopotential heights (associated with low humidity values) favoring the occurrence of o-t-events. These findings are not just in good agreement with the results of the MDA8O3-MLR models at these stations, but also confirm the underlying physical processes and key factors known to determine temperature and ozone levels. The relevance of these drivers at the specific stations may also be associated with their location in the westerly wind zone close to the North Atlantic. Transport of moist air masses from the ocean inlands leads generally to increased relative humidity levels, the evolution of clouds, and precipitation in coastal regions. No distinct differences were found regarding station

characteristics, so main drivers of o-t-events are primary related to synoptic influences rather than individual station classes.
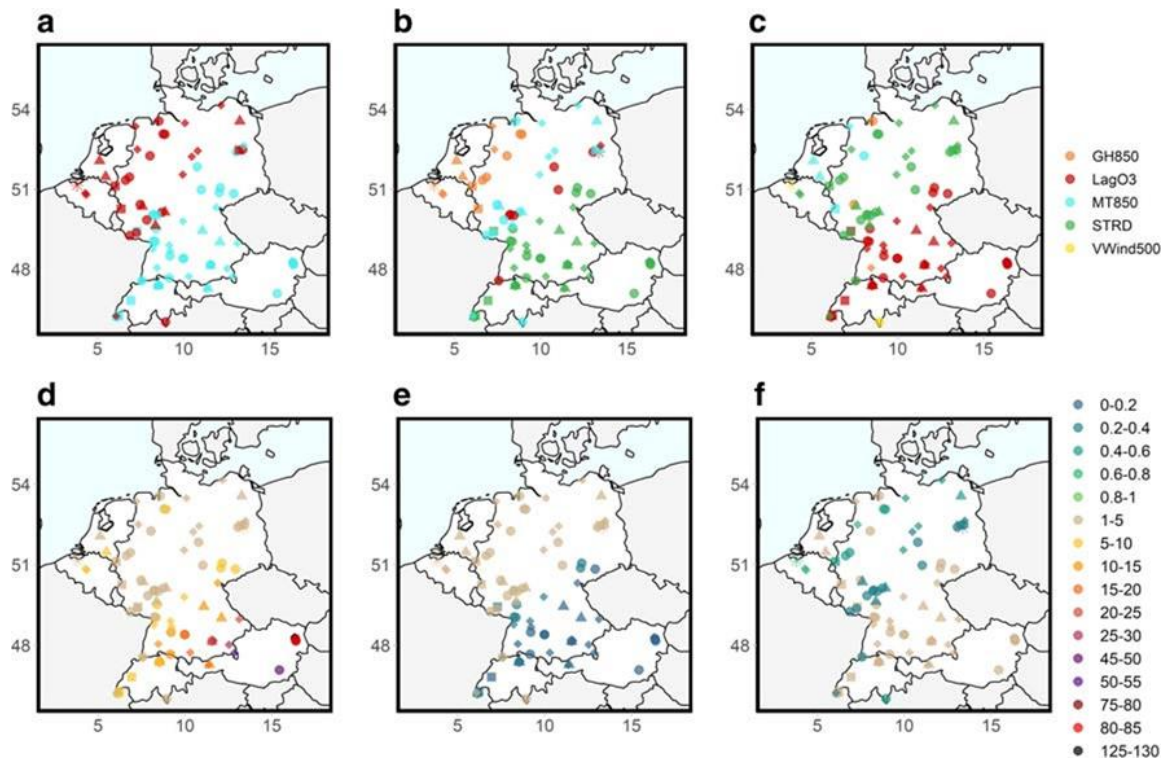
Fig. 2.6 Spatial distribution of the most important (a), second most important (b), and third most important (c) driver of o-t-events in LR. The odds ratio is shown for the respective identified main driver at each station (d-f)
The shape of the legend symbols has no meaning.

Projections for the twenty-first century

Projections of MDA8O3

A comparison of values statistically modeled using historical ESM predictor data with reanalysis-modeled data in the historical period from 1993 to 2005 showed good agreement. Monthly biases were extracted by calculating the monthly mean differences between the statistically modeled values using either historical ESM predictor data or reanalysis-based data. Biases were normalized by the standard deviations of the reanalysis-based data. Throughout this section, numbers in brackets refer to minimum and maximum values grounded on ESM projection results averaged across all stations. Mean and median monthly biases across all ESMs amounted to 0.28 (min -0.60, max 0.66) and 0.24, respectively. Across all seven ESMs, only one station (AT900ZA) showed for two ESMs significant monthly distributional differences between the statistically modeled time series (α = 0.05).
As the downscaling models per se showed a good performance in the historical period over Central Europe, statistical MDA8O3 projections were conducted by exchanging the ERA5 predictor data with corresponding ESM data. MDA8O3 values were modeled for 1993 to 2100 under both scenario conditions. Considering the ensemble mean over Central Europe across all seven ESMs under RCP4.5 scenario assumptions, a mean and median change of -0.19% (min -9.84, max 35.12) and -0.59% for the mid-century as well as -0.10% (min -11.68, max 40.15) and -0.54% for the late-century period were assessed. Thus, on average, no relevant overall change became apparent, under the assumption of stationarity of the start value of MDA8O3 concentrations as well as of governing statistical relationships. Similar results became apparent for RCP8.5 scenario conditions with a mean and median change of 1.09% (min -18.65, max 19.74) and 1.05% for the mid-century as well as -0.32% (min -25.27, max

12.68) and -0.22% for the late-century period. With respect to spatial distributions, no distinct pattern became evident with only one station (CH0011A) showing elevated multi-model mean increases of MDA8O3 concentrations of 24.54% (mid-century) and 27.34% (late-century) under RCP4.5 and multi-model mean decreases of 0.01% (mid-century) and 16.06% (late-century) under RCP8.5 scenario assumptions. Although the projections for this station were comparably strong across all applied ESMs, the very different ensemble-mean percentage changes of this station for almost all time slices were highly determined by the results of one ESM (IPSL-CM5A-MR) with a modeled change of over 185% and 210% (RCP4.5) and over -70% and -80% (RCP8.5), respectively. As the multi-model mean of this station is highly dependent on one model outlier, a note of caution should be sounded with regard to projections for this station. In summary, stabilized MDA8O3 concentrations throughout the twenty-first century were assessed for Central Europe under both scenario conditions and the previously outlined, underlying modeling assumptions showing no relevant spatial differences across the vast majority of stations.

Projections of combined events

Table 2.3 provides an overview of the multi-model time slice differences, statistically downscaled under RCP4.5 and RCP8.5 scenario assumptions. It is evident that projections point to an on average growing number of days with concurrent occurrences of thermal load and ozone pollution in Central Europe. Not surprisingly, considering the identified main drivers in LR and the stronger radiative forcing by greenhouse gases and the related enhanced rise in global mean temperatures, comparably stronger frequency shifts were assessed under RCP8.5 scenario assumptions for mid- and late-century climate conditions. For example, a substantial projected increase of o-t-events in the period 2081-2100 compared to the period 1993-2012 was revealed for both scenarios, but for RCP4.5 with about 17% only being less than half as strong as for RCP8.5 with about 38%.

Table 2.3 Changes [%] regarding the amount of days with o-t-events between the periods 2031-2050 as well as 2081-2100 compared with 1993-2012 under RCP4.5 and RCP8.5 scenarios
Numbers refer to the ensemble mean and median across all seven ESMs. Numbers in brackets give minimum and maximum changes based on single ESM projections averaged across all 85 stations.

Scenario	Period	Mean [%]	Median [%]
RCP4.5	2031-2050	8.94 [-0.39, 22.70]	7.80
	2081-2100	16.84 [-1.23, 39.77]	16.22
RCP8.5	2031-2050	13.33 [0.04, 33.18]	11.37
	2081-2100	37.52 [-1.85, 96.42]	33.92

The shown multi-model results were based on the climate change signal of seven individual ESMs showing for almost all periods the same sign, but a different magnitude of change. The respective projected changes of each single ESM can be found in Table S4 in the Supplementary Material (Online Resource 2).

An overview of the spatial distribution is provided in Figure 2.7 showing the multi-model mean changes for every single station under RCP4.5 (upper) and RCP8.5 (lower) scenario conditions for mid- (left) and late-century (right section of figure) climate. In general, stronger frequency shifts over Central Europe for late-century and under RCP8.5 scenario conditions became apparent. The single most striking observation to emerge from the spatial analysis was the clear identification of hotspot regions across all scenarios and periods. In general, the respective strongest increases in o-t-events were projected for south- to mid-eastern Central

Europe. Under RCP4.5 scenario, assumptions projected changes ranged from -0.39 (BETR740) to 22.70% (DEBY079), with 83 stations for mid-century climate showing an increase of o-t-event days. For comparison, late-century changes ranged from -1.23 (BETR740) to 39.77% (DEBY088) with a growing number of event days projected for 84 stations. Similar results became apparent under RCP8.5 scenario conditions. For the mid-century period, all 85 stations showed an increase in o-t-events. Projected changes reached from 0.04 (DEHB002) up to 33.18% (DEBY079). Until the end of the twenty-first century, a higher frequency of o-t-events was assessed for 84 stations, ranging in general between -1.85 (BETR740) and 96.42% (DEBY063).
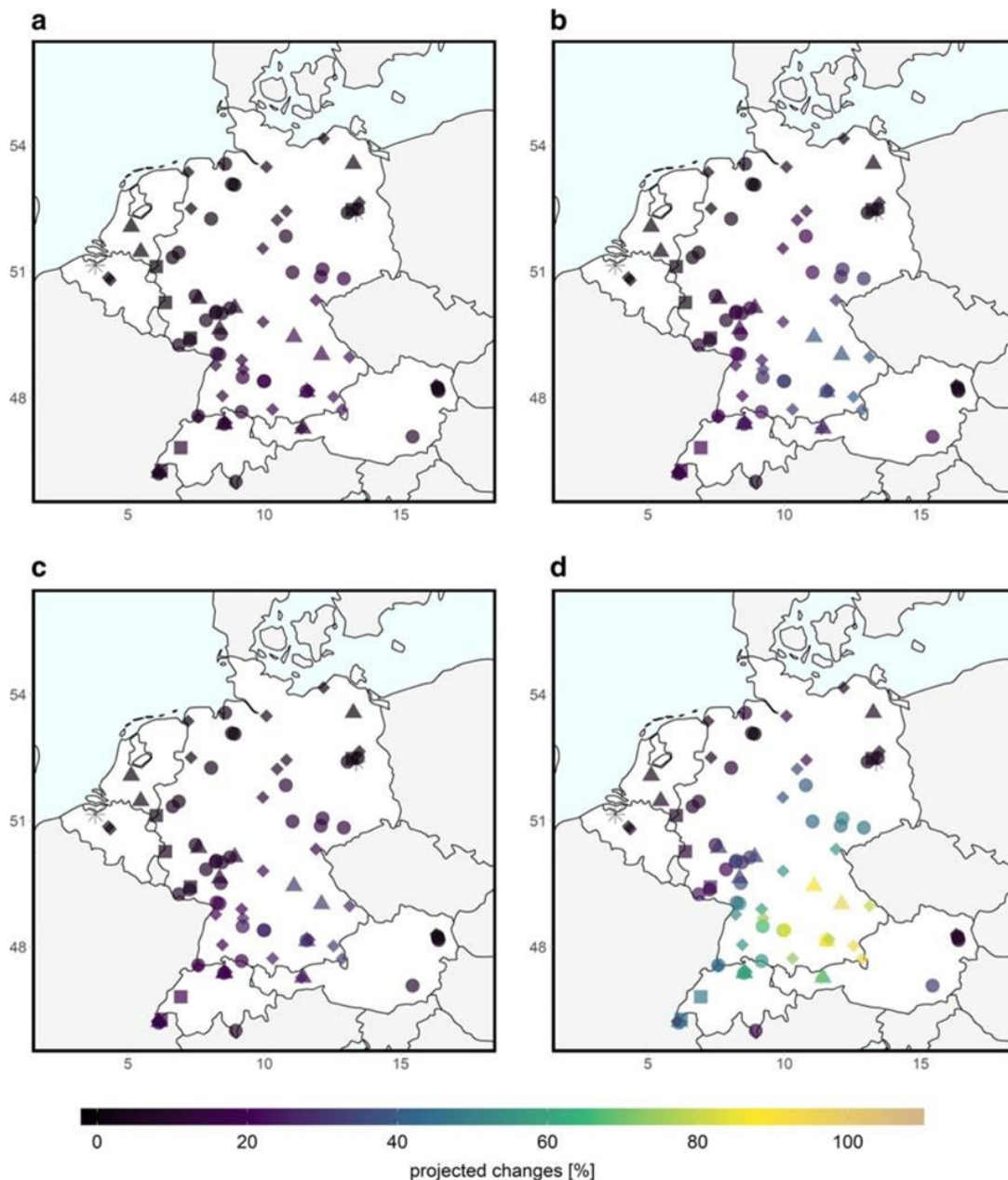
Fig. 2.7 Spatial distribution of projected changes (%) with respect to the number of days with o-t-events between the periods 2031-2050 (left) and 2081-2100 (right) compared with 1993-2012 under RCP4.5 (top) and RCP8.5 (bottom) scenario
Numbers refer to the ensemble mean across all seven ESMs.

The stations showing a late-century increase of at least 60% (16 stations) under RCP8.5 were all located in the German federal states of Bavaria and Baden-Wuerttemberg or close to the southern German border in Austria and Switzerland. As in general south- to central-eastern

parts of the study region could be identified as hotspots of regional change, a low climate change signal became apparent in general at stations in the northern and northwestern part of Central Europe. As shown in Figure 2.6, the most influencing drivers for the vast majority of stations in the identified hotspot regions are MT850, LagO3, and STRD according to the LR models. The MDA8O3-MLR models assessed stabilized MDA8O3 concentrations throughout the twenty-first century (refer to chapters Projections and Projections of MDA8O3 for detail). These values entered later as LagO3 predictor the LR model-based projection process. Consequently, primary projected changes of MT850 and STRD may mainly affect the projected frequency increases of o-t-events under both scenario assumptions, also highlighted by the substantial OR. In agreement with the previous analysis of main drivers of o-t-events, other than regional hotspots, no significant and consistent dependence of the changes from station characteristics became apparent. Additional analysis about monthly mid-century to late-century percentage changes in the future occurrences of o-t-events based on multi-model means under RCP4.5 and RCP8.5 can be found in the Supplementary Material (Figures S1-S4, Online Resource 3). In summary, the downscaling results indicated a considerable increase in the occurrence of combined o-t-events from April to September and hence of thermal and air pollution load in the future. Regional hotspots of rising frequencies of o-t-events became apparent. Projected high frequency shifts became primarily evident in south- to mid-eastern regions of Central Europe.

Discussion

The occurrence of combined ozone-temperature-events for Central Europe based on the selection of 85 stations with different air quality settings in Austria, Germany, Belgium, The Netherlands, and Switzerland was assessed. The primary presumption of a strong positive correlation between surface daily maximum temperature and surface daily maximum ozone concentrations was confirmed for all analyzed stations. Due to the photochemical ozone formation with increased reactivity at higher temperatures and enhanced solar radiation, this relationship was evident primarily within the defined o-t-season from April to September. Burden-inducing, combined were defined by quantile (75th) as well as threshold exceedances (100 µg/m^3). Different modeling approaches were tested to model the occurrence of combined o-t-events. As a result of an extensive model performance evaluation, statistical downscaling models based on logistic regression were the final chosen modeling approach in this context. The models were at first developed to assess the relationship between large-scale predictors, ozone pollution levels, and local-scale events in the observational period. A holistic approach for Central Europe was chosen, accompanied by the greatest possible standardization of the model building process across all stations. Using a screening procedure primary based on lasso regression, a unified predictor set was assessed for all individual LR station models over Central Europe. MT500, STRD, and LagO3 were found to be the main drivers of co-occurring high levels of MDA8O3 concentrations and TX levels.

The LR models were then used for projections under future scenarios. For this purpose, ESM data entered the statistical models and projections of o-t-events under RCP4.5 and RCP8.5 scenario assumptions to account for the ongoing climate change until the end of the twenty-first century. As the seven chosen ESMs of the CMIP5 project did not provide surface daily maximum ozone levels, a MLR modeling approach to generate MDA8O3 projections until the end of the twenty-first century subsequently integrated as LagO3 predictor in the LR models was used. Multi-model mean changes (%) in the occurrence of o-t-events of 8.94% and 16.84% for mid- and late-century climate in comparison to 1993-2012 were found for the RCP4.5 scenario across all stations. Accordingly, changes of 13.33% and 37.52% under RCP8.5 scenario assumptions were generated. Regarding spatial distributions, regional hotspots in south- to central-eastern parts of Central Europe became apparent, but no obvious dependence of the projections on station classes was evident.

Concerning this study, it is plausible that a number of limitations may have influenced the results obtained. All findings need to be interpreted with regard to the chosen holistic focus of the study on Central Europe as the main spatial scale. In order to identify more subtleties and differences within the study area and thus to highlight, e.g., station class-specific differences, a more individual approach would have to be used. An initial focus of the study was to generate a homogenized database based on preselected ozone and temperature station pairs with similar boundary conditions (e.g., altitude levels) showing a strong relationship between ozone and temperature. To incorporate a sufficient number of stations spread across the study region, no further selection process based on the types of air quality settings (e.g., urban traffic stations vs. rural background stations) was incorporated. Consequently, the direct influence of emissions of precursors and hence reactive pollutants affecting ozone production and depletion as well as air pollution transport processes on varying spatial scales were not further considered and incorporated in the analysis. A more detailed and differentiated approach concerning the varying ozone production chemistry and underlying processes should be integrated in further analysis. As the investigations presented here have mainly focused on an European-wide scale, for comparison, a more regional- and station-specific approach should be the target of future work. Thus, along with a more individualized predictor screening process, final station models based on their station-specific predictor optimum could be generated and applied for projections. As a result, frequency shifts of o-t-events until the end of the twenty-first century based on station-specific models and on the here presented unified approach could be compared and relevant differences assessed. Additionally, combined events for both underlying target variables could be more station- or region-specific and might not just integrate worldwide air quality guidelines and percentile thresholds but also use, e.g., individual recommendations of national- or regional-wide institutions. This would also account for current and future demographic and health-relevant developments of the Central European population, as, e.g., aging, and pre-existing conditions lead to a more vulnerable population to thermal load and concurrent air pollution.

A major source of uncertainty is based on the method applied to assess future MDA8O3 concentrations later used for projecting o-t-events. Even though the statistically modeled values were in good agreement with observations and reanalysis-modeled values, the assumed stationarity of the start value of MDA8O3 concentrations as well as the performance of the MLR models themselves influenced and may lead to inaccuracies in the subsequent projections. The performance of the generated MDA8O3-MLR models was in general satisfactory for Central Europe, but slightly disappointing for some individual stations. This is to a large part due to the objective to find holistic downscaling models with a fixed predictor set for all stations, but it has to be especially kept in mind when interpreting station-specific developments and projections. The here presented findings should be read with regard to the chosen framework conditions of the study. The projected MDA8O3 levels should be interpreted to be a result of recent and future mitigation strategies and policies not comprising new or other sources of precursor emissions counteracting or strengthening these measures under future European climate conditions. Hence, the results must be interpreted against the background of these stabilized projected MDA8O3 concentrations entering as LagO3 predictor the LR models to project future o-t-events under both scenario assumptions. Consequently, as comparably stable ozone persistence conditions are assumed, changes of all meteorological predictors - mostly future projected MT850 and STRD conditions showing the highest standardized regression coefficients in the LR models (see Table 2.2) - may strongly affect the general projected increase in future o-t-events across Central Europe.

One negative factor regarding the projections for the twenty-first century is inevitable and is connected to the in general coarse resolution of the seven ESMs being regridded to match the spatial resolution of the ERA5 reanalysis data. Data errors and inaccuracies might have emerged due to interpolation, processing, generalizations, and uncertainties in the CMIP5 climate projections themselves. Associated limitations were accounted for by not just only bias-

correct the data but as well as pre-select predictor data based on significant distributional differences between reanalysis and ESM data. Even if the initial shortcomings and limitations of the ESM data are accounted for in the predictor preparation, modeling, and projection process, the use of ESMs with higher spatial resolution would be beneficial. Thus, future work needs to be undertaken by means of global climate model simulations of subsequent Coupled Model Intercomparison Project phases (i.e., CMIP6). Furthermore, longer MDA8O3 and TX time series with more recent observational data should be integrated in future studies to confirm the modeled relationships and to assess even more reliable statistical downscaling models and projections.

Conclusion

In general, a strong correlation between daily maximum ozone concentrations and temperature values was found from April to September in Central Europe accompanied by a high frequency of concurrent elevated levels of both variables. MLR and LR models describing the relationship between large-scale meteorological predictors, prevailing high pollution levels and local-scale events, performed well enough to become practical tools for predicting daily MDA8O3 concentrations as well as combined ozone-temperature events. Projections of o-t-events assuming stationary of the statistical relationships under historical and scenario conditions until the end of the twenty-first century were evaluated for the 2031-2050 and 2081-2100 time windows. A sharp increase of o-t-events was projected under RCP4.5 and RCP8.5 scenario assumptions. It became evident that south- to central-eastern parts of the study area represented hotspot regions with more frequent occurrences of these combined events in the o-t-season. High levels of ozone and temperature will increasingly coincide in these areas, thus posing an even intensified threat to human life as a result of their associated individual and combined health effects. Special attention should be paid to these vulnerable regions by the formulation and implementation of consensual European climate change mitigation strategies. MT500, LagO3, and STRD can be considered as powerful predictors to assess days with concurrent thermal and air pollution load and should consequently be interpreted as main drivers of o-t-events. GH850, VWind500, and RH500 became also apparent to substantially influence co-occurring elevated levels of surface daily ozone and temperature levels. The results suggest that ozone persistence is particularly relevant for subsequent pollution levels.

Compliance with ethical standards

Conflict of interest The authors declare that they have no conflicts of interest.

Code availability Not applicable

Publisher's note Springer Nature remains neutral with regard to jurisdictional claims in published maps and institutional affiliations.

3. Chapter 3 - Research Article 2

Using Clustering, Statistical Modeling, and Climate Change Projections to Analyze Recent and Future Region-Specific Compound Ozone and Temperature Burden Over Europe

Publication:

This chapter contains one original research article submitted to the transdisciplinary, Gold Open Access journal *GeoHealth* published by Wiley Periodicals LLC on behalf of American Geophysical Union and received in November 2021. The article was accepted in March 2022 and published in Volume 6, issue 4, in April 2022:

JAHN, S.* & HERTIG, E. 2022. Using Clustering, Statistical Modeling, and Climate Change Projections to Analyze Recent and Future Region-Specific Compound Ozone and Temperature Burden Over Europe. *GeoHealth*, 6, e2021GH000561. https://doi.org/10.1029/2021gh000561

*Sally Jahn is first and corresponding author.

The layout, and citation style of the original article, including figure and table designs, numbers, and captions, were adapted and adjusted to be consistent with the rest of the manuscript. No changes in spelling, including e.g., used abbreviations and acronyms, were made and the main text of this chapter is still in this regard as published. The Supplementary Information is available online alongside the original article as well as is additionally added to this dissertation without further adjustments as Appendix E.

Individual author contributions (as in Appendix C):

The study was conceived and designed by Sally Jahn, in discussion with Elke Hertig. Literature review, all data processing and computations including implementation and development of the regionalization approach along with the identification of representative stations were performed by Sally Jahn, with valuable comments and feedback from Elke Hertig. The statistical downscaling model and projection design was developed and conducted by Sally Jahn in agreement with Elke Hertig. Figures were provided by Sally Jahn. Discussion and interpretation of the results were done by Sally Jahn with support from Elke Hertig, who also aided to improve the manuscript initially prepared by Sally Jahn. The authors thank Irena Kaspar-Ott for the final proof-reading of the manuscript.

Using Clustering, Statistical Modeling, and Climate Change Projections to Analyze Recent and Future Region-Specific Compound Ozone and Temperature Burden Over Europe

Sally Jahn[1] and Elke Hertig[2]

[1]Regional Climate Change and Health, Institute of Geography and Faculty of Medicine, University of Augsburg, Augsburg, Germany

[2]Regional Climate Change and Health, Faculty of Medicine, University of Augsburg, Augsburg, Germany

Supporting Information: Supporting Information may be found in the online version of this article.

Correspondence to: S. Jahn, sally.jahn@med.uni-augsburg.de

Abstract

High ground-level ozone concentrations and high air temperatures present two health-relevant natural hazards. The most severe health outcomes are generally associated with concurrent elevated levels of both variables, representing so-called compound ozone and temperature (o-t-) events. These o-t-events, their relationship with identified main meteorological and synoptic drivers, as well as ozone and temperature levels themselves and the linkage between both variables, vary temporally and with the location of sites. Due to the serious health burden and its spatiotemporal variations, the analysis of o-t-events across the European domain represents the focus of the current work. The main objective is to model and project present and future o-t-events, taking region-specific differences into account. Thus, a division of the European domain into six o-t-regions with homogeneous, similar ground-level ozone and temperature characteristics and patterns built the basis of the study. In order to assess region-specific main meteorological and synoptic drivers of o-t-events, statistical downscaling models were developed for selected representative stations per o-t-region. Statistical climate change projections for all central European o-t-regions were generated to assess potential frequency shifts of o-t-events until the end of the 21st century. The output of eight Earth System Models from the sixth phase of the Coupled Model Intercomparison Project considering SSP245 and SSP370 scenario assumptions was applied. By comparing midcentury (2041-2060) and late century (2081-2100) time slice differences with respect to a historical base period (1995-2014), substantial increases of the health-relevant compound o-t-events were projected across all central European regions.

Plain Language Summary

Compound events with concurrent high levels of ozone, being a major pollutant present in the air near Earth's surface, and of air temperature, have strong negative impacts on the health of humans. In this study, these compound events were investigated under present and future European climate. Six regions of similar ozone and temperature characteristics and patterns were defined. For each region, representative stations being typical examples for the overall region were extracted. Models for these stations were developed and their results analyzed to define factors that highly influence the occurrence of compound ozone and temperature events in each region, for example, mean air temperature or humidity levels. The generated models were later applied to project future frequency shifts of these compound events under climate change in central Europe. As a major result of the study, the future health-relevant compound

ozone and temperature events were projected to occur more frequently in the middle as well as at the end of the 21st century across all central European regions.

Key Points

- A clustering approach based on ground-level ozone and air temperature leads to a division of Europe into six ozone and temperature regions

- Statistical downscaling models identify region-specific main meteorological and synoptic drivers of compound ozone and temperature events

- Climate change projections point to an increase in these compound events until the end of the 21st century in central Europe

1. Introduction

Simultaneous occurrences of elevated levels of tropospheric, ground-level ozone (O_3) concentrations, and surface air temperatures can be defined as so-called compound events (Zscheischler et al., 2020). O_3 and air temperatures are often strongly correlated and elevated levels repeatedly coincide. Their relationship and joint occurrences have already presented the focus of a variety of recent health-related environmental studies (e.g., Abdullah et al., 2017, Hertig, 2020, Schnell and Prather, 2017). There is evidence that the co-occurrence of both variables results in a human health risk beyond the sum of their individual effects (Hertig et al., 2020, Katsouyanni and Analitis, 2009, Pattenden et al., 2010).

The variations, linkage, and co-occurrences of O_3 and air temperatures are based on the specific nonlinear, temperature-dependent and sunlight-driven chemistry of ozone formation determined by the overall ambient, photochemical conditions and precursor emissions (Pusede et al., 2015). O_3 is influenced by a large variety of often also temperature-dependent and partly interacting, chemical-based factors (e.g., composition of VOCs or the cycle and supply of odd hydrogen radicals). O_3 is also strongly dependent on meteorological variables and synoptic conditions (please refer to Sillman, 2003, Sillman, 1999 for more background information on ozone formation). Porter and Heald (2019) analyzed the summertime ozone-temperature (o-t-) relationship in the United States and Europe. They found that a high portion of the o-t-correlation can be attributed to four temperature-dependent, chemistry-based mechanisms (i.e., soil NO_x and biogenic VOC emissions, PAN dissociation and O_3 dry decomposition). But, especially in Europe, the correlation is linked to meteorological phenomena. Consequently, ozone and air temperature levels, their linkage, and respective compound events can be expected to differ regionally across Europe.

Recent work confirms that the linkage between ozone and temperature must be evaluated over a broad range of temperatures. Especially, ozone levels in polluted regions show strong dependences on temperature. Elevated levels are generally associated with air temperatures surpassing 20°C (Sillman, 2003). Steiner et al. (2010) analyzed the o-t-relationship in four air basins in California. They found an approximately linear increase in maximum ground-level ozone concentrations between 295 and 312 K (about 22-37°C), but they also provided evidence that ozone may plateau or decrease under extremely high temperatures (>37°C). This is due to a decrease in PAN and a reduction of isoprene emissions at these high-temperature levels. Varotsos et al. (2019) confirmed by their analysis of two major European heatwave episodes (2003 and 2014) that higher O_3 concentrations are in general accompanied by higher air temperatures. However, a break of the o-t-relationship in the higher percentiles of both variables was present during the 2003 heatwave. This was mainly due to reduced biogenic emissions under very high temperatures in southern parts of their European study domain. The linkage between both variables under current and future emission and climatic conditions has been the focus of further studies (e.g., Bloomer et al., 2009, Coates et al., 2016, Colette et al., 2015, Rasmussen et al., 2013). In previous work from Jahn and Hertig (2021),

co-occurring elevated O_3 and air temperature levels in Europe were considered. A strong o-t-correlation accompanied by a high frequency of concurrent high levels of both variables becomes evident in central Europe (i.e., Austria, Belgium, Germany, The Netherlands, and Switzerland). However, a strong o-t-relationship is not observable in more northern- and southern-located stations (i.e., in Great Britain, Greece, Finland, and Sweden). These findings also suggest that the o-t-linkage regionally varies across Europe.

Considering the meteorological and synoptic conditions influencing compound o-t-events, various previous studies exist focusing on the identification of respective mechanisms affecting ozone alone or in combination with air temperature levels (e.g., Hertig, 2020, Jahn and Hertig, 2021, Kerr et al., 2019). Regional variations have already become evident. For example, Otero et al. (2016) found that over central Europe meteorological variables play an important role as drivers of maximum daily ozone and its extreme values. However, in northern and southern parts of the study domain, the influence of ozone persistence and hence precursor emissions is comparably strong on ozone exceedances. These results suggest a stronger role of preceding ozone conditions compared to meteorological variables in northern and southern Europe. Hertig et al. (2020) analyzed single and concurrent heat and ozone waves in two climatically different regions, Portugal and Bavaria. They found that for Portugal, representative for southern Europe, synoptic circulation weather types (WT), promoting the inflow of hot and dry air masses, and the advection of ozone and its precursors from remote areas highly influence observed O_3 levels.

One way of addressing regional differences consists of dividing the European domain into regions of coherent spatiotemporal o-t-characteristics and patterns, which may be affected by different main drivers under climatic and environmental changes. Regionalizations, comprising the classification of sites and resulting in the spatial division into zones or regions, have been generated in previous studies based on ozone (Boleti et al., 2020, Carro-Calvo et al., 2017, Lehman et al., 2004, Lyapina et al., 2016, Varotsos et al., 2013) or temperature (Bador et al., 2015, Chidean et al., 2015, Scotto et al., 2011). However, to the best of our knowledge, a spatial clustering based on both target variables over Europe in order to account for recent and future spatiotemporal variations has not been conducted so far.

The present study fills this gap by presenting a regionalization approach based on O_3 and air temperatures to account for spatiotemporally varying environmental and climatic conditions across Europe. Additionally, regionally different recent and future health burden over Europe is highlighted. The definition of robust, geographically, and environmentally meaningful European o-t-regions using a clustering approach constitutes a novelty and builds the basis of the presented work. Based on the identified o-t-regions, statistical downscaling models of health-relevant compound o-t-events were generated. Only distinct meteorological variables and synoptic conditions that carry physically meaningful and relevant information were considered. WT to analyze synoptic conditions has been applied in various recent air quality studies already (e.g., Otero et al., 2016, Russo et al., 2015). In this study, Self-Organizing Maps (SOM), an artificial neural network algorithm based on unsupervised learning, was used. SOM has been applied within a climatic or synoptic context in several existing studies (e.g., Gibson et al., 2017, Odoulami et al., 2020, Sheridan and Lee, 2011, Tian et al., 2014, Vesanto and Alhoniemi, 2000). Region-specific projections based on statistical downscaling models using the climate change scenario assumptions SSP245 and SSP370 until the end of the 21st century based on the updated Coupled Model Intercomparison Project Phase 6 (CMIP6) were generated.

The main contributions of the presented work are hence the following: first, the identification of six European o-t-regions highlighting the regional phenomena of o-t-characteristics, patterns, and variabilities. Second, the specification and comparison of region-specific variations of o-t-relationships. Third, statistical models and downscaling climate change projections of compound o-t-events, including the evaluation of the suitability of the applied study framework for all central European o-t-regions.

The remainder of this paper is structured as follows. Section 2 presents the initial selection and preprocessing of station-based ozone and temperature data and the application of the regionalization process. Section 3 introduces the preparation of predictands as well as the selection and prepossessing of predictor data. All applied statistical models and projection approaches are presented in Section 4. Section 5 summarizes the main contributions with discussion and limitations presented in Sections 6 and 7. Section 8 contains concluding remarks. In the Table S1 in Supporting Information S1, an overview of all abbreviations and acronyms used in this paper is provided.

2. Station-Based Data and Regionalization

2.1. Data and Station Selection

This section describes the collection, preprocessing, and selection of European stations, providing measurement data on surface maximum daily ozone and air temperature. Ozone and temperature stations were paired based on the location of sites and on the extracted and processed observation data. Station pairs represented the final locations of combined ozone and temperature observations.

2.1.1. Data Sources

The processing and preselection of daily maximum surface air temperature (TX) and O_3 data were conducted to generate a homogenized database with consistently submitted and prepared air quality and temperature monitoring data. Station-based, valid TX data based on the available adjusted, homogenized blended temperature series of the European Climate Assessment and Data set project (ECA&D) (Klein Tank et al., 2002) were obtained. Air Quality eReporting ozone pollution data from the European Environment Agency with an originally reported hourly time resolution were extracted (EEA, 2017). Daily 8-hr running means and subsequently daily maximum 8-hr running means (MDA8O3) were calculated by only considering valid labeled hourly measurements. Valid MDA8O3 data finally used for further analysis were only calculated if at least 18 valid 8-hr running means were available for a particular day. In order to achieve a suitable and sufficient coverage with ozone stations across the whole European domain, the years from 2004 to 2018 built the temporal focus. This specific period of time is hereinafter referred to as base period. To reduce the direct influence of emissions of precursors and hence reactive pollutants affecting ozone formation and depletion processes, only urban, suburban, and rural background stations (hereinafter referred to as station types) were incorporated in the analysis. In general, only ozone and temperature stations providing data for each year in the base period were selected. If not otherwise specified, temperature or TX as well as ozone or MDA8O3 refer to the finally approved station-based daily maximum air temperature and ozone values. All further analyses were based on the o-t-season from April to September.

2.1.2. Station Pairs

Station pairs, combining temperature and ozone measurements, were built assigning a temperature station with a maximum distance of 15 km and a maximum altitude difference of 200 m to each ozone station. In order to minimize the influence of missing values, station pairs with daily data for both ozone and temperature with a data coverage of more than 75% in the o-t-season from 2004 to 2018 were selected. If another ozone station matched with the same temperature station, only the station pair with an overall higher data coverage was kept for further analysis to avoid the occurrence of the same temperature data series for different ozone locations. As a result, 161 station pairs represent the final database. The mean distance between all paired stations is 5.39 km (min 0.09 km, max 14.99 km, and median 4.45 km) and the mean altitude difference is 28.47 m (min 0 m, max 189 m, and median 13 m). An overview of all chosen station pairs with more detailed station metadata and characteristics is available

in the Table S2 in Supporting Information S1. Hereinafter, the linked station pairs are simplified referred to as station. All spatial station information is represented by the respective station pair's ozone site. Station altitudes in the final database vary between min -1.0 m and max 3,106.0 m (mean 219.93 m and median 111.0 m).

2.2. Regionalization

The overall goal of the regionalization is a spatial division of the study domain into distinct o-t-regions. A common hierarchical clustering technique based on MDA8O3 and TX conditions in Europe is applied to produce stable clusters, that is, the final o-t-regions.

2.2.1. Ozone and Temperature Regions

Regionalization aims to generate homogenous regions, showing the highest dissimilarities between each other. An agglomerative hierarchical clustering approach, which is an unsupervised learning algorithm, was applied to primarily account for region-specific temporal variabilities like day-to-day variations in ozone and air temperatures. The algorithm builds nested clusters by merging them successively based on the computation of distances. The Ward variance minimization algorithm (hereinafter referred to as Ward's method) was selected out of a large variety of possible linkage methods. Ward's method not only relies on a simple (Euclidean) distance calculation, but also accounts for cluster variances by minimizing the total within-cluster and maximizing the between-cluster variance. The separability of clusters can finally be clearly measured by Ward's distance (e.g., Backhaus et al., 2016, Wilks, 2006). In future work, new instances can be easily assigned to a generated cluster by simply calculating and minimizing Ward's distance. This represents a significant advantage if, for example, the database is expanded by additional stations within the given European domain. Ward's method also shows the most promising results regarding the generation of geographically and environmentally meaningful regions with distinct o-t-characteristics and patterns (please refer to Section 5 for details).

The selection of the optimum number of clusters is generally challenging and several metrics can be applied. In this study, the overall goal is to find distinct o-t-regions, which yield a balance between a sufficient number of regions to explain spatiotemporal variability while still providing a reasonable degree of generalization. A minimum of at least four distinct o-t-regions to account for general geographical differences was thus chosen. In this context, besides a manual evaluation, the within-cluster similarity and thus distances and height calculations based on Ward's method were considered. Primarily, the dendrogram as well as the elbow method were used to define the optimum number of clusters.

Station-based MDA8O3 and TX data were separately preprocessed by filling missing values with daily means in order to perform the cluster procedure. Considering joint TX and MDA8O3 time series data for clustering, the station-based data were at first standardized by removing the mean to center the data and by scaling it to unit variance. Standardization in this study was always conducted following this procedure.

2.2.2. Representative Stations

Representative stations were defined for each region to build statistical downscaling models valid for the whole o-t-region. The stations were selected based on the Euclidean distance of a station to its respective cluster centroid. While the regionalization mainly aims to group similar daily variability, absolute station-based values may highly differ within an o-t-region. This may be particularly true between different site-specific station characteristics. If available, one urban, suburban, and rural representative stations per region were hence selected. Thus, MDA8O3- and TX-level differences per station type in an o-t-region and so intraregional differences were accounted for by selecting more than one representative station per region. Even if all stations of a region vary similarly and variances of each cluster were minimized by

the chosen clustering procedure, type-specific ozone, and temperature-level variations were hence be represented in subsequent modeling and projection processes. The hypothesis that compound o-t-events in each region depend on the same main drivers could thus be tested and possible different future sensitivities under future climate change were accounted for.

3. Predictor and Predictand Data

3.1. Compound Events

Health-relevant, concurrent high levels of MDA8O3 and TX were used to define o-t-events regarding each specific representative station. For MDA8O3, pollution levels surpassing a threshold of 100 µg/m³ determined an ozone event. The threshold is in accordance with recommended standards of the World Health Organization (WHO, 2006, WHO, 2021). A local and station-specific percentile-based approach was chosen for TX to define non-optimum ambient temperatures per site. Based on a 31-day window, the 80th percentiles (similar to e.g., Della-Marta et al., 2007) were calculated for each individual day based on the respective daily TX values across all years in the base period (hereinafter referred to as ^{80}TX). This uniform 80th percentile value for all regions and stations eases the comparability and interpretation of o-t-events across the whole study domain. Additionally, the station-based approach regards the fact that individuals generally adapt to their local weather conditions. So, spatial but also seasonal acclimatization processes as well as, to some extent, location-based (population) characteristics are taken into account. If an o-t-event was observed, temperature levels as well as ozone concentrations are needed to exceed these predefined thresholds on the same day. Compound events were in general coded as 1 (event) and 0 (nonevent) in statistical models and climate change projections.

3.2. ERA5 Reanalysis Data

The selection of suitable variables to predict compound o-t-events was primarily determined by an analysis and a literature review (e.g., Hertig et al., 2019, Jahn and Hertig, 2021, Otero et al., 2016), data availability in the chosen ERA5 reanalysis, as well as Earth System Models (ESM). Predictor metrics used in this study are hence split into two types, meteorological predictors and synoptic WT. Even if nonphysical predictors may provide an additive value for predictions, further metrics like persistence of ozone or the inclusion of harmonic functions to assess regional variations of the seasonal cycle were not included in the statistical models as they do not represent direct physical drivers of ozone and temperature.

3.2.1. Meteorological Predictors

Meteorological predictors were selected to include one circulation dynamic, humidity, thermal, and radiation-based predictor to cover each climate change-relevant information. Simultaneously, overfitting in the modeling process by not including several predictors of almost the same information was avoided. The following meteorological variables provided by the ERA5 reanalysis data set from the European Centre for Medium-Range Weather Forecasts (Hersbach and Dee, 2016) were retrieved (units in square brackets): geopotential heights (GH) (m), specific humidity (SH) (kg/kg), and mean air temperatures (MT) (°C). The predictors were all downloaded at the 850 hPa level for the whole European domain (25°N-70°N, 40°E-25°W) with a 1 × 1° resolution. Hence, predictor data approximately directly above the boundary layer not being strongly influenced by varying orographic and topographic conditions were selected. Furthermore, surface solar radiation downward (SSRD) was extracted (W/m^2). For the purpose of including for each specific location the best-fitting predictor data, the mean of the nine grid boxes covering the area over and around each representative site was used to define station-based daily predictor time series. The daily meteorological predictor time series were all standardized before entering the statistical modeling process.

The agreement of predictors across all stations of one o-t-region was evaluated by manual inspection and correlation analysis. Similar monthly meteorological conditions with comparable variations were observable within a region in the o-t-seasons from 2004 to 2018. Spearman rank correlation coefficients of at least 0.5, by considering daily pairwise station-based predictor time series within a region, were computed. In summary, the presented meteorological information of each representative station fits quite well its overall region conditions. The same predictors show similar characteristics and variations and are highly correlated across all stations of an o-t-region.

3.2.2. Synoptic Weather Types

Daily ERA5 mean sea level pressure (MSLP) was used to classify synoptic WT, representing the second group of predictors. The data were extracted with the same spatial resolution and coverage as the meteorological predictors. SOM was applied on the preprocessed European MSLP data. WT patterns commonly show the MSLP-"weight" of each node of the generated SOM grid.

In general, a SOM grid needs to be defined by size and hence number of nodes. A balance must be found between a too high complexity of the model and choosing enough nodes to represent all needed information. With a too small grid size, the output patterns are too general and important differences are missed. If the grid size is too large, the differences between neurons are too detailed. In projection studies, a not too high number of nodes with a more even distribution across all WT are favorable to avoid a significant number of "empty" nodes when applying ESM data.

In this study, the classification comprises all months in the o-t-season from 2004 to 2018. The WT are based on a rectangular SOM grid. Several grid sizes were tested within the classification from a minimum of four to a maximum of 20 WT. The topographic product as a measure for the degree of topology preservation was used to define an appropriate grid size. This metric can be combined with a detailed, far-reaching hyperparameter tuning. Hyperparameter tuning was conducted by adjusting the parameters sigma, learning rate, and iterations of the SOM algorithm.

New samples are in general classified by evaluating the Euclidean distance between the sample and the weights of all nodes. Accordingly, WT were assigned to each day in the o-t-season from 2004 to 2018 by evaluating the Euclidean distance between each daily MSLP field and the weights of all nodes. A respective synoptic WT predictor time series based on numerical codes was hence created, later used for model building.

3.3. Earth System Model Data

For climate change projections, predictor data were extracted for the European study domain using output from eight CMIP6-ESM (Eyring et al., 2016): BCC-CSM2-MR, CanESM5, FGOALS-g3, INM-CM5-0, IPSL-CM6A-LR, MIROC6, MPI-ESM1-2-HR, and MRI-ESM2-0. Historical ESM runs from 1995 to 2014 as well as SSP245 and SSP370 scenario runs from 2015 to 2100 (e.g., Gidden et al., 2019, O'Neill et al., 2016, Turnock et al., 2020) were downloaded under r1i1p1f1 initial conditions in a daily temporal resolution. The spatial resolution of the ESM data varies from 0.9° (MPI-ESM1-2-HR) to more than 2.5° (CanESM5). Consequently, model data were regridded by bilinear interpolation to match the ERA5 resolution. Station-specific meteorological time series were generated in accordance with the reanalysis predictor data by considering nine grid-cell means. A specific WT was assigned to each day in the historical ESM as well as for both scenarios in accordance with the approach used in reanalysis. Thus, for each chosen ESM, daily WT time series consisting of numerical codes were generated by the evaluation of Euclidean distances.

A simple linear scaling bias correction technique, also used by for example, Gohar et al. (2017) and Teutschbein and Seibert (2012), was chosen and adapted to remove the monthly mean bias between climate model data and reanalysis. The monthly mean difference between

station-based meteorological reanalysis and historical ESM data was used to bias-correct the respective ESM data. Based on the two-sample Kolmogorov-Smirnov test, the distributional similarity between meteorological ERA5 and monthly bias-corrected ESM data was considered. The evaluation was conducted for each predictor variable across all representative stations and ESM. ESM and ERA5 predictor data show in general a high consistency across all ESM and variables with significant distributional differences only present for 12 ERA5-ESM pairs (please refer to Table S3 in Supporting Information S1 for details). Thus, the ESM meteorological predictors are suitable to exchange the ERA5 predictor data to generate projections. For MSLP data, the bias correction was first conducted based on every grid cell in the European domain before the respective WT time series was generated. An overview and comparison of the occurrences of WT considering all eight ESM as well as ERA5 reanalysis data is given in Table S4 in Supporting Information S1.

ESM data were standardized before entering projections. Hereby, historical and one scenario, SSP245 or SSP370, time series were first merged and subsequently standardized with respect to their means and standard deviations. Consequently, variability and mean changes per scenario assumption could be evaluated.

4. Statistical Models and Climate Change Projections

4.1. Statistical Downscaling Models

Statistical models to establish the relationships between meteorological and synoptic conditions and o-t-events were generated. All representative stations of each individual o-t-region were considered. A station-based approach with an individualized predictor screening process was chosen to assess suitable station-specific predictors. Thus, the identification of specifics and differences within as well as between o-t-regions was simplified. Logistic regression (LR) was used to assess the likelihood of o-t-events. Site-specific main drivers were identified. Statistical downscaling models were evaluated by considering model fit and performance.

4.1.1. Logistic Regression

A specific type of generalized linear models, LR, was used to assess the probability of threshold exceedances, hence o-t-events. By applying LR, a sufficient number of events with respect to the number of selected predictors is generally needed. Even if, as rule of thumb, a common ratio of 10-20 events per variable is often used, existing studies suggest and apply a smaller ratio of 5-10 (Otero et al., 2016, Peduzzi et al., 1996). For modeling, strong imbalanced data sets with an unequal distribution of majority and minority classes (here o-t-events) are unfavorable. In this study, the minority class represents under 20% of all data points across all representative stations. Thus, data were resampled using the SMOTE (Synthetic Minority Oversampling Technique) algorithm. SMOTE creates synthetic samples from the minority class to get equally distributed data sets. At first, a station model was built on all available predictor data. The significance of a predictor was tested on the 95% significance level by applying Wald's Test. If the p-value of a predictor exceeded 0.05, the predictor was excluded, and the station model was generated again based on the new subset of predictors. The process was repeated until only significant predictors entered the final station model.

A special focus in the presented work is set on the identification of the most important (MID), second (SMID) and third most important drivers (TMID) of o-t-events. In the statistical models, a predictor variable's effect on prediction can be expressed by its regression coefficient in terms of the log-odds. If a predictor variable's effect on prediction is significantly different from zero, it contributes to the prediction of o-t-events. Leading drivers of o-t-events are identified by the strength of the relationship between each predictor and the target variable, given by the absolute value and the sign of its standardized regression coefficient. Predictor variables can hence be ranked by importance to identify station-based main drivers.

4.1.2. Model Fit and Performance

McFadden's Pseudo-R^2 (MF-R^2) based on the maximum likelihood concept is a common metric applied to assess model fit considering LR. By comparing two models, the one with higher MF-R^2 values represents generally a better-fitted model. Common performance metrics with respect to imbalanced data sets in machine learning are Precision (P), Recall (R), and the F1-Score (He and Ma, 2013), all applied for model evaluation. All metrics indicate performance by values between zero and one with higher values showing a better model performance. The performance evaluation of the final station-based LR models was embedded in a tenfold cross-validation procedure. In general, a modeled probability value of 0.5 is often used to differ between event and nonevent days. To ensure a more balanced relationship between the fraction of actual observed events that were correctly predicted (P) and the fraction of the predicted events that did actually occur (R), a suitable probability threshold value was evaluated within an own, upstream tenfold cross-validation procedure. The threshold for which P and R were closest to each other was selected. This model-specific threshold was used in performance evaluation as well as for projections.

4.2. Climate Change Projections

Statistical climate change projections of compound o-t-events under future scenario assumptions were generated by replacing reanalysis with corresponding, preprocessed ESM predictor data in the final station-specific statistical downscaling models. Only representative stations in regions having shown their suitability to project o-t-events under future scenario assumptions were incorporated. Thus, all regions with stations not showing a substantial, positive linkage between MDA8O3 and TX levels as well as a strong relationship of o-t-events and selected predictors were excluded from further analysis. Projected changes (%) and thus potential frequency shifts of o-t-event occurrences until the end of the 21st century were assessed by comparing time slice differences with respect to the number of o-t-event days. Potential frequency shifts were evaluated by comparing midcentury (2041-2060) and late century (2081-2100) time windows to a historical ESM period (1995-2014). Multi-model (ensemble) means based on the climate change signal from eight CMIP6-ESM were considered.

5.   Results

5.1.   Present-Day Ozone and Temperature

The regionalization led to a division of the study domain in six o-t-regions. Representative stations were selected for each region. Region- and site-specific characteristics as well as relationships between MDA8O3 and TX were analyzed. An in-depth evaluation and interpretation of respective results are presented subsequently in Section 6.

5.1.1. Ozone and Temperature Regions

The regionalization resulted in the following northern, southern, and four central European o-t-regions: 1-CE (**C**entral **E**astern), 2-CN (**C**entral **N**orthern), 3-CW (**C**entral **W**estern), 4-HA (Central **H**igh **A**ltitude), 5-NE (**N**orthern **E**uropean), and 6-SE (**S**outhern **E**uropean o-t-region). The location of all stations used in the cluster analysis and their assignments to each o-t-region are highlighted in Figure 3.1. In addition, Table 3.1 gives an overview of region-specific ozone and temperature characteristics. Not taking 4-HA into account, Table 3.1 reveals that the highest and lowest mean MDA803 and TX values are observable in 5-NE and 6-SE, located at the northern and southern rims of the study domain. The lowest, medium, and highest daily TX levels are generally accompanied by the lowest, medium, and highest daily MDA8O3 concentrations, not considering 4-HA.
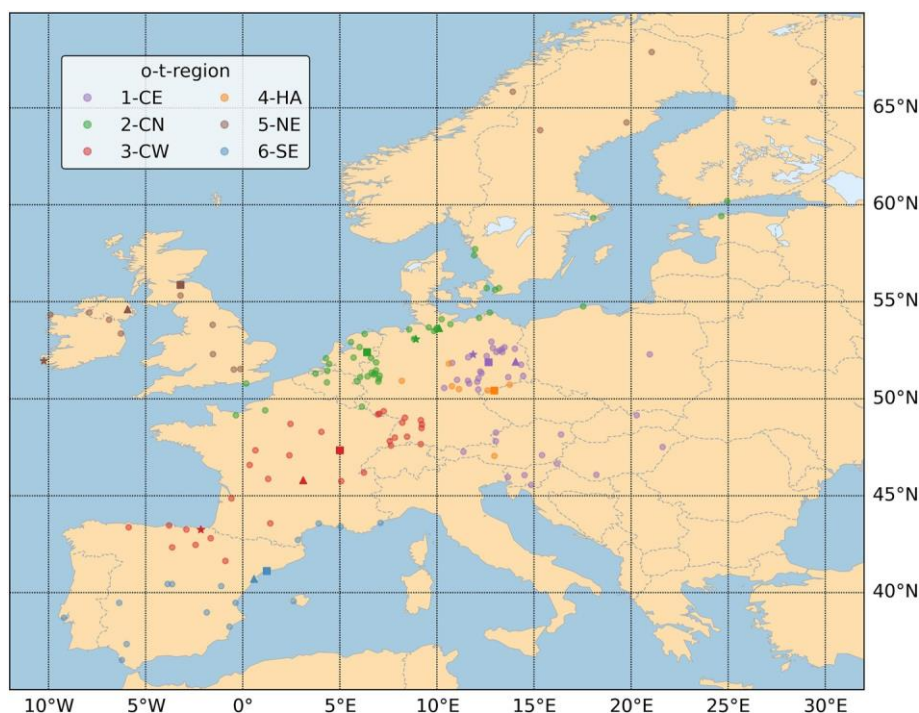
Fig. 3.1 Location of all 161 stations in Europe
Color of points indicate to which of the following o-t-region each station is assigned: 1-CE (**C**entral **E**astern), 2-CN (**C**entral **N**orthern), 3-CW (**C**entral **W**estern), 4-HA (Central **H**igh **A**ltitude), 5-NE (**N**orthern **E**uropean), and 6-SE (**S**outhern **E**uropean o-t-region). Representative stations are highlighted by shape (squares = first, triangles = second, stars = third representative station) and color saturation.

Table 3.1 Region-specific ozone and temperature characteristics

O-t-region	Altitude	MDA8O3	MDA8O3	MDA8O3	TX	TX	TX
	mean / median	mean	median	25th / 75th	mean	median	25th / 75th
1-CE	205.67 / 140.00	97.58	95.44	79.37 / 114.00	21.75	21.90	17.80 / 25.80
2-CN	37.86 / 19.00	85.94	82.55	69.00 / 98.24	19.78	19.80	16.50 / 23.10
3-CW	273.94 / 275.00	96.24	93.20	78.20 / 111.00	22.68	22.60	18.80 / 26.60
4-HA	1205.13 / 916.5	105.86	104.00	87.75 / 122.40	13.41	14.10	9.00 / 18.60
5-NE	170.59 / 130.00	71.02	69.40	57.00 / 84.16	16.28	16.70	13.40 / 19.50
6-SE	236.88 / 81.00	105.85	104.00	91.00 / 119.00	27.17	27.50	23.40 / 31.00

Note. MDA8O3 (in µg/m^3) and TX (in °C) characteristics are based on the o-t-season from 2004 to 2018. Mean, median, as well as 25th and 75th percentile values for each region are shown. Additionally, the mean and median altitude levels (in m) are depicted. Numbers are calculated on the basis of all available stations of an o-t-region.

Central European o-t-region 4-HA is geographically scattered. The region contains mainly higher altitude stations with mean and median levels of 1205.13 m and 916.5 m (min 641 m and max 3,106 m), with two stations being located above 1000 m (representative station DESN053 and DEST039) and only one above 2,000 m (AT0SON1). Stations of 4-HA show comparably low TX next to high MDA8O3 values due to their outstanding location characteristics, that is, high-altitude levels determine relatively cold air temperatures, and

stratospheric influences often affect daily ozone concentration levels. The separate clustering of these stations due to their deviant environmental and air pollution conditions is hence reasonable, outlined more in detail in the subsequent section and in Section 6.

Figure 3.2 provides the main information that a strong linkage of ozone and temperature is primarily present in central Europe. Very strong relationships between MDA8O3 concentrations and TX values in the o-t-season become mainly apparent for 1-CE, 2-CN, and 3-CW. Regions 5-NE and 6-SE, representing comparably low- and high-temperature areas, show in general lower correlation coefficients. This is also evident for the o-t-season from April to September.
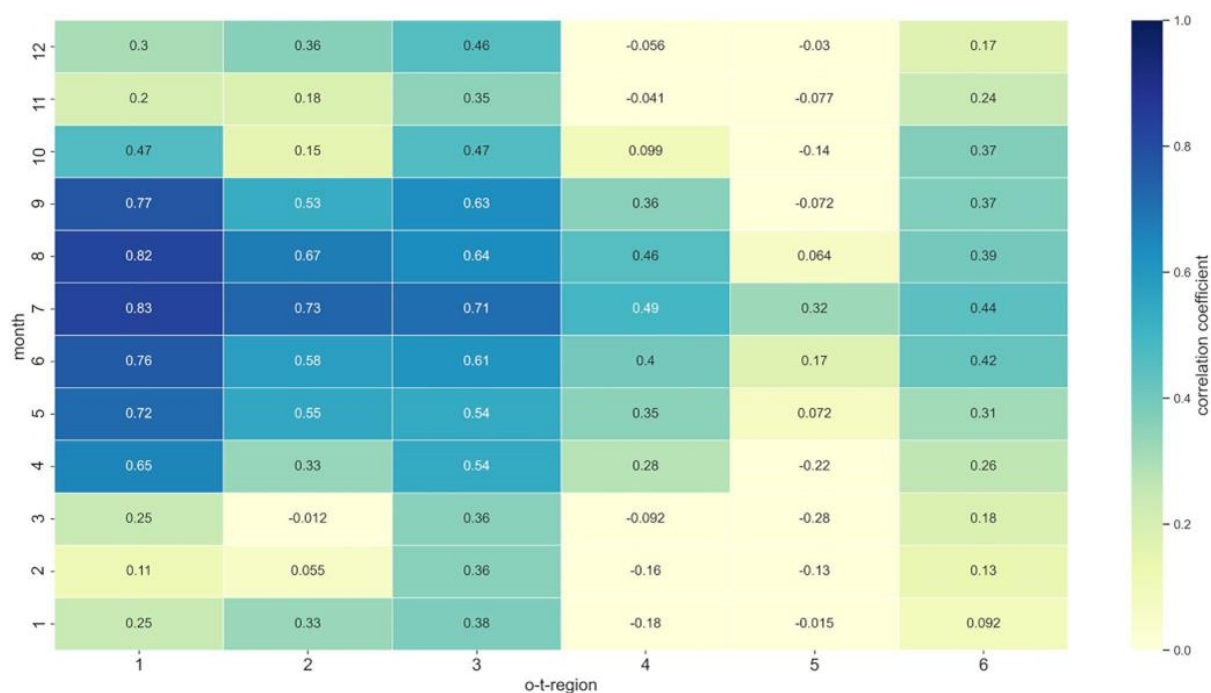
Fig. 3.2 Spearman rank correlation coefficients between daily MDA8O3 concentrations and TX values for each o-t-region in Europe from 2004 to 2018
O-t-regions are specified by their respective numbers and depicted on the x axis. Months are shown as numbers (1 = January to 12 = December) on the y axis.

If site-specific ozone chemistry characteristics highly determine ozone levels and related o-t-relationships, the observed deviant correlation levels could be associated with the varying number of stations per station type in each o-t-region. For example, 2-CN consists of 61% urban stations, while only 35% of all stations in 5-NE are urban (please refer to Table S5 in Supporting Information S1 for details). The different number of urban stations hence might affect the presented region-specific o-t-correlations of 2-CN and 5-NE shown in Figure 3.2. Respective possible relationships were tested and could be ruled out by the analysis. Hence, station-type influences do not generally determine region-specific o-t-correlations.

The same evaluation as shown in Figure 3.2 was conducted on a station level. Monthly spearman rank correlation coefficients were calculated for each individual station of an o-t-region. The station-specific monthly o-t-linkage from January to December based on all years from 2004 to 2018 was evaluated. The results were in accordance with the patterns shown in Figure 3.2. For the vast majority of stations, similar o-t-correlations as for the respective overall o-t-region could be observed. Considering 4-HA, a high correlation of at least 0.6 for each month in the o-t-season becomes apparent for all stations but one (AT0SON1). AT0SON1 shows deviant o-t-correlations with coefficients of 0.4 or higher only computed for the months from June to August. AT0SON1 is located above 3,000 m, so it is primary installed to monitor background free-tropospheric ozone concentrations. But as in three summer months, the o-t-correlation is still substantially observable, and to maintain consistency in the approach,

AT0SON1 is kept in the database. Nevertheless, all subsequent results for 4-HA can only partly be transferred to station AT0SON1.

5.1.2. Representative Stations

Fifteen representative stations were extracted. The analysis revealed that the proximity of a station to its centroid, based on Euclidean distances, is in general independent of station types, including all representative stations. All but one representative station (ES1599A representing the only rural station in 3-CW) are nearby their respective cluster centroids. Representative stations are also highlighted and further described in Table S2 and S5 in Supporting Information S1. Not taking 4-HA into account, the highest numbers of o-event days are visible for both representative stations in 6-SE and the by far lowest numbers in 5-NE. Due to the definition of t-events based on the chosen percentile-based approach, a similar number of t-event days is observable across all regions and representative stations. Considering ^{80}TX in 5-NE and 6-SE, t-events are defined based on generally low or high values in comparison to central European o-t-regions 1-CE, 2-CN, and 3-CW. A comparably small number of o-t-events is observable in 5-NE and 6-SE, even if many o-event days are present in 6-SE. This fact underlines the calculated low correlation coefficients between ozone and temperature in 6-SE presented above.
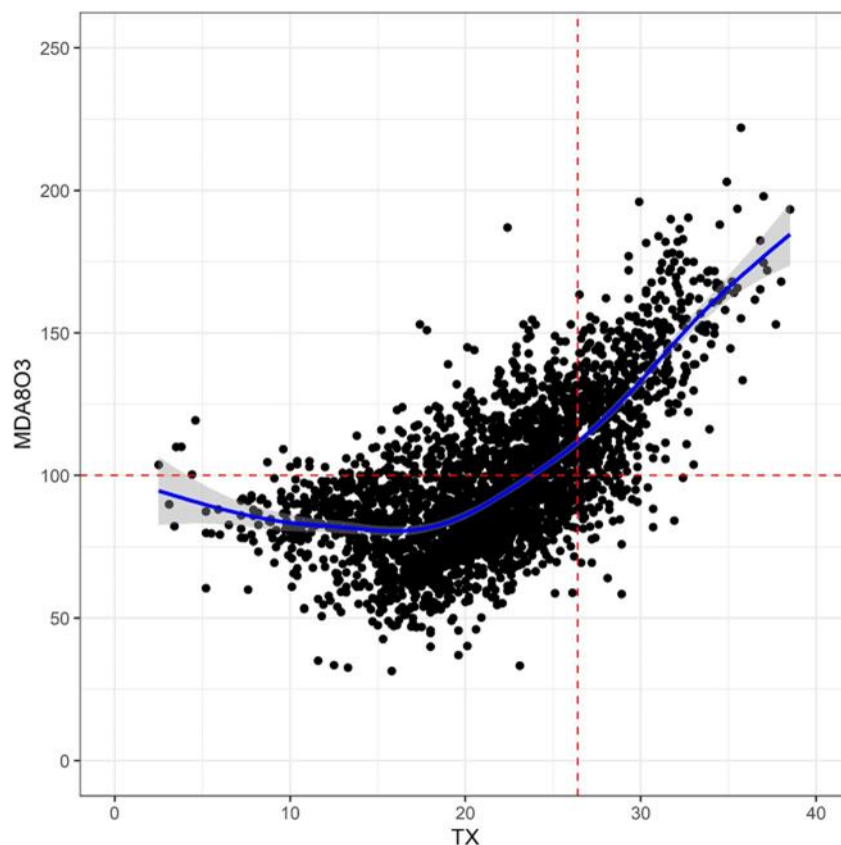
Fig. 3.3 Relationship between MDA8O3 and TX for representative station DEST002 of 1-CE (Burg in Saxony-Anhalt)
All daily observations from April to September across all years from 2004 to 2018 are considered. A Generalized additive models between both target variables is shown to highlight the linkage between both variables (blue line). Gray shadings illustrate the used confidence interval (0.95). The red horizontal line illustrates the World Health Organisation guideline of 100 µg/m³. The red vertical line shows the 80% quantile of all respective observed TX values across all months and years, amounting to 26.4°C.

Generalized additive models (GAM) were applied to analyze the o-t-linkage for each o-t-region in more depth. Figure 3.3 shows the o-t-relationship exemplarily for the representative suburban background station of 1-CE, DEST002 (Burg in Saxony-Anhalt). Please refer to

Figure S1 in Supporting Information S1 for all other representative stations. Figure 3.3 underlines a very direct, approximately linear linkage between both variables as temperature levels approach 20°C. A high proportion of observations lies in the area of a direct response of ozone with clear increases of MDA8O3 at higher TX values. The direct linkage associated with a strong positive ozone response on temperature is also observable as TX levels approach 20°C or 10°C for representative stations of 1-CE, 2-CN, and 3-CW and for the high-altitude station DESN053 (1214 m) of 4-HA, respectively.

While comparable results become evident for all four central European regions, deviant relationships are observable for the northern and southern representative stations. The majority of observations in 5-NE are in lower temperature ranges with 80% quantiles not reaching 20°C. But even for these stations, the upper 20% of TX values already indicate a positive o-t-linkage. This observation suggests that similar relationships above 20°C are present at higher air temperature levels. For 6-SE, it becomes apparent that TX values are by far higher than for all other representative stations. Also, 20% and 80% quantiles surpass 25°C and 33°C as well as 22°C and 30°C for representative stations ES1215A and ES1666A, respectively. Thus, o-t-events are associated with higher temperatures. The distinct direct linkage with increases of ozone levels due to rising air temperatures is not generally observed for the majority of observations in 6-SE.

Please note that direct is used in this context throughout the paper to describe the strong relationship between MDA8O3 and TX, relating to a large positive response of MDA8O3 on rising TX levels. This has to be seen independent of the various different direct and indirect causalities determining the o-t-relationship. Just to name one of these direct and indirect causalities, respectively: ozone is formed from a complex series of reactions accelerated by warm temperatures (direct); the sunlight-driven photochemical production of ozone influences the o-t-relationship as high solar radiation induces usually also warm air temperatures (indirect).

5.2. Statistical Modeling and Climate Change Projection Results

Statistical downscaling models were generated based on the identified station-specific predictor sets. Similarities and differences in main drivers of compound o-t-events across all o-t-regions were analyzed. Statistical downscaling models were subsequently applied with ESM data to project frequency shifts of o-t-events under two scenario assumptions.

5.2.1. Models and Main Drivers

LR statistical downscaling models were generated based on all selected and preprocessed meteorological and synoptic predictors. Given the geographical proximity of both representative stations of 6-SE (ES1215A and ES1666A), the nine grid-cell means to generate station-based meteorological predictor time series are identical. Considering the synoptic predictor, the SOM result showing the smallest topographic product of -0.0374 was selected. The final nine WT, entering the modeling process as numerical codes from one to nine, are shown in Figure S2 in Supporting Information S1. As the array of nodes self-organizes into a pattern with more similar nodes being in closer proximity and more dissimilar nodes further away, simple clusters can be detected. Please refer to Table S6 in Supporting Information S1 for a more detailed evaluation of the generated WT and an in depth-analysis of their association with o-, t-, and o-t-events in the base period.

Table 3.2 gives an overview of the final LR statistical downscaling model results. Across all stations, a similar, balanced performance considering P and R is achieved. Model fit and performance are in general high for stations in the central European regions. The F1-Score of the LR models for all but one central European station (ES1599A) amounts to at least 0.65 (DEHH047) with a maximum of 0.72 (DEST066). A station-specific maximum F1-Score of 0.41 is observable across all stations of 5-NE and 6-SE. Hence, the LR models in central European

regions 1-CE, 2-CN, 3-CW, and 4-HA clearly outperform the models of 5-NE and 6-SE in capturing o-t-events.

Table 3.2 Overview of the logistic regression station model results

Station	Ratio	Regression coefficient					P	R	F1-Score	MF-R^2
		GH	MT	SH	SSRD	WT				
DEST066	102.60	-0.44	**4.29**[1]	**-1.66**[2]	**0.76**[3]	0.61	0.72	0.72	0.72	0.58
DEBB066	98.60	-0.64	**3.84**[1]	**-1.37**[2]	**0.82**[3]	0.66	0.70	0.70	0.69	0.55
DEST002	95.80	-0.53	**4.00**[1]	**-1.35**[2]	**0.80**[3]	0.63	0.70	0.70	0.69	0.57
NL00807	83.80	-0.67	**2.74**[1]	-0.48	**1.46**[2]	**0.84**[3]	0.68	0.68	0.68	0.56
DEHH047	82.20	-0.41	**2.68**[1]	-0.51	**1.27**[2]	**0.75**[3]	0.65	0.64	0.64	0.53
DEHB002	77.00	-0.76	**3.05**[1]	-0.59	**1.84**[2]	**0.82**[3]	0.69	0.68	0.68	0.61
FR26010	94.00	-0.28	**3.29**[1]	**-1.24**[2]	0.48	**0.52**[3]	0.65	0.66	0.66	0.51
FR07004	88.20	-0.26	**3.46**[1]	**-1.23**[2]	**0.39**[3]	0.16	0.68	0.69	0.68	0.54
ES1599A	68.40	**-0.64**[3]	**2.25**[1]	**-0.87**[2]	0.39	0.18	0.46	0.44	0.45	0.36
DESN053	129.75	-0.21	**4.63**[1]	**-1.93**[2]	-	**0.28**[3]	0.70	0.70	0.70	0.54
GB0033R	16.00	-0.28	**1.57**[1]	**-0.63**[3]	**0.77**[2]	0.50	0.26	0.26	0.29	0.32
GB0567A	9.20	**-1.09**[3]	**2.18**[1]	-0.25	**1.84**[2]	0.95	0.28	0.38	0.41	0.54
IE0001R	23.20	-0.22	**0.99**[2]	-0.33	**1.15**[1]	**0.74**[3]	0.26	0.32	0.31	0.28
ES1666A	55.20	0.39	**0.78**[1]	**-0.50**[3]	**0.61**[2]	-0.17	0.34	0.32	0.32	0.20
ES1215A	58.20	**0.60**[2]	**0.69**[1]	**-0.44**[3]	0.43	-0.07	0.27	0.27	0.27	0.17

Note. The final statistical downscaling model results for all representative stations are shown. Standardized regression coefficients for each predictor variable (GH = geopotential heights, SH = specific humidity, MT = mean air temperatures, SSRD = surface solar radiation downward) are shown. Station-specific main drivers are highlighted in bold and specified by superscript (MID = 1, SMID = 2, TMID = 3). Model fit and performance are given by Precision (P), Recall (R), F1-Score, and McFadden's R^2 (MF-R^2). The ratio based on the number of events with respect to the number of predictors is shown as well. Stations are ordered by region (from 1-CE to 6-SE) and are framed, respectively, in the table by dashed lines. Within a region, stations are ordered from the first to the last representative station based on the Euclidean distances to their region centroid.

For all stations but one (DESN053), all predictors are significant and included in the model. The standardized regression coefficients as well as the identification of main drivers revealed no clear station-type-related differences. Thus, main drivers of o-t-events seem to be primary related to larger scale regional influences rather than individual station characteristics. In general, the identified MID and SMID represent by far the most influencing factors of o-t-events, especially in central Europe. MT mainly governs o-t-events as MID with varying magnitudes. SH and SSRD represent a further influential factor for the vast majority of locations with low humidity and high solar radiation levels favoring the occurrence of o-t-events. More sporadically, for some stations, WT and GH are selected as SMID and TMID.

For DESN053 of 4-HA, SSRD is not a significant predictor and was not kept in the final station model. This might indicate that 4-HA stations are not as strongly dependent on the local,

photochemical in-situ formation of ozone, but are stronger influenced by, for example, stratospheric O_3 exchange processes. Nevertheless, DESN053 results show high model fit and performance values with an F1-Score above 0.7. This as well as the high regression coefficients of other predictors indicate that the selected meteorological and synoptic drivers generally influence compound o-t-events at this high-altitude station.

5.2.2. Climate Change Projections

Table 3.3 Projected midcentury and late 21st century ensemble mean changes (%)

Station	SSP245		SSP370	
	2041-2060	2081-2100	2041-260	2081-2100
DEST066	34.72	56.32	47.60	111.41
DEBB066	38.87	59.42	49.40	118.40
DEST002	40.08	65.76	56.89	130.31
NL00807	52.01	75.88	62.66	139.92
DEHH047	50.52	74.02	61.87	138.07
DEHB002	54.73	79.99	68.46	152.66
FR26010	51.45	79.02	65.77	147.89
FR07004	55.20	87.06	76.56	177.67
ES1599A	65.59	110.45	102.93	221.31
DESN053	36.17	61.63	54.98	124.89

Note. Climate change projection results for the representative station of all central European o-t-regions 1-CE to 4-HA, separated by dashed lines, are shown. The ensemble results are based on the number of days with o-t-events between the periods 2041-2060 (midcentury) as well as 2081-2100 (late century) compared to the historical Earth System Models (ESM) period 1995-2014 under SSP245 and SSP370 scenario assumptions. The climate change signals of all selected individual ESM showing the same sign, but a different magnitude of change, are considered. Hence, numbers refer to the multi-model mean across all eight ESM. Stations are listed in accordance with Table 2.

Climate change projections were generated for all representative stations of central European o-t-regions 1-CE, 2-CN, 3-CW, and 4-HA. Table 3.3 provides an overview of projected ensemble mean changes statistically downscaled under SSP245 and SSP370 scenario assumptions. Projected frequency shifts range from an increase of about 35%-66% (midcentury) and 56%-110% (late century) for SSP245 and from 48% to 103% (midcentury) and 111%-221% (late century) for SSP370, respectively. Stations DEST066 (1-CE) and ES1599A (3-CW) always show the lowest and highest values, respectively. On average, a growing number of compound event days in central Europe with midcentury and late 21st century projected frequency changes being stronger for SSP370 in comparison to SSP245 becomes apparent. Stronger frequency shifts are assessed for corresponding late century climatic conditions. By considering spatial patterns of projected change, a general gradient from 1-CE, over 2-CN, to 3-CW can be observed across all scenario assumptions and time slice differences. For station DESN053, similar responses comparable to surrounding, low-altitude stations of 1-CE become apparent. Respective median, minimum, and maximum projected changes can be found in Table S7 in Supporting Information S1.

An overall assumption of stationarity of governing statistical and causal relations regarding the predictors themselves as well as between predictors and predictand forms the basis of the applied modeling and climate change projection framework. This includes that all ozone chemistry, transport, and formation conditions and o-t-characteristics retain their main characteristics throughout the 21st century. To examine if these basic assumptions are met, projected multi-model mean midcentury and late century warmings under SSP245 and SSP370 scenario assumptions were analyzed. Region-specific MT anomalies per scenario and time window, presented in the Table S8 in Supporting Information S1, were hence considered. Projected increases of MT levels do not in general surpass 2.7°C for SSP245 (both midcentury and late century) and SSSP370 (only midcentury conditions) in any central European o-t-region. So strong deviant statistical relationships leading to a break of the observed relationships in the modeling periods are rather unlikely under these assumptions. But for late century SSP370 scenario assumptions, in some regions, late century MT anomalies amount to over 4°C.

6. Discussion

6.1. Regionalization

A regionalization of the European domain based on a hierarchical clustering approach considering daily surface maximum ozone concentrations and air temperature levels from April to September is presented. The result reflects a consistent and robust geographical clustering. O-t-regions consist of stations showing comparable spatiotemporal ozone and temperature variabilities, patterns, and characteristics. Region-specific dynamics seem to have a stronger impact than local site conditions and station types. This includes that station types did not highly influence the assignment of a station to an o-t-region. In accordance, the proximity of a station to its centroid, based on Euclidean distances, could not be connected to site characteristics. The observed station-based patterns generally fit the overall region-specific conditions of both target variables. This is also particularly true for the representative stations of varying station types identified for all six o-t-regions. The results give evidence that interregional dissimilarities are strong in comparison to intraregional variability and differences, including that station types do not substantially affect o-t-relationships in comparison to region-wide influences. This hints to the fact that o-t-events in Europe are phenomena of a broader regional scale influenced by larger scale processes. Thus, a region-specific approach to model and project compound events can uncover widespread, regional variations. The results also highlight the usefulness of synoptic WT in modeling and climate change projection studies.

6.2. Present-Day Relationships and Models

6.2.1. Central Europe

For central European o-t-regions 1-CE, 2-CN, 3-CW and to a lesser extent, also for 4-HA, a strong positive correlation and direct relationship between MDA8O3 and TX in the o-t-season from April to September is confirmed. Statistical downscaling models based on logistic regression to assess the relationship between four selected meteorological predictors, synoptic WT, and o-t-events verify the physical processes behind ground-level ozone formation as well as elevated temperature levels. The validity of the models is emphasized as not only model fit and performance values, but also the magnitude of the standardized regression coefficients hint to a strong relationship between the selected predictors and the occurrence of o-t-events. The results point to the circumstances that central Europe temperature conditions support a direct o-t-linkage with a large portion of observations lying in ranges with linear MDA8O3 responses to rising air temperatures. A clear relationship between compound o-t-events and meteorological and synoptic mechanisms is observed for all central European regions. In general, mean air temperatures, specific humidity levels (both at 850 hPa

levels) as well as downward-directed surface solar radiation can be regarded as powerful predictors to assess compound o-t-events.

Even though the presented results indicate a substantial relationship between compound o-t-events and the identified main drivers also for stations in high-altitude o-t-region 4-HA, station AT0SON1 shows a lesser o-t-linkage due to its unique site conditions. Therefore, results should only be transferred to all other stations of 4-HA. In future work with differing framework conditions (e.g., by considering variable time periods as base period), further stations being located at similar altitude levels as AT0SON1 may be included in the database and lead to a separation of this station from the given cluster 4-HA. This will probably result in the formation of a new, separate o-t-region, consisting of primarily stations monitoring background, free troposphere ozone values.

6.2.2. Northern and Southern Europe

For 5-NE and 6-SE, a deviant picture emerged. Presented results point to the fact that existing temperature and environmental conditions determine a comparably weak o-t-linkage and correlation. An absent or low direct dependence of MDA8O3 on temperature levels is reasonable for 5-NE as the majority of TX observations lay under 20°C. In contrast, high TX values determine o-t-events at both representative stations in 6-SE. A break of the direct o-t-relationship with plateauing or even decreasing ozone concentrations under very high air temperatures might be in general anticipated (e.g., Steiner et al., 2010 above 37°C). However, as most of the observations in 6-SE still lay inside moderate temperature ranges, the weak observed linkage and correlation between TX and MDA8O3 cannot be substantially attributed to this relation. The general presumption of a strong direct relationship of local ozone and air temperature conditions is further based on the assumption of a high proportion of O_3 in-situ formation by photochemical reactions. If long-range transport processes of ozone from various locations outside the specific o-t-region strongly determine pollution levels, as for example, Hertig et al. (2020) found for Portugal, a weaker connection of station-based MDA8O3 levels on local air temperatures can be anticipated. Similar influences and further non-in-situ formation factors might be present in 6-SE with stations spread across Portugal and mainly southern parts of Spain and France. This is further underlined by the observed, comparable low number of co-occurring o-t-events in 6-SE although a high number of o-event days are present (in contrast to 5-NE showing in general low o- and o-t-event occurrences).

All central European station models clearly outperform the ones of 5-NE and 6-SE. The deviant o-t-characteristics and linkages as well as the generally observed lower number of o-t-events in 5-NE and 6-SE may determine the comparably weak predictive power of all southern and northern station models. This might also rely on a general relatively weak role of direct physical predictors on combined elevated ozone concentration and temperature levels in northern and southern Europe. This is also in accordance with the results of previous studies, for example, Otero et al. (2016) who found that preceding conditions based for example, on precursor emissions rather than meteorological variables impact ozone concentrations in these parts of Europe. Furthermore, daily exceedances based on [80]TX values in 6-SE already represent comparably high levels (amounting to rounded median values of 30°C and 33°C). Hence, the modeled o-t-events are in air temperature ranges approaching the environmental conditions for which a weaker response of MDA8O3 concentrations on TX values can already be expected.

6.3. Climate Change Projections

Using the output of eight ESM of the CMIP6 project, the LR models together with ESM data were used for climate change projections. 5-NE and 6-SE did not show a strong direct linkage between MDA8O3 and TX levels as well as between selected physical drivers and o-t-events, visible by low model fit and performance values. Hence, both o-t-regions were discarded for climate change projections. Multi-model mean changes point in general to an increase in the

occurrence of o-t-events until the end of the 21st century. This is in accordance with the statistical downscaling modeling results across all central European o-t-regions. MT, SH, and SSRD represent in general the most important drivers of o-t-events over central Europe. Consequently, projected increases of future air temperatures, solar radiation levels, and related specific humidity changes impact future mean O_3 concentrations and temperature levels. Hence, a growth in future compound o-t-event occurrences under global warming can be expected. Clear interregional differences, but no obvious dependences of the projections on site-specific characteristics, and hence station types become evident. Assuming stationarity of recent ozone chemistry conditions and underlying processes, this indicates that overall region-specific environmental changes lead to a similar response to the climate change signals across all stations. For late century SSP370 scenario assumptions, a break of the observed relationships cannot be ruled out for some o-t-regions. For 3-CW, statistically modeled relationships of the base period could not simply be assumed to hold in a projected, warmer central European climate. So, respective climate change projections need to be interpreted with caution. Even if a substantial frequency shift is projected for all central European o-t-regions, some areas (e.g., in 2-CN) that already show nowadays comparably high levels of both variables may be more affected by future changes and should be emphasized in future European-wide mitigation and adaption strategies.

7.   Limitations

Some of the results might be influenced by limitations from the study design. The study relies on a strong and direct linkage between MDA8O3 and TX levels as well as on stationarity of all statistical relationships and characteristics. This includes, for example, all ozone chemistry influencing processes and conditions not directly incorporated in the statistical downscaling models. A major source of uncertainty is thus based on the assumption that present-day o-t-relationships are expected to hold across all central European o-t-regions under future warming. This fact was accounted for by only considering central European o-t-regions for climate change projections and by the evaluation of MT anomalies based on all scenarios and time slice differences. But, nevertheless, this approach relies on the postulation that precursor emissions are anticipated to behave accordingly, which must be considered as a major assumption of the given work. The aim of the study was to analyze o-t-events considering future climatic changes, including, but not limited to, temperature. Precursor emissions and their possible future reductions, for example, with regard to European climate neutrality goals, but also further factors like future land use and vegetational changes, may influence the governing present-day relationships in magnitude and characteristic, but were not directly included in this work. However, a break of the observed and modeled statistical associations of ozone, temperature, meteorology, and synoptic conditions can also not simply be anticipated as a variety of influences, such as for instance precursors emissions transported from extracontinental sources to the identified European o-t-regions, might determine future European o-t-event occurrences. Station and site characteristics might also influence future changes in o-t-events and vary not only in an inter- but also intraregional perspective. This fact was mitigated by two primary decisions. At first, only background stations installed to monitor regional background levels representative of the average exposure of the general population rather than locally limited and site-specific pollution levels like major roads or industrial areas were selected. Second, several representative stations per region based on deviant station characteristics were selected. This selection also enables to include varying site characteristics with alternating pollution regimes and influences in the model and projection process. As in general more NO_x-sensitive regimes in rural and VOC-sensitive regimes in urbanized areas can be expected, the results of the regionalization, modeling, and projection process show primary regional, not station-type dependences, and so underline the minor role of regimes in this context. Nevertheless, individual sites of a region might still show strongly deviant developments based on specific local environmental conditions, and a selected station may

not be representative for the general exposure of a region anymore. This cannot be accounted for by the chosen approach. The performance of the generated LR models was in general good for central Europe, but individual station model fit, and performance values have always to be kept in mind when interpreting station-specific developments and climate change projections.

Limitations based on the different resolution of the ESM and ERA5 reanalysis data and thus related interpolation and preprocessing as well as general uncertainties of the CMIP6 climate change projections themselves might exist. ESM data were thus bias-corrected and the significant distributional differences between the climate model and reanalysis data were evaluated. Nevertheless, the general coarse resolution of some ESMs used for 21st century projections must be pointed out.

Most importantly, it becomes apparent that the applied study framework is to a large extent only suitable for all central European stations. Consequently, for northern and southern parts of Europe, a revised and adapted approach needs to be developed in future health-relevant o-t-event-studies. Frequency shifts of o-t events until the end of the 21st century based on adjusted northern and southern European region-specific, station-based statistical models, and related projections could subsequently be compared with the here presented central European results and possible relevant differences assessed.

8.   Conclusions

Six ozone and temperature regions together with 15 representative stations with different site characteristics and air quality settings were identified. A region-specific analysis of both target variables, including the evaluation of the relationship between meteorological and synoptic conditions and compound o-t-events, was conducted. A strong and direct relationship and correlation between ozone and temperature as well as a good performance of the statistical downscaling models were primarily found in all central European o-t-regions. Consequently, climate change projections were only generated for central Europe. Sharp increases of o-t-events, considering 20-year time slice differences under SSP245 and SSP370 scenario assumptions, were in general assessed resulting in a considerable intensified health burden for the central European population until the end of the 21st century.

Concluding, compound ozone and temperature events combining two natural hazards and composing a substantial health risk throughout different regions of central Europe should be the focus of further studies, but also upcoming European climate change mitigation and adaption strategies. An adjusted and adapted approach focusing on northern and southern parts of Europe should be incorporated in future work of health-relevant o-t-event-studies.

Conflict of Interest The authors declare that they have no conflicts of interest.

Data Availability Statement The authors acknowledge the data providers of the ECA&D and Air Quality eReporting data sets. Respective ECA&D data (Klein Tank et al., 2002) used in this study are available at the following website: https://www.ecad.eu/dailydata/predefinedseries.php (accessed 3 July 2020). Air Quality eReporting data (EEA, 2017) are available at https://aqportal.discomap.eea.europa.eu/ with the raw data accessible via and downloaded on 3 July 2020 at https://discomap.eea.europa.eu/map/fme/AirQualityExport.htm (since 2013) and https://discomap.eea.europa.eu/map/fme/AirQualityExportAirBase.htm (2004-2012). The authors also acknowledge the European Centre for Medium-Range Weather Forecasts for provision of the ERA5 data set as well as the World Climate Research Programme's Working Group on Coupled Modelling, which is responsible for CMIP, and we thank the climate modeling groups for producing and making available their model output. ERA5 (Hersbach and Dee, 2016) and CMIP6 (Eyring et al., 2016) data are available at https://cds.climate.copernicus.eu/ and https://esgf-node.llnl.gov/projects/cmip6/, respectively. Most of the data preparation and analysis including regionalization, model building, and projections were conducted using the Python programming language (version 3.7.4, IDE PyCharm).

4. Chapter 4 - Research Article 3

Future Local Ground-level Ozone in the European area from Statistical Downscaling Projections Considering Climate and Emission Changes

Publication:

*Elke Hertig is first and corresponding author.

The layout, and citation style of the original article, including figure and table designs, numbers, and captions, were adapted and adjusted to be consistent with the rest of the manuscript. No changes in spelling, including e.g., used abbreviations and acronyms, were made and the main text of this chapter is still in this regard as published. The Supplementary Information is available online alongside the original article as well as is additionally added to this dissertation without further adjustments as Appendix F.

Individual author contributions (as in Appendix C):

The main topic and specific design of this study was formulated and developed by Elke Hertig. Sally Jahn collected all observational and together with Irena Kaspar-Ott all meteorological reanalysis data. Observational and meteorological reanalysis data were processed and preselected by Sally Jahn. Ozone reanalysis and climate model data were downloaded and processed by Irena Kaspar-Ott. The detailed bias correction of the climate model data was conceived and designed by Elke Hertig and performed and evaluated by Irena Kaspar-Ott, while Elke Hertig contributed to the analysis and interpretation of the results along with an extensive discussion of the choice of a suitable ozone reanalysis product. The implementation and development of statistical downscaling models along with a prior predictor selection procedure, model evaluation and main driver analysis was performed by Sally Jahn in consultation with Elke Hertig and Irena Kaspar-Ott. The model setup was substantially extended and improved by Elke Hertig providing the support for the development of a sensitivity analysis evaluating primarily the impact of different predictor types on model and projection results. Projections were generated and final figures were provided by Irena Kaspar-Ott and Sally Jahn. Final analysis of the model and projection output, discussions, and interpretations of the main results were primarily done by Elke Hertig and Irena Kaspar-Ott. The literature studies and the preparation of the manuscript were mainly conducted by Elke Hertig, with contributions from Irena Kaspar-Ott and Sally Jahn who provided primarily main text parts for the sections on data and methods. The manuscript was finalized by Elke Hertig with the aid of all co-authors.

Future Local Ground-level Ozone in the European area from Statistical Downscaling Projections Considering Climate and Emission Changes

Elke Hertig[1], Sally Jahn[1] and Irena Kaspar-Ott[1]

[1]Regional Climate Change and Health, Faculty of Medicine, University of Augsburg, Universitätsstrasse 2, 86159 Augsburg, Germany

Supporting Information: Supporting Information may be found in the online version of this article.

Correspondence to: E. Hertig, elke.hertig@med.uni-augsburg.de

Abstract

Ground-level ozone is a major air pollutant harmful for human health. In the scope of climate change, it is essential to provide high-quality local-scale assessments of the anticipated changes for public health and policy interventions. Assessments and projections of ground-level ozone usually rely on numerical modeling, but statistical approaches are also available. The present study enhances the validity of statistical downscaling by taking climate change as well as air pollution changes into account. Besides considering meteorological predictors such as air temperature, short-wave radiation, humidity, and wind, ozone trends from changes in precursor emissions were included in the statistical models. Meteorological and ozone predictor information extracted from reanalysis data for the observational period and output of seven Earth System Models (ESMs) for the projection periods were used, with three of them having interactive chemical modeling, while the other four used prescribed ozone changes. Ground-level ozone, more precisely daily maximum 8-hr running means (MDA8) as well as daily maximum 1-hr values (MDA1), at 798 measurement stations across the European area in the "ozone season" from April to September were assessed. Results depended strongly on whether only meteorological information or additional information about emission changes were considered. As a general picture under the consideration of climate and emission changes, decreasing ground-level ozone concentrations were projected under the moderate SSP2-4.5 scenario, while for the more pessimistic scenario SSP3-7.0 increasing ozone concentrations over Europe, especially at the end of the 21st century, were assessed.

Plain Language Summary

Ground-level ozone is a gaseous air pollutant that is formed under sunlight from other air pollutants. Ground-level ozone is harmful to human health. There are concerns that under climate change, ground-level ozone will increase. To assess changes on a local-scale various methods are available, which can roughly be divided into numerical models and statistical approaches. The present study developed statistical models further, to give a more realistic picture of future changes in ground-level ozone in the European area. Information about meteorological changes such as air temperature, atmospheric humidity, and wind as well as changes in air pollutants like nitrogen oxides was considered. During the 21st century decreasing ground-level ozone concentrations were projected under a moderate climate change scenario, while for a more pessimistic scenario increasing ozone concentrations over Europe, especially at the end of the century, were assessed. This result highlights the

necessity to further reduce greenhouse gases and air pollution, bringing forth better protection of human health.

Key Points

- Precursor emission changes are represented by the inclusion of ozone trend in the statistical downscaling models

- Statistical projections results are sensitive to the predictor types and Earth System Model output used

- Climate change scenarios have a major impact on future ozone, greenhouse gas and air pollution reductions can mitigate health risks

1. Introduction

Ground-level ozone (O_3) is a photochemical oxidant formed from precursors in a polluted atmosphere, mainly nitrogen oxides (NO_x) and non-methane volatile organic compounds (VOCs). O_3 at the surface is harmful to human health and the World Health Organization recently tightened the air quality guidelines based on new epidemiological evidence (WHO, 2021).
While already many regions of the world frequently exceed the recommended levels, concerns have been raised that in the scope of ongoing climate change ground-level O_3 concentrations will further increase despite efforts for rigorous air pollution control. This "climate penalty" implies the need for stronger emission controls to achieve a given air quality standard (Wu et al., 2008). Processes that are discussed to contribute to elevated O_3 concentrations due to climate change comprise warming-induced biogenic VOC emission enhancements, faster chemistry kinetics, and faster peroxyacetyl nitrate decomposition (Lu et al., 2019). Porter and Heald (2019) found that temperature-dependent deposition and soil NO_x emissions contribute to the "climate penalty". Furthermore, enhanced stratosphere-troposphere exchange, changes in the large-scale atmospheric circulation and synoptic patterns, increased stagnancy, and changes in atmospheric humidity may lead to increases in surface O_3 (Porter and Heald, 2019, Lu et al., 2019). In general, models project increases in surface O_3, and most notably of extreme O_3 episodes, in polluted regions and decreases over rural areas and oceans (Schnell et al., 2016). This trend was found in Europe already in the observational period 2000-2015, with daily mean O_3 decreasing at rural sites, while in suburban and urban sites stable or increasing trends occurred (Boleti et al., 2020). This rural-urban difference is commonly attributed to the reduction of precursor emissions, which are most effective in rural regions with low NO_x concentrations. At low NO_x conditions, ozone production is limited by the supply of NO_x (NO_x-limited regime), whereas at high NO_x levels, ozone production linearly increases with VOCs concentration, but decreases with NO_x concentrations (VOC-limited regime) (Lu et al., 2019). For Europe, projections by Orru et al. (2019) indicate that the health burden due to O_3 increases due to climate change and the size of susceptible populations. However, because of reductions of O_3 precursor emissions, an overall decrease in the total health burden in 2050 was estimated. Extreme O_3 events are expected to increase in combination with rising heat events, in particular over mid-latitude regions like Central Europe or the Northeast of the United States (Jahn and Hertig, 2022, Shen et al., 2016). Thus, O_3 health risks could combine with increased health risks from heat exposure.
Projections of future tropospheric O_3 under climate change are commonly conducted using climate chemistry models coupled with general circulation models and regional climate models, respectively (a recent overview is given in Lu et al., 2019). Since these dynamical models are computationally expensive, the number of considered models and model runs is usually limited. For downscaling to regional to local scales, besides dynamical downscaling, various statistical analyses have been conducted, mostly focusing on the relationship between

meteorological factors and synoptic conditions with ozone concentrations (e.g, Jahn and Hertig, 2022, Jahn and Hertig, 2021, Hertig et al., 2020, Hertig, 2020, Otero et al., 2016). Statistical analysis has the advantage of being computationally inexpensive, but it mostly comes with the limitation that it considers meteorological drivers, while the impact and changes of precursor emissions are not regarded.

Here, we used a statistical downscaling framework based on the Perfect Prognosis (PP) approach (for an overview on statistical downscaling methods see e.g., Gutiérrez et al., 2019) to assess future changes of local, ground-level O_3 in the European area. The PP models were established in the observational period using local, station-based O_3, as the target variable, more precisely daily maximum 8-hr running means (MDA8) as well as daily maximum 1-hr values (MDA1). Reanalysis-based variables served as predictors. To generate future projections, predictors simulated by the latest generation of Earth System Models (ESMs) from the Coupled Model Intercomparison Project Phase 6 were used.

In addition to the inclusion of information on meteorological changes, we factored changes in precursor emissions into the statistical downscaling models. This was done via the incorporation of O_3 time series derived from the ESM model output. These ESM O_3 time series reflect the larger-scale total changes of O_3, resulting from climate change and from changes of precursor emissions under different scenario assumptions. Thus, the precursor gases were not used as predictors in the statistical models. Yet the information about their change and impact on O_3 progression was included by directly taking ESM modeled O_3. To assess the impact of different choices within the statistical downscaling, a sensitivity analysis was conducted, analyzing the impact of different predictor types (emission-related and meteorological, i.e., radiative and thermal, thermo-dynamic, and circulation-dynamic), different ESMs (with interactive computation of the atmospheric chemistry vs. prescribed O_3 changes), and different scenario assumptions (using the shared socioeconomic pathways SSP2-4.5 and SSP3-7.0). Section 2 presents the data and methods used in this study, while Section 3 elaborates first on the statistical downscaling models in the observational period, followed by the projection results for local MDA8 in the European area until the end of the 21st century, including the comparison of different predictor sets. Section 4 discusses the results further, while in Section 5 conclusions are drawn. Results for MDA1 were generally similar to MDA8 and can be found in the Supporting Information.

2. Data and Methods

2.1. Data

2.1.1. Station-Based Data

Hourly Air Quality eReporting O_3 pollution data from the European Environment Agency (EEA, 2017) were extracted. MDA8 as well as MDA1 were calculated and converted from µg/m^3 to ppbv. Stations with data from 2005 to 2019 and having more than 80% complete data per month were considered. To reduce the impact of direct formation and depletion processes next to emission sources of precursors (mainly NO_x), only urban, suburban, and rural background stations were incorporated in the analysis. Hence, no stations in traffic or industrial areas, located near major roads or industrial areas or sources, were included in the analysis. Consequently, we focus in our analysis on stations which are installed to monitor background concentration levels of ozone. These background levels are commonly considered to be representative for a given region and regarded as the average exposure of the general population. In summary, the initial selection led to an ozone station database with 798 background stations. The location of the stations, station type, and mean MDA8 concentrations for April-September 2005-2019 are illustrated in Figure 4.1. The distribution of the ozone stations per country is given in Table S1 in the Supplementary Material.
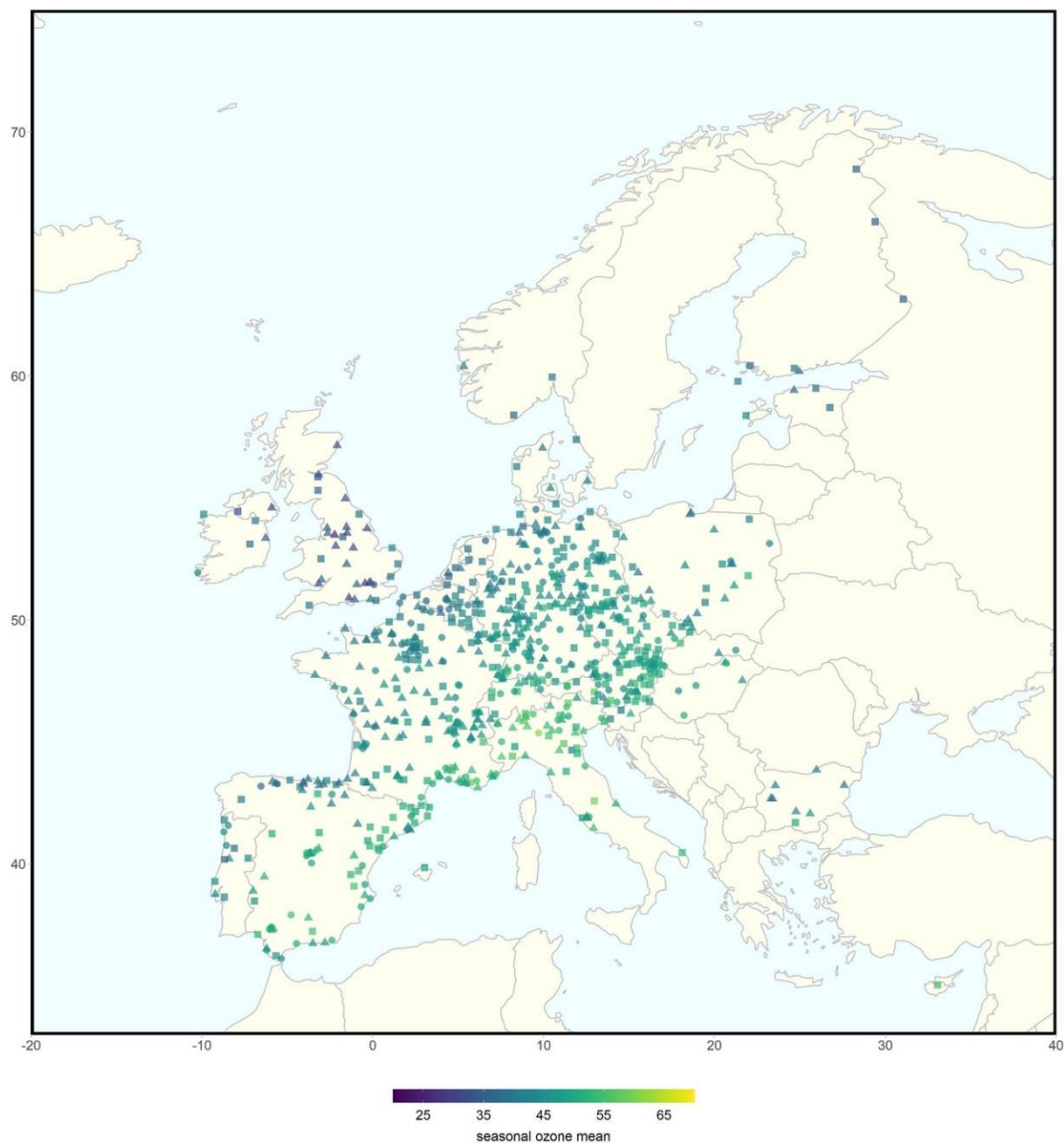
Fig. 4.1 Location of all 798 ozone stations across Europe
Color indicates MDA8 concentrations as mean values [ppbv] in the season April to September for the period 2005-2019 and shape of points indicate the type of each station (triangle = urban, circle = suburban and rectangle = rural).

2.1.2.   Reanalysis Data

The main meteorological drivers of O_3 in the European area comprise solar radiation, air temperature, atmospheric humidity, wind speed and direction, and air pressure (Otero et al., 2016, Hertig et al., 2020, Hertig, 2020, Jahn and Hertig, 2021). The meteorological variables enter the station-specific statistical downscaling models as predictors. Predictor data was retrieved from the ERA5 reanalysis data set from the European Centre for Medium-Range Weather Forecasts (Hersbach and Dee, 2016). Data was downloaded for the whole European domain with a 1° x 1° resolution. Variables were extracted at the 850 hPa level and preprocessed to get the following daily predictors for the period 2005 to 2019 (units in brackets): mean air temperature T850 (°C), specific humidity SH850 (g/kg), geopotential heights GH850 (m) as well as wind speed WS850 (m/s) and direction WD850(.), the two latter calculated from the zonal and meridional wind components UW850 (m/s) and VW850 (m/s). Furthermore, surface solar radiation downward SRD (W/m²) was downloaded. Only variables which carry physically meaningful and relevant information to model MDA8 and MDA1 were included. Atmospheric changes due to climate change were covered by selecting circulation-

dynamic, thermo-dynamic, thermal, and radiation-based predictors. The mean of the nine grid boxes covering the area over and around each ozone station location was used to define station-based daily predictor data.

For O_3, the Copernicus Atmosphere Monitoring Service (CAMS) reanalysis from the European Centre for Medium-Range Weather Forecasts (ECMWF) was used (Inness et al., 2019). The CAMS reanalysis contains information about atmospheric composition and is assimilated from satellite retrievals of total column CO, tropospheric column NO_2, aerosol optical depth, and total column, partial column, and profile O_3 retrievals. For our study, we used O_3 data at the 850 hPa level from 2005 to 2019 at a monthly resolution (O3month), spatially interpolated to 1°x1° grid boxes of latitude and longitude.

In preparation for our study, we analyzed two other tropospheric O_3 reanalysis products in addition to the CAMS reanalysis: the O_3 data from the ERA5 reanalysis and the TCR-2 reanalysis from Miyazaki et al. (2020), the latter showing good results in the O_3 evaluation study from Park et al. (2020) for East Asia. A correlation analysis with the O_3 station data showed that the CAMS reanalysis had the best agreement with the observational data over most of our study area. The ERA5 O_3 data could reflect the spatial patterns of O_3 distribution over Europe to a very limited extent.

2.1.3. Earth System Model (ESM) Data

To estimate tropospheric O_3 concentrations over Europe on a station basis for the mid (2041-2060) and late 21st century (2081-2100), all available data from the Coupled Model Intercomparison Project Phase 6 (CMIP6, Eyring et al., 2016) were used. The number of ESMs available depends on the availability of data at the time of this publication. The atmospheric predictors (T850, SRD, GH850, UW850, VW850, SH850) were used at daily resolution. O_3 data at the 850 hPa level was only available at a monthly resolution. Data was extracted for the historical period and the two scenarios SSP2-4.5 and SSP3-7.0 (for a description of the SSPs see e.g., O'Neill et al., 2014). Seven ESMs could be used, which can be divided into two groups: models with O_3 prescribed from a data set (BCC-CSM2-MR, IPSL-CM6A-LR, MPI-ESM1-2-HR and MPI-ESM1-2-LR), and models which interactively compute the atmospheric chemistry by themselves (CESM2-WACCM, MRI-ESM2-0 and UKESM1-0-LL). Note that IPSL-CM6A-LR did not provide predictor data for 21 O_3 station locations in the alpine region.

For those ESMs that do not have an interactive chemistry model themselves, an O_3 dataset is provided as part of CMIP6. This CMIP6 O_3 dataset (Checa-Garcia, 2018) uses simulations of the CMAM and CESM-WACCM models that are part of the Chemistry-Climate Model Initiative (Eyring et al., 2013, Morgenstern et al., 2017). Thus, a dataset is available that contains a complete three-dimensional field for both the stratosphere and troposphere, spanning from pre-industrial times to the present, and to the end of the 21st century under the various SSP scenarios (O'Neill et al., 2015, Keeble et al., 2020). This is a key difference from the O_3 data used for CMIP5, which were based on stratospheric O_3 values from a combination of model and observational data between the 1970s and 2011, extended into the past and future under assumptions about changes in stratospheric chlorine and the 11-year solar cycle (Cionni et al., 2011). Note that for the models which do not model the O_3 concentrations interactively, the O_3 output is identical.

One of the three models with interactive chemical modeling is the CESM2-WACCM version of the Community Earth System Model version 2 (CESM2), which uses the Model for Ozone and Related chemical Tracers family of chemical mechanisms, covering the troposphere, stratosphere, mesosphere, and lower thermosphere (Gettelman et al., 2019, Emmons et al., 2020). The MRI-ESM2-0 model includes an interactive chemistry model, called MRI-CCM2.1 module, which simulates the distribution and evolution of O_3 and other trace gases in the troposphere and middle atmosphere (Yukimoto et al., 2019). The third model in our study with interactive chemical modelling, UKESM1-0-LL, uses the UKCA model (United Kingdom

Chemistry and Aerosol model) with unified stratospheric-tropospheric chemistry and close coupling between chemistry and aerosols (Sellar et al., 2019).

All ESM simulation output were re-gridded onto a 1° x 1° spatial resolution to align with the reanalysis data. The units were converted accordingly, and WS850 and WD850 were calculated from UW850 and VW850.

2.2. Methods

Figure 4.2 provides a schematic diagram illustrating the methodology used in this study. Detailed information is given in the following subsections.
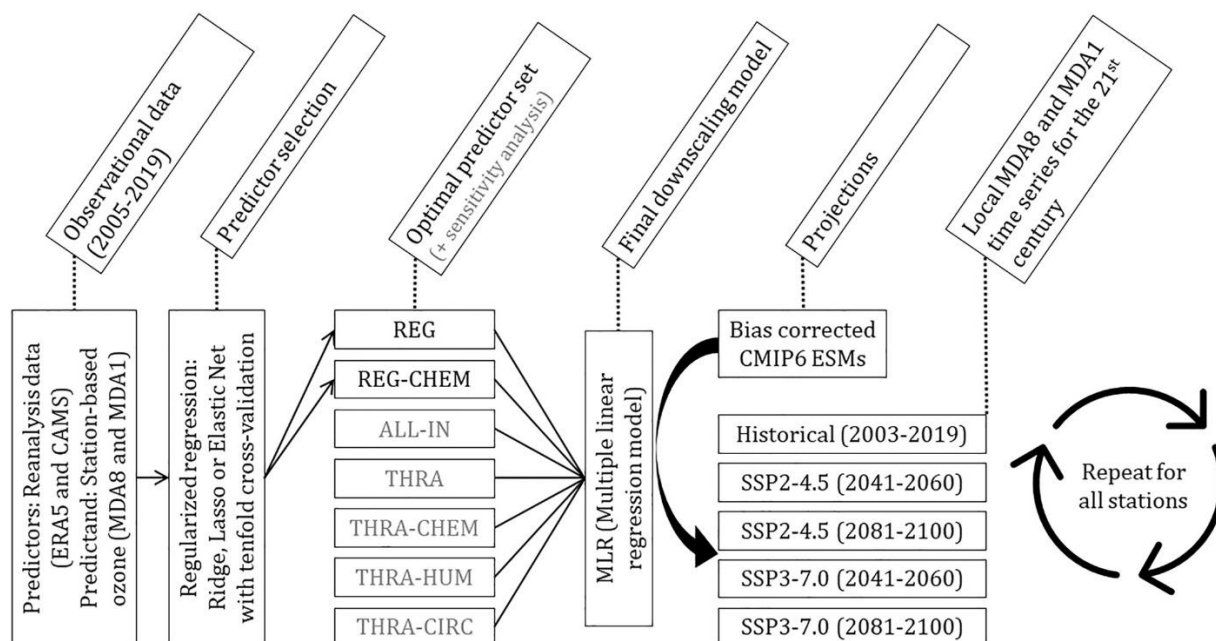
Fig. 4.2 Schematic diagram of the downscaling methodology

2.2.1. Statistical Downscaling Models and Sensitivity Analysis

Statistical downscaling models were built for the O_3 season from April to September, the time of the year when the highest O_3 concentrations occur over Europe. The models were used to establish station-specific relationships of meteorological and chemical predictors with MDA8 and MDA1. Daily time series of all selected and preprocessed meteorological variables as well as the monthly resolved O_3 data were used as initial predictors. Before entering any statistical model building process, each predictor was standardized by subtracting from the values the respective mean and then dividing it by the respective standard deviation. A station-specific modeling approach was chosen with an individualized predictor screening to generate site-specific optimums. Predictor selection was conducted using regularization with varying shrinkage methods (Hastie et al., 2009). Multiple Linear Regression (MLR), representing an effective tool to study the impact of predictors on the mean of the response variable, was used to model the relationship between all selected predictors and MDA8/MDA1.

A sensitivity analysis was conducted analyzing further varying settings of the statistical downscaling models, mainly differing in terms of the predictor variables used, to quantify more detailed the influence of specific predictors on the downscaling and projection results. A special focus was given to O3month as an emission-related predictor. All statistical downscaling models were evaluated by considering various model fit and performance metrics. Most of the data preparation and analysis including predictor selection, and hence regularized regression, model building as well as projections, were conducted using the R programming language (R version 4.1.0, IDE RStudio).

2.2.1.1. Predictor Selection and Main Models

Predictor selection was conducted using regularization with varying shrinkage methods to generate site-specific optimum predictor sets. Ridge, Lasso and Elastic Net regularized regression (Hastie et al., 2009) were considered. In this regard, ridge regression is considered best if all variables are useful as it shrinks all parameters but does not remove them. Lasso regression will be the best choice if the initial predictor set contains a lot of useless variables as these are excluded from the equation and simpler and easy to interpret results are generated. Elastic Net combines Lasso and Ridge regression penalty and thus combines the strengths of both options. It is the preferred option if, as in our case, there exist strong correlations between predictors. Elastic Net groups and shrinks the parameters associated with the correlated variables and leaves them in the equation or removes them all at once. The R package glmnet was applied for regularized regression and predictor selection. In an upstream tenfold cross-validation, the station-specific optimum value for alpha was defined. Lambda.1se instead of lambda.min was used as the former results in models with in general fewer parameters. This was preferred in our analysis since we aimed to identify the main drivers of O_3 at each site. As a result, MLR models based on site-specific predictor optimums were generated to establish the relationships between MDA8/MDA1 and their main drivers and to use these statistical downscaling models for station-based projections.

2.2.1.2. Model Fit and Performance

Fit and performance of the MLR statistical downscaling models were evaluated using two typical performance metrics: the adjusted coefficient of determination R^2 and the Root Mean Square Error RMSE. The fit and performance evaluation of the final station-based MLR models was embedded in its own tenfold cross-validation procedure. To judge overall performance, mean values were calculated for both metrics, and averaged for the 10 calibration (cal) and 10 validation (val) periods, respectively. Furthermore, adjusted R^2 was extracted from the final MLR models (R^2). Stations showing a sufficient model fit and performance were considered for further analysis and projections. In this regard, stations showing an R^2 value of at least 0.25 were selected.

2.2.1.3. Main Drivers

The final station-based statistical MLR downscaling models represent the results of the multistep predictor selection and model building approach that aimed to define the linkage between MDA8/MDA1 and their optimum predictor set. The impact of a predictor on the target variable can in general be interpreted in terms of the magnitude and the sign of the predictor's standardized regression coefficient. Thus, predictor variables can be ranked by importance to identify station-based main drivers. The most important drivers of MDA8/MDA1 were identified for each analyzed O_3 station location. This allows for the investigation of possible station-type- and region-specific differences and sensitivities under current and future climatic conditions.

2.2.1.4. Sensitivity Analysis

In addition to the station-specific optimal choice of predictors, different predictor configurations were tested to investigate the influence of specific predictor groups on downscaled MDA8/MDA1. The main model-building process and its framework described in the previous sections are used as a baseline and the following settings, differing mainly in terms of the predictors used, were evaluated.

1. Regularized (REG): Statistical models using the station-specific optimum predictor set from the regularized predictor selection described in section 2.2.1.1.

2. Regularized and chemistry (REG-CHEM): Statistical models using the station-specific optimum predictor set from the predictor selection described in section 2.2.1.1., with always

setting by default O3month as predictor to ensure the inclusion of the emissions-related information content.

3. All in (ALL-IN): Statistical models with all predictor variables included (O3month, T850, SH850, GH850, SRD, WS850 and WD850). Thus, no regularization was used, and all predictor variables were kept.

4. Thermal, radiative (THRA): Statistical models using only T850 and SRD to assess the isolated role of these most important meteorological predictors for ground-level O_3.

5. Thermal, radiative and chemistry (THRA-CHEM): Statistical models including T850, SRD, and O3month to measure the combined impact of the essential meteorological predictors and of emission changes.

6. Thermal, radiative and thermo-dynamic (THRA-HUM): Statistical models using the predictors T850, SRD, and SH850 to assess the additional influence of atmospheric humidity.

7. Thermal, radiative and circulation-dynamic (THRA-CIRC): Statistical models using T850, SRD, GH850 as well as WS850 and WD850. This setting was used to identify the role of atmospheric circulation dynamics on O_3 and its change.

For the first two options, a feature selection based on regularized regression in accordance with the described approach for the original model-building process was conducted to generate station-specific optimum predictor sets. For all other options, station-based MLR models were directly generated with the respective predictor sets. Model fit and performance were evaluated for all settings. The relationships of the predictors with MDA8/MDA1 established in the observation period for each option were subsequently used to assess the response of MDA8/MDA1 to future changes in the respective predictor sets. Consequently, the projections of all varying settings from the sensitivity analysis could be compared.

2.2.2. Bias Correction of ESM Data

Prior to using the ESM data within the statistical downscaling models, they were bias corrected using a univariate quantile mapping method (using the R package MBC; Cannon, 2018). The atmospheric variables from the ERA5 reanalysis and the CAMS reanalysis for O_3 were used as the correction basis. Since the historical CMIP6 runs ended in 2014, they were extended to 2019 using data from scenario SSP3-7.0. Bias correction was performed for each grid point in the entire European study area. Similar to Cannon (2018) three consecutive months in a shifting window were used, and only the central month was kept. If less than 20% of the days per grid point and 3-month window were missing, the bias correction was calculated, otherwise, the grid point was flagged as missing value. Bias correction was calculated separately for each scenario (SSP2-4.5 and SSP3-7.0), and for each time slice (2041-2060 and 2081-2100) using the reference period 2003-2019.

2.2.3. Statistical Projections

Statistical projections under climate and emission changes were generated by replacing reanalysis predictor data with bias-corrected ESM output in the MLR models. Time slice differences under the two selected scenarios SSP2-4.5 and SSP3-7.0 for the future periods 2041-2060 and 2081-2100 compared with the historical period 2003-19 were used to illustrate the local O_3 changes under future climate change.

3. Results

Results are shown for MDA8 since most health-relevant guidelines and threshold values refer to this value. Results for MDA1 are similar and can be found in the Supplement. Note that

differing numbers of ozone measuring stations were included in the various analyses, due to the different statistical downscaling performances of the stations under different predictand and predictor sets.

3.1. Statistical Downscaling Model Performance

Table 4.1 Statistical downscaling model performance of the different predictor sets based on 623 stations

Option	Predictor	R^2	R^2.cal	R^2.val	RMSE.cal	RMSE.val
1	REG	0.52	0.46	0.46	8.09	8.11
2	REG-CHEM	0.52	0.46	0.46	8.09	8.10
3	ALL-IN	0.52	0.48	0.47	8.01	8.03
4	THRA	0.46	0.40	0.40	8.55	8.55
5	THRA-CHEM	0.49	0.44	0.44	8.22	8.23
6	THRA-HUM	0.46	0.41	0.41	8.50	8.50
7	THRA-CIRC	0.48	0.43	0.42	8.37	8.38

Note. Given are the adjusted coefficient of determination R^2 and the Root Mean Square Error RMSE [in ppbv] as means over the 10 calibration (cal) and validation (val) periods as well as final R^2 for MDA8.

The performance of the MLR models was evaluated using a tenfold cross-validation. To judge and compare the different predictor sets performance was calculated as mean values over the 10 calibration and 10 validation periods as well as for the final MLR models using the whole time series. Stations showing a final R^2 value of at least 0.25 were selected. This led to a reduction of the originally 798 stations to 716 stations for the predictor set REG, and to 720 stations for both predictor sets ALL-IN and REG-CHEM. The criterion for exclusion of 0.25 led to 682 stations for the set THRA-CHEM, 671 stations for the set THRA-CIRC, 635 stations for the set THRA-HUM, and down to 623 stations for the predictor set THRA. Thus, with the predictor sets REG, REG-CHEM, and ALL-IN the vast majority of stations could be assessed, whereas the reductions of the number of assessable stations for the other predictor sets point to missing predictor information in these sets to adequately capture ozone variation in some regions.

The over all predictor combinations shared set of 623 stations was used for a further comparison of the predictor performance in the observational period. Interestingly, all predictor sets yielded a comparable performance for the stations considered (Table 4.1). Thus, the predictors T850 and SRD (THRA) could already explain a large fraction of the daily MDA8 variability. The inclusion of other meteorological and chemical information did not substantially increase statistical performance. However, keep in mind that using the sets REG, REG-CHEM, and ALL-IN resulted in almost 100 stations more which could be assessed compared to the set THRA, indicating that THRA is a decisive predictor set only for some regions of Europe. Thus, stations with high model performance using THRA concentrated mainly over Central Europe, while for southern, western, and north-western European stations further predictors were needed.

For further analysis, we chose the predictor set REG-CHEM since it combines a good model performance, robust downscaling models derived from regularization and assures the inclusion of information on meteorology as well as emission changes in the projections. Thus, the results of the predictor set REG-CHEM for MDA8 from April to September at 720 measuring stations are discussed in the following.

3.2.   Main Predictors

Specific predictors emerged as prominent factors governing daily MDA8 variability. Figure 4.3 shows the three most important predictors of the predictor set REG-CHEM for MDA8 in the O_3 season from April to September. In the majority of the statistical downscaling models O3month, SRD and T850 were selected. For most of the stations in Central and southern Europe, the most important predictor was either T850 or SRD, whereas for stations in northern Europe O3month was selected. For some maritime stations in southern Europe SH850 or WS850 constituted the most important predictor, indicating the role of meso-scale land-sea circulation systems (Figure 4.3, left). In Central Europe, the second most important predictor was still a thermal or radiative one. However, for many stations, O3month was selected. In southern Europe, SH850 emerged as an important driving factor (Figure 4.3, middle). O3month constituted the third most important predictor at most stations in Central Europe, but SH850 played a role for stations in eastern Europe as well as WD850 in western Europe (Figure 4.3, right), the latter pointing to the importance of inflow of polluted air masses.
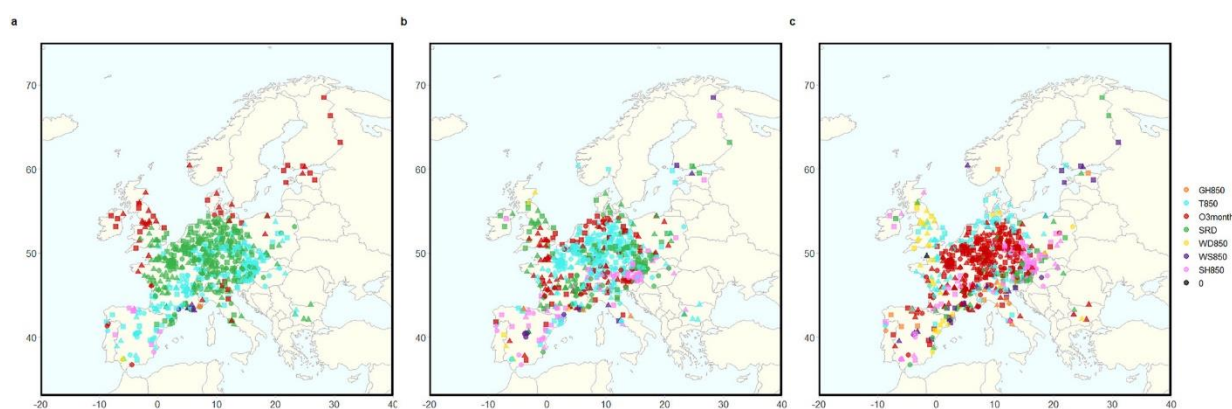
Fig. 4.3 Predictors chosen in the multiple linear regression models using the predictor set REG-CHEM
From left to right: most important predictor, second most important predictor, third most important predictor for MDA8 (0 = no third predictor variable).

Overall, for all of the 720 stations O3month was selected as a predictor, for 715 stations SRD and 686 stations T850. All three predictors had strong positive regression coefficients in the MLR models. SH850 was included in the statistical downscaling models only for 339 stations, with a medium strong, negative coefficient. WS850 was selected for 613 stations, WD850 for 513 stations, and GH850 for 308 stations, all of them with relatively low, negative coefficients. In summary, O3month plays a decisive role in the statistical downscaling models to explain daily MDA8 variability, implying that the emission-related predictor information is important and enhances statistical downscaling model quality. The selection of SRD and T850 as prominent meteorological predictors reflects the photochemical, temperature-dependent build-up of O_3. SH850 only played an important role in some European regions, whereas the frequent selection of the negative association of WS850 with MDA8 points to in-situ O_3 formation under low-flow conditions.

3.3.   Bias Correction

With the bias correction method QDM, the partly strong model deviations of the individual climate models could be satisfactorily adjusted. Figure 4.4 gives the raw and the adjusted output for the three most important predictors T850, SRD as well as O3month for the months April to September in the historical period 2003-2019.
The raw output of the seven ESMs showed for T850 and SRD different amounts of biases, which were spatially different, compared to the observation-based ERA5 reanalysis. For T850 deviations of up to ± 4.5°C were found, for SRD up to ±60 W/m² at individual locations.

O3month, shown at the bottom of Figure 4.4, had compared to the CAMS reanalysis an almost identical pattern for the models with no interactive chemistry modeling, with slightly too high O_3 values over Europe, strongest over the Alps and Turkey and small negative biases in the European North. The ESM UKESM1-0-LL with active chemistry modeling had the highest biases in the summertime, especially in the Mediterranean area.

The bias correction satisfactorily minimized model errors for all predictors. Model errors after bias correction were within ±0.35°C for T850, ±4 W/m^2 for SRD, and ±0.6 ppbv for O3month (see again Figure 4.4). The remaining errors for the other predictors were also very small. We also examined whether the bias correction modified the change signals in future scenarios. It was found that the change signals were not affected by the bias correction (not shown here).
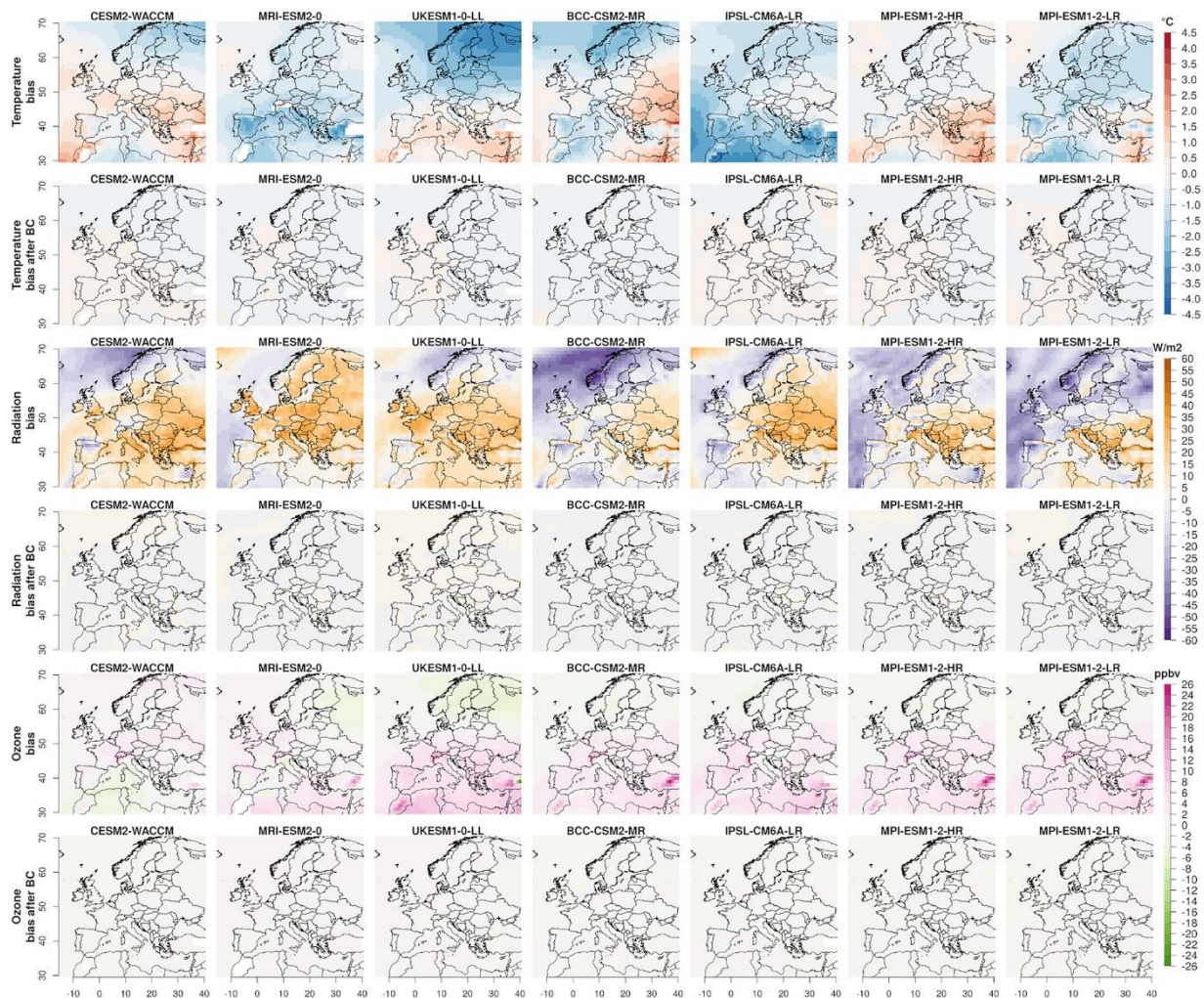
Fig. 4.4 Biases before and after bias correction (BC) of the three most important predictors T850 [°C], SRD [W/m^2], and O3month at 850 hPa [ppbv] for the O$_3$ peak season April-September in the historical period 2003-2019
Bias correction reference for T850 and SRD: ERA5 reanalysis, for O3month: Copernicus Atmosphere Monitoring Service reanalysis.

3.4.   Statistical Projections Under Climate and Emission Changes

The results in Sections 3.4.1. and 3.4.2. are based on the statistical models using the station-specific optimum predictor set from the predictor selection described in Section 2.2.1.1. with always setting by default O3month as predictor (REG-CHEM). Results are given for MDA8 from April to September for the 720 stations which could be assessed using this predictor set. A discussion about the role of the other predictor sets on projected MDA8 is given in Section 3.4.3.

3.4.1. Individual ESM Results

Figure 4.5 shows the downscaled MDA8 changes for the single ESM ensemble members. The two top rows show the downscaled near future changes as average in the period 2041-2060, and the bottom rows illustrate the change signals for the end of the 21st century (2081-2100) for each station. The two scenarios SSP2-4.5 and SSP3-7.0 are shown one above the other in each case. A general trend can be seen from the figures of the individual models. SSP2-4.5 led to decreasing MDA8 concentrations for almost all ESMs, while the more pessimistic scenario SSP3-7.0 projected increasing concentrations over Europe, especially at the end of the 21st century. However, there were exceptions for the individual ESMs. For example, the MRI-ESM2-0 model consistently projected almost only negative trends even in the pessimistic scenario, while the UKESM1-0-LL model simulated predominantly increases in ground-level MDA8 concentrations even in the more optimistic scenario SSP2-4.5. At the end of the century, these were particularly strong.
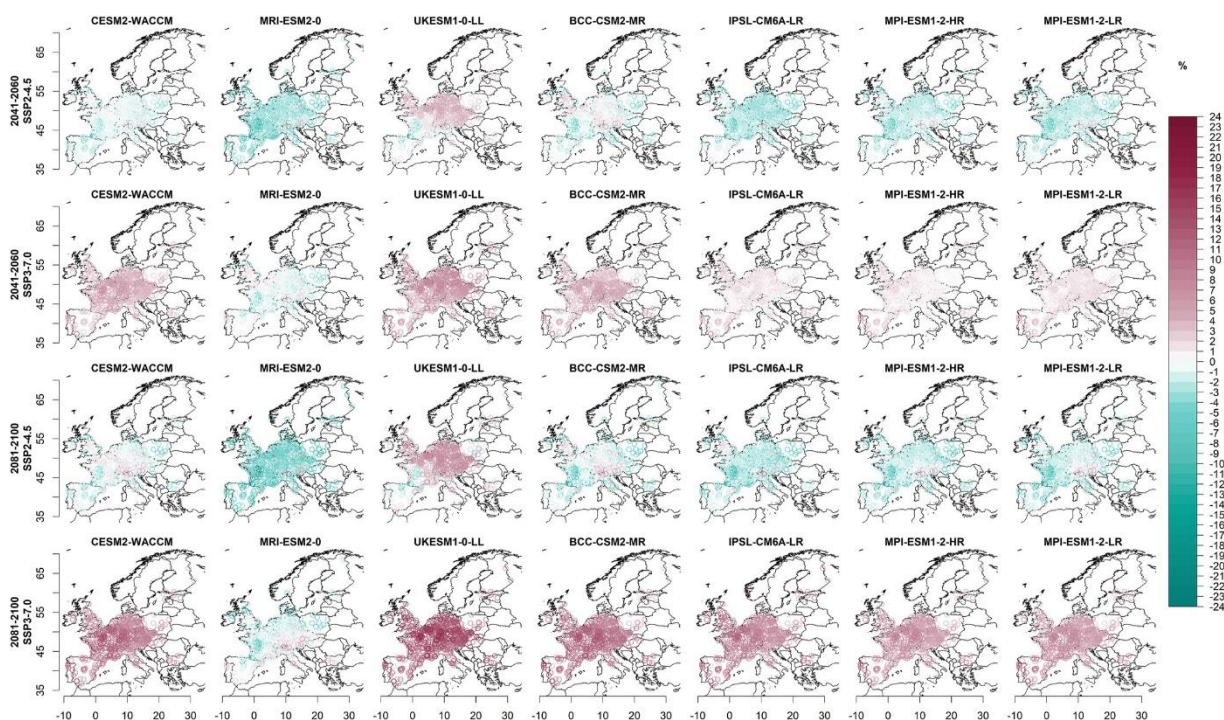
Fig. 4.5 Change signals [%] of downscaled ground-level MDA8 concentrations at 720 O$_3$ measuring stations across Europe for all investigated CMIP6 earth system models. Shown are results for SSP2-4.5, SSP3-7.0, and the years 2041-2060 and 2081-2100.

To understand the reasons for the differing MDA8 projection results from the individual climate models, the change signals of the three most important predictors are examined below.

Figure 4.6 shows the projected T850 progression in the 21st century for the O$_3$ peak season April to September. For each individual model of the CMIP6 ensemble, the change signals of the bias-corrected data are given for the periods 2041-2060 and 2081-2100, and for the two scenarios SSP2-4.5 and SSP3-7.0. In the mid 21st century, the two scenarios were not yet very different from each other and projected a temperature increase of about 2°C, compared to the historical period 2003-2019 (shown in the top two rows of Figure 4.6). However, toward the end of the 21st century, especially scenario SSP3-7.0 yielded a further temperature increase over Europe. The differences between the individual climate models increased as well. In all projections, the UKESM1-0-LL model stood out with particularly strong warming trends, reaching up to 8°C in the more pessimistic scenario.

The change of SRD (Figure 4.7) shows a very heterogeneous picture of increasing and decreasing tendencies. With some exceptions, over the European land areas, an increase of

radiation was projected and over the sea decreasing radiation sums. UKESM1-0-LL stood out, again, with strongly increasing SRD north of the Mediterranean Sea at the end of the 21st century. The two very strong positive trends of T850 and SRD in the UKESM1-0-LL model induced the consistently increasing, partly very pronounced O_3 concentrations, seen in Figure 4.5.
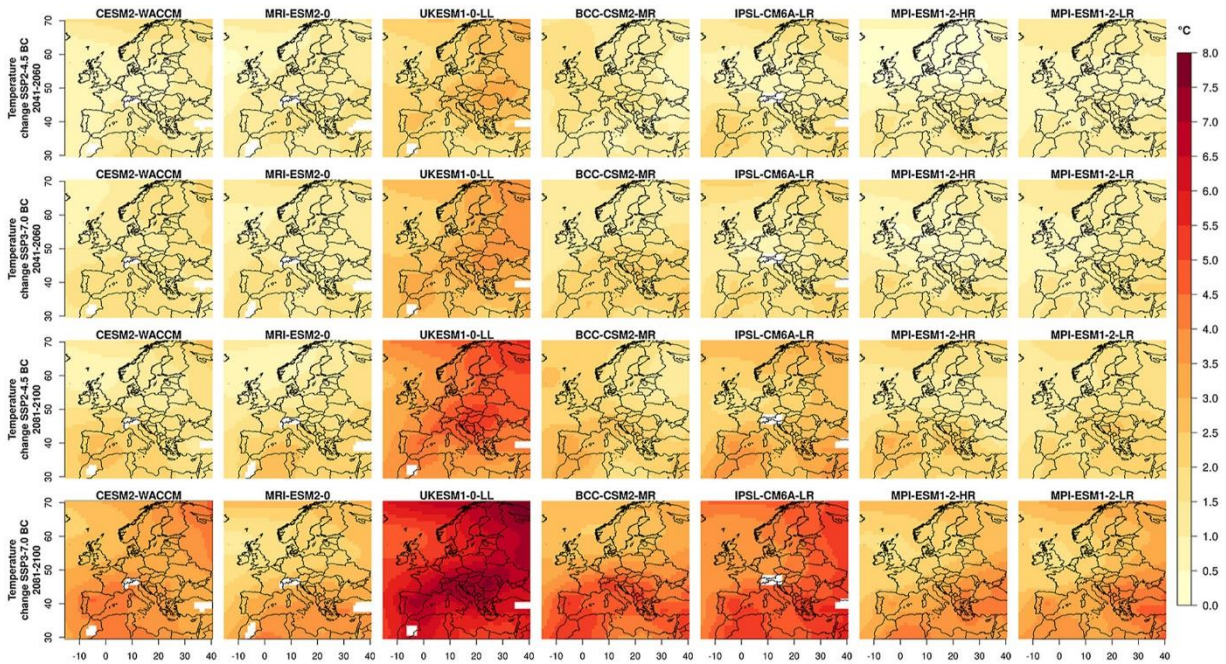
Fig. 4.6 Change signals of bias-corrected (BC) CMIP6 T850 [°C] for the O_3 peak season April-September for the years 2041-2060 (top rows) and 2081-2100 (bottom rows) compared to 2003-2019 and the two scenarios SSP2-4.5 and SSP3-7.0
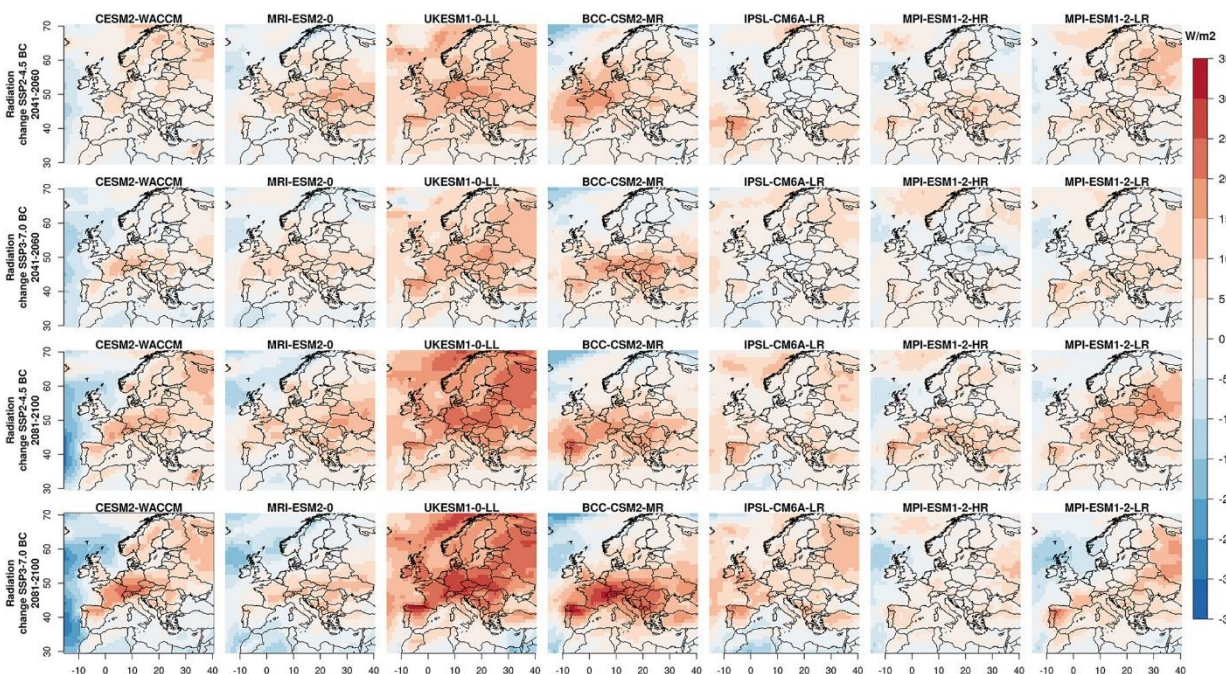
Fig. 4.7 As Figure 4.6, but for SRD [W/m²]

Figure 4.8 shows the projected changes in O3month from the CMIP6 ensemble. As expected, the four models with prescribed O_3 concentrations from the Chemistry-Climate Model Initiative O_3 data set yielded an almost identical O3month projection. The CESM2-WACCM model also exhibited a very similar picture because it is part of the Chemistry-Climate Model Initiative and

thus provided O₃ data for the other models without active chemistry modeling. It is noticeable that the two scenarios were fundamentally different from each other in their change signals. Scenario SSP2-4.5 led to decreasing O3month concentrations, while scenario SSP3-7.0 resulted in O3month increases. An exception was the MRI-ESM2-0 model with active chemistry, which also simulated predominantly decreasing O3month levels over Europe for scenario SSP3-7.0. This was reflected then in the results of the downscaled station MDA8 from Figure 4.5, where negative MDA8 concentrations occurred despite increasing T850 and SRD.
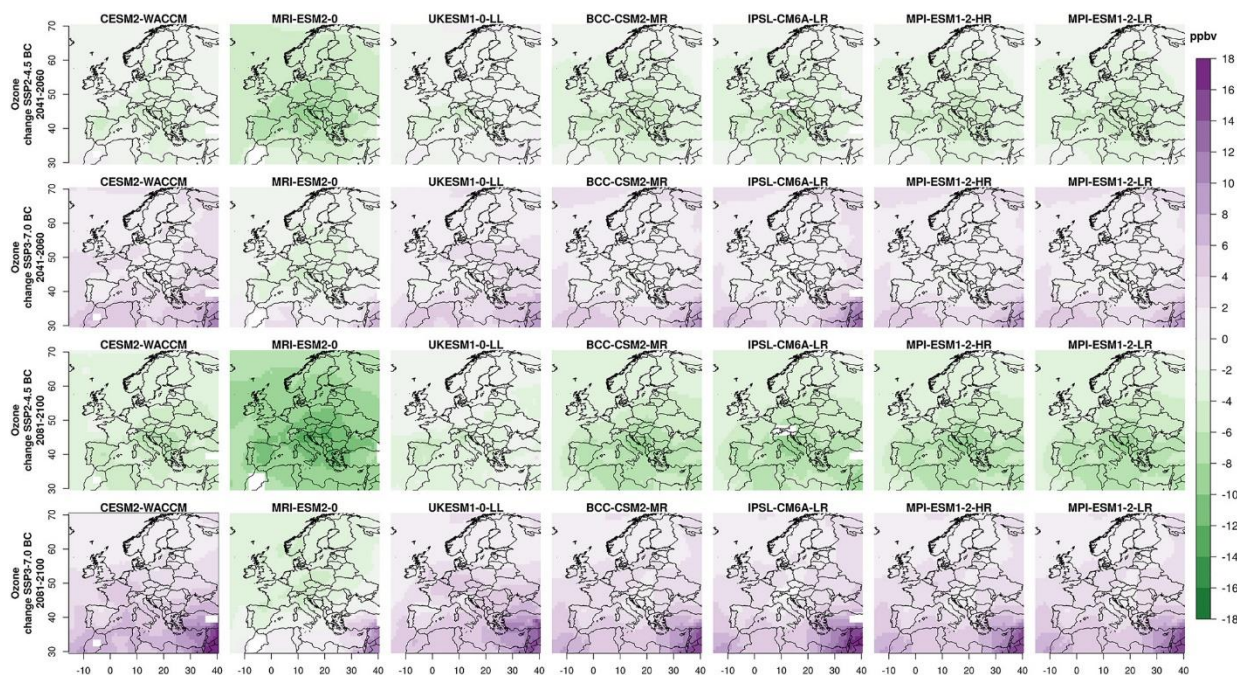
Fig. 4.8 As Figure 4.6, but for O3month [ppbv]

The individual analysis of the climate models showed that a distinction between models with and without an active chemical component was not decisive for the downscaling results, since the other predictors could determine the future MDA8 concentrations, as shown for the model UKESM1-0-LL.

3.4.2. Multi-Model Mean

Figure 4.9 shows the projection results of the CMIP6 models as Multi-Model Mean (MMM). In a world that follows the SSP2 scenario, called "Middle of the Road", in which social, economic, and technological trends do not shift markedly from historical patterns and climate protection measures are adopted, the MDA8 concentrations over Europe were projected to decrease. The mean decrease over all stations was -1.75% at the mid-century and about -1.94% at the end of the century. Thus, most of the MDA8 reduction might already be achieved by mid-century, with a small additional decrease occurring in subsequent years. The negative trend was not simulated for the center of the United Kingdom and at some stations in the Alps. Some weak positive trends were observed here. The strongest decreases occurred in western France, where all CMIP6 models in our ensemble showed a consistent decline. However, if the world develops according to scenario SSP3, which is characterized by regional rivalries and a revival of nationalism, pushing global issues into the background, causing severe environmental degradation, and making mitigation and adaptation to climate change more difficult, projected ground-level MDA8 concentrations look very different. On average, the model ensemble projected a +1.82% increase in MDA8 concentrations across Europe by the mid-century, increasing considerably to +5.49% by 2100. By the end of the 21st century, increases of up to 16% were projected at some European stations. All regions were affected by strong increases, no clear regional differences could be identified.
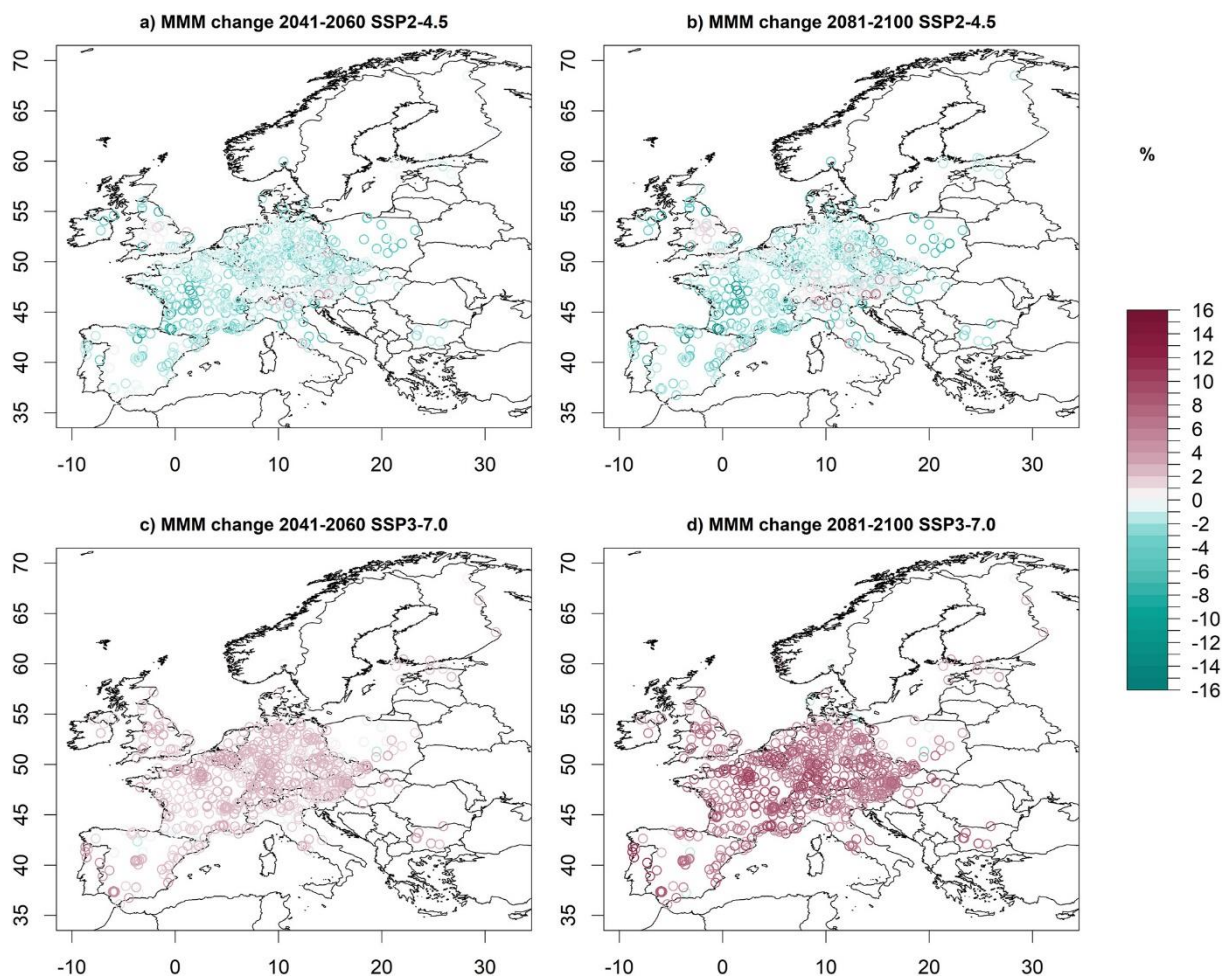
Fig. 4.9 Multi-Model Mean (MMM) change [%] of downscaled ground-level MDA8 for 720 O$_3$ measuring stations over Europe
Shown are results for SSP2-4.5, SSP3-7.0 and the years 2041-2060 and 2081-2100 compared to the historical period 2003-2019.

3.4.3. Impact of Different Predictor Settings

The model performance in the observational period is just one indicator for the overall statistical downscaling model performance since it does not necessarily guarantee the suitability of a predictor set to assess future MDA8 changes. While a good observational model performance hints at the successful capture of the relationships under current climate and environmental conditions, for projections a predictor set has also to carry the relevant signals of climate and emission changes that impact future MDA8 progression.

As for the comparison of the model performance in Section 3.1, the common set of 623 stations was used, again. The comparison of the impact of different predictor settings on future MDA8 concentrations showed that there are considerable differences when using only meteorological information compared to the inclusion of information on emission changes.

Table 4.2 shows the downscaled MDA8 changes as mean across the 623 measuring stations and the different ESMs. Using only meteorological predictors (THRA, THRA-HUM, THRA-CIRC) resulted in projected increases of MDA8 for both scenarios and time slices. At the middle of the century MDA8 increased by about 1.5% for both scenarios and at the end of the century increased by 2.6%-2.8% under SSP2-4.5, and 3.6%-3.8% under SSP3-7.0. Despite the differing importance of the meteorological predictors across Europe to explain MDA8 variability (see section 3.2) and their differing climate change signals, the increases were visible for almost all stations across the European area with no specific regional pattern (not shown). In contrast, the inclusion of information on emission changes (REG, REG-CHEM, ALL-

IN, THRA-CHEM) modified the sign of change under SSP2-4.5 scenario assumptions, yielding decreases of about -1.7% to -1.9% during the 21st century. This points to the effectiveness of the emission reductions of the precursor gases which outweigh the O_3 increases caused by climate change. Under the more pessimistic SSP3-7.0 scenario, which does not include effective emission reductions, MDA8 was projected to increase. These increases were even stronger compared to the assessments using only meteorological information and amounted to 1.8%-1.9% at the mid-century and 5.6%-5.8% at the end of the century, implying that there is a combined "climate change and emission penalty" on future O_3 concentrations. For all emission-including predictor sets the spatial pattern of MDA8 changes followed the patterns illustrated in Figure 4.9.

Table 4.2 Multi-model mean (MMM) change [%] of downscaled ground-level MDA8 as mean over 623 O_3 measuring stations over Europe using different predictor sets

Option	Predictors	SSP2-4.5 2041-2060 minus 2003-2019	SSP2-4.5 2081-2100 minus 2003-2019	SSP3-7.0 2041-2060 minus 2003-2019	SSP3-7.0 2081-2100 minus 2003-2019
1	REG	-1.76	-1.88	1.80	5.69
2	REG-CHEM	-1.75	-1.86	1.79	5.57
3	ALL-IN	-1.81	-1.92	1.81	5.64
4	THRA	1.64	2.78	1.64	3.81
5	THRA-CHEM	-1.69	-1.78	1.91	5.79
6	THRA-HUM	1.60	2.74	1.63	3.79
7	THRA-CIRC	1.54	2.62	1.53	3.63

Note. Shown are results for SSP2-4.5, SSP3-7.0 and the years 2041-2060 and 2081-2100 compared to the historical period 2003-2019.

4. Discussion

A PP downscaling approach was adopted to assess local ground-level MDA8 and MDA1 concentrations in the European area. Despite many advancements in the current ESMs, there is still the need for downscaling to provide highly-resolved climate change information. In this regard, knowledge about local future ground-level O_3 concentrations is of particular interest to protect human health and to design corresponding mitigation and adaptation strategies. According to Liu et al. (2022) methods to obtain O_3 estimates can be divided into regional and global chemical transport models, statistical models, geostatistical data fusion, and machine learning models. While dynamical climate chemistry models are a useful tool to assess future O_3, they come with the drawback of being computationally expensive and thus the number of model runs is limited. Machine learning models have a very good performance, but they are generally characterized by low interpretability (Liu et al., 2022). Statistical models, which are very flexible, computationally inexpensive, and easy to interpret, have so far only used meteorological information to assess future O_3 concentrations, neglecting information about the precursor emissions. In this study, this shortcoming was addressed by incorporating information about the precursor emissions into the statistical downscaling models. This was done not by using NO_x or VOCs directly as predictors, but via the inclusion of O_3 as predictor,

thus providing information about their final impact, including emission, transport, transformation, and deposition processes, as assessed in the reanalysis and climate model products.

The statistical downscaling models were calibrated and validated in the observational period using a regularization approach to carefully capture the predictors-predictand relationships. The selection of the predictors and their association with MDA8/MDA1 in the statistical models was in accordance with previous studies (e.g., Jahn and Hertig, 2022, Jahn and Hertig, 2021, Otero et al., 2016). Model performance was assessed using R^2 and RMSE. The overall assessable stations mean model performance amounted to about 50% explained variance (R^2 of approx. 0.5), which shows that local MDA8/MDA1 concentrations are not only governed by larger-scale factors, but also by local characteristics, which cannot be captured in such a downscaling approach. Furthermore, the model performance varied across the European area, pointing to a differing sensitivity of local MDA8/MDA1 variability to the larger-scale forcings, confirming the findings of Jahn and Hertig (2022) who showed that there exists a strong connection between ground-level O_3 to the larger-scale meteorology in Central Europe, whereas for northern and southern Europe other processes must be considered.

There has been large progress in chemistry-climate modeling leading to an advanced representation of O_3, but models still show partly large biases and considerable uncertainties exist (Young et al., 2018). The output of seven CMIP6 models was used in the current study, with three of them having interactive chemical modeling, while the other four used prescribed O_3 from the CMIP6 ozone dataset. However, statistically downscaled future MDA8/MDA1, assessed using the CMIP6 model output variables as predictors, could not be divided into two groups, interactive versus prescribed. Rather, the differences between the individual models across all models were dominant. The use of MRI-ESM2-0 output as predictors in the predictor set REG-CHEM yielded mainly negative MDA8/MDA1 trends, whereas UKESM1-0-LL output led to increases of MDA8/MDA1, with the other models providing assessment results in between. A general feature across almost all ESMs was decreasing MDA8/MDA1 concentrations under the SSP2-4.5 scenario, while the use of the more pessimistic scenario SSP3-7.0 led to increasing concentrations over Europe, especially at the end of the 21st century.

This general picture emerged when using meteorological factors as well as information about emission changes, while the pure meteorological predictor sets led to projected increases of MDA8/MDA1 in both scenarios. Regarding content this highlights the necessity to further reduce air pollution in the European area, bringing forth better protection of human health from direct emissions like NO_x as well as indirect pollutants such as O_3. From a methodological viewpoint, this points to the necessity to include information about emission changes in statistical projections to provide a more realistic assessment of future O_3 progression.

Multiple uncertainties exist within statistical downscaling assessments of ground-level O_3 under climate change which must be addressed properly. First, these uncertainties are related to the chosen downscaling method. Here, MLR with regularization and a thorough calibration/validation procedure was used which was appropriate for the intended application and led to robust and reproducible results. Further, the choice of predictors affects the results and predictors were selected which are physically related to the predictand and contain information about climate change as well as changes of the precursor emissions. Climate change scenarios depend per se on the assumptions made within them and more than one scenario was regarded to illustrate a range of possible future evolution. Advancements in climate-chemistry modeling have led to more realistic assessments, but there are still many uncertainties. One way to attenuate these uncertainties was the use of multiple models spanning the range of possible future O_3 progression.

Recently, modern ESM ensemble learning methods for O_3 have been developed. These methods combine multiple algorithms and show high performance and stability. Thus, Requia et al. (2020) and Sun and Archibald (2021) developed multi-stage ensemble-learning

frameworks based on random forest, gradient boosting, and neural network approaches, the latter also a 2-stage space-time Bayesian neural networks approach. While these methods greatly improve surface O_3 modeling, they are computationally relatively expensive, and the cannot treat the fusion of a small number of ESMs very well. So far, these methods have only been used with monthly O_3 data. Because the availability of daily data from the CMIP6 models is limited and yields a relatively small ensemble of models, complex model weighting or model fusion was not feasible in the present study. However, with our downscaling methodology, a weighting method of the individual ESMs would be possible as postprocessing. This was not done in this work, because the focus was rather on the sensitivity study of the predictors (particularly the influence of ozone as a predictor) and the influence of the different SSPs in the scenarios.

5. Conclusions

The provision of accurate estimates of local-scale ground-level O_3 under current conditions as well as under climate change is still a challenging task. Ground-level O_3 concentrations depend on the chemical and physical processes that govern the formation, transport, transformation, and deposition. These processes are controlled by multiple factors such as the characteristics and distribution of precursors, the larger-scale meteorology, and local-scale environmental conditions. Besides state-of-the-art chemical transport modeling, statistical approaches are useful tools to analyse and assess O_3. Under climate change, there are major concerns that O_3 concentrations will increase, despite efforts for a better air pollution control. The results of the present study for local-scale ground-level ozone across the European area confirm this rating, with projected MDA8/MDA1 decreases under the SSP2-4.5 scenario, but increases under the scenario SSP3-7.0.

The present study contributes to the health-relevant topic of O_3 air pollution under climate and emission changes by assessing local-scale daily MDA8/MDA1 changes using the latest data and statistical methodology. In this regard, state-of-the-art ESM fusion methods (e.g., Liu et al., 2022, Sun and Archibald, 2021) are promising approaches to further improve the methodology presented in this study. Besides, for health impact assessments and public health and policy interventions, it is important to provide further information about changes in health-relevant thresholds such as the MDA8 value of 100 μg/m^3 for short-term O_3 exposure and of 60 μg/m^3 in the peak season (highest average in six consecutive months) for long-term exposure (WHO, 2021). Furthermore, there is a need to refine exposure-response relationships from epidemiological studies to accurately estimate associated health burdens (Seltzer et al., 2018). Also, information about co-occurring heat stress as well as changes with respect to the susceptible population, as for instance considered in an assessment of future ozone and heat-related mortality by Orru et al. (2019), is useful information in this context. In this regard, the downscaling results of the present study provide a valuable basis for future studies.

5. Chapter 5 - Summary and Synthesis

This dissertation investigated the relationship between ground-level ozone and surface air temperature as well as the influence of meteorological, (prevailing) air pollution and synoptic conditions on surface ozone alone and in the context of health-relevant compound ozone-temperature occurrences across Europe. Spatiotemporal patterns and characteristics of ozone and temperature by analyzing regional variabilities of and the link between both target variables as well as by assessing the general and region-specific most important key drivers of compound o-t-events were revealed. In addition, the influence of recent but also projected future region- and site-specific health burden induced by ground-level ozone alone or in combination with heat was assessed regarding single and combined changes in climate and precursor emissions. In Chapter 1.3 four research areas were postulated with several leading research questions raised within. The proposed solutions were subsequently set out in Chapters 2-4. In the following, the main conclusions obtained for each RA are outlined with respect to each RQ alongside a general, summarizing synthesis and discussion of results and central, most important findings.

5.1 RA1: European O-t-Associations and Main Drivers

(Research Article 1)

A variety of assessments investigated ground-level ozone as well as heat occurrences separately for Europe, as both target variables represent severe health stressors inducing a substantial health burden for the general population. But there exists, as already outlined, only a rare number of studies analyzing concurrent health-relevant elevated air temperature and ozone pollution levels in Europe, which is especially true for projection studies (also refer to RA3 in this regard). The first study of this dissertation outlined in Chapter 2 - Research Article 1 hence complemented previous work and examined the relationship between both target variables as well as the capability of two different statistical downscaling model and projection approaches based on lasso logistic, and multiple linear regression to capture the current and future occurrence of health-relevant compound o-t-events. In the following, to address RQ1 of RA1, results of the initial descriptive and correlation analysis are presented that were conducted within Research Article 1. Main design and results of the statistical downscaling models are subsequently outlined, with the key findings of the main driver analysis specifically and separately described, to give answer to RQ2 of RA1. This chapter ends with a short summary highlighting the most important findings and contributions to RA1.

> **RA1-RQ1:** Is there an association between day-to-day variation in surface ozone and air temperature levels in Europe?

To address RA1-RQ1, a descriptive analysis of and spearman rank correlation evaluation between ground-level ozone and surface air temperature was conducted. Based on the higher observed correlation between daily and monthly maximum daily surface ozone and air temperature values from April to September, a respective o-t-season was defined. In this season, a strong relationship between both variables was indicated, in which also a higher frequency of compound o-t-event days was observed. However, notable discrepancies alongside lower site-specific correlations were found in southern and northern parts of Europe, leading to an exclusion of certain locations outside central Europe in this first study comprising Research Article 1. The presumption of a strong positive correlation between surface ozone and air temperature was hence confirmed for all further analyzed stations in central Europe. More than half of all days with thermal load also showed ozone exceedances. A high proportion of days (almost a fifth of all observed days) in the observation period and season showed threshold exceedances of both variables. The findings highlighted and confirmed the strong

relationship between thermal load and ozone pollution. These results hence already revealed that there exist clear associations between daily surface ozone and air temperature variabilities and between health-relevant levels of both target variables, at least and particularly in central Europe.

RA1-RQ2: How do statistical regression-based downscaling models represent the influence of main drivers based on meteorological variables and prevailing ozone persistence on health-relevant compound o-t-events in central Europe?

Statistical regression- and station-based downscaling models representing the results of two multistep modeling approaches were generated to capture central European compound o-t-events. As previous studies had already revealed the important role of prevailing ozone concentration levels or pollution episodes on current ozone concentrations at least in parts of Europe (e.g., Otero et al., 2016, Hertig et al., 2019), beside a preliminary meteorological predictor screening process based on reanalysis and climate model data, several prevailing ozone pollution metrics were evaluated. Finally, the first previous day was selected of all initial chosen persistence metrics and entered the statistical downscaling station-based models as ozone persistence predictor. Furthermore, by a further screening procedure primary based on lasso regression, a unified meteorological predictor set was defined and used for all station-based statistical downscaling models across central Europe. The models were thus developed to initially capture the relationship between large-scale predictors, ozone pollution levels, and local-scale compound o-t-events in the observational period.

Results revealed that the logistic regression approach directly assessing the probability of combined o-t-events clearly outperformed the second approach based on multiple linear regression. The inclusion of ozone persistence, i.e., the ozone concentrations from the pervious day, as predictor generally improved substantially the statistical model performance of both modeling approaches. Evaluation revealed a clear variation of model performance across the European study domain. The in general by far lesser performance of the second model approach in assessing compound o-t-events already indicated the general inability of the multiple linear regression-based models to capture elevated levels of both target variables. But, in accordance that multiple linear regression commonly represents an effective tool to model the mean of a response variable, respective generated models predicted on the other hand ozone concentrations reasonably well across central Europe. Consequently, as the result of the extensive model performance evaluation, statistical downscaling models based on logistic regression were evaluated to be the best and final chosen approach in modeling and later projecting (please refer to RA3 for more detail) compound o-t-events, while multiple linear regression was evaluated suitable to predict the single surface ozone response.

In general, a predictor variable's effect on prediction can be expressed by its regression coefficient, with values significantly different from zero contributing to the prediction. Regarding the relative importance of drivers, primarily expressed by the absolute value and the sign of the respective standardized regression coefficients, site-specific key mechanisms and factors were evaluated for each station location. The results generally revealed distinct regional patterns in terms of not only statistical model performance, but also in the dominance of the three most important main drivers. Ozone persistence and mean temperatures represented the most important influencing factors of compound o-t-events in northwestern and southern to eastern parts of the study domain, respectively. Regarding the findings for the mean of the response variable assessed by multiple linear regression as well, ozone persistence became evident to be the governing factor in surface ozone at each single station location across central Europe. Hence, results presented in Chapter 2 - Research Article 1 indicated in general the important role of ozone persistence, causing long-lasting or obstinately elevated ozone levels on several subsequent days, on the occurrence of surface ozone as well as health-relevant concurrent elevated levels of both target variables.

RA1: Summary and Contributions

To sum up, the first assessment (Chapter 2 - Research Article 1) provided further insights into the impacts of key drivers on ground-level ozone and compound o-t-events over Europe during the here defined o-t-season from April to September. The contributions to RA1 were mainly achieved by a preliminary analysis and evaluation of statistical regression-based downscaling models capturing the relationship between both target variables as well as between large-scale meteorological predictors, prevailing ozone pollution levels, and local-scale compound o-t-events in central Europe. The analysis therefore built the basis of the subsequent research work (Research Articles 2 and 3 outlined in Chapters 3 and 4). The prior suitability of logistic regression to model compound elevated levels of both target variables was identified and hence the following modeling and projection study (Chapter 3 - Research Article 2) designed accordingly. So, the results of the extensive model performance evaluation conducted to address RA2-RQ2 also determined the choice of statistical downscaling models to capture region-specific compound o-t-events (RA2), with logistic regression being also considered to be in general the superior method for projecting compound o-t-events (RA3). The weaker performance of models based on multiple linear regression to capture high percentiles of the ozone distribution became apparent, while the approach revealed valuable model results regarding the mean of the ozone response. This was also in good agreement with and considered in subsequent research (Chapter 4 - Research Article 3) to address all raised questions of RA4. Furthermore, main physical and nonphysical drivers of ground-level ozone alone or in combination with air temperature were already evaluated based on this holistic central European focus and main parts of the results also transferred to subsequent research studies (Research Articles 2 and 3), focusing on models with station-specific predictor optimums to account more for subtleties and region- as well as site-specific differences in the respective study domain. In addition, the results also pointed out that the varying air quality settings of each location played a minor role with regard to model results, already indicating the superior importance of regional, rather than site-specific, variations and linkages for compound o-t-event occurrences. This key finding was further focused on and confirmed in subsequent analysis, outlined in Chapter 3 - Research Article 2.

5.2 RA2: Region-specific Relationships and Compound O-t-Event Occurrences

(Research Article 2)

As already indicated by the results obtained addressing RA1 and previous work (e.g., Jahn and Hertig, 2021, Hertig et al., 2020, Otero et al., 2016), main meteorological and synoptic drivers of ground-level ozone alone or in combination with heat, including compound o-t-event occurrences, as well as levels of and linkages between both variables, can be assumed to vary temporally and with the location of sites. This is especially true with regard to the strong variations in the observed relationships, patterns and characteristics between and of both target variables by comparing northern, southern, and central parts of Europe. The previous findings had already specified a comparably stronger role of advection and preceding conditions of ozone and hence precursor emissions regarding the occurrence of surface ozone as well as the weaker correlation between both target variables outside of central Europe. Based on these already indicated regional phenomena of surface ozone alone or in combination with air temperature, research questions of RA2 were raised. A regionalization based on both target variables was conducted and built the basis of the second research work presented in Chapter 3 - Research Article 2 to address all raised research questions of RA2. The o-t-season from April to September, defined in the previous study (Chapter 2 - Research Article 1), represented again the temporal focus. Updated surface ozone and air temperature time series data comprising more recent observational information in comparison to Research

Article 1 were used in Research Article 2. In the following, the main contributions of Research Article 2 outlined in Chapter 3 to RQ1 and RQ2 of RA2 are presented. Results of the statistical downscaling models, including the results regarding a region-and site-specific main driver analysis, are specifically highlighted by addressing RA2-RQ2. This chapter ends with a short summary of the most important findings and contributions to RA2.

RA2-RQ1: How is the European domain dividable into regions based on the regional phenomena of surface ozone and air temperature?

A hierarchical clustering approach based on daily surface maximum ozone concentrations and air temperature levels led to a division of the European domain into six ozone-temperature regions showing distinct spatiotemporal variabilities, patterns, and characteristics of both target variables. The in Chapter 3 - Research Article 2 presented regionalization result, leading to a consistent and robust geographical and environmentally meaningful clustering, hence confirmed the regional phenomena of o-t-variabilities and linkages. A region- and site-specific analysis regarding characteristics of and relationships between both target variables identified similarities within and differences between o-t-regions, with a strong and direct linkage and correlation between surface ozone and air temperature found in central, but not in northern and southern parts of Europe. Concluding, results highlighted that interregional dissimilarities, including region-specific dynamics, were strong in contrast to intraregional variabilities and differences regarding surface ozone and air temperature occurrences in Europe. This included in accordance that local site and station conditions were not found to substantially affect o-t-relationships in comparison to region-wide influences. This key finding hence emphasized as well the already indicated and assumed minor role of air quality settings regarding the occurrence of daily surface ozone and air temperature levels as well as of health-relevant compound o-t-events.

RA2-RQ2: How do statistical downscaling models incorporating meteorological variables and synoptic conditions capture region-specific compound o-t-events?

Research Article 2 presented in Chapter 3 specifically aimed to analyze regional variations in compound o-t-event occurrences, including the identification of region- and site-specific main meteorological and synoptic drivers. Following the results of the model evaluation outlined in Chapter 2 - Research Article 1, logistic regression was used to build site-specific statistical downscaling models to capture region-specific health-relevant compound o-t-events. Several stations of varying characteristic per o-t-region, being identified as representative and station-based results considered valid for the whole o-t-region, were selected in this regard. Deviant from the previous Research Article 1 presented in Chapter 2, only distinct physical drivers, i.e., meteorological variables and synoptic conditions, that in general carry physically meaningful and relevant information in this respect, were focused on in Research Article 2. Background stations were thus only included in the analysis to reduce the direct influence of emissions of precursors and hence reactive pollutants affecting ozone formation and depletion processes. While all findings of the previous work (Research Article 1) had to be interpreted with regard to the chosen holistic focus of the study on central Europe as the main spatial scale, a more regional- and station-specific modeling approach was chosen in Research Article 2 with a station-based individualized predictor screening process. Overall model fit and performance was in general good for central Europe. So, beside a stronger and more direct relationship and correlation between surface ozone and air temperature, central European site-specific models also clearly outperformed northern and southern station-based models in capturing compound o-t-events.

Regarding the evaluation of the most important meteorological and synoptic drivers of compound o-t-events, the approach presented in Chapter 2 - Research Article 1 was adapted to the analysis of the region- and site-specific modeling framework of Chapter 3 - Research Article 2. The results showed that the identified most and second most important drivers were

by far the most influencing factors of compound o-t-events, specifically in central Europe. Mean air temperature as predictor generally represented the governing determinant of compound o-t-event occurrences, being in good agreement with the results of Research Article 1. Specific humidity as well as solar radiation were found to be further powerful predictors to assess compound o-t-events for most locations in central Europe, with low humidity and high solar radiation levels favoring the occurrence of compound o-t-events. One of the most striking results regarding RQ2-RA2 was that beside the region-specific variation of o-t-correlations and linkages, also model results along with the identification of main drivers revealed not to be mainly determined or strongly influenced by site- or station-characteristics. This key finding agreed again with the central European model results presented in Chapter 2 - Research Article 1, already indicating the minor influence of air quality settings on compound o-t-event occurrences. Consequently, compound o-t-events and their underlying main drivers in Europe can be seen as well as phenomena of a broader regional scale and seem to be primarily related to larger-scale processes.

RA2: Summary and Contributions

To sum up, while most of the previous studies had analyzed the relationship between ozone, air temperature and meteorological and/or synoptic conditions at specific locations or regarding a smaller scale in Europe, this dissertation provided a comprehensive analysis of the spatiotemporal characterization of both target variables and related compound event occurrences over the whole European domain by also uncovering widespread, regional variations. All questions of RA2 were addressed in Chapter 3 - Research Article 2. Results revealed that the variabilities and levels of as well as the link and connection between both target variables indeed represent regional phenomena. The hierarchical clustering result led not only to the identification of six ozone-temperature regions showing coherent spatiotemporal o-t-characteristics and patterns, which were assumed to be affected by different main drivers under current and future climatic and environmental changes. The regionalization was also the basis of the region-specific modeling approach to capture compound o-t-events. Respective results highlighted the comparably weak predictive power of all southern and northern European station-based models, being also grounded on an in comparison to central Europe lower total number of compound o-t-events. Furthermore, the findings of Research Article 2 confirmed the results of the previous holistic central European study (Chapter 2 - Research Article 1), in which strong positive correlations between and elevated levels of surface ozone and air temperature in the o-t-season from April to September became primarily evident in central parts of Europe. The results of Research Article 2 hence not only confirmed the in Research Article 1 indicated strong linkage of ground-level ozone and surface air temperature but also the clear relationship between compound o-t-events and meteorological and synoptic mechanisms in central Europe, while the weak role of direct physical predictors regarding combined elevated surface ozone concentration and air temperature levels in northern and southern Europe became apparent as well.

The key findings of the evaluation of the suitability of the applied model framework for all identified European o-t-regions was and is relevant not only with respect to questions raised in RA3, but also for external environmental health science and projection studies relying on statistical downscaling models and climate change projections. In this context, the repetitive study results of a needed adjusted and adapted study framework for areas outside central Europe, being stronger influenced by advection and preceding conditions of ozone conditions and precursors emissions, generally highlight the importance to also include information on precursor emission changes under different scenario assumptions in projection studies. Lastly, this key finding of this dissertation introduced and demonstrated the importance of the results of the last Research Article 3 of this dissertation, addressing RA4 and being presented in Chapter 4.

5.3 RA3: Future Compound Ozone and Temperature Burden under Climate Change

(Research Article 1 and 2)

The occurrence of elevated levels of ground-level ozone and air temperature are substantially influenced by meteorological and air pollution conditions, both expected to alter due to ongoing climate change throughout the 21st century. Both health stressors are hence target variables to assess recent and future health burden occasions for the European population with concurrent ozone pollution and heat events depending not just on recent but also future climatic conditions. Thus, future changes of these health stressors need to be analyzed in terms of anthropogenic induced global climate change, especially as only a rare number of studies, as already outlined before, have so far investigated concurrent elevated surface ozone concentration and air temperature levels under future European climate.

The projected future changes in the frequency of compound o-t-event occurrences were assessed in the first two of the three research articles of this dissertation outlined in Chapters 2 and 3. Both relied on using climate change projections considering respective selected scenarios provided by two consecutive phases of the Coupled Model Intercomparison Project (CMIP5/6). Single and multi-model results based on the climate change signal of several selected individual ESM, showing for almost all periods the same sign, but a different magnitude of change, were evaluated in this regard. In the following, the general application of statistical climate change projections regarding European compound o-t-events based on several main criteria is outlined. Specific projection results are subsequently presented with respect to Research Articles 1 and 2 to give answer to RQ1 of RA3. Subsequently, the key findings in both articles regarding RQ2 of RA3 are summarized. This chapter ends with a short summary highlighting the most important findings and contributions to RA3.

RA3: General Application of Climate Change Projections

Statistical climate change projections were conducted by exchanging the initial predictor data with corresponding climate model data. In the formulation of RA3, future assessments of compound o-t-events are solely referred to be based on mere climate change projections. This was also true for Research Article 1 outlined in Chapter 2, even if, deviant to the in Chapter 3 presented Research Article 2, the statistical downscaling models and projections included not only direct physical drivers but also ozone persistence information. But the in this regard applied future ozone concentrations were themselves assessed based on climate change projections, as the provided ESM of CMIP5 did not include ozone persistence predictor data with necessary resolution. Statistical climate change projections of compound o-t-events under future scenario assumptions in both assessments needed to fulfill several requirements and prerequisites, with the following main ones being particularly essential to be met:

1) Statistical downscaling models had to be based on predictors carrying relevant and essential information to capture current as well as future physical relationships.

2) Models showing good performance in the historical period to assess, and later project compound o-t-events needed to be selected.

3) As compound occurrences of health-relevant elevated levels of surface ozone and air temperature were considered, strong and direct current and future linkages between both target variables were crucial.

4) All statistically modeled relationships and characteristics, including present-day o-t-relationships, had to be expected to hold under future projected warming in Europe.

All four main criteria were evaluated in the first two research articles of this dissertation presented in Chapters 2 and 3, and study designs and approaches adjusted and adapted accordingly. The first three criteria were already referred to and partly addressed above by answering the research questions of RA1 and RA2. In order to select relevant predictor information for models and projections, an extensive predictor screening based on the holistic focus on central Europe was at first conducted (Chapter 2 - Research Article 1), with findings transferred and predictor selection finally refined to meet the subsequently chosen more region- and site-specific approach (Chapter 3 - Research Article 2). As already mentioned, logistic regression represented the final modeling technique based on its prior evaluated performance and suitability to model and thus project compound o-t-events. Results of the first two research articles revealed mainly a substantial, positive linkage between both target variables as well as a strong relationship between compound o-t-events and selected predictors in central Europe. So, respective projections focused solely on central European stations, but relied on the individual study framework and design chosen for the corresponding holistic and region-/site-specific approaches of Research Article 1 and Research Article 2, respectively. The possibility of a break of the observed statistical associations due to future warming incorporated in climate change projections was partly accounted for in Research Article 2 by the evaluation of mean temperature anomalies based on all time slice differences and chosen scenarios of CMIP6. Results indicated relationships could be assumed to hold in a projected warmer climate for at least most examined regions and scenarios across central Europe.

> **RA3-RQ1:** What are the expected changes in future health burden induced by compound o-t-events until the end of the 21st century under central European climate change projections?

Research Article 1 outlined in Chapter 2 presented the projected future central European mid- and end-century changes of compound o-t-events based on the climate change signal from seven ESM under CMIP5's RCP4.5 and RCP8.5 scenario assumptions. The evaluation was based on time slice differences regarding two selected twenty-year periods in the 21st century with respect to a historical twenty-year long base period by assuming stationary statistical relationships. Projections of compound o-t-events pointed to an on average growing number of days with concurrent occurrences of thermal load and ozone pollution. While the projected future ozone concentrations, entering as persistence metric projections of compound o-t-events, showed no relevant spatial differences, hotspot regions of regional change in event occurrences in south- to central-eastern parts of the study domain across all scenarios and periods became apparent. These regional hotspots showing strongest compound o-t-event frequency increases were based on the underlying future changes of the main drivers identified with respect to the logistic regression model and projection approach. High levels of surface ozone and of mean air temperature were hence expected to increasingly coincide in these areas, thus resulting in an intensified threat to human life. Therefore, the health burden for the central European population induced by compound o-t-events became evident to worsen throughout the 21st century, especially in the identified hotspot regions in south- to central-eastern parts of the study domain. Regarding the impact of location and site characteristics on projection results, no obvious, significant, and consistent dependences on the varying types of air quality settings became apparent.

Subsequent work presented in Chapter 3 - Research Article 2 assessed potential central European region-specific frequency shifts of compound o-t-event occurrences until the end of the 21st century regarding the climate change signal from eight ESM under CMIP6's SSP2-4.5 and SSP3-7.0 scenario assumptions by comparing historical, mid-, and end-century time slices based on selected twenty-year periods. Furthermore, alongside a more individualized predictor screening, statistical climate change projections of compound o-t-events were generated based on the formulated station-based models including site-specific physical and climate

change relevant information. As a result, the slightly disappointing model results from some individual stations based on the generated holistic downscaling model approach with a fixed predictor set across all stations of previous work presented in Chapter 2 - Research Article 1 could hence be partly accounted for by this in Chapter 3 - Research Article 2 outlined new approach. In general, sharp increases of compound o-t-events in central Europe primarily due to changes in mean air temperature and specific humidity levels as well as solar radiation were projected, resulting in a strong future by compound o-t-events induced health burden for the general population. Projections of Research Article 2 were hence also in good agreement with the results of Research Article 1 that focused entirely on and was completely attuned to central Europe. Based on the projection approach of Research Article 2 and by considering spatial patterns of projected change, a general east-west gradient across all scenario assumptions and time slices became apparent, but no obvious dependences on site-specific characteristics and hence air quality settings emerged.

RA3-RQ2: To what extent are the proposed projection frameworks suitable across the whole European domain?

The analysis regarding both research articles presented in Chapter 2 and Chapter 3 revealed that climate change projections based on the so far applied statistical downscaling model and projection frameworks were only valid for central Europe. In Chapter 2 - Research Article 1 clear associations between surface ozone and air temperature variabilities and between health-relevant levels of both target variables became evident for central Europe, but the comparably weak correlation for locations in northern (i.e., Great Britain, Finland, and Sweden), and southern (i.e., Greece) parts of Europe led to an exclusion of eight respectively located stations. In Chapter 3 - Research Article 2 only central European o-t-regions were considered for projections, all showing a substantial, positive linkage between surface ozone and air temperature. Furthermore, model results for all representative stations revealed a strong relationship of compound o-t-events and selected predictors only within central European o-t-regions. Consequently, o-t-regions outside central Europe were excluded from further analysis regarding future compound o-t-event occurrences. On top of that, the evaluation regarding possible breaks of the observed statistical associations due to future warming highlighted that even if strong deviant or a break of the statistical relationships in the future were rather unlikely under the given framework in central Europe, possible deviant conditions had to be considered in northern and southern Europe. Concluding, results of both research articles presented in Chapters 2 and 3 revealed that climate change projections based on the so far applied general PP statistical downscaling model and projection framework could only be regarded as valid for central Europe, but revised and adapted approaches were hence needed and should be developed for northern and southern parts.

RA3: Summary and Contributions

In summary, the slightly varying statistical downscaling model and projection approaches of Research Article 1 and 2 presented in Chapter 2 and Chapter 3 both indicated a considerable increase in the occurrence of compound o-t-events from April to September under future central European climate, resulting in a considerable intensified health burden for the respective exposed population until the end of the 21st century. Special attention should be paid and highlighted in the formulation and implementation of consensual European climate change and air pollution mitigation and adaption strategies to specifically vulnerable parts of the continent, e.g., the hotspot regions identified in Research Article 1. Regarding the impact of local characteristics, no obvious, significant, and consistent dependences of the projected changes on station areas and characteristics and hence site-specific air quality settings became apparent. Additionally, results of both in Chapter 2 and Chapter 3 presented research articles revealed that climate change projections based on the so far applied statistical downscaling model and projection frameworks were only valid for central Europe. Revised and

adapted approaches need to be developed for northern and southern parts of the continent. This is especially true as, even if deviant correlations and relationships between both health stressors were found outside of central Europe under current ambient conditions, future climate change might lead to temperature shifts resulting in stronger and more direct o-t-relationship outside central Europe, e.g., also in northern European areas. Furthermore, results showed that especially for southern Europe a strong health risk induced by both health stressors became already evident in the recent past, as high elevated levels of both variables repeatedly occurred. Therefore, an intensification of the by compound occurrences induced health burden in the southern parts of Europe should also be the focus of future work. Concluding, all research questions posed in RA3 were addressed by the first two research articles of this dissertation presented in Chapter 2 and Chapter 3 focusing on current and future compound o-t-event occurrences.

5.4 RA4: Future Local, Ground level O$_3$ under Climate and Emission Changes

(Research Article 3)

The relationship between surface ozone and air temperature is, as already mentioned, usually highly influenced by precursor gases (e.g., Bloomer et al., 2009, Coates et al., 2016, Sillman, 1999). Future ground-level ozone concentrations as well as compound ozone-temperature events are so not only determined by altering ambient conditions due to ongoing climate change but also by future pollution and mitigation strategies incorporating e.g., strong reductions in precursor emissions. However, previous, and most recent statistical analysis considering surface ozone alone or alongside air temperature have so far ignored to consider the impact and changes of precursor substances. This was also true for Research Articles 1 and 2 of this dissertation presented in Chapters 2 and 3 assessing future frequency shifts in compound o-t-events in central parts of Europe by solely using CMIP's climate change projections. The limitation of an overall assumption of stationary governing statistical and causal relations regarding the predictors themselves as well as between predictors and predictand throughout the 21st century, including the stationarity of ozone chemistry, transport, and formation conditions and o-t-characteristics, was hence present in Research Article 1 as well as in Research Article 2. But in Research Article 1, the importance of ozone persistence as predictor became already apparent, generally improving substantially statistical model performance over central Europe. This was true for both evaluated modeling approaches, already indicating the determining factor of prolonged or preceding pollution levels and precursor emissions on the occurrence of ozone pollution alone or in combination with thermal load. All in all, the necessity to consider determining emission changes in future assessments of compound o-t-events and hence to also include ozone trend in environmental health science and projection studies focusing on a statistical model and projection framework has more and more emerged in the recent past, also as a result of the two research articles presented in Chapters 2 and 3.

The main contribution of the last part of this dissertation outlined in Chapter 4 - Research Article 3 was hence the generation and analysis of site-specific local, ground-level O$_3$ time series data for Europe projected by a statistical downscaling framework including information on climate but also on precursor emission changes. Therefore, one further major goal of the final research work at hand was to enhance the validity of statistical downscaling with respect to assessments and projections of ground-level ozone by also incorporating air pollution beside climatic changes into the analysis. Based on the generated results, the limitation of stationary governing statistical and causal relations of preceding statistical analysis neglecting information on precursor emissions can be addressed in future ozone-related research work, including studies focusing on compound o-t-event occurrences. Therefore, future changes of local, ground-level ozone in the European area generated and described in Chapter 4 -

Research Article 3 need to be included in upcoming environmental health sciences and projections studies. In this regard, Research Article 3 addressed both research questions of RA4. In the following, a general summary of the statistical downscaling model and projection framework is given at first, including the presentation of all lessons learned and referring to the transfer and application of knowledge from previous research work outlined before in Chapters 2 and 3. Specific model and projection results focusing on the presentation of the generated time series data of future ground-level O_3 at more than 700 European sites are also described to give answer to R4-RQ1. Secondly, the most important conclusions of the sensitivity analysis based on varying predictor configurations, several selected ESM, and different scenario assumptions is presented to address RQ2 of RA4. This section ends with a short summary highlighting the most important findings and contributions to RA4.

> **RA4-RQ1:** How are local, ground-level O_3 concentrations modeled, and future changes projected by a statistical downscaling framework including information on climate and precursor emission changes under different scenario assumptions in the European area?

Future changes of site-specific ground-level O_3 over Europe based on a statistical downscaling framework were assessed under mid- and end-21st century conditions considering respectively selected time slices, as outlined in Chapter 4 - Research Article 3. Statistical station-based downscaling models based on the in Chapter 2 - Research Article 1 defined and in Chapter 3 - Research Article 2 adapted season from April to September were at first generated to assess site-specific relationships between meteorological and chemical predictors and local, ground-level O_3. Multiple linear regression, already showing good performance in Research Article 1 in capturing the mean surface ozone response, was applied to model and later project local O_3 concentrations. In accordance with Research Article 2, CMIP6's SSP2-4.5 and SSP3-7.0 scenario assumptions as well as seven respective ESM were used in this regard. To primarily consider background concentration levels of ozone, being seen as representative for a given region and regarded as the average exposure of the general population, as in Research Article 2, only urban, suburban, and rural background stations were incorporated in the analysis.

Statistical downscaling models and projections relied on the inclusion of main meteorological drivers that in general carry physically meaningful and relevant information, also in the context of global climate change. Respective drivers had already been evaluated for surface ozone alone and in combination with air temperature in Research Articles 1 and 2. The primary applied statistical downscaling and projection framework to assess future local, ground-level O_3 in Europe was based on models using station-specific predictor set optimums from a preceding predictor selection process by always including monthly resolved O_3 predictor data. So, the inclusion of emission-related information content in projections was ensured and the direct influence of emissions of precursors and hence reactive pollutants affecting ozone production and depletion as well as air pollution emission and transport processes on varying spatial scales accounted for. The impact and changes of precursor emissions were factored into models and projections via the incorporation of monthly O_3 time series data derived from reanalysis and model output of seven ESM, not by including information on precursors themselves. In general, ozone data in CMIP6 extracted for the historical period and the two scenarios, SSP2-4.5 and SSP3-7.0, were merely available for some ESM, being dividable, as already outlined, into two groups (with ozone information prescribed from a dataset or interactively computed), and only at a monthly resolution.

Model fit and performance in Chapter 4 - Research Article 3 was evaluated following the approaches incorporated in Research Articles 1 and 2 and only stations showing sufficient evaluation results were considered for projections. All in all, central European models clearly outperformed the ones in northern and southern parts of the study domain, being in good agreement with the results regarding compound o-t-event occurrences of the previous two research articles. In accordance with these previous studies, predictor variables were also ranked by importance to identify station-based most important drivers determining local

ground-level ozone. Results revealed a large contribution of the large-scale predictors solar radiation and mean air temperature on surface ozone concentrations for most stations in southern and central Europe, while especially in northern parts of the study domain the total large-scale monthly ozone predictor highly influenced ground-level ozone. At some maritime sites in southern Europe, specific humidity and wind speed emerged as the prominent factor in governing daily ozone variability, indicating e.g., the important influence of meso-scale land-sea circulation systems on surface ozone levels in these areas.

Projection results under climate and emission changes until the end of the 21st century regarding the signal of all seven ESM under CMIP6's moderate SSP2-4.5 scenario assumption showed on average a substantial decrease in ozone concentrations over Europe until 2050, with slight further reductions projected towards the end of the 21st century. Results for some smaller-scaled areas and sites in United Kingdom and in the Alps revealed occasionally some weak positive trends. In contrast, for CMIP6's more pessimistic SSP3-7.0 scenario assumptions, results showed in general increasing O_3 concentrations over Europe, especially at the end of the 21st century. Projections results showed no clear dependences on site characteristics, i.e., regarding urban, suburban, or rural station types and hence air quality settings.

> **RA4-RQ2:** How does the variation of the chosen statistical downscaling models, mainly differing in terms of the predictor variables used, impact model and projection results?

Furthermore, beside the incorporation of several ESM and two varying scenario assumptions, the impact of different predictor configurations based on seven respectively defined model options was evaluated to quantify more detailed the influence of specific predictor types and sets on the downscaling model and projection results. Therefore, the impact of different predictor settings based on these selected, different model choices on assessed current and future ozone concentrations over Europe could be evaluated and respective results compared in Chapter 4 - Research Article 3. All in all, for two options, a feature selection based on regularized regression was incorporated, while all other options were directly generated from predefined predictor sets. One model option represented the plain result of the regularized predictor selection process using only the generated station-specific predictor set optimums, while the main model option presented above always additionally included monthly resolved O_3 predictor data. Considering the model choices not relying on regularization, for three model choices, the monthly resolved explanatory ozone variable O3month as emission-related predictor was always included, while three further ones only used meteorological information in all their generated, site-specific models.

The findings of Research Article 3 revealed a substantial impact of emission changes on modeled and projected current and future local-scale surface ozone in Europe. Results became evident to depend strongly on whether underlying models include only meteorological predictors or also considered emission-related information. Considering model performance, even if a comparable performance regarding a common set of stations across all model options was assessed, model choices not including emission-related information in general led to an exclusion of more stations. This was specifically true for models based solely on thermal-radiative (THRA) forcing, indicating that it was only a decisive predictor set for some, especially central, regions of Europe. Thus, stations with high model performance using THRA were mainly concentrated over central Europe, while for southern, western, and north-western European stations further predictors were obviously needed to sufficiently capture compound o-t-events in these areas. One major striking result of the analysis was that statistical projections taking only meteorological changes into account generally resulted in projected European-wide increases in ground-level ozone not only under the more pessimistic, by rivalry characterized SSP3-7.0 but also under the comparably positive middle of the road SSP2-4.5 scenario assumptions.

RA4: Summary and Contributions

To sum up, the final assessment of this dissertation presented in Chapter 4 - Research Article 3 addressed RA4 and led to the generation of time series data of future ground-level O_3 at more than 700 European sites. This major scientific output was achieved by a statistical downscaling model and projection approach based on site-specific predictor optimums by always including large-scaled, monthly resolved O_3 data to give answer to RQ1 of RA4. Model performances, predictor selections and ozone-predictor associations as well as related regional variations were in good agreement with results presented in Chapter 2 - Research Article 1 and Chapter 3 - Research Article 2. The strong role of large-scale meteorology in ground-level O_3 occurrences in central Europe was confirmed, while further evidence emerged that additional governing forcings were needed in northern and southern parts of the continent. These key findings were also in good agreement with e.g., results from Otero et al. (2016) outlined before in Chapter 1 - Introduction. Results revealed no clear dependences of projection results on the two ESM groups or site characteristics and hence air quality settings and regimes. One major finding of the study was that the efforts of air pollution control might mitigate future O_3 concentrations as results revealed in general decreases under the moderate SSP2-4.5 scenario but increases under the more pessimistic SSP3-7.0 scenario. The sensitivity analysis regarding varying predictor configurations, aimed at RQ2 of RA4, revealed that projection results could highly depend on whether information on impact and changes of precursors emissions beside meteorological drivers was considered. The results hence confirmed not only variations in magnitude but also in the sign of the projected local surface O_3 changes under SSP2-4.5 scenario assumptions, based on whether emission-related information was or was not included in projections. The results highlighted that in environmental health science and projection studies predictor sets need not only to be evaluated regarding their ability to capture physical relationships under most recent ambient conditions, but also in consideration of the necessity to include relevant information on future climate and emission changes.

In conclusion, the enhanced ground-level ozone modeling and projection approach used in Research Article 3 addressed known limitations. Preceding, especially statistical, studies did not commonly incorporate the impact and changes of precursor emissions in their ozone-related research work and based their projections solely on meteorological and synoptic conditions as well as climate change projections. The results in Chapter 4 - Research Article 3 emphasized the general necessity to include information on emission changes into statistical assessments of future ozone pollution. The presented generated time series data of future ground-level O_3 need hence to be applied in upcoming environmental health science and projection studies focusing on the European health burden induced by surface ozone alone or in combination with air temperature. The findings must thus also be transferred to future work regarding statistical analysis assessing concurrent health-relevant compound surface ozone and air temperature occurrences. Local, future ground-level ozone time series data generated and described in Research Article 3 are already planned to be included in upcoming statistical European projection studies, as outlined more in detail in Chapter 6 - Conclusion and Outlook.

6. Chapter 6 - Conclusion and Outlook

The work documented in this dissertation provided a comprehensive assessment of health-relevant compound occurrences of surface ozone and air temperature under current and future European climate. Furthermore, future local-scale ground-level ozone in the European area was assessed by not only considering climate, but also emission changes. The aims of this dissertation were initially specified by four main research areas with several guiding research questions formulated and addressed in the given thesis. Methodologically, all analysis was primarily based on a Perfect Prognosis statistical downscaling and projection framework, including the implementation and evaluation of several context-specific statistical approaches in the three individual research articles (Research Articles 1-3) outlined in the main part of this manuscript (Chapters 2-4).

In the following, the main contributions and findings of this work are summarized and their relevance regarding the general scientific knowledge is highlighted. Therefore, the key findings that emerged by the analysis of all four addressed research areas and across all three research articles presented in this manuscript are outlined and evaluated with respect to their general significance and the current scientific state of the art. Subsequently, an outlook on the ongoing and possible applications of the main contributions and findings in current and future research is given.

On major goal of this dissertation was to complement existing work regarding the occurrence of O_3 alone or alongside thermal load, by also particularly focusing on regional and site-specific variations across Europe, with key findings not only confirming but also deepening and expanding existing knowledge in this regard.

The period from April to September was identified as ozone and ozone-temperature season, representing the time of the year when health-relevant O_3 concentrations alone or alongside increased thermal load generally occurred over Europe. Furthermore, a strong connection between ozone and temperature became apparent during these months, especially in central parts of Europe. The results agreed with preceding ozone- and temperature-related research that commonly identified or applied the same time frame of this extended summer period (e.g., Hertig, 2020, Otero et al., 2022, Schnell and Prather, 2017, Lacour et al., 2006).

The regional phenomena of ozone and temperature became apparent in a large variety of findings of the given work. In this regard, the regionalization of Europe based on both target variables, surface ozone, and air temperature, constituted a novelty. The generation of geographically, and environmentally meaningful European ozone-temperature regions underlined and confirmed the regional phenomena of both variables, also in their combined occurrence. In general, main differences emerged especially between central, northern, and southern Europe. Strong associations and direct linkages of both variables were found mainly in central parts of Europe, along with higher performances of model approaches capturing ozone variability or compound o-t-event occurrences. Furthermore, model results and main driver analysis confirmed the importance of meteorological and synoptic conditions in central Europe. Deviant pictures emerged for all these aspects in northern and southern parts of the European study domain. Similar results were reported by Otero et al. (2016) indicating a comparably higher importance of ozone persistence and precursor emissions in southern and northern parts of Europe, while daily maximum temperature was found as a key driver of ozone and health-relevant ozone exceedances. The results of this thesis nevertheless also confirmed that meteorology influenced the (concurrent) occurrence of ozone and temperature across the whole European domain, being in good agreement with the findings of Porter and Heald (2019) who underlined in their work the important role of meteorology regarding the o-t-relationship in Europe. The spatiotemporal variation of ozone and air temperature, their linkage as well as main drivers of their single as well as compound occurrence were also indicated by further

research studies, as outlined in Chapter 1 - Introduction, with the current contribution now giving further, deepened, and extended evidence in this regard.

The key findings of this dissertation also provided new insights into the projection of site- and region-specific compound o-t-events as well as local-scale ground-level ozone over Europe based on climate change alone or alongside emission changes. Even if the relevance of the addressed research questions and the main contributions of this thesis regarding future single and compound occurrences of surface ozone and air temperature were emphasized and highlighted by previous research work, the existing evidence has still been limited and extended research has been needed.

Considering climate change projections, in this thesis, substantial increases in ground-level ozone concentrations, but especially in compound o-t-event occurrences were assessed for central Europe. The lack of recent research focusing on both target variables, ozone, and temperature, under climate change has so far been especially true for Europe. There exist only a small number of studies regarding and indicating, in accordance with the results of this dissertation, the increase in compound occurrences of both variables. For example, Hertig (2020) assessed at least for a smaller scale, i.e., for the state of Bavaria in Southern Germany, an increase of concurrent exceedances of surface ozone and air temperature until the end of the 21st century. A recent study of Ban et al. (2022) regarding compound heatwave and ozone pollution identified a substantial increase in compound event days worldwide in the 2080s alongside an enhanced respective exposure under SSP3-7.0 scenario assumptions, while regional patterns revealed also a clear health-relevant increased exposure risk for large parts of Europe.

The dissertation contributed as well to the investigation of the predefined and already repeatedly investigated ozone-climate penalty. Previous work indicated that ozone pollution might increase in the future if anthropogenic mitigation strategies and emission controls were not implemented and/or emissions and ambient conditions maintained at current levels (see Chapter 1 and the references therein). These findings were in good agreement with the results regarding future frequency shifts in compound o-t-events by not directly including emission changes in models and projections obtained during this thesis. However, some results in the first two studies (Chapter 2 - Research Article 1 and Chapter 3 - Research Article 2) but especially the key findings of the last research work (Chapter 4 - Research Article 3) revealed the need to include information on impact and changes of precursor emissions, at least in the form of an ozone trend or ozone persistence, into projections capturing future surface ozone alone or alongside air temperature. Further research work regarding varying scenarios and taking emission changes into account (Meehl et al., 2018, Orru et al., 2019) gave evidence as well in this regard, with respectively assessed decreases in projected future ozone pollution and related health burden, being in contrast to the also therein presented assessments of future increased ground-level ozone levels projected by solely including climate change. Therefore, the last contribution of this dissertation assessed future ground-level ozone in the European area by a sole PP statistical downscaling modeling and projection framework considering not only climate but also emission changes. Limitations regarding surface ozone projections that neglect to include information on emission changes, influencing model and projection results and weakening the significance of some findings, were thereby addressed. Additionally, the research work also constituted a specificity in statistical analysis as the impact and changes of precursor emissions were here taken into account. The key findings of this last contribution confirmed previous evidence of the importance of air pollution control and strategies, with decreases of future local-scale ground-level ozone becoming evident across Europe under the middle of the road SSP2-4.5 but increases under the more pessimistic SSP3-7.0 scenario with enhanced regional rivalry, the latter incorporating no climate change mitigation and only weak air pollution control strategies. These findings were also in accordance with the recent scientific basis of the IPCC (2021), with future assessments

incorporating no or not all-encompassing measures to reduce air pollution and ozone precursor emissions are expected to lead to a worsening of projected O_3 pollution for much of the 21st century under respective scenario assumptions such as SSP3-7-0 and SSP5-8.5 (high confidence). The statistical analysis and generated results of Research Article 3 presented in Chapter 4 hence not only now complement existing work based on dynamical models, i.e., climate chemistry models, or chemical transport model, commonly used to model and project surface ozone in this regard (Lu et al., 2019), but also support current research regarding the ozone-climate penalty.

An evaluation of the applied general PP statistical downscaling and projection framework for the whole European domain was conducted as part of the dissertation. Respective lessons learned and drawn conclusions should be therefore integrated in future, upcoming research. In accordance and alongside the results listed above, the specific applied statistical downscaling model and projection frameworks were evaluated to be primarily suitable for central Europe. This conclusion was underlined by the fact that the observed and modeled statistical associations could generally be expected to be only valid under certain ambient conditions and might deviate or break under current extreme summer heat or future warming, as already indicated in previous work (e.g., Steiner et al., 2010, Shen et al., 2016, Varotsos et al., 2013). But in contrast to the findings of some previous studies (e.g., Boleti et al., 2020) indicating a substantial impact of air quality regimes on ground-level ozone concentrations, the analysis revealed a minor role of air quality settings regarding the occurrence of surface ozone alone or alongside air temperature, including that no clear dependences of model and projection results on site characteristics became evident. This key finding emerged across all three research articles, whether beside climate change, also emission changes were regarded or not in the assessment of ground-level ozone or compound o-t-events. Consequently, as a main conclusion of this thesis, in future assessments adapted and adjusted approaches need to be designed for northern and southern parts of Europe, but not necessarily separately for local-scaled urban, suburban, and rural sites.

Based on the main scientific findings and contributions described in the previous chapters and summarized above, a number of recommendations and suggestions can be drawn for future work and health impact assessments as well as public health and policy interventions and strategies. A general increase in the health burden induced by compound occurrences of health-relevant surface ozone and air temperature levels is to be expected due to the shown results, pointing out the vulnerability of central European regions to future episodes of concurrent ozone pollution and heat under climate change. So, beside solely focusing on ozone-induced risk in environmental health science and projection studies, compound ozone-temperature events should be the focus of future work. In this regard, it is of utter importance to not just focus on climate, but also emission changes based on e.g., European climate neutrality goals, land use or vegetational changes. Future work and follow-up research projects grounded on the contributions and findings of the presented dissertation are already in progress and respective research articles currently in preparation. For instance, the downscaling output of the last Research Article 3 presented in Chapter 4 regarding future local ground-level ozone across various sites in Europe from projections considering climate and emission changes forms a valuable basis for further studies. The generated O_3 time series data for Augsburg, Southern Germany generated in this study, are currently used in an ongoing research project focusing on recent and future ground-level ozone- and temperature-related daily myocardial infarction (MI) frequencies in the city and two adjacent counties. Furthermore, the output is also planned to be applied in a follow-up European-wide study assessing future health burden induced by co-occurring ozone pollution and thermal load during prolonged episodes of heat in the form of heatwaves. Therefore, the key findings of the previous assessments regarding future compound o-t-events can be transferred and limitations and shortcomings addressed by this

new and updated study designs, including now information about impact and changes of precursor emissions in statistical downscaling models and projections.

Concluding, this work presents useful information and new insights regarding the current and future health burden induced by surface ozone alone or in combination with air temperature. Especially in the scope of ongoing climate change, it is essential to provide high-quality local-scale assessments of the anticipated changes in natural hazards composing a substantial health risk for the European population. The contributions and results of this thesis hence supply key findings not only essential for the formulation and implementation of future work, but also for current and future warning systems and protection strategies focusing on the interplay between air quality, heat, and human health in Europe. Compound o-t-events represent specifically harmful occasions that should be intensively focused on in consensual climate change and air pollution mitigation, adaption, and protection strategies. Particular attention should be paid in this context to the areas in Europe particularly affected by ozone pollution and thermal stress under current and future conditions.

Appendix A

Abbreviations and Acronyms

Symbol Formula	Description	Further Information
CH_4	Methane	
CMIP5	Coupled Model Intercomparison Project Phase 5	Projections are based on the Representative Concentration Pathway (RCP) scenarios. Future scenarios of anthropogenic forcing range from a low (RCP 2.6), through two intermediate scenarios (RCP 4.5 and RCP6.0), to a high emission scenario (RCP 8.5)
CMIP6	Coupled Model Intercomparison Project Phase 6	Projections are based on the SSP (Shared Socioeconomic Pathways) scenarios. Future scenarios SSPs are labelled as follows: SSP1 (sustainability), SSP2 (middle of the road), SSP3 (regional rivalry), SSP4 (inequality) and SSP5 (fossil-fuel development). SSP are combined with a corresponding RCP, with e.g., SSP2-4.5 and SSP3-7.0 representing two possible combinations
GCM	General Circulation Model(s)	
EEA	European Environment Agency	
ESM	Earth System Model(s)	
EU	European Union	
EU-AQD	Ambient Air Quality Directive of the EU	
EU-120	EU-AQD long-term objective target ozone value of 120 µg/m^3	The value is based on maximum daily 8-hour running ozone means (MDA8O3)
HNO_3	Nitric acid	
HO_2	Hydroperoxyl radical(s)	
IPCC	Intergovernmental Panel on Climate Change	
MDA8O3	Daily ozone concentration(s) based on maximum daily 8-hour running ozone means	
NO, NO_2, NO_x	Nitrogen oxide, nitrogen dioxide, nitrogen oxides	
O_3	Tropospheric, surface, ground-level ozone	Standard units used to depict O_3 concentrations are ppb or µg/m^3. As simple approximation (EU Directive 2008/50), units are convertible into each other as follows: 2 x O_3 [ppb] = O_3 [µg/m^3]

OH	Hydroxyl radical(s)	
o-t-	Ozone-temperature-	e.g., o-t-association, o-t-correlation, o-t-event, o-t-linkage, o-t-region, o-t-relationship, o-t-season, o-t-slope
PAN	Peroxyacetyl nitrate	
PP	Perfect Prognosis	
RA	Research area(s)	
RCM	Regional Climate Model(s)	
RQ	Research question(s)	
THRA	Thermal-radiative	
WHO	World Health Organization	
WHO-AQG	WHO Air Quality Guidelines	
WHO-100	The WHO-AQG value for short-term exposure to ozone of 100 µg/m^3	The value is based on MDA8O3
VOCs	Volatile organic compounds	

Appendix B

List of Publications and Conference Contributions

List of Publications

JAHN, S.* & HERTIG, E. 2021. Modeling and projecting health-relevant combined ozone and temperature events in present and future Central European climate. *Air Quality, Atmosphere & Health*, 14, 563-580. https://doi.org/10.1007/s11869-020-00961-0
*first and corresponding author

JAHN, S.* & HERTIG, E. 2022. Using Clustering, Statistical Modeling, and Climate Change Projections to Analyze Recent and Future Region-Specific Compound Ozone and Temperature Burden Over Europe. *Geohealth,* 6**,** e2021GH000561.
https://doi.org/10.1029/2021gh000561
*first and corresponding author

HERTIG, E.*, JAHN, S. & KASPAR-OTT, I. 2023. Future Local Ground-level Ozone in the European area from Statistical Downscaling Projections Considering Climate and Emission Changes. *Earth's Future,* 11, e2022EF003317.
https://doi.org/10.1029/2022EF003317
*first and corresponding author

JAHN, S.*, HERTIG, E*., LINSEISEN, J. & MEISINGER, C ---. Analysis and projection of ground-level ozone- and temperature-related daily myocardial infarction (MI) frequencies in Augsburg, Southern Germany. ---, in perparation (status as of December 2022).
*shared co-first authorship

List of Conference Contributions

Presentations

JAHN, S.* & HERTIG, E. 2022. Relationships of compound temperature-ozone pollution-events with myocardial infarction (MI) frequencies in Augsburg, Southern Germany. *EMS Annual Meeting 2022*, Session OSA2.5 Atmospheric effects on humans, Bonn, September 04-09. On-site presentation. Young Researchers Travel Scholarship Program of the University of Augsburg. https://doi.org/10.5194/ems2022-9
*presenter

JAHN, S.* & HERTIG, E. 2022. Health-relevant, compound ozone and temperature events over Europe. *EGU General Assembly 2022*, Session CL3.2.6 Climate extremes, biosphere and society: impacts, cascades, feedbacks, and resilience, Vienna, May 23-27. On-site presentation. Young Researchers Travel Scholarship Program of the University of Augsburg. https://doi.org/10.5194/egusphere-egu22-2936
*presenter

JAHN, S.* & HERTIG, E. 2022. PC1 - COVID-19, haze, and ozone impacts on human health. Invited Press Conference Speaker, *EGU General Assembly 2022,* PC1 - first press conference, Vienna, May 22. On-site presentation.
https://www.egu.eu/gamedia/2022/press-conferences/
*invited press conference speaker and presenter

JAHN, S.* & HERTIG, E. 2021. Gesundheitsrelevante, kombinierte Temperatur-Ozon-Ereignisse in Europa. *AK Klima 2021*, 39. Jahrestagung des Arbeitskreis Klima der

Deutschen Gesellschaft für Geographie, Passau, November 05-11. On-site presentation.
*presenter

JAHN, S.* & HERTIG, E. 2021. Current and future occurrences of health-relevant, compound heat and ozone pollution events in six European ozone-temperature regions. *EMS Annual Meeting 2021*, Session OSA2.4 Atmospheric effects on humans, September 06-10. Online presentation (Lightning Talk). https://doi.org/10.5194/ems2021-61
*presenter

JAHN, S.* & HERTIG, E. 2021. Health-relevant, concurrent ground-level ozone and temperature events in recent and future European climate. *EGU General Assembly 2021*, Session NH1.7 Extreme meteorological and hydrological events induced by severe weather and climate change, April 19-30. Online presentation (vPICO). https://doi.org/10.5194/egusphere-egu21-451
*presenter

JAHN, S.* & HERTIG, E. 2020. Statistical modelling of combined ozone-temperature events in Europe. *EGU General Assembly 2020*, Session AS3.22 Urban Air Quality and Greenhouse Gases, May 04-08. Online presentation. Young Researchers Travel Scholarship Program of the University of Augsburg. https://doi.org/10.5194/egusphere-egu2020-1314
*presenter

Posters

JAHN, S.* & HERTIG, E. 2020. Statistical modeling of combined ozone and temperature extremes in Central Europe. Symposium on Challenges in Applied Human Biometeorology 2020, Freiburg, March 02-03. Poster presentation.
*presenter

JAHN, S.* & HERTIG, E. 2019. Statistische Modellierung kombinierter Ozon- und Temperaturextremereignisse in Zentraleuropa. AK Klima 2019, 38. Jahrestagung des Arbeitskreis Klima der Deutschen Gesellschaft für Geographie, Hamburg, October 25-27. Poster presentation. Young Researchers Travel Scholarship Program of the University of Augsburg.
*presenter

Appendix C

Contribution of the Author to the Different Research Articles of the Dissertation

Contribution to Research Article 1

The main topic of this study was formulated by Elke Hertig. The specific study design was developed by Sally Jahn and Elke Hertig. Statistical downscaling modeling and projection approaches were designed by Sally Jahn in discussion with Elke Hertig, who also provided the idea and support for the integration of ozone persistence into the projection process. Literature review, data download and processing, all computations including statistical downscaling model and projection development and implementation, the final analysis, and preparation of figures were performed by Sally Jahn. Discussions and interpretation of the main results were done during the evaluation meetings with Elke Hertig. Sally Jahn prepared the manuscript, which was improved with the aid and contributions of Elke Hertig. The authors thank Irena Kaspar-Ott for the final proof-reading of the manuscript.

Contribution to Research Article 2

The study was conceived and designed by Sally Jahn, in discussion with Elke Hertig. Literature review, all data processing and computations including implementation and development of the regionalization approach along with the identification of representative stations were performed by Sally Jahn, with valuable comments and feedback from Elke Hertig. The statistical downscaling model and projection design was developed and conducted by Sally Jahn in agreement with Elke Hertig. Figures were provided by Sally Jahn. Discussion and interpretation of the results were done by Sally Jahn with support from Elke Hertig, who also aided to improve the manuscript initially prepared by Sally Jahn. The authors thank Irena Kaspar-Ott for the final proof-reading of the manuscript.

Contribution to Research Article 3

The main topic and specific design of this study was formulated and developed by Elke Hertig. Sally Jahn collected all observational and together with Irena Kaspar-Ott all meteorological reanalysis data. Observational and meteorological reanalysis data were processed and preselected by Sally Jahn. Ozone reanalysis and climate model data were downloaded and processed by Irena Kaspar-Ott. The detailed bias correction of the climate model data was conceived and designed by Elke Hertig and performed and evaluated by Irena Kaspar-Ott, while Elke Hertig contributed to the analysis and interpretation of the results along with an extensive discussion of the choice of a suitable ozone reanalysis product. The implementation and development of statistical downscaling models along with a prior predictor selection procedure, model evaluation and main driver analysis was performed by Sally Jahn in consultation with Elke Hertig and Irena Kaspar-Ott. The model setup was substantially extended and improved by Elke Hertig providing the support for the development of a sensitivity analysis evaluating primarily the impact of different predictor types on model and projection results. Projections were generated and final figures were provided by Irena Kaspar-Ott and Sally Jahn. Final analysis of the model and projection output, discussions, and interpretations of the main results were primarily done by Elke Hertig and Irena Kaspar-Ott. The literature studies and the preparation of the manuscript were mainly conducted by Elke Hertig, with contributions from Irena Kaspar-Ott and Sally Jahn who provided primarily main text parts for the sections on data and methods. The manuscript was finalized by Elke Hertig with the aid of all co-authors.

Appendix D

Supplementary Information

Research Article 1

The Supplementary Material (Online Resources 1-3) of Research Article 1 (Chapter 2) as submitted and available online alongside the original article.

Article title: Modeling and projecting health-relevant combined ozone and temperature events in present and future Central European climate
Journal name: Air Quality, Atmosphere & Health
Author names: Sally Jahn*, Elke Hertig

*Corresponding author
E-mail address: **sally.jahn@geo.uni-augsburg.de**
Regional Climate Change and Health, Institute of Geography and Faculty of Medicine,
Augsburg University, Alter Postweg 118, 86159 Augsburg, Germany

Table S1 Overview of all used abbrevations and acronyms. Common institutional, statistical and projection-based abbreviations and acronyms are not listed.

General	Explanation
AQD	Ambient Air Quality Directive (EU)
AQG	Air Quality Guidelines (WHO)
MDA8O3	Daily maximum ozone values based on running 8-hour means
MI	Myocardial infarction
o-t-events	Ozone and temperature events
o-t-season	Ozone and temperature season
TX	Daily maximum surface air temperature

Predictors	Explanation
GH850, GH500	Geopotential heights at 850 and 500 hPa
LagO3	Ozone persistence (ozone pollution levels of the previous day)
MSLP	Mean sea level pressure
MT850, MT500, MT2m	Mean air temperatures at 850 and 500 hPa and 2m
RH850, RH500	Relative humidity at 850 and 500 hPa
SSRD	Surface solar radiation downwards
STRD	Surface thermal radiation downwards
TCC	Total cloud cover
UWind850, UWind 500	Zonal winds at 850 and 500 hPa
VWind850, VWind500	Meridional winds at 850 and 500 hPa

Station-based	Explanation
r, s, u	EEA's predefined station type of area (rural, suburban, urban)
b, i, t	EEA's predefined type of station (background, industrial, traffic)
rb	Rural background
ri	Rural industrial
sb	Suburban background
ub	Urban background
ut	Urban traffic

Models and projections	Explanation
ESM	Earth System Model
LR	Logistic regression
MLR	Multiple linear regression
MDA8O3-MLR	Multiple linear regression to assess MDA8O3
MID	Most important driver
SMID	Second most important driver
TMID	Third most important driver
TX-MLR	Multiple linear regression to assess TX

Table S2 Overview of all 85 MDA8O3 stations with station code, station name, location and further statistics and characteristics. Station codes of the assigned temperature stations are also depicted for each ozone station. Daily MDA8O3 concentrations and daily TX levels in the months from April to September are shown with numbers respresenting the mean for each station over the years.

number	code	name	class	longitude [°]	latitude [°]	altitude [m a.s.l.]	temperature station code	distance [km]	altitude difference [m]	MDA8O3 [µg/m³]	TX [°C]
1	AT30601	Klosterneuburg Wisentgasse	sb	16.30	48.30	200	16	8.31	2	99.08	22.80
2	AT60018	Graz Schlossberg	ub	15.44	47.08	450	12	1.08	84	98.85	22.95
3	AT72106	Innsbruck Reichenau	ut	11.42	47.27	570	13	1.45	7	79.52	22.29
4	AT72113	Innsbruck Sadrach	sb	11.37	47.27	670	13	2.56	93	91.71	22.32
5	AT900ZA	Wien Hohe Warte - Zentralanstalt für Meteorologie und Geodyn	ub	16.36	48.25	207	16	1.88	9	96.30	22.81
6	AT90LAA	Wien Laaer Berg	ub	16.39	48.16	250	16	8.58	52	88.86	22.80
7	AT9STEF	Wien Stephansplatz	ub	16.37	48.21	173	16	3.22	25	89.02	22.81
8	BETB011	41B011 - BERCHEM S.A	sb	4.29	50.86	30	17	8.57	70	79.62	20.14
9	BETR012	41R012 - UCCLE	sb	4.36	50.80	100	17	0.71	0	83.26	20.14
10	BETR740	44R740 - ST.KRUIS-WI	ri	3.81	51.15	5	2571	9.01	4	72.10	20.09
11	CH0002R	Payerne	rb	6.94	46.81	489	2180	0.58	1	100.23	21.09
12	CH0005A	Dübendorf-EMPA	sb	8.61	47.40	432	244	4.16	123	95.30	20.33
13	CH0008A	Basel-Binningen	sb	7.58	47.54	316	239	0.89	0	95.57	21.76
14	CH0010A	Zürich-Kaserne	ub	8.53	47.38	409	244	2.80	146	91.87	20.32
15	CH0011A	Lugano-Università	ub	8.96	46.01	280	242	1.44	7	115.22	22.91
16	CH0013A	Zürich-Stampfenbachstrasse	ut	8.54	47.39	445	244	2.06	110	86.55	20.32
17	CH0017A	Basel-St-Johann	ub	7.58	47.57	260	2192	7.62	3	81.99	22.22
18	CH0021A	Zürich-Schimmelstrasse	ut	8.52	47.37	415	244	3.52	140	71.32	20.09

19	CH0045A	Anières-Débarcadère	rb	6.22	46.28	375	240	7.47	45	96.97	22.28
20	CH0046A	Thônex-Foron	sb	6.21	46.20	422	240	8.53	2	93.90	22.25
21	CH0048A	Genève-Wilson	ut	6.15	46.22	376	241	1.80	29	74.58	22.18
22	CH0049A	Genève-Ste-Clotilde	ub	6.13	46.20	374	241	1.37	31	82.33	22.26
23	CH0050A	Meyrin-Vaudagne	sb	6.07	46.23	439	240	5.00	19	88.12	22.25
24	DEBB021	Potsdam-Zentrum	ub	13.06	52.40	31	54	2.02	50	88.73	21.11
25	DEBE027	B Marienfelde-Schichauweg	ri	13.37	52.40	45	4588	9.75	0	92.55	20.86
26	DEBE032	B Grunewald (3.5 m)	rb	13.23	52.47	50	41	5.29	1	83.44	20.99
27	DEBE034	B Neukölln-Nansenstraße	ub	13.43	52.49	35	4563	5.83	0	80.35	21.05
28	DEBE051	B Buch	sb	13.49	52.64	60	4529	1.56	0	89.53	21.14
29	DEBW019	Ulm	ub	9.98	48.40	481	4708	2.31	86	83.83	19.70
30	DEBW024	Ludwigsburg	sb	9.17	48.90	302	3506	8.06	12	95.32	21.32
31	DEBW027	Reutlingen	ub	9.21	48.49	385	4554	2.54	25	87.15	21.60
32	DEBW039	Villingen-Schwenningen	sb	8.46	48.05	700	4712	0.35	20	96.45	19.36
33	DEBW042	Bernhausen	sb	9.23	48.68	370	2763	1.25	1	85.96	20.79
34	DEBW052	Konstanz	ub	9.17	47.66	403	495	2.22	40	94.68	21.69
35	DEBW076	Baden-Baden	sb	8.22	48.77	148	4284	5.40	92	95.36	21.43
36	DEBW081	Karlsruhe-Nordwest	ub	8.36	49.03	114	2762	6.41	2	96.37	22.99
37	DEBY020	Hof/LfU	sb	11.90	50.32	525	490	1.65	40	81.24	18.41
38	DEBY031	Kempten (Allgäu)/Westendstraße	sb	10.31	47.73	678	496	2.23	27	88.85	19.42
39	DEBY037	München/Stachus	ut	11.56	48.14	521	4431	2.84	0	59.68	20.82
40	DEBY039	München/Lothstraße	ub	11.55	48.15	521	4431	3.63	0	83.43	20.96

41	DEBY052	Neu-Ulm/Gabelsbergerstraße	ub	10.01	48.40	470	4708	4.26	97	82.60	19.70
42	DEBY053	Nürnberg/Bahnhof	ut	11.09	49.45	307	4127	9.76	6	78.23	21.04
43	DEBY062	Regen/Bodenmaiser Straße	sb	13.13	48.97	545	4805	7.09	70	86.76	19.12
44	DEBY063	Regensburg/Rathaus	ut	12.10	49.02	335	4465	5.02	6	62.89	22.00
45	DEBY077	Würzburg/Kopfklinik	sb	9.96	49.80	226	489	3.71	42	84.89	21.55
46	DEBY079	Bad Reichenhall/Nonn	sb	12.86	47.72	465	4547	1.26	5	82.27	21.12
47	DEBY088	Trostberg/Schwimmbadstraße	sb	12.54	48.02	488	4699	1.13	71	87.96	20.59
48	DEBY089	München/Johanneskirchen	sb	11.65	48.17	513	52	7.77	2	89.91	20.94
49	DEHB001	Bremen-Mitte	ub	8.82	53.08	10	42	3.60	6	78.62	19.94
50	DEHB002	Bremen-Ost	ub	8.92	53.06	7	42	8.02	3	75.86	19.97
51	DEHB005	Bremerhaven	ub	8.57	53.56	3	4885	3.16	4	76.44	18.68
52	DEHE008	Frankfurt-Ost	ub	8.75	50.13	100	4107	6.11	9	81.29	22.22
53	DEHE011	Hanau	ut	8.92	50.13	106	4189	1.55	0	80.78	22.10
54	DEHE018	Raunheim	ub	8.45	50.01	90	2761	9.73	22	87.61	22.02
55	DEHE022	Wiesbaden-Süd	ub	8.24	50.05	121	4381	9.46	74	84.87	22.14
56	DEHH021	Hamburg Tatenberg	sb	10.08	53.49	2	11781	9.91	0	74.98	19.83
57	DEMV003	Neubrandenburg	ut	13.27	53.56	15	4698	5.36	54	68.67	19.80
58	DEMV007	Rostock-Stuthof	sb	12.17	54.16	5	472	6.40	1	81.69	18.36
59	DENI011	Braunschweig	sb	10.47	52.23	98	4880	8.33	15	87.01	20.05
60	DENI020	Wolfsburg	sb	10.82	52.44	66	4785	9.78	16	85.08	20.83
61	DENI029	Ostfriesland	sb	7.21	53.36	1	4054	1.55	1	85.37	18.77
62	DENI038	Osnabrück	ub	8.05	52.26	95	4499	0.20	0	82.86	20.02

63	DENI042	Göttingen	sb	9.95	51.55	170	4151	5.50	3	88.48	20.18
64	DENI043	Emsland	sb	7.32	52.50	30	4360	2.38	8	86.43	20.16
65	DENW038	Mülheim-Styrum	ub	6.87	51.45	37	4031	9.25	16	75.55	21.25
66	DENW042	Krefeld-Linn	ub	6.64	51.34	32	4030	7.75	1	79.57	21.12
67	DERP001	Ludwigshafen-Oppau	ub	8.40	49.52	91	4369	6.17	4	82.18	22.67
68	DERP007	Mainz-Mombach	ub	8.22	50.02	120	4381	5.46	75	84.27	22.14
69	DERP013	Westpfalz-Waldmohr	rb	7.29	49.42	455	4595	8.17	55	97.09	19.67
70	DERP015	Westeifel Wascheid	rb	6.38	50.27	680	4618	4.64	31	94.74	16.71
71	DERP021	Neuwied-Hafenstraße	ub	7.48	50.42	65	4447	7.72	62	80.49	22.04
72	DERP022	Bad Kreuznach-Bosenheimer Straße	ub	7.87	49.84	108	4577	1.15	6	77.73	22.40
73	DERP023	Worms-Hagenstraße	ut	8.36	49.63	97	4787	2.58	9	78.23	22.36
74	DERP024	Koblenz-Friedrich-Ebert-Ring	ut	7.60	50.35	68	4447	6.70	59	63.44	22.10
75	DERP025	Wörth-Marktplatz	ub	8.25	49.05	104	51	8.26	8	93.65	23.05
76	DESL002	Bexbach Schule	ub	7.26	49.36	273	4458	3.09	37	87.97	21.11
77	DESL017	Völklingen-City Stadionstr.	ub	6.87	49.25	189	4850	5.08	1	82.71	21.90
78	DESN011	Chemnitz-Mitte	ub	12.92	50.83	300	4954	5.41	118	87.43	19.05
79	DEST011	Wernigerode/Bahnhof	ub	10.79	51.84	230	4758	1.70	4	90.09	19.88
80	DEST028	Zeitz	ub	12.14	51.05	160	4797	0.21	10	87.39	20.61
81	DETH009	Gera Friedericistr.	ub	12.07	50.88	190	3990	3.91	121	84.35	19.91
82	DETH020	Erfurt Krämpferstr.	ub	11.04	50.98	195	487	5.27	121	80.69	19.57
83	NL00107	Posterholt-Vlodropperweg	rb	6.04	51.12	32	4207	9.66	25	83.41	20.66
84	NL00236	Eindhoven-Genovevalaan	ut	5.47	51.47	17	2566	7.03	5	63.78	20.54

| 85 | NL00639 | Utrecht-Erzeijstraat | ut | 5.12 | 52.07 | 1 | 162 | 5.20 | 0 | 60.99 | 19.85 |

Article title: Modeling and projecting health-relevant combined ozone and temperature
events in present and future Central European climate
Journal name: Air Quality, Atmosphere & Health
Author names: Sally Jahn*, Elke Hertig

*Corresponding author
E-mail address: **sally.jahn@geo.uni-augsburg.de**
Regional Climate Change and Health, Institute of Geography and Faculty of Medicine,
Augsburg University, Alter Postweg 118, 86159 Augsburg, Germany

Table S3 Evaluation metrics used for LR model performance evaluation. Mean and median metric scores across all stations are shown for Central Europe. Minimum and maximum values are given in brackets. The following abbreviations are used: tp for true positives, tn for true negatives, fp for false positives and fn for false negatives.

Metrics	Description	Formula	Mean	Median
True Positive Rate (TPR) *Or* Sensitivity (SN) *Or* Recall (R)	Metric is used to measure the fraction of actual, observed events that are correctly predicted.	$\dfrac{tp}{tp + fn}$	0.83 [0.74, 0.89]	0.84
True Negative Rate (TNR) *Or* Specificity (SP)	Metric is used to measure the fraction of actual, observed non-events that are correctly predicted.	$\dfrac{tn}{tn + fp}$	0.81 [0.75, 0.85]	0.81
False Positive Rate (FPR)	Metric is used to measure the fraction of actual, observed non-events thare are incorrectly predicted.	$\dfrac{fp}{fp + tn}$	0.19 [0.15, 0.25]	0.19
False Negative Rate (FNR)	Metric is used to measure the fraction of actual, observed events thare are incorrectly predicted.	$\dfrac{fn}{fn + tp}$	0.17 [0.11, 0.26]	0.16
False Alarm Ratio (FARatio)	Metric is used to measure the fraction of the predicted events that did actually not occur.	$\dfrac{fp}{tp + fp}$	0.50 [0.37, 0.64]	0.49
Precision (P)	Metric is used to measure the fraction of the predicted events that did actually occur.	$\dfrac{tp}{tp + fp}$	0.51 [0.36, 0.63]	0.51
F1-Score	Metric represents the harmonic mean and thus maintains a balance between recall and precision.	$2 \times \dfrac{P \times R}{P + R}$	0.63 [0.49, 0.74]	0.63
Area under the ROC curve (AUCROC)	ROC curves show how the number of correctly predicted events varies with the number of incorrectly predicted non-events. AUC measures the entire two-dimensional area underneath curve. Thus, AUC can be used as a summary of the overall model skill.	Area under ROC (Receiver Operating Characteristics) curve created by plotting TPR (y-axis) against FPR (x-axis) at various threshold settings	0.90 [0.85, 0.94]	0.90
Area under the PR curve (AUCPR)	PR curves are similar to ROC curves, but are based on P and R. As both metris are focused on the positive class (events), the area under the PR curve is better to assess the perfomance of the model to predict the minority class. Thus, the metric is especially suitably for highly imbalanced datasets.	Area under PR (Precision-Recall) curve created by plotting P (y-axis) against R (x-axis) at various threshold settings	0.69 [0.5, 0.83]	0.69

Table S4 Changes [%] regarding the amount of days with combined ozone-temperature events between the periods 2031-2050 as well as 2081-2100 compared with 1993-2012 under RCP4.5 and RCP8.5 scenario. Numbers refer to the mean across all stations with respect to each specific ESM. Minimum and maximum values are given in brackets.

	ACCESS1-0	CanESM2	CMCC-CMS	CNRM-CM5	IPSL-CM5A-MR	MIROC-ESM	MPI-ESM-MR
RCP4.5							
2031-2050	17.59 [0.14, 55.00]	12.57 [0.03, 27.21]	4.78 [-5.15, 24.35]	4.93 [-2.59, 15.25]	8.18 [-3.09, 35.13]	7.98 [-9.07, 29.07]	6.52 [-4.54, 33.69]
2081-2100	33.92 [0.25, 95.19]	12.10 [-1.08, 27.11]	6.11 [-5.05, 44.86]	15.13 [0.03, 36.81]	18.38 [-2.58, 56.06]	24.27 [-1.19, 57.84]	7.97 [-9.47, 53.07]
RCP8.5							
2031-2050	29.94 [-1.45,80.00]	14.51 [0.08, 30.73]	-2.13 [-12.44, 13.60]	5.92 [-0.90, 14.20]	14.11 [-0.12, 43.84]	23.74 [0.11, 56.71]	7.25 [-2.06, 30.36]
2081-2100	61.56 [-1.96, 184.10]	39.30 [-8.61, 85.02]	19.01 [-10.47, 93.57]	20.28 [-0.03, 47.92]	51.98 [0.27, 143.62]	49.75 [0.11, 129.49]	20.75 [-9.92, 108.40]

Article title: Modeling and projecting health-relevant combined ozone and temperature events in present and future Central European climate
Journal name: Air Quality, Atmosphere & Health
Author names: Sally Jahn*, Elke Hertig

*Corresponding author
E-mail address: **sally.jahn@geo.uni-augsburg.de**
Regional Climate Change and Health, Institute of Geography and Faculty of Medicine,
Augsburg University, Alter Postweg 118, 86159 Augsburg, Germany
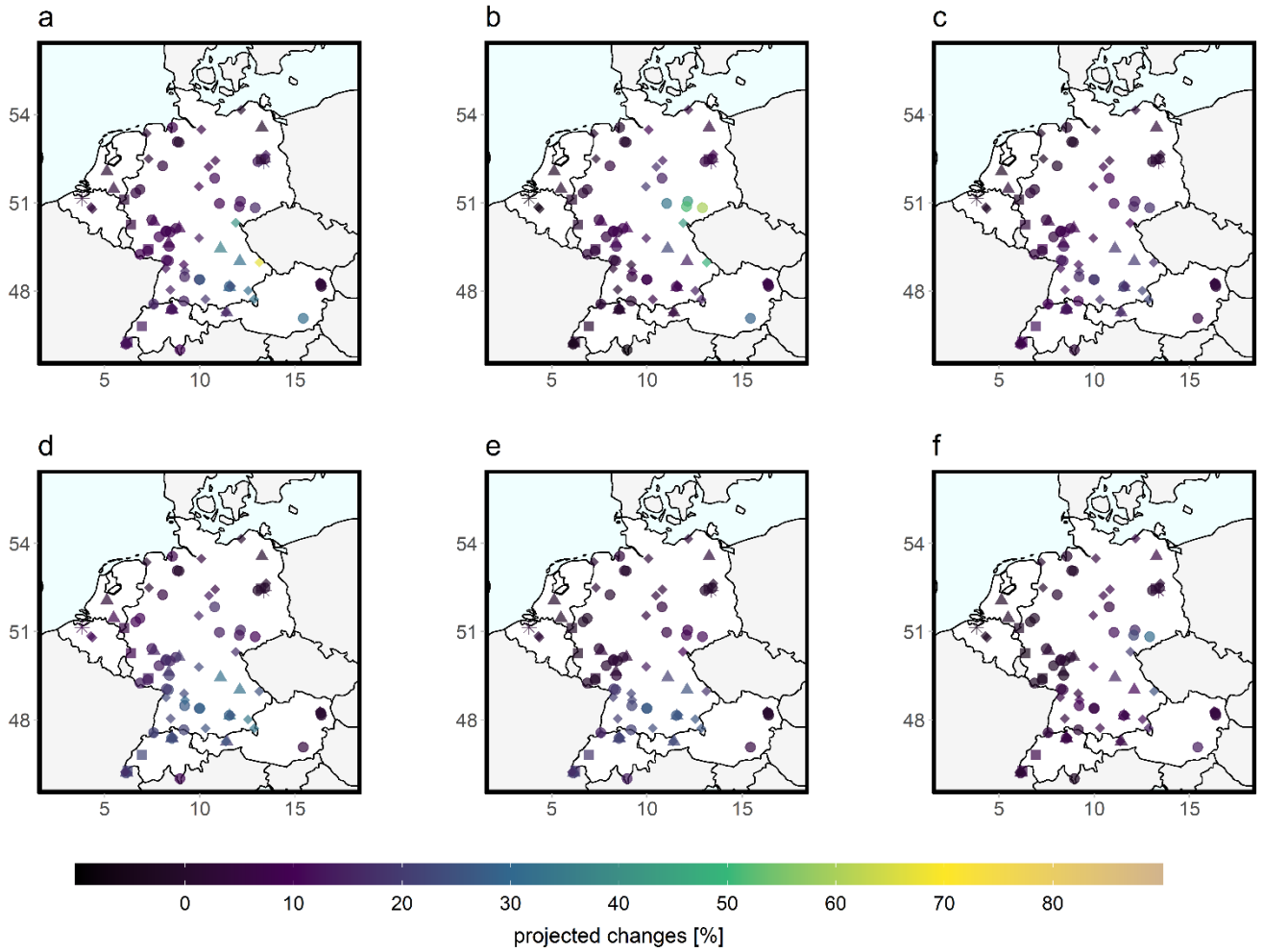
Fig. S1 Spatial distribution of monthly changes [%] regarding the amount of days with combined o-t-events between the period 2031-2050 compared with 1993-2012 under RCP4.5 scenario. Months April to September are shown from a to f. Numbers refer to the ensemble mean across all seven ESMs.
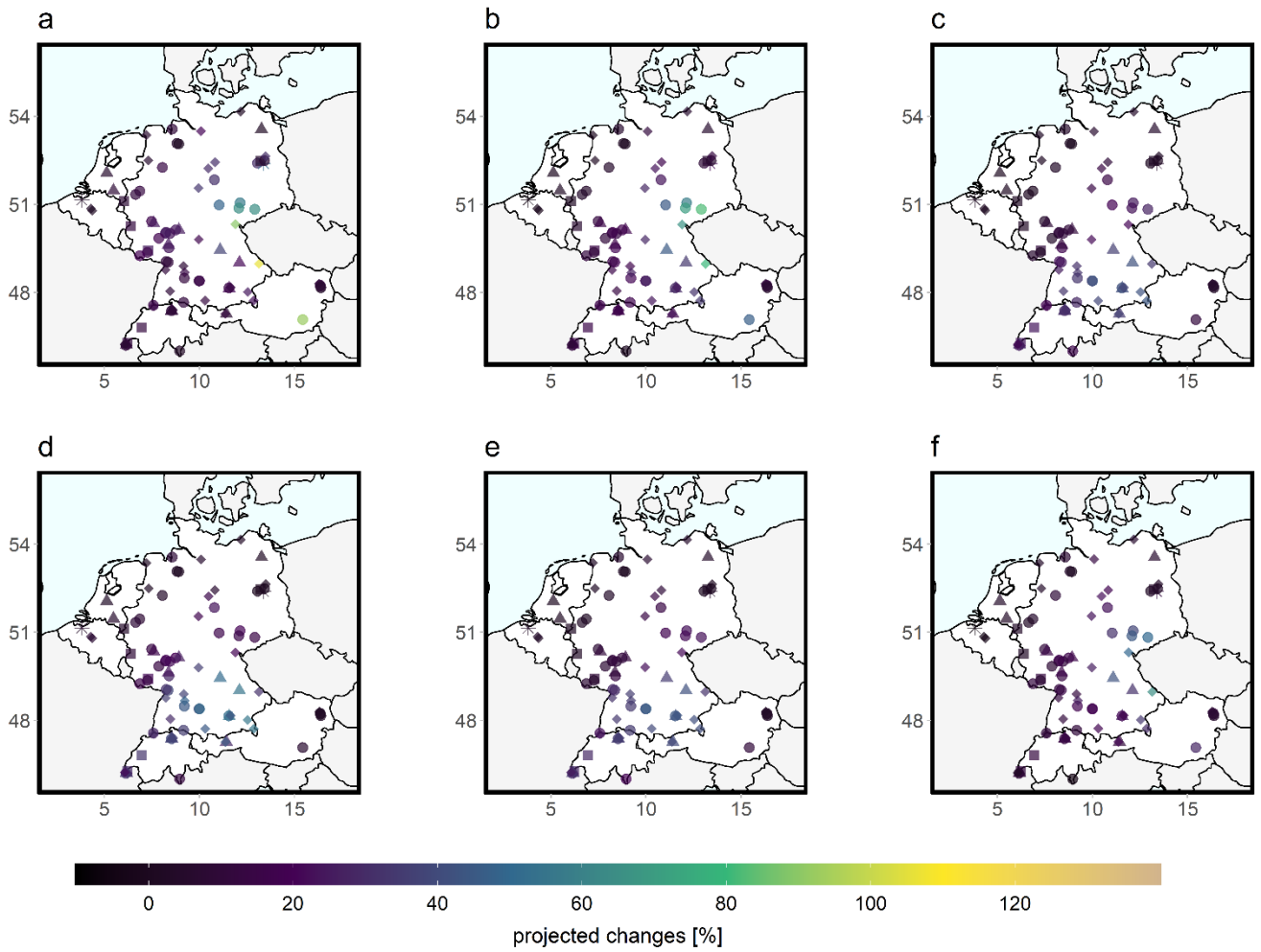
Fig. S2 Spatial distribution of monthly changes [%] regarding the amount of days with combined o-t-events between the period 2081-2100 compared with 1993-2012 under RCP4.5 scenario. Months April to September are shown from a to f. Numbers refer to the ensemble mean across all seven ESMs.
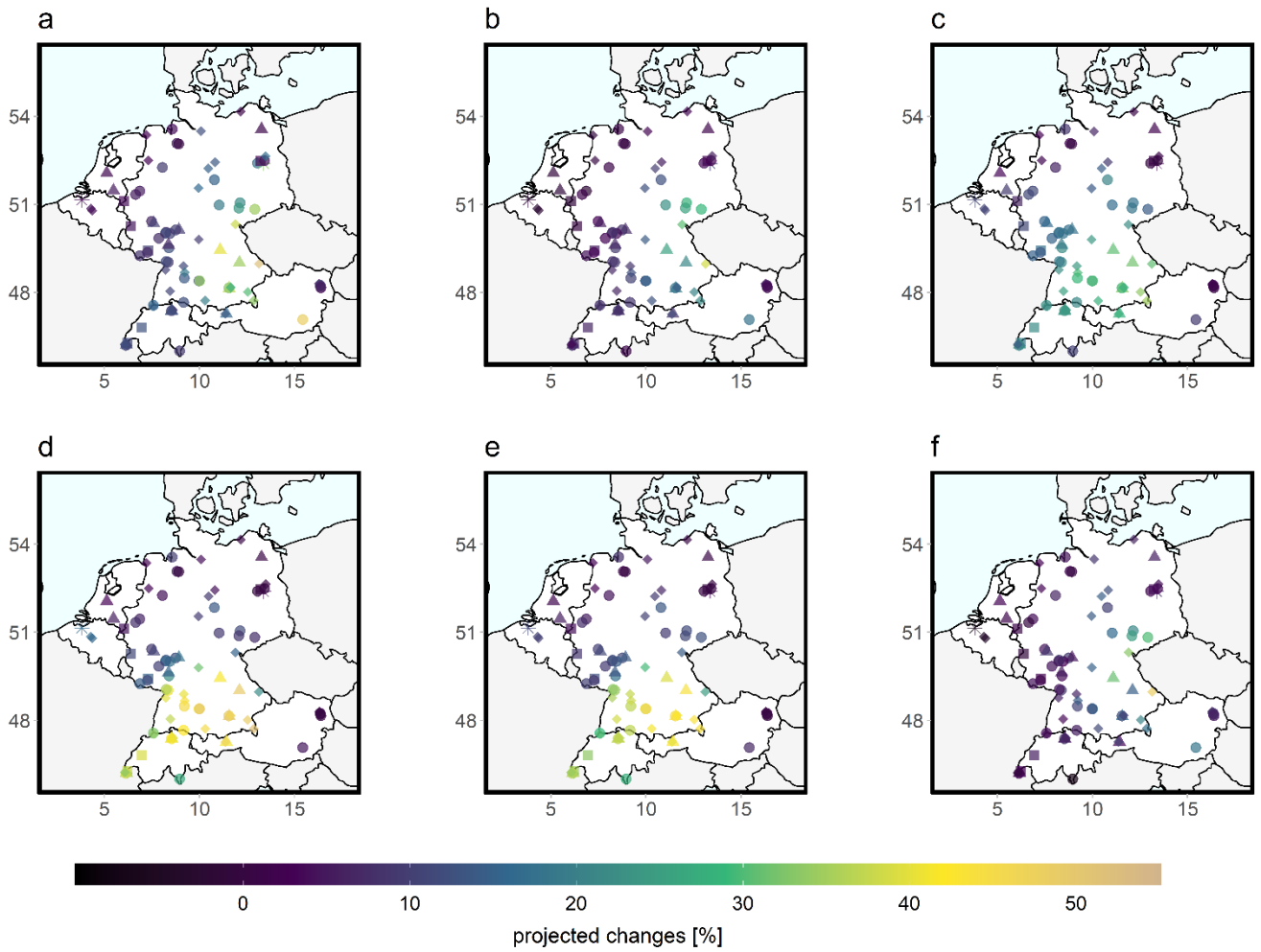
Fig. S3 Spatial distribution of monthly changes [%] regarding the amount of days with combined o-t-events between the period 2031-2050 compared with 1993-2012 under RCP8.5 scenario. Months April to September are shown from a to f. Numbers refer to the ensemble mean across all seven ESMs.
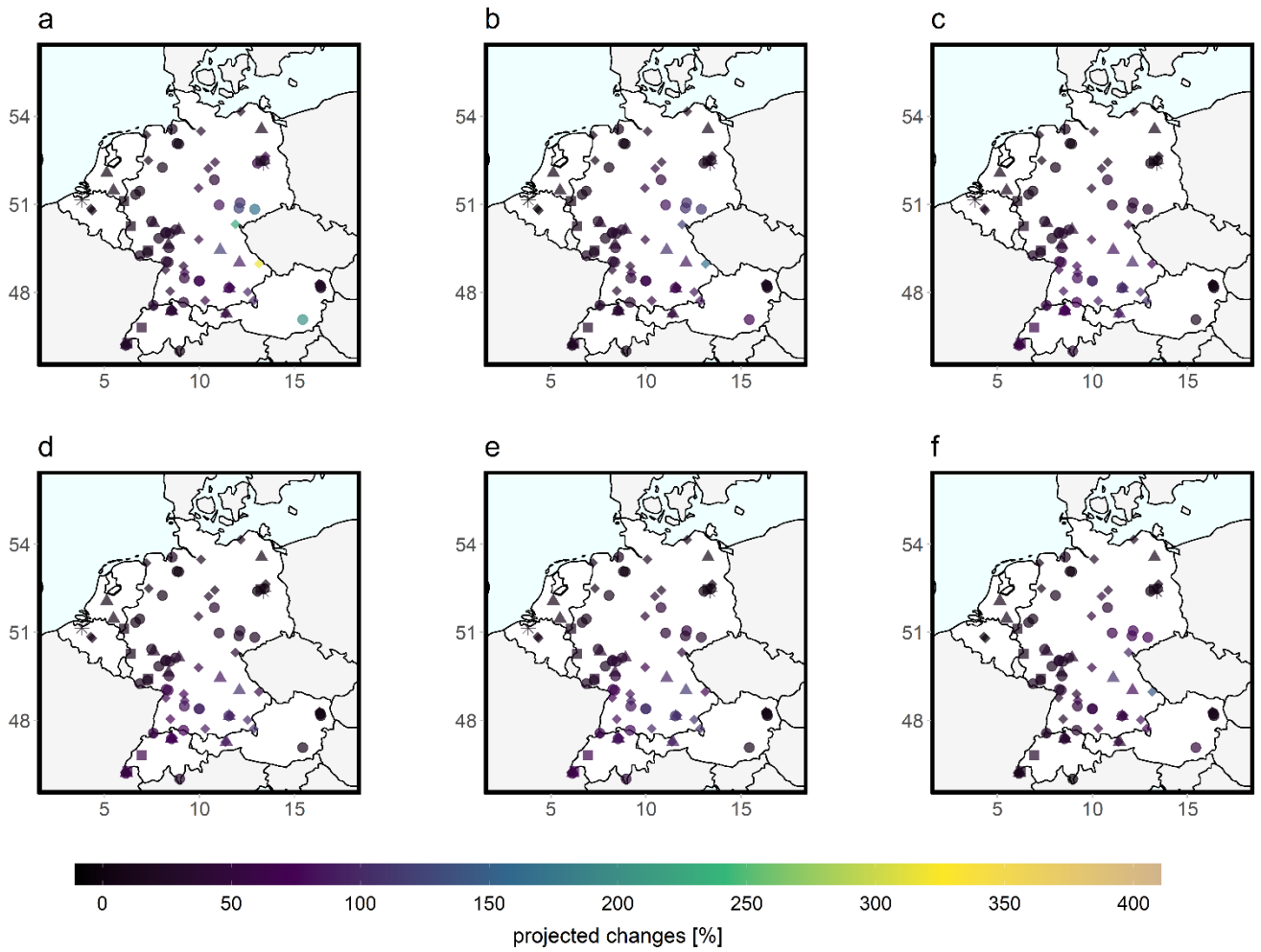
Fig. S4 Spatial distribution of monthly changes [%] regarding the amount of days with combined o-t-events between the period 2081-2100 compared with 1993-2012 under RCP8.5 scenario. Months April to September are shown from a to f. Numbers refer to the ensemble mean across all seven ESMs.

Appendix E

Supplementary Information

Research Article 2

The Supplementary Information of Research Article 2 (Chapter 3) as submitted and available online alongside the original article.

Using clustering, statistical modeling, and climate change projections to analyze recent and future region-specific compound ozone and temperature burden over Europe

Sally Jahn[1], Elke Hertig[2]

[1]Regional Climate Change and Health, Institute of Geography and Faculty of Medicine,

University of Augsburg, Werner-von-Siemens-Straße 6, 86159 Augsburg, Germany

[2]Regional Climate Change and Health, Faculty of Medicine,

University of Augsburg, Werner-von-Siemens-Straße 6, 86159 Augsburg, Germany

Contents of this file

Table S1 *Abbreviations and Acronyms*

General	Explanation
MDA8O3	Daily maximum ozone values based on 8-hour running means
NO_x	Nitrogen oxides
O_3	Tropospheric, ground-level ozone
o- / t- / o-t-(events, season etc.)	Ozone- / temperature- / Ozone - temperature (events, season etc.)
PAN	Peroxyacetyl nitrate
TX; [80]TX	Daily maximum surface air temperature; Daily 80th percentiles based on a 31-day window, 2004-2018
VOCs	Volatile organic compounds
Ward's method	Ward variance minimization algorithm
WHO	World Health Organization

Predictors	Explanation
GH	Geopotential heights at 850 hPa
MID	Most important driver
MT	Mean air temperatures at 850 hPa
SH	Specific humidity at 850 hPa
SMID	Second most important driver
SSRD	Surface solar radiation downwards
TMID	Third most important driver
WT	Weather type(s)

O-t-Regions	Explanation
1-CE	Central Eastern
2-CN	Central Northern
3-CW	Central Western
4-HA	Central High Altitude
5-NE	Northern European
6-SE	Southern European

Models/Projections	Explanation
CMIP5/6	Coupled Model Intercomparison Project Phase 5/6
ESM	Earth System Model(s)
F1-Score	Metric represents the harmonic mean and maintains a balance between R and P.
GAM	Generalized additive model(s)
LR	Logistic Regression
MF-R^2	McFadden's R^2
P	Precision. Metric is used to measure the fraction of the predicted events that did actually occur.
R	Recall. Metric is used to measure the fraction of actual, observed events that are correctly predicted.
SMOTE	Synthetic Minority Oversampling Technique

Table S2 *Overview Station Pairs*

No.	O₃ station code	O₃ station name	O₃ station type	O₃ station longitude [°]	O₃ station latitude [°]	O₃ station altitude [m a.s.l.]	TX station code	TX station name	Distance [km]	Altitude difference [m]	O-t-region
1	AT0SON1	Sonnblick	1	12.96	47.05	3106	15	SONNBLICK	0.81	0	4-HA
2	AT4S156	Braunau Zentrum, Kolpingplatz	3	13.04	48.26	350	4647	SIMBACH/INN	1.81	-10	1-CE
3	AT51200	Salzburg Lehener Park, Franz-Martin-Straße 1	2	13.03	47.82	455	14	SALZBURG	3.01	18	1-CE
4	AT60138	Graz Nord Gösting	3	15.41	47.10	348	12	GRAZ	3.05	-18	1-CE
5	AT72113	Innsbruck Sadrach	3	11.37	47.27	670	13	INNSBRUCK	2.57	93	1-CE
6	AT90LAA	Wien Laaer Berg	2	16.39	48.16	250	16	WIEN	8.58	52	1-CE
7	BETR001	41R001 - MOLENBEEK	2	4.33	50.85	20	17	UCCLE	5.98	-80	2-CN
8	DEBB021	Potsdam-Zentrum	2	13.06	52.40	31	54	POTSDAM	2.02	-50	1-CE
9	DEBB048	Neuruppin	3	12.81	52.93	43	475	NEURUPPIN	2.96	5	1-CE
10	DEBB053	Hasenholz	1	14.02	52.56	88	4430	MUNCHEBERG	8.95	25	1-CE
11	DEBB064	Cottbus	2	14.33	51.75	75	4014	COTTBUS	3.59	6	1-CE
12	DEBB065	Lütte (Belzig)	1	12.56	52.19	111	4766	WIESENBURG	10.61	-76	1-CE
13	**DEBB066**	**Spreewald**	**1**	**14.06**	**51.90**	**52**	**4370**	**LUBBEN-BLUMENFELDE**	**12.48**	**-5**	**1-CE**
14	DEBB067	Nauen	3	12.89	52.61	31	4808	BERGE	6.64	-9	1-CE

3

15	DEBE010	Berlin Wedding	2	13.35	52.54	35	4563	BERLIN-MITTE	2.54	0	1-CE
16	DEBE027	Berlin Marienfelde	1	13.37	52.40	45	4556	BERLIN-LICHTENRADE	3.30	-2	1-CE
17	DEBE032	Berlin Grunewald (3.5 m)	1	13.23	52.47	50	4588	BERLIN-ZEHLENDORF	4.81	5	1-CE
18	DEBE051	Berlin Buch	3	13.48	52.64	60	4529	BERLIN-BUCH	1.91	0	1-CE
19	DEBW023	Weil am Rhein	3	7.63	47.59	275	4042	EIMELDINGEN	5.35	11	3-CW
20	DEBW024	Ludwigsburg	3	9.17	48.90	302	3506	STUTTGART-SCHNARRENBERG	8.06	-12	3-CW
21	DEBW027	Reutlingen	2	9.21	48.49	385	4554	REUTLINGEN-BETZINGEN	2.54	25	3-CW
22	DEBW039	Villingen-Schwenningen	3	8.46	48.05	700	4712	VILLINGEN-SCHWENNINGEN	0.35	-20	3-CW
23	DEBW042	Bernhausen	3	9.23	48.68	370	2763	STUTTGART/ECHTERDINGEN	1.25	-1	3-CW
24	DEBW052	Konstanz	2	9.17	47.66	403	495	KONSTANZ	2.22	-40	3-CW
25	DEBW073	Neuenburg	3	7.57	47.82	223	4286	MULLHEIM	5.49	-50	3-CW
26	DEBW076	Baden-Baden	3	8.22	48.77	148	4284	BADEN-BADEN-GEROLDSAU	5.40	-92	3-CW
27	DEBW081	Karlsruhe-Nordwest	2	8.36	49.03	114	51	KARLSRUHE	1.36	2	3-CW
28	DEBW084	Freiburg	2	7.83	48.00	262	4115	FREIBURG IM BREISGAU-HERDERN	2.46	7	3-CW

29	DEHB001	Bremen-Mitte	2	8.82	53.08	10	4884	BREMEN-SEEFAHRTSCHULE	3.45	6	2-CN
30	**DEHB002**	**Bremen-Ost**	**2**	**8.92**	**53.06**	**7**	**42**	**BREMEN**	**8.02**	**3**	**2-CN**
31	DEHB005	Bremerhaven-Hansastraße	2	8.57	53.56	3	4885	BREMERHAVEN	3.16	-4	2-CN
32	DEHH008	Hamburg Sternschanze	2	9.97	53.56	15	4180	HAMBURG-BOTANISCHER GARTEN	1.39	1	2-CN
33	DEHH033	Hamburg Flughafen Nord	2	10.00	53.64	13	47	HAMBURG FUHLSBUETTEL	0.64	2	2-CN
34	**DEHH047**	**Hamburg Bramfeld**	**3**	**10.11**	**53.63**	**31**	**4186**	**HAMBURG-WANDSBEK**	**5.08**	**13**	**2-CN**
35	DEHH050	Hamburg Neugraben	3	9.86	53.48	3	4182	HAMBURG-NEUWIEDENTHAL	2.73	0	2-CN
36	DEMV007	Rostock-Stuthof	3	12.17	54.16	5	472	ROSTOCK-WARNEMUNDE	6.40	1	2-CN
37	DENW038	Mülheim-Styrum	2	6.87	51.45	39	4074	ESSEN-BREDENEY	8.93	-111	2-CN
38	DENW042	Krefeld-Linn	2	6.64	51.34	36	4030	DUISBURG-FRIEMERSHEIM	7.75	5	2-CN
39	DENW059	Köln-Rodenkirchen	3	6.99	50.89	50	4298	KOLN-BOTANISCHER GARTEN	8.16	5	2-CN
40	DENW065	Netphen Rothaargebirge	1	8.19	50.93	641	4514	BAD-STUNZEL BERLEBURG	13.81	31	4-HA
41	DENW071	Düsseldorf-Lörick	2	6.73	51.25	38	4029	DUSSELDORF-SUDFRIEDHOF	5.67	1	2-CN

42	DENW078	Ratingen-Tiefenbroich	3	6.82	51.30	42	479	DUSSELDORF	3.54	5	2.CN
43	DENW079	Leverkusen-Manfort	3	7.00	51.03	50	4351	KOLN-STAMMHEIM	4.66	7	2-CN
44	DENW080	Solingen-Wald	3	7.05	51.18	208	4651	SOLINGEN-HOHENSCHEID	5.59	54	2-CN
45	DENW081	Borken-Gemen	1	6.87	51.86	44	4841	BORKEN IN WESTFALEN	1.59	-4	2-CN
46	DENW096	Mönchengladbach-Rheydt	3	6.43	51.15	83	4423	MONCHENGLADBACH	5.14	34	2-CN
47	DESH001	Altendeich	1	9.59	53.67	8	4195	HASELDORF	4.09	5	2-CN
48	DESH008	Bornhöved	1	10.24	54.09	45	4578	RUHWINKEL	1.14	9	2-CN
49	DESH023	Lübeck-St. Jürgen	2	10.70	53.84	12	4372	LUBECK-BLANKENSEE	2.86	7	2-CN
50	DESL002	Bexbach Schule	3	7.26	49.36	275	4458	NEUNKIRCHEN-WELLESWEILER	3.10	39	3-CW
51	DESL011	Saarbrücken-Eschberg	2	7.04	49.24	315	4584	SAARBRUCKEN-SANKT JOHANN	1.99	122	3-CW
52	DESN004	Bautzen	2	14.44	51.18	203	4384	KR. BAUTZEN KUBSCHUTZ	4.58	-29	1-CE
53	DESN049	Carlsfeld	1	12.61	50.43	896	4950	CARLSFELD	0.14	-1	4-HA
54	DESN051	Radebeul-Wahnsdorf	1	13.68	51.12	246	43	DRESDEN WAHNSDORF	0.65	0	1-CE
55	DESN052	Zinnwald	1	13.75	50.73	877	4801	ZINNWALD-GEORGENFELD	0.18	0	4-HA
56	**DESN053**	**Fichtelberg**	**1**	**12.95**	**50.43**	**1214**	**488**	**FICHTELBERG**	**0.15**	**1**	**4-HA**

57	DESN059	Leipzig-West	2	12.30	51.32	115	4344	LEIPZIG-HOLZHAUSEN	10.44	-23	1-CE
58	DESN080	Schkeuditz	1	12.23	51.40	122	482	LEIPZIG-SCHKEUDITZ	4.45	-9	1-CE
59	DESN081	Plauen-DWD	3	12.13	50.48	385	4522	PLAUEN	0.17	-1	1-CE
60	**DEST002**	**Burg**	**3**	**11.86**	**52.27**	**47**	**4679**	**THEESSEN**	**13.21**	**-14**	**1-CE**
61	DEST011	Wernigerode/Bahnhof	2	10.79	51.84	235	4758	WERNIGERODE	1.70	1	1-CE
62	DEST028	Zeitz	2	12.14	51.05	156	4797	ZEITZ	0.21	-14	1-CE
63	DEST039	Brocken	1	10.62	51.80	1130	2006	BROCKEN	0.19	-12	4-HA
64	**DEST066**	**Wittenberg/Bahnstrasse**	**2**	**12.66**	**51.87**	**71**	**4776**	**WITTENBERG**	**2.46**	**-34**	**1-CE**
65	DEST077	Magdeburg/West	2	11.61	52.13	58	477	MAGDEBURG	3.33	-18	1-CE
66	DETH009	Gera Friedericistr.	2	12.07	50.88	190	3990	GERA-LEUMNITZ	3.89	-121	1-CE
67	DETH020	Erfurt Krämpferstr.	2	11.04	50.98	195	487	ERFURT-BINDERSLEBEN	5.27	-121	1-CE
68	DETH026	Dreißigacker	1	10.38	50.56	450	486	MEININGEN	0.14	0	1-CE
69	DETH027	Neuhaus	1	11.13	50.50	840	4450	NEUHAUS AM RENNWEG	0.17	-5	4-HA
70	DETH041	Jena Dammstr.	2	11.60	50.93	140	49	JENA STERNWARTE	1.18	-15	1-CE
71	DETH061	Hummelshain	1	11.66	50.79	357	4415	SCHMIERITZ-WELTWITZ	11.15	8	1-CE
72	DEUB028	Zingst	1	12.72	54.44	1	4353	BARTH	10.75	-2	2-CN
73	DEUB029	Schmücke	1	10.77	50.65	937	4617	SCHMUCKE	0.19	0	4-HA

74	DK0045A	"Copenhagen/1259"	2	12.56	55.70	25	116	KOEBENHAVN: LANDBOHOJSKOLEN-1	2.61	16	2-CN
75	EE0018A	Oismäe	2	24.65	59.41	6	11363	TALLINN	3.19	-27	2-CN
76	ES0124A	ARTURO SORIA	2	-3.64	40.44	698	230	MADRID - RETIRO	4.56	31	6-SE
77	**ES1215A**	**Amposta (Sant Domènec - Itàlia)**	**3**	**0.58**	**40.71**	**8**	**236**	**TORTOSA - OBSERVATORIO DEL EBRO**	**14.77**	**-36**	**6-SE**
78	ES1421A	TERUEL	2	-1.11	40.34	915	3966	TERUEL	1.68	15	6-SE
79	ES1443A	BURGOS 4	2	-3.64	42.34	929	414	BURGOS-VILLAFRIA	2.21	39	3-CW
80	ES1472A	ITURRAMA	2	-1.65	42.81	449	3950	PAMPLONA (OBSERVATORIO)	1.67	7	3-CW
81	ES1516A	RIO SAN PEDRO	2	-6.23	36.52	1	415	CADIZ	3.73	0	6-SE
82	ES1529A	TETUÁN	2	-3.79	43.47	30	1392	SANTANDER CENTRO	2.34	-34	3-CW
83	ES1535A	ALBACETE	3	-1.85	38.98	686	3906	ALBACETE OBS.	3.13	12	6-SE
84	ES1572A	PURIFICACIÓN TOMÁS	2	-5.87	43.37	276	3913	OVIEDO	2.06	-60	3-CW
85	**ES1599A**	**PAGOETA**	**1**	**-2.16**	**43.25**	**225**	**234**	**SAN SEBASTIAN - IGUELDO**	**11.32**	**-26**	**3-CW**
86	ES1602A	LA CIGÜEÑA	2	-2.43	42.46	385	1398	LOGRONO-AGONCILLO	8.09	32	3-CW
87	ES1604A	BELLVER	3	2.62	39.56	117	3918	PALMA DE MALLORCA CMT	1.00	114	6-SE
88	ES1612A	MAJADAHONDA	3	-3.87	40.45	722	3947	MADRID/CUATROVIENTOS	10.17	35	6-SE

89	ES1615A	CÁCERES	2	-6.36	39.47	389	3921	CACERES CIUDAD	1.27	-70	6-SE
90	ES1619A	VALÈNCIA-VIVERS	2	-0.37	39.48	11	237	VALENCIA	0.32	0	6-SE
91	ES1624A	ELX-AGROALIMENTARI	3	-0.68	38.24	44	309	ALICANTE EL ALTET	10.79	1	6-SE
92	ES1638A	BERMEJALES	2	-5.98	37.35	26	423	SEVILLA/SAN PABLO	11.77	-8	6-SE
93	ES1641A	RENOVALES	2	-0.89	41.64	220	238	ZARAGOZA AEROPUERTO	9.95	-27	3-CW
94	**ES1666A**	**Tarragona (parc de la Ciutat)**	**2**	**1.24**	**41.12**	**13**	**1401**	**REUS/AEROPUERTO**	**6.35**	**-58**	**6-SE**
95	ES1713A	PARQUE EUROPA	2	-2.90	43.25	76	1393	BILBAO AEROPUERTO	4.81	34	3-CW
96	FI00352	Oulanka	1	29.40	66.32	310	7765	KUUSAMO KIUTAKONGAS	6.33	150	5-NE
97	FI00425	Kallio 2	2	24.95	60.19	18	28	HELSINKI KAISANIEMI	1.39	14	2-CN
98	FR02004	Martigues P. Central	2	5.04	43.42	107	39	MARIGNANE	14.15	98	6-SE
99	FR04149	MONTGERON	2	2.46	48.71	68	11249	ORLY	5.47	-21	3-CW
100	**FR07004**	**Montferrand**	**2**	**3.11**	**45.80**	**340**	**750**	**CLERMONT-FERRAND**	**2.98**	**9**	**3-CW**
101	FR08017	Périurbaine Sud	3	3.91	43.57	5	2207	MONTPELLIER-AEROPORT	4.20	3	6-SE
102	FR08712	St Estève	3	2.84	42.72	61	36	PERPIGNAN	3.29	19	6-SE
103	FR09015	Les Couronneries	3	0.36	46.59	119	749	POITIERS - BIARD	3.48	-4	3-CW
104	FR12004	ECOLE M.JACQUIER	2	1.42	43.58	143	33	TOULOUSE-BLAGNAC	5.97	-8	3-CW

105	FR14033	STE SAVINE	2	4.05	48.30	119	11243	TROYES-BARBEREY	3.98	7	3-CW
106	FR20048	SAINT EXUPERY	3	5.07	45.75	217	37	LYON - ST EXUPERY	3.02	-18	3-CW
107	FR21019	IFS Caen sud	2	-0.35	49.15	22	738	CAEN-CARPIQUET	8.13	-45	2-CN
108	FR22014	Spicheren(14)	3	6.96	49.20	340	4850	SAARBRUCKEN-BURBACH	5.40	150	3-CW
109	FR24007	ANTIBES JEAN MOULIN	3	7.09	43.60	81	757	NICE	10.70	79	6-SE
110	FR25040	Mesnil Esnard	3	1.16	49.41	160	2184	ROUEN - BOOS	3.21	9	2-CN
111	**FR26010**	**Station DAIX**	**3**	**5.00**	**47.35**	**332**	**745**	**DIJON-LONGVIC**	**10.80**	**113**	**3-CW**
112	FR31001	GRAND PARC	2	-0.58	44.86	3	34	BORDEAUX-MERIGNAC	9.47	-44	3-CW
113	FR33211	ANNEMASSE	2	6.24	46.20	441	241	GENEVE OBSERVATOIRE	6.99	36	3-CW
114	FR34024	Joué lès Tours	2	0.65	47.34	90	2190	TOURS	12.39	-18	3-CW
115	FR34032	Leblanc	2	2.40	47.08	133	32	BOURGES	4.30	-28	3-CW
116	FR35007	PALAIS S/ V.- Garros	3	1.31	45.87	333	2195	LIMOGES - BELLEGARDE	10.51	-69	3-CW
117	GB0002R	Eskdalemuir	1	-3.21	55.32	255	272	ESKDALEMUIR	0.42	13	5-NE
118	GB0006R	Lough Navar	1	-7.90	54.44	130	1822	LOUGH NAVAR FOREST	0.19	4	5-NE
119	**GB0033R**	**Bush Estate**	**1**	**-3.21**	**55.86**	**180**	**1831**	**PENICUIK**	**4.45**	**-5**	**5-NE**
120	GB0038R	Lullington Heath	1	0.18	50.79	125	1864	EASTBOURNE	8.14	118	2-CN
121	GB0566A	London Bloomsbury	2	-0.13	51.52	20	1859	HAMPSTEAD	5.64	-117	5-NE

122	GB0567A	**Belfast Centre**	2	-5.93	54.60	10	1821	**STORMONT CASTLE**	6.45	-46	5-NE
123	GB0584A	Leeds Centre	2	-1.55	53.80	78	1847	BRADFORD	14.84	-56	5-NE
124	GB0642A	London Hillingdon	2	-0.46	51.50	34	1860	HEATHROW	2.11	9	5-NE
125	GB0643A	Leamington Spa	2	-1.53	52.29	55	1853	WELLESBOURNE	10.39	8	5-NE
126	HU0023A	"Debrecen Kalotaszeg"	2	21.62	47.51	111	852	DEBRECEN AIRPORT	2.77	4	1-CE
127	HU0029A	"Pecs Boszorkany	3	18.21	46.08	200	849	PECS POGANY	8.48	-2	1-CE
128	IE0001R	**Kerry Valentia Observatory**	3	-10.24	51.94	10	123	**VALENTIA OBSERVATORY**	1.30	1	5-NE
129	IE0028A	Dublin Rathmines Wynnefield Road	2	-6.28	53.35	25	1704	DUBLIN (GLASNEVIN)	1.93	4	5-NE
130	IE0031R	Galway Mace Head	1	-9.90	54.33	8	2143	BELMULLET	12.41	-1	5-NE
131	IE0090A	Monaghan Kilkitt Waterworks	1	-6.88	54.07	170	968	CARRICKMACROSS (DUNOGE)	12.96	82	5-NE
132	LU0101A	Luxembourg Bonnevoie	2	6.14	49.60	275	203	LUXEMBOURG AIRPORT	5.68	-101	2-CN
133	NL00107	"Posterholt-Vlodropperweg"	1	6.04	51.12	32	4207	HEINSBERG-SCHLEIDEN	9.66	-25	2-CN
134	NL00133	"Wijnandsrade-Opfergeltstraat"	3	5.88	50.90	96	168	MAASTRICHT	8.46	-18	2-CN
135	NL00235	"Huijbergen-Vennekenstraat"	1	4.36	51.43	18	604	WOENSDRECHT	1.92	4	2-CN
136	NL00318	"Philippine-Stelleweg"	1	3.75	51.30	5	2571	WESTDORPE	11.05	4	2-CN
137	NL00404	"Den Haag-Rebecquestraat"	2	4.29	52.08	2	10961	VOORSCHOTEN	12.16	3	2-CN

138	NL00437	"Westmaas-Groeneweg"	1	4.45	51.79	-1	3192	ROTTERDAM-GEULHAVEN	14.99	-4	2-CN
139	NL00722	"Eibergen-Lintveldseweg"	1	6.61	52.09	19	454	HUPSEL	4.43	-10	2-CN
140	NL00738	"Wekerom-Riemterdijk"	1	5.71	52.11	18	2563	DEELEN	12.87	-32	2-CN
141	**NL00807**	**"Hellendoorn-Luttenbergerweg"**	**1**	**6.40**	**52.39**	**7**	**453**	**HEINO**	**11.02**	**4**	**2-CN**
142	NL00818	"Barsbeek-De Veenen"	1	6.02	52.65	1	411	MARKNESSE	10.22	4	2-CN
143	NL00918	"Balk-Trophornsterweg"	1	5.57	52.92	1	596	STAVOREN	12.97	2	2-CN
144	NL00934	"Kollumerwaard-Hooge Zuidwal"	1	6.28	53.33	1	413	LAUWERSOOG	10.31	-1	2-CN
145	NO0015R	Tustervatn	1	13.91	65.83	440	18266	VARNTRESK	13.11	34	5-NE
146	PL0004R	IMGW Łeba - Rąbka	3	17.53	54.75	2	332	LEBA	0.09	0	2-CN
147	PL0044A	Warszawa-Podleśna	2	20.96	52.28	98	209	WARSZAWA-OKECIE	13.14	-9	1-CE
148	PT03087	Restelo	2	-9.21	38.70	143	214	LISBOA GEOFISICA	5.39	66	6-SE
149	SE0001A	Malmö Rådhuset	2	13.00	55.61	25	5177	MALMO_2	1.55	22	2-CN
150	SE0004A	Göteborg Femman	2	11.97	57.71	31.3	462	GOTEBORG A	1.61	26.3	2-CN
151	SE0005R	Bredkälen	1	15.32	63.85	380	5696	HALLHAXASEN_A	8.41	5	5-NE
152	SE0013R	Esrange	1	21.06	67.88	524	5859	ESRANGE	1.30	189	5-NE
153	SE0014R	Råö	1	11.91	57.39	10	3512	NIDINGEN A	9.99	8	2-CN
154	SE0022A	Stockholm Torkel Knutssongatan	2	18.06	59.32	58	5464	STOCKHOLM_A	2.57	14	2-CN

155	SE0035R	Vindeln	1	19.77	64.24	271	5714	VINDELN-SUNNANSJONAS	5.42	34	5-NE
156	SE0054A	Lund Spyken	2	13.20	55.70	60	463	LUND	0.11	-13	2-CN
157	SI0003A	Ljubljana Bezigrad	2	14.51	46.07	299	228	LJUBLJANA BEZIGRAD	0.33	0	1-CE
158	SI0008R	Iskrba	1	14.86	45.56	540	3311	KOCEVJE	5.42	73	1-CE
159	SI0033A	Murska Sobota-Rakican	1	16.19	46.65	188	3335	MURSKA SOBOTA-RAKICAN	5.43	0	1-CE
160	SI0034A	Nova Gorica	2	13.65	45.96	113	3326	BILJE	7.39	58	1-CE
161	SK0004R	"Stara Lesna - AU SAV EMEP/O3"	1	20.29	49.15	808	334	POPRAD/TATRY	10.47	114	1-CE

Note. All 161 ozone stations with station code, name, type and specific location metadata. O_3 station types are specified as follows: 1 = rural, 2 = urban, 3= suburban. Station codes and names of the assigned temperature stations are given. Respective distance and altitude difference values for each station pair are depicted. The o-t-region each station pair is assigned to is given as well. Stations are listed in alphabetical order based on the O_3 station code. Representative stations are framed and highlighted in bold.

Table S3 *ERA5-ESM pairs with Significant Distributional Differences*

ESM	Station	O-t-region	Variable
CanESM5	DESN053	4-HA	GH
	ES1599A	3-CW	SH
	ES1215A	6-SE	SH
FGOALS-g3	ES1666A	6-SE	SH
	NL00807	2-CN	GH
	ES1215A	6-SE	SH
INM-CM5-0	ES1599A	3-CW	SH
	ES1666A	6-SE	SH
	FR07004	3-CW	SH
IPSL-CM6A-LR	DEBB066	1-CE	SSRD
	DEST066	1-CE	SSRD
MIROC6	GB0033R	5-NE	MT

Note. 12 ERA5-ESM pairs that show significant distributional differences for a specific meteorological predictor based on the evaluation of monthly time series data by applying a two-sample Kolmogorov-Smirnov test. Distribution differences were tested on the 95% significance level. In general, 4 (predictor variables) x 15 (representative stations) x 8 (ESM) = 480 ERA5-ESM predictor variable pairs were tested. No statistical downscaling projections were generated for 5 of the 12 depicted representative stations, as all stations of 5-NE and 6-SE were discarded from further analysis after the evaluation of o-t-characteristics in the base period and the subsequent modeling process.

Table S4 *Daily Weather Type Occurrences (%)*

ESM	WT1	WT2	WT3	WT4	WT5	WT6	WT7	WT8	WT9
BCC-CSM2-MR	13.09	8.55	13.72	9.59	9.67	9.40	9.97	12.40	13.61
CanESM5	13.36	12.38	9.48	12.95	8.22	9.13	7.84	14.21	12.43
FGOALS-g3	12.65	11.17	10.79	11.53	12.19	9.26	8.72	12.35	11.34
INM-CM5-0	12.27	15.77	10.27	12.35	8.66	10.96	3.72	15.27	10.74
IPSL-CM6A-LR	11.80	12.65	10.93	13.55	9.64	9.95	9.86	13.33	8.28
MIROC6	13.61	14.89	5.82	13.91	9.86	11.12	6.64	15.77	8.39
MPI-ESM1-2-HR	12.54	12.19	10.79	13.50	8.77	10.98	10.38	12.73	8.11
MRI-ESM2-0	12.87	11.45	10.49	12.19	10.55	9.75	10.46	12.62	9.62
ERA5	14.32	12.20	9.22	11.99	11.07	9.18	9.76	12.31	9.95

Note. The relative numbers (%) of daily weather type occurrences per ESM as well as for ERA5 reanalysis data are shown. The relative numbers are based on daily WT time series data considering the chosen historical ESM period 1995-2014 for all eight climate models, while reanalysis WT numbers refer to the base period 2004-2018.

Table S5 *Overview Representative Stations*

Station	Position	MDA8O3 mean (min / max)	MDA8O3 median (25th / 75th)	TX mean (min / max)	TX median (25th / 75th)	80TX mean (min / max)	80TX median (25th / 75th)	Total number of o-/ t- / o-t-event days [-]	Relative number of ozone / temperature / o-t-events [%]
			1-CE - 12 rural, 18 urban and 9 suburban (total: 39) stations						
DEST066 (urban)	1	100.31 (27.00 / 231.37)	96.51 (81.00 / 116.17)	21.63 (1.80 / 37.80)	21.80 (17.80 / 25.50)	25.58 (16.54 / 29.92)	26.60 (23.10 / 28.00)	1226 / 547 / 513	44.66 / 19.93 / 18.69
DEBB066 (rural)	3	98.68 (21.00 / 195.00)	96.17 (81.69 / 113.80)	22.12 (2.30 / 37.90)	22.40 (18.30 / 25.90)	26.02 (17.60 / 30.40)	26.92 (23.62 / 28.52)	1188 / 540 / 493	43.28 / 19.67 / 17.96
DEST002 (suburban)	9	98.32 (31.40 / 222.01)	94.01 (79.80 / 113.00)	21.63 (2.50 / 38.50)	21.90 (17.90 / 25.30)	25.53 (16.72 / 29.80)	26.50 (23.40 / 27.92)	1105 / 547 / 479	40.26 / 19.93 / 17.45
			2-CN - 16 rural, 20 urban and 11 suburban (total: 47) stations						
NL00807 (rural)	1	88.08 (11.96 / 242.48)	83.09 (68.88 / 101.71)	20.05 (6.00 / 36.70)	20.10 (16.90 / 23.20)	23.36 (16.20 / 27.00)	24.10 (21.44 / 25.30)	720 / 544 / 419	26.23 / 19.82 / 15.26
DEHH047 (suburban)	4	86.12 (15.00 / 225.05)	83.00 (69.05 / 99.18)	20.02 (3.30 / 37.80)	20.00 (16.50 / 23.40)	23.65 (15.30 / 28.22)	24.40 (21.52 / 25.72)	652 / 548 / 411	23.75 / 19.96 / 14.97
DEHB002 (urban)	5	83.54 (8.44 / 211.02)	80.21 (65.45 / 98.24)	20.32 (3.80 / 36.80)	20.40 (16.90 / 23.80)	23.92 (16.20 / 28.30)	24.70 (21.82 / 25.90)	611 / 538 / 385	22.26 / 19.60 / 14.03
			3-CW - 1 rural, 20 urban and 12 suburban (total: 33) stations						
FR26010 (suburban)	1	100.30 (32.00 / 204.00)	97.00 (83.00 / 114.50)	22.62 (5.40 / 37.70)	22.70 (19.00 / 26.40)	26.51 (19.00 / 30.80)	27.12 (23.80 / 29.40)	1204 / 538 / 470	43.86 / 19.60 / 17.12
FR07004 (urban)	2	98.18 (24.00 / 185.00)	96.75 (83.00 / 112.00)	22.98 (5.20 / 39.80)	23.00 (19.10 / 26.90)	27.01 (19.22 / 31.12)	27.80 (24.72 / 29.94)	1136 / 538 / 441	41.38 / 19.60 / 16.07

16

ES1599A (rural)	27	94.25 (43.00 / 180.00)	94.00 (80.00 / 106.00)	20.11 (7.00 / 37.20)	20.00 (17.20 / 22.60)	22.81 (18.62 / 25.14)	23.50 (21.30 / 24.50)	916 / 542 / 342	33.37 / 19.74 / 12.46

4-HA - 8 rural, 0 urban and 0 suburban (total: 8) stations

DESN053 (rural)	1	111.39 (49.74 / 230.00)	109.00 (93.66 / 127.00)	13.36 (-6.40 / 30.60)	13.50 (9.60 / 17.50)	17.64 (9.30 / 21.90)	18.70 (15.00 / 20.22)	1706 / 546 / 519	62.15 / 19.89 / 18.91

5-NE - 10 rural, 6 urban and 1 suburban (total: 17) stations

GB0033R (rural)	1	75.67 (24.10 / 158.00)	73.64 (63.91 / 87.31)	16.50 (2.50 / 28.60)	16.60 (14.00 / 18.80)	18.75 (13.50 / 22.00)	19.50 (17.00 / 20.40)	193 / 510 / 80	7.03 / 18.58 / 2.91
GB0567A (urban)	2	66.38 (16.00 / 188.00)	64.00 (54.00 / 76.67)	16.92 (4.30 / 29.00)	17.10 (14.70 /19.10)	18.92 (13.70 / 21.40)	19.80 (17.40 / 20.50)	87 / 524 / 46	3.17 / 19.09 / 1.68
IE0001R (suburban)	7	74.03 (1.85 / 89.40)	72.20 (60.40 / 89.40)	16.15 (7.00 / 28.50)	16.40 (14.40 / 17.80)	17.50 (13.50 / 19.10)	18.50 (16.10 / 18.70)	341 / 512 / 116	12.42 / 18.65 / 4.23

6-SE - 0 rural, 9 urban and 8 suburban (total: 17) stations

ES1666A (urban)	1	103.33 (29.00 / 233.00)	101.00 (90.00 / 114.00)	26.49 (11.30 / 39.80)	27.40 (23.40 / 29.90)	28.65 (21.30 / 32.50)	29.70 (25.84 / 31.70)	1287 / 495 / 276	46.89 / 18.03 / 10.05
ES1215A (suburban)	2	101.01 (33.00 / 195.00)	100.00 (91.00 / 110.00)	29.33 (10.60 / 42.30)	30.10 (26.20 / 33.10)	31.84 (24.60 / 35.00)	33.00 (29.10 / 35.00)	1248 / 499 / 291	45.46 / 18.18 / 10.60

Note. The 15 selected representative stations per o-t-region are shown. O-t-regions are framed in the table by dashed lines. The total number as well as the number of stations per type are given as well. Position values refer to the proximity of a representative station to its respective cluster centroid based on the ranking of all region-specific stations with respect to their Euclidean distances to their cluster centroid (for example, considering the ranking of stations in 3-CW based on all computed Euclidean distances, station FR07004 is on position 2 of 33 being the second closest to its region's centroid). Please keep in mind that the shown positions also depend on the number of stations present in a region for each station type (i.e., ES1599A being the only rural station in 3-CW). Mean, median, minimum, maximum as well as 25% and 75% quantiles based on the months from April to September across all years are depicted for both target variables. The absolute and relative numbers of o-, t- and o-t-events with respect to the total number of days in the base period from 2004 to 2018 are shown as well.

Table S6 *Association of Weather Types with Event Days*

Region events		WT1	WT2	WT3	WT4	WT5	WT6	WT7	WT8	WT9	Total
1-CE											
Ozone	n	135	165	102	162	222	153	155	202	151	1447
	%	9.33	11.4	7.05	11.2	**15.34**	10.57	10.71	13.96	10.44	
Temperature	n	48	40	46	62	108	84	69	107	96	660
	%	7.27	6.06	6.97	9.39	16.36	12.73	10.45	**16.21**	14.55	
Ozone - Temperature	n	43	39	31	61	105	75	66	102	87	609
	%	7.06	6.4	5.09	10.02	**17.24**	12.32	10.84	**16.75**	14.29	
2-CN											
Ozone	n	59	84	39	104	194	101	144	154	99	978
	%	6.03	8.59	3.99	10.63	**19.84**	10.33	14.72	**15.75**	10.12	
Temperature	n	41	46	17	61	137	87	102	121	103	715
	%	5.73	6.43	2.38	8.53	**19.16**	12.17	14.27	**16.92**	14.41	
Ozone - Temperature	n	25	40	10	54	123	60	92	102	68	574
	%	4.36	6.97	1.74	9.41	**21.43**	10.45	**16.03**	**17.77**	11.85	
3-CW											
Ozone	n	232	170	107	210	229	150	182	231	180	1691
	%	13.72	10.05	6.33	12.42	13.54	8.87	10.76	13.66	10.64	
Temperature	n	112	72	73	77	162	105	70	130	107	908
	%	12.33	7.93	8.04	8.48	**17.84**	11.56	7.71	14.32	11.78	

Ozone - Temperature	n	98	51	37	63	135	83	64	121	88	740
	%	13.24	6.89	5	8.51	**18.24**	11.22	8.65	**16.35**	11.89	

4-HA

Ozone	n	179	204	142	193	235	186	158	226	183	1706
	%	10.49	11.96	8.32	11.31	13.77	10.9	9.26	13.25	10.73	
Temperature	n	51	47	44	54	68	80	31	82	89	546
	%	9.34	8.61	8.06	9.89	12.45	14.65	5.68	**15.02**	**16.3**	
Ozone - Temperature	n	50	43	41	53	65	75	30	79	83	519
	%	9.63	8.29	7.9	10.21	12.52	14.45	5.78	**15.22**	**15.99**	

5-NE

Ozone	n	232	170	107	210	229	150	182	231	180	908
	%	13.72	10.05	6.33	12.42	13.54	8.87	10.76	13.66	10.64	
Temperature	n	112	72	73	77	162	105	70	130	107	1691
	%	12.33	7.93	8.04	8.48	**17.84**	11.56	7.71	14.32	11.78	
Ozone - Temperature	n	98	51	37	63	135	83	64	121	88	740
	%	13.24	6.89	5	8.51	**18.24**	11.22	8.65	**16.35**	11.89	

6-SE

Ozone	n	260	173	121	222	187	135	192	206	163	1659
	%	**15.67**	10.43	7.29	13.38	11.27	8.14	11.57	12.42	9.83	
Temperature	n	130	72	89	74	68	61	57	78	69	698
	%	**18.62**	10.32	12.75	10.6	9.74	8.74	8.17	11.17	9.89	

	n	94	42	41	47	45	28	42	48	45	432
Ozone - Temperature										
	%	**21.76**	9.72	9.49	10.88	10.42	6.48	9.72	11.11	10.42	

Note. An overview of the association of weather types with o-, t- as well as o-t- events in the o-t-season from April to September across all years from 2004 to 2018 is given. Shown are the absolute (n) and relative (%) numbers of event days by considering all representative stations of an o-t-region (from 1-CE to 6-SE). Event days of a type which occurred simultaneously at multiple stations of a region are only counted once. Relative contributions of a weather type to an event above 15% are marked in bold. Note that minor differences in the depicted percentage values are due to rounding.

Table S7 *Projected Ensemble Changes [%]*

Station	SSP245						SSP370					
	2041-2060			2081-2100			2041-2060			2081-2100		
	median	min	max	median	min	max	median	min	max	median	min	max
DEST066	33.06	9.60 FGOALS-g3	86.92 CanESM5	56.32	14.40 FGOALS-g3	122.62 CanESM5	41.22	15.19 MPI-ESM1-2-HR	138.75 CanESM5	78.05	17.68 FGOALS-g3	332.92 CanESM5
DEBB066	36.40	10.21 INM-CM5-0	102.49 CanESM5	57.21	18.04 FGOALS-g3	138.63 CanESM5	44.01	14.93 MPI-ESM1-2-HR	140.85 CanESM5	90.37	19.26 FGOALS-g3	358.69 CanESM5
DEST002	39.64	13.89 INM-CM5-0	100.00 CanESM5	65.52	18.65 FGOALS-g3	148.57 CanESM5	45.94	17.00 MPI-ESM1-2-HR	168.37 CanESM5	93.45	22.92 FGOALS-g3	419.39 CanESM5
NL00807	39.66	15.40 MPI-ESM1-2-HR	109.06 CanESM5	75.88	19.56 FGOALS-g3	147.46 CanESM5	62.66	28.47 FGOALS-g3	141.34 CanESM5	115.45	35.41 FGOALS-g3	421.79 CanESM5
DEHH047	49.37	20.85 INM-CM5-0	108.99 CanESM5	74.02	31.33 FGOALS-g3	148.92 CanESM5	48.25	31.90 MPI-ESM1-2-HR	153.45 CanESM5	99.15	25.83 FGOALS-g3	445.98 CanESM5
DEHB002	42.24	19.71 INM-CM5-0	112.95 CanESM5	79.99	31.15 FGOALS-g3	160.71 CanESM5	57.38	35.03 IPSL-CM6A-LR	170.68 CanESM5	113.46	26.37 FGOALS-g3	500.00 CanESM5
FR26010	48.51	20.45 INM-CM5-0	112.46 IPSL-CM6A-LR	76.92	12.13 FGOALS-g3	163.67 IPSL-CM6A-LR	58.88	27.36 FGOALS-g3	158.69 CanESM5	127.66	61.15 MPI-ESM1-2-HR	330.52 CanESM5
FR07004	53.68	24.08 INM-CM5-0	130.97 IPSL-CM6A-LR	82.83	29.31 FGOALS-g3	199.56 IPSL-CM6A-LR	75.99	29.58 MPI-ESM1-2-HR	162.84 CanESM5	159.80	54.63 MPI-ESM1-2-HR	361.70 IPSL-CM6A-LR
ES1599A	49.47	18.39 INM-CM5-0	203.55 IPSL-CM6A-LR	110.45	41.10 FGOALS-g3	273.76 IPSL-CM6A-LR	100.39	41.94 INM-CM5-0	194.90 CanESM5	179.02	81.36 INM-CM5-0	509.18 CanESM5
DESN053	32.57	10.70 FGOALS-g3	78.05 CanESM5	58.35	8.72 FGOALS-g3	122.92 IPSL-CM6A-LR	47.12	8.24 MPI-ESM1-2-HR	160.57 CanESM5	94.46	26.40 FGOALS-g3	323.58 CanESM5

Note. Ensemble median changes [%] regarding the number of days with o-t-events between the periods 2041-2060 (mid-century) as well as 2081-2100 (end-century) compared to the historical ESM period 1995-2014 for all representative stations of 1-CE, 2-CN, 3-CW and 4-HA are shown. O-t-regions are separated by dashed lines. Minimum and maximum changes with respective ESM names in brackets based on single ESM projections are given as well. SSP245 and SSP370 scenario assumptions are considered.

**Table S8** *Region-Specific MT Anomaly Mean Warmings*

O-t-region	SSP245		SSP370	
	2041-2060	**2081-2100**	**2041-2060**	**2081-2100**
1-CE	1.22 (0.31 / 3.41)	2.03 (0.77 / 3.97)	1.58 (0.49 / 3.56)	3.26 (1.64 / 4.96)
2-CN	1.20 (0.40 / 3.11)	1.99 (0.82 / 3.60)	1.52 (0.59 / 3.35)	3.14 (1.56 / 5.02)
3-CW	1.74 (0.42 / 3.39)	2.67 (0.65 / 4.68)	2.06 (0.65 / 4.09)	4.15 (1.86 / 6.25)
4-HA	1.34 (0.24 / 3.63)	2.19 (0.55 / 4.26)	1.70 (0.23 / 3.62)	3.51 (1.50 / 5.16)

Note. Based on o-t-seasonal daily ESM data, mean warmings per time window (2041-2060 and 2081-2100) are calculated for the two SSP scenarios in the chosen CMIP6 ensemble for all Central European o-t-regions (from 1-CE to 4-HA). Warmings are expressed by MT anomalies and are shown per region. Averages across daily time series data of all representative stations of an o-t-region are considered to get one region-specific daily time series data. Means of this region-specific daily historical ESM data from 1995 to 2014 build the baseline to define MT anomalies. The ensemble warming anomalies per time window are calculated based on this baseline mean across all eight chosen ESM per scenario and o-t-region. While the depicted values represent the multi-model mean results of all eight ESM, numbers in brackets refer to the minimum and maximum values grounded on one specific ESM.

Figure S1

Relationship between MDA8O3 and TX for all representative stations and o-t-regions. All daily observations from April to September across all years from 2004-2018 are considered. GAM between both target variables are shown to highlight the linkage between both variables (blue line). Grey shadings illustrate the used confidence interval (0.95). Red horizontal lines illustrate the WHO guideline of 100 µg/m^3. Vertical lines show the 80% quantile of all respective observed TX values across all months and years. Note that representative station DEST002 of 1-CE is not depicted, again.

1-CE

a) DEST066   b) DEBB066
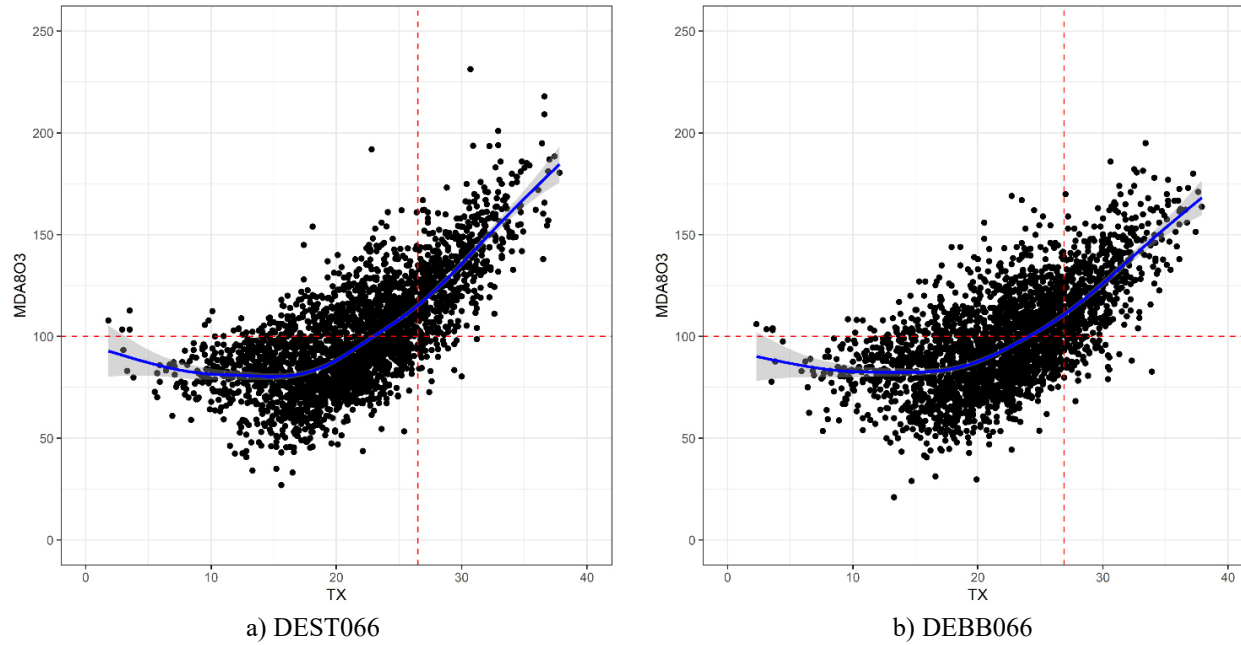
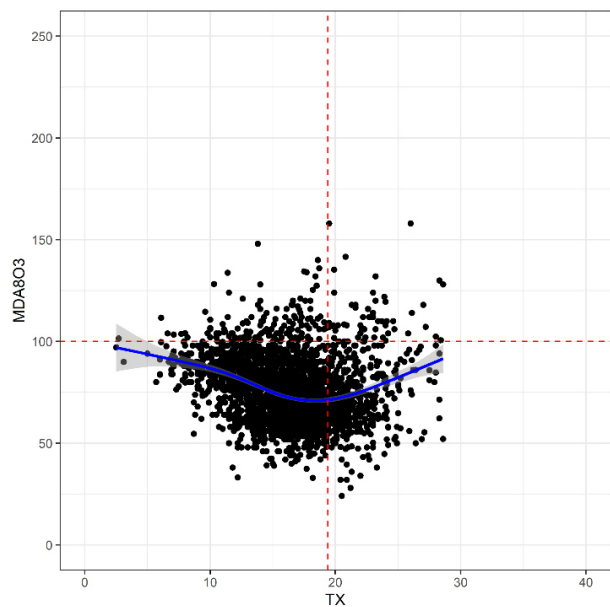**2-CN**
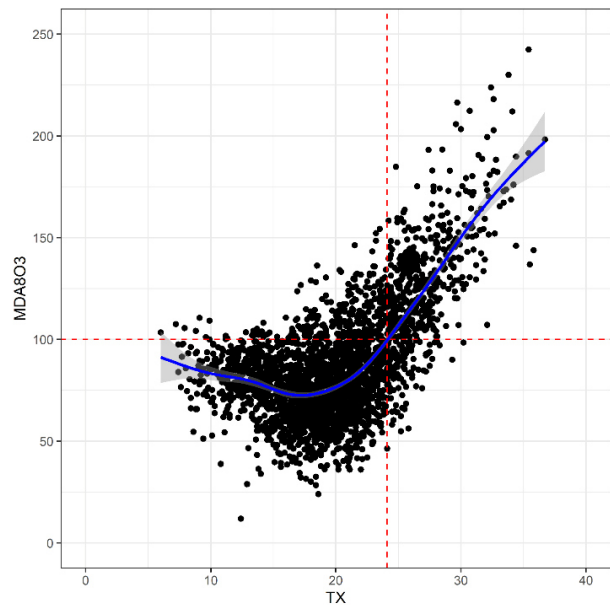
c) NL00807
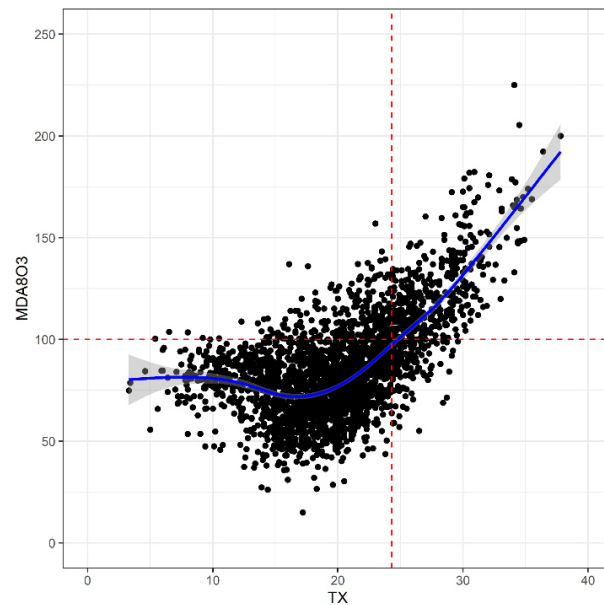
d) DEHH047
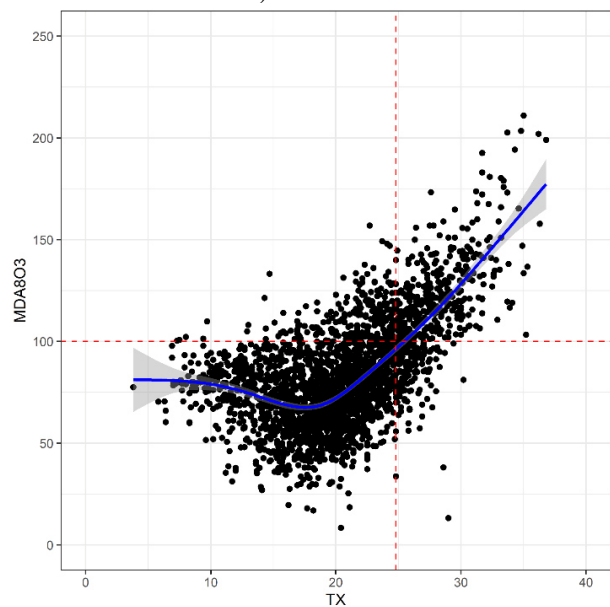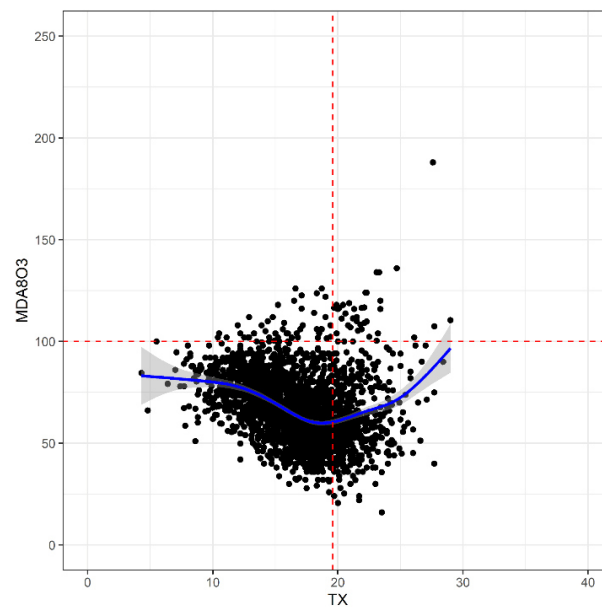

e) DEHB002

3-CW
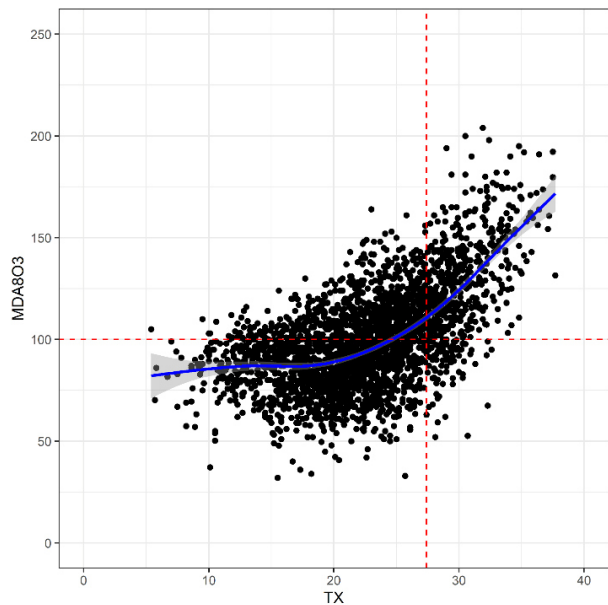
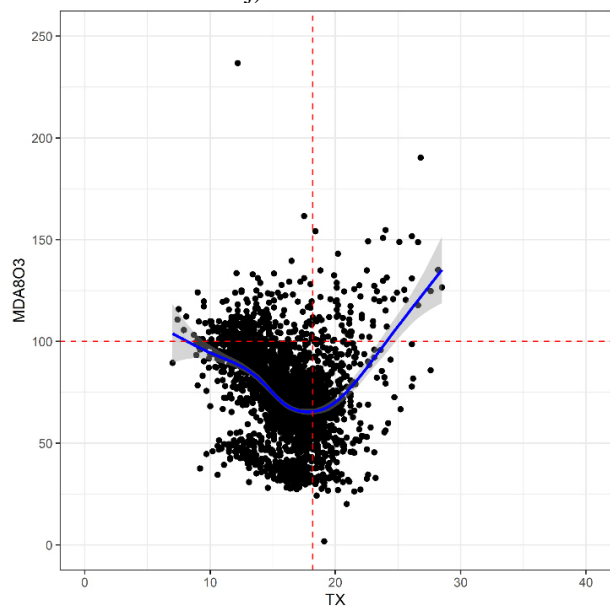
f) FR26010
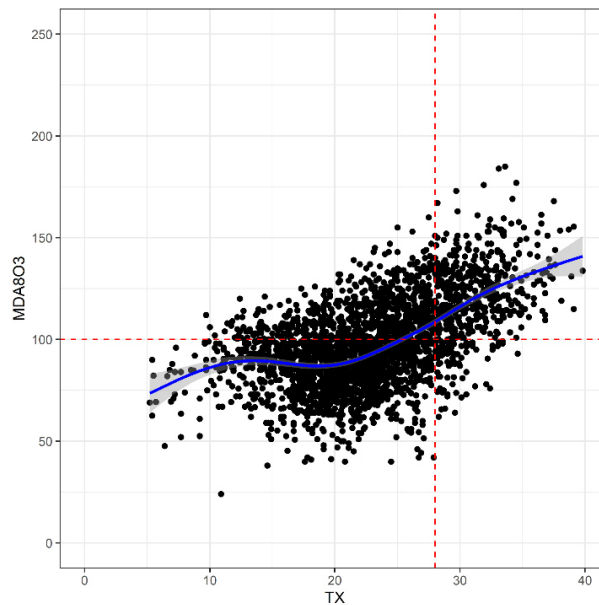
g) FR07004
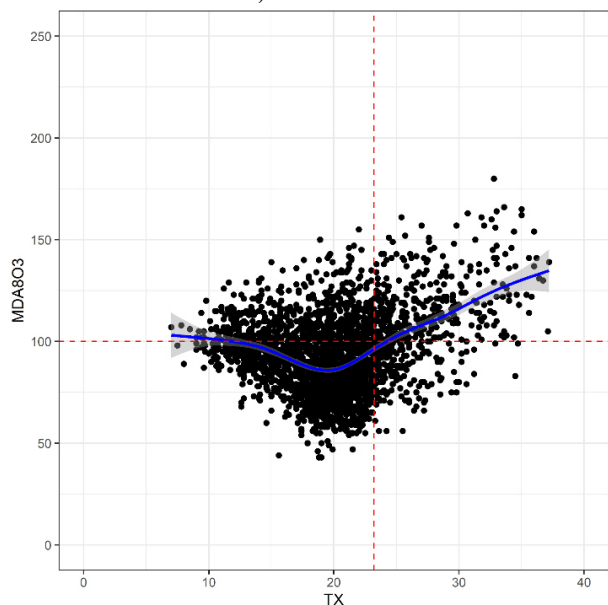
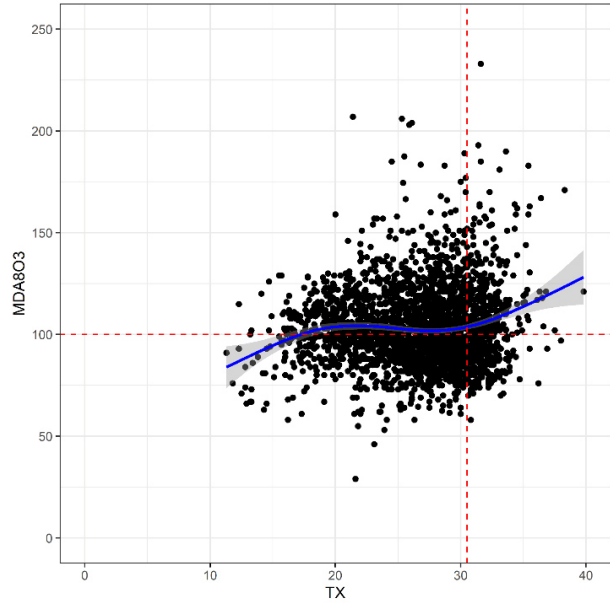h) ES1599A

4-HA
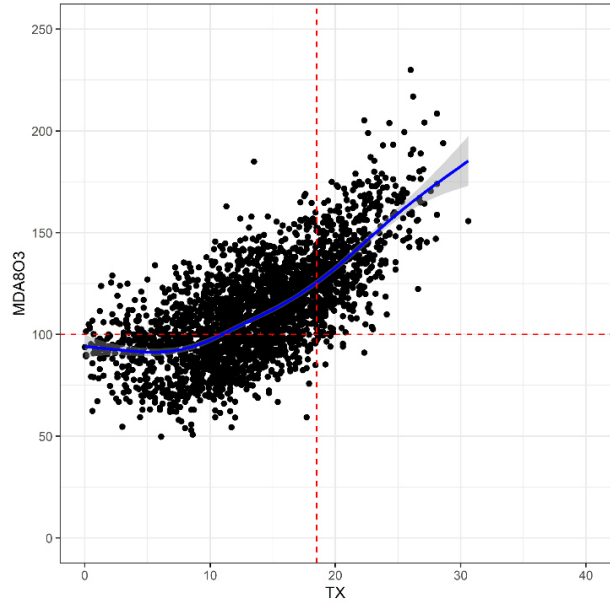
i) DESN053
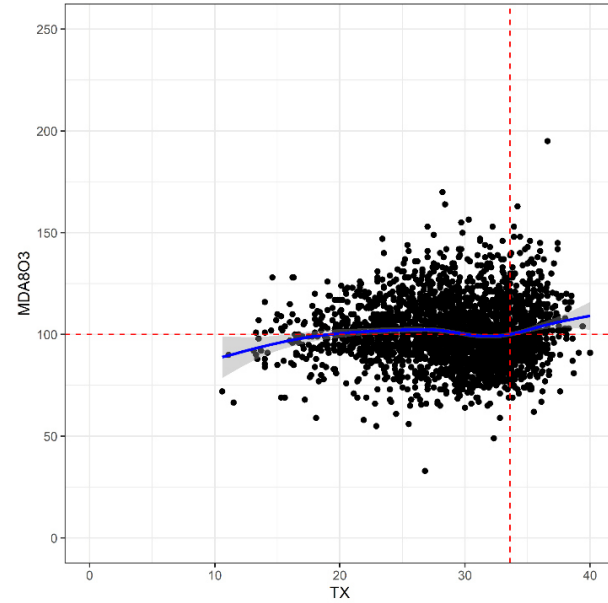
j) GB0033R


k) GB0567A

l) IE0001R

6-SE

m) ES1666A

n) ES1215A

Figure S2

Overview of the final 9 synoptic weather types in Europe created by the applied weather classification scheme using the SOM algorithm. Classification grounds on the o-t-season from 2004 to 2018. Each weather type is based one node of the SOM. The respective patterns shown are the MSLP- "weights" of each node. As the array of nodes self-organize into a pattern with more similar nodes being into closer proximity and more dissimilar nodes further away, simple clusters can be detected. Consequently, weather types WT1 (upper left corner) to WT9 (bottom right corner) are presented. Atmospheric pressure levels are shown in hPa.
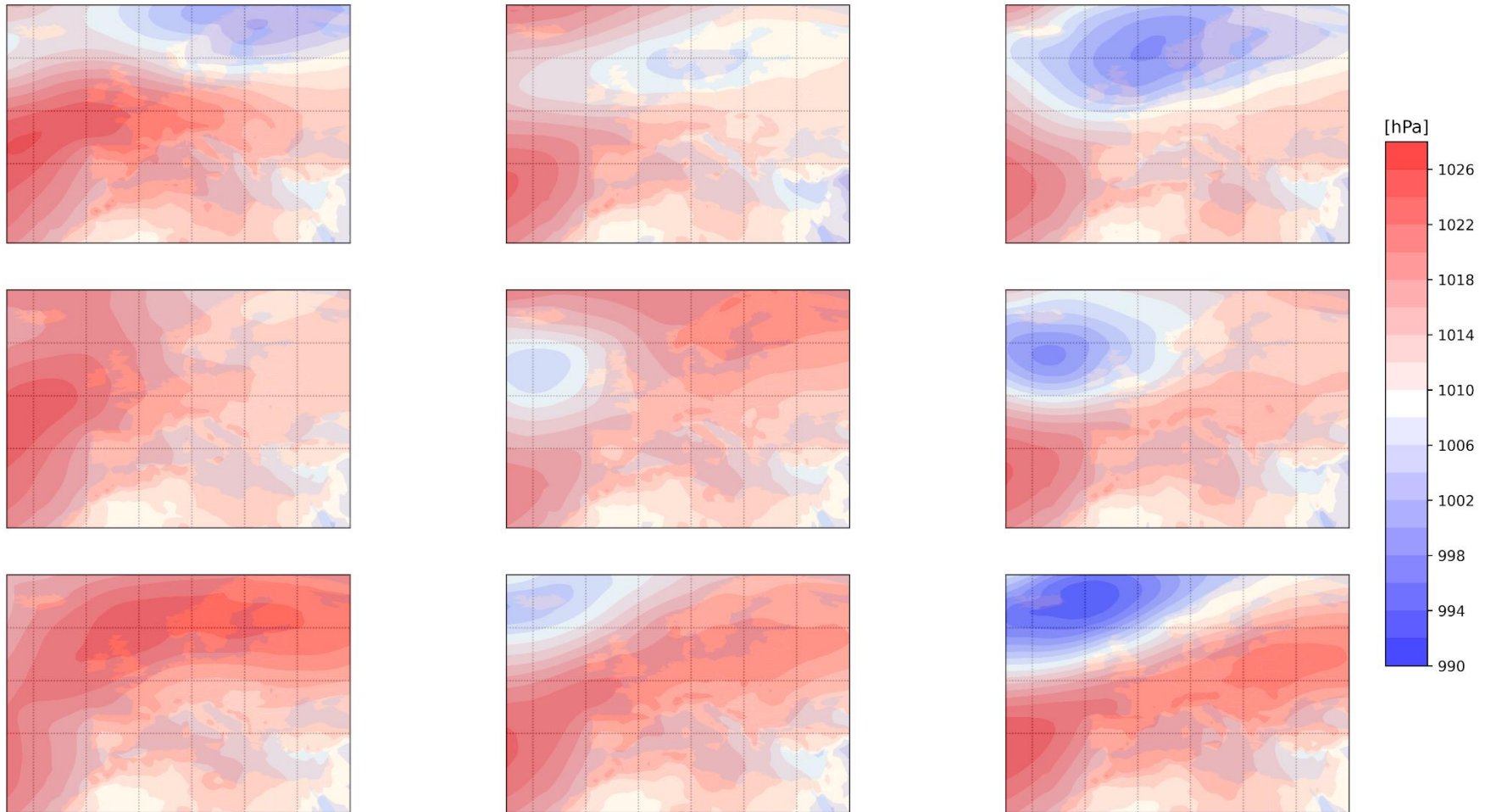
Appendix F

Supplementary Information

Research Article 3

The Supplementary Information of Research Article 3 (Chapter 4) as submitted and available online alongside the original article.

Supporting Information for

Future Local Ground-level Ozone in the European area from Statistical Downscaling Projections Considering Climate and Emission Changes

Elke Hertig[1], Sally Jahn[1], and Irena Kaspar-Ott[1]

[1]Regional Climate Change and Health, Faculty of Medicine, University of Augsburg, Universitätsstrasse 2, 86159 Augsburg, Germany.

Contents of this file

Introduction

This supplement contains the results for the daily maximum 1-hr values of ozone (MDA1). All methods leading to these results correspond to the procedure for MDA8 described in the main manuscript.

Text S1.

This supplement contains the results for MDA1.

Figure S1 shows the location of the stations, station type, and mean MDA1 concentrations in April-September 2005-2019.

The performance of the statistical downscaling models for MDA1 are comparable to the results for MDA8 (Table S2).

Figure S2 shows the three most important predictors of the predictor set REG-CHEM for MDA1 in the O_3 season from April to September. In the majority of the statistical downscaling models O3month, SRD and T850 were selected. The regional distribution is similar to the pattern for MDA8.

Figure S3 shows the downscaled MDA1 changes for the single ESM ensemble members. The two top rows show the downscaled near future changes from 2041-2060, the bottom rows include the change signals for the end of the 21st century (2081-2100) for each station.

36   The two scenarios SSP2-4.5 and SSP3-7.0 are shown one above the other in each case. A
37   general trend can be seen from the figures of the individual models. SSP2-4.5 led to
38   decreasing MDA1 concentrations for almost all ESMs, while the more pessimistic scenario
39   SSP3-7.0 projected increasing concentrations over Europe, especially at the end of the 21st
40   century. The differences between the individual models are very similar to the results of
41   MDA8.
42
43   Figure S4 shows the projection results of the CMIP6 models as Multi-Model Mean (MMM)
44   for MDA1. As for MDA8, the two scenarios differ in the direction of the change signal: SSP2-4.5
45   results in decreasing ozone concentrations, while increasing MDA1 concentrations are
46   projected for SSP3-7.0. However, the ozone reductions in SSP2-4.5 are on average not as large
47   as for MDA8; stations in and around the Alps also show significant increases, especially
48   towards the end of the 21st century.
49
50   Table S3 depicts the Multi-Model Mean (MMM) change [%] of downscaled ground-level
51   MDA1 as mean over 623 O3 measuring stations over Europe using different predictor sets.
52   Results are in accordance with the findings for MDA8, albeit with some differences in the
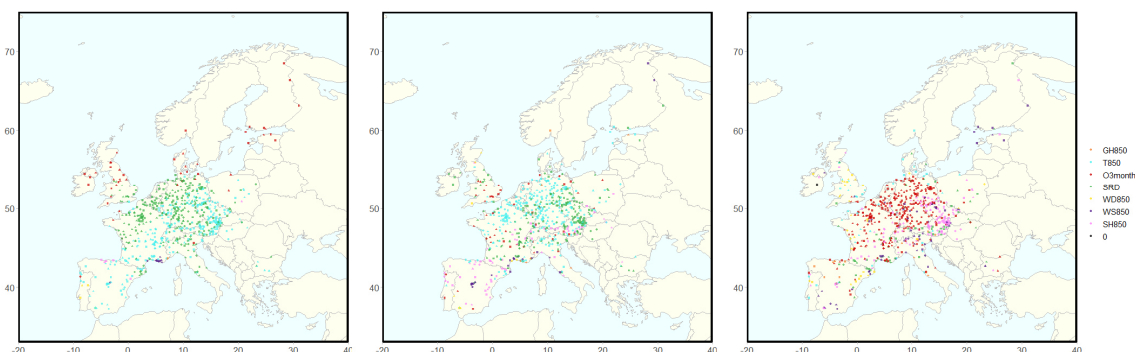53   magnitude of change.
54
55
56   **Figures:**
57
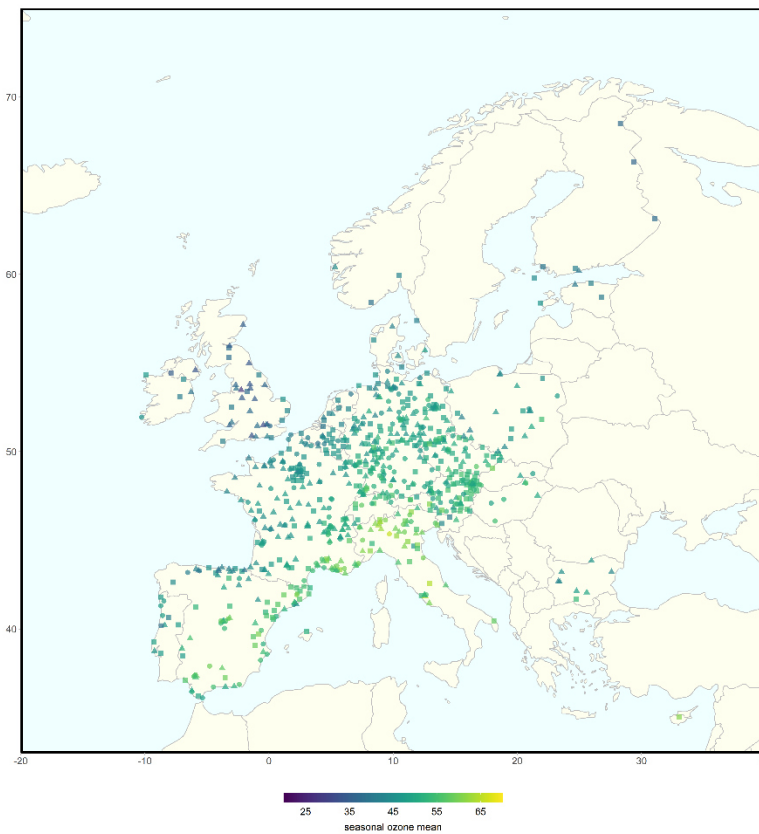
59   **Figure S1.** Location of all 798 ozone stations across Europe. Color indicates MDA1
60   concentrations as mean values in the season April to September for the period 2005-2019 and

2

shape of points indicate the type of each station (triangle = urban, circle = suburban and rectangle = rural).

Figure S2. Predictors chosen in the MLR models for MDA1 using the predictor set REG-CHEM. Left: most important predictor, middle: second most important predictor, right: third important predictor (0 = no third predictor variable).
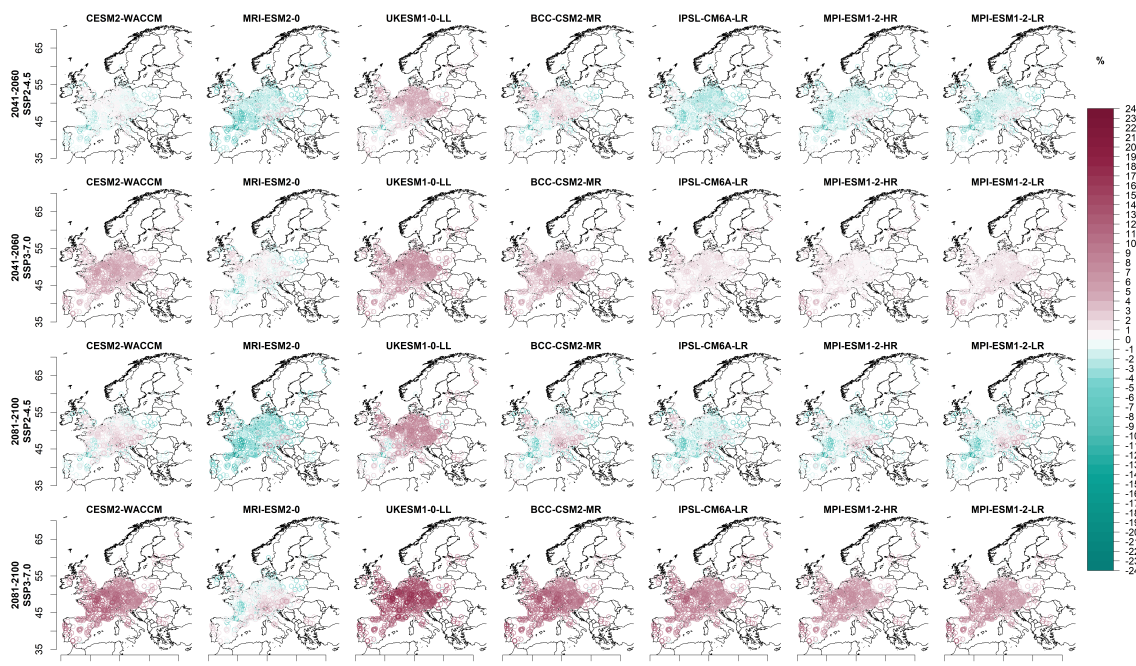
Figure S3. Change signals [%] of downscaled ground-level MDA1 concentrations at 720 O_3 measuring stations across Europe for all investigated CMIP6 ESMs. Shown are results for SSP2-4.5, SSP3-7.0, and the years 2041-2060 and 2081-2100.
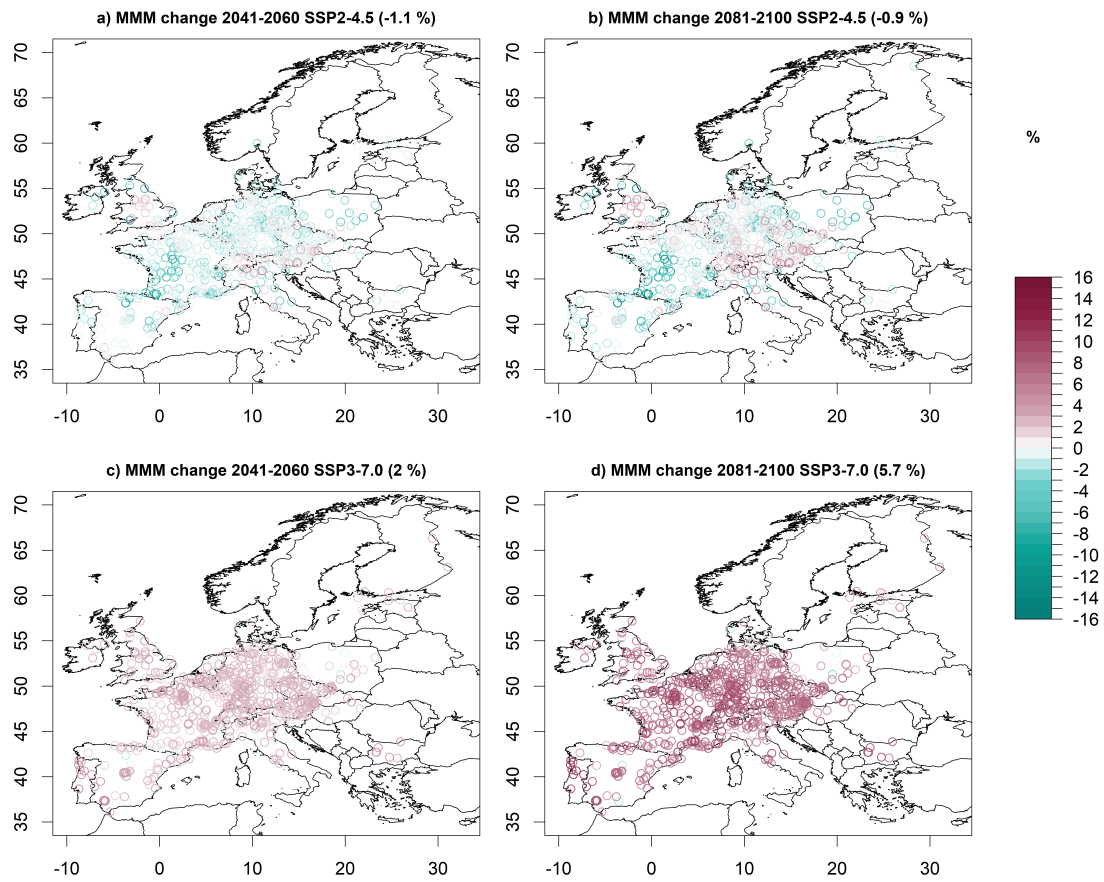
Figure S4. Multi-Model Mean (MMM) change [%] of downscaled ground-level MDA1 for 720 O₃ measuring stations over Europe. Shown are results for SSP2-4.5, SSP3-7.0 and the years 2041-2060 and 2081-2100 compared to the historical period 2003-2019. Percentages in parentheses in the image headings represent the area average of the change signals.

83 **_Tables:_**

84 **Table S1.** Distribution of the initially selected ozone stations across Europe. The number of
85 stations per country is depicted.

AT	BE	BG	CH	CY	CZ	DE	DK	EE	ES	FI	FR
80	19	8	16	1	45	191	5	4	87	7	187
GB	GI	HU	IE	IT	NL	NO	PL	PT	SE	SI	SK
34	1	6	5	48	10	3	23	11	1	4	2

86

87 **Table S2.** Statistical Downscaling Model Performance of the Different Predictor Sets based on
88 629 stations for MDA1. Given are the adjusted coefficient of determination R^2 and the Root
89 Mean Square Error RMSE as means over the ten calibration (cal) and validation (val) periods as
90 well as final R^2.

Option	Predictors	R^2	R2.cal	R2.val	RMSE.cal	RMSE.val
1	REG	0.52	0.47	0.46	8.78	8.79
2	REG-CHEM	0.52	0.47	0.47	8.77	8.79
3	ALL-IN	0.52	0.48	0.48	8.68	8.70
4	THRA	0.47	0.41	0.41	9.24	9.24
5	THRA-CHEM	0.49	0.44	0.44	8.98	8.98
6	THRA-HUM	0.47	0.42	0.42	9.17	9.17
7	THRA-CIRC	0.49	0.44	0.44	9.00	9.01

91

92 **Table S3:** _Multi-Model Mean (MMM) change [%] of downscaled ground-level MDA1 as mean over_
93 _629 O_3 measuring stations over Europe using different predictor sets. Shown are results for SSP2-4.5,_
94 _SSP3-7.0 and the years 2041-2060 and 2081-2100 compared to the historical period 2003-2019._

Option	Predictors	SSP2-4.5 2041-2060 minus 2003-2019	SSP2-4.5 2081-2100 minus 2003-2019	SSP3-7.0 2041-2060 minus 2003-2019	SSP3-7.0 2081-2100 minus 2003-2019
1	REG	-1.12	-0.92	1.93	5.76
2	REG-CHEM	-1.12	-0.92	1.94	5.77
3	ALL-IN	-1.19	-0.98	1.95	5.82
4	THRA	1.79	3.04	1.82	4.24
5	THRA-CHEM	-1.05	-0.83	2.05	5.98

5

6	THRA-HUM	1.74	3.03	1.82	4.26
7	THRA-CIRC	1.68	2.87	1.69	4.04

95

Bibliography

ABDULLAH, A. M., ISMAIL, M., YUEN, F. S., ABDULLAH, S. & ELHADI, R. 2017. The Relationship between Daily Maximum Temperature and Daily Maximum Ground Level Ozone Concentration. *Polish Journal of Environmental Studies,* 26**,** 517-523.

AKAIKE, H. 1974. A new look at the statistical model identification. *IEEE Transactions on Automatic Control,* 19**,** 716-723.

ANALITIS, A., KATSOUYANNI, K., PEDELI, X., KIRCHMAYER, U., MICHELOZZI, P. & MENNE, B. 2008. Investigating the Independent and Synergistic Effects of Heat Waves and Air Pollution on Health: The EuroHEAT Project. *Epidemiology,* 19**,** 214-215.

ANALITIS, A., MICHELOZZI, P., D'IPPOLITI, D., DE'DONATO, F., MENNE, B., MATTHIES, F., ATKINSON, R. W., XF, IGUEZ, C., BASAGA, XF, A, X., SCHNEIDER, A., LEFRANC, A., XE, PALDY, A., BISANTI, L. & KATSOUYANNI, K. 2014. Effects of Heat Waves on Mortality: Effect Modification and Confounding by Air Pollutants. *Epidemiology,* 25**,** 15-22.

ANDERSON, G. B. & BELL, M. L. 2011. Heat waves in the United States: mortality risk during heat waves and effect modification by heat wave characteristics in 43 US communities. *Environmental Health Perspectives,* 119**,** 210-218.

BACCINI, M., BIGGERI, A., ACCETTA, G., KOSATSKY, T., KATSOUYANNI, K., ANALITIS, A., ANDERSON, H. R., BISANTI, L., D'IPPOLITI, D., DANOVA, J., FORSBERG, B., MEDINA, S., PALDY, A., RABCZENKO, D., SCHINDLER, C. & MICHELOZZI, P. 2008. Heat Effects on Mortality in 15 European Cities. *Epidemiology,* 19**,** 711-719.

BACKHAUS, K., ERICHSON, B., PLINKE, W. & WEIBER, R. 2016. *Multivariate Analysemethoden,* Berlin Heidelberg, Springer.

BADOR, M., NAVEAU, P., GILLELAND, E., CASTELLÀ, M. & ARIVELO, T. 2015. Spatial clustering of summer temperature maxima from the CNRM-CM5 climate model ensembles & E-OBS over Europe. *Weather and Climate Extremes,* 9**,** 17-24.

BAN, J., LU, K. L., WANG, Q. & LI, T. T. 2022. Climate change will amplify the inequitable exposure to compound heatwave and ozone pollution. *One Earth,* 5**,** 677-686.

BLACK, E., BLACKBURN, M., HARRISON, G., HOSKINS, B. & METHVEN, J. 2004. Factors contributing to the summer 2003 European heatwave. *Weather,* 59**,** 217-223.

BLOOMER, B. J., STEHR, J. W., PIETY, C. A., SALAWITCH, R. J. & DICKERSON, R. R. 2009. Observed relationships of ozone air pollution with temperature and emissions. *Geophysical Research Letters,* 36**,** L09803.

BOLETI, E., HUEGLIN, C., GRANGE, S. K., PRÉVÔT, A. S. H. & TAKAHAMA, S. 2020. Temporal and spatial analysis of ozone concentrations in Europe based on timescale decomposition and a multi-clustering approach. *Atmospheric Chemistry and Physics,* 20**,** 9051-9066.

BRANCO, P., TORGO, L. & RIBEIRO, R. P. 2016. A survey of predictive modeling under imbalanced distributions. *ACM Computing Surveys,* 49**,** 1-48.

BRANDS, S., HERRERA, S., FERNÁNDEZ, J. & GUTIÉRREZ, J. M. 2013. How well do CMIP5 Earth System Models simulate present climate conditions in Europe and Africa? *Climate Dynamics,* 41**,** 803-817.

CAMALIER, L., COX, W. & DOLWICK, P. 2007. The effects of meteorology on ozone in urban areas and their use in assessing ozone trends. *Atmospheric Environment,* 41**,** 7127-7137.

CANNON, A. J. 2018. Multivariate quantile mapping bias correction: an N-dimensional probability density function transform for climate model simulations of multiple variables. *Climate Dynamics,* 50**,** 31-49.

CARRO-CALVO, L., ORDÓÑEZ, C., GARCÍA-HERRERA, R. & SCHNELL, J. L. 2017. Spatial clustering and meteorological drivers of summer ozone in Europe. *Atmospheric Environment,* 167**,** 496-510.

CHAWLA, N. V., BOWYER, K. W., HALL, L. O. & KEGELMEYER, W. P. 2002. SMOTE: synthetic minority over-sampling technique. *Journal of Artificial Intelligence Research,* 16**,** 321-357.

CHECA-GARCIA, R. 2018. *CMIP6 Ozone forcing dataset: supporting information (Initial)* [Online]. Zenodo. Available: https://doi.org/10.5281/zenodo.1135126 [Accessed 12.11.2022].

CHIDEAN, M. I., MUÑOZ-BULNES, J., RAMIRO-BARGUEÑO, J., CAAMAÑO, A. J. & SALCEDO-SANZ, S. 2015. Spatio-temporal trend analysis of air temperature in Europe and Western Asia using data-coupled clustering. *Global and Planetary Change,* 129**,** 45-55.

CIONNI, I., EYRING, V., LAMARQUE, J. F., RANDEL, W. J., STEVENSON, D. S., WU, F., BODEKER, G. E., SHEPHERD, T. G., SHINDELL, D. T. & WAUGH, D. W. 2011. Ozone database in support of CMIP5 simulations: results and corresponding radiative forcing. *Atmospheric Chemistry and Physics,* 11**,** 11267-11292.

COATES, J., MAR, K. A., OJHA, N. & BUTLER, T. M. 2016. The influence of temperature on ozone production under varying NOx conditions – a modelling study. *Atmospheric Chemistry and Physics,* 16**,** 11601-11615.

COLETTE, A., ANDERSSON, C., BAKLANOV, A., BESSAGNET, B., BRANDT, J., CHRISTENSEN, J. H., DOHERTY, R., ENGARDT, M., GEELS, C., GIANNAKOPOULOS, C., HEDEGAARD, G. B., KATRAGKOU, E., LANGNER, J., LEI, H., MANDERS, A., MELAS, D., MELEUX, F., ROUÏL, L., SOFIEV, M., SOARES, J., STEVENSON, D. S., TOMBROU-TZELLA, M., VAROTSOS, K. V. & YOUNG, P. 2015. Is the ozone climate penalty robust in Europe? *Environmental Research Letters,* 10**,** 084015.

DELLA-MARTA, P. M., LUTERBACHER, J., VON WEISSENFLUH, H., XOPLAKI, E., BRUNET, M. & WANNER, H. 2007. Summer heat waves over western Europe 1880–2003, their relationship to large-scale forcings and predictability. *Climate Dynamics,* 29**,** 251-275.

DEMUZERE, M., TRIGO, R. M., VILA-GUERAU DE ARELLANO, J. & VAN LIPZIG, N. 2009. The impact of weather and atmospheric circulation on O_3 and PM_{10} levels at a rural mid-latitude site. *Atmospheric Chemistry and Physics,* 9**,** 2695-2714.

DEUTSCHER WETTERDIENST (DWD). 2020. *Wetterlexikon* [Online]. Deutscher Wetterdienst. Available: https://www.dwd.de/DE/service/lexikon/lexikon_node.html [Accessed 25.04.2020].

DUEÑAS, C., FERNÁNDEZ, M. C., CAÑETE, S., CARRETERO, J. & LIGER, E. 2002. Assessment of ozone variations and meteorological effects in an urban area in the Mediterranean Coast. *Science of the Total Environment,* 299**,** 97-113.

EBI, K. L., CAPON, A., BERRY, P., BRODERICK, C., DE DEAR, R., HAVENITH, G., HONDA, Y., KOVATS, R. S., MA, W., MALIK, A., MORRIS, N. B., NYBO, L., SENEVIRATNE, S. I., VANOS, J. & JAY, O. 2021. Hot weather and heat extremes: health risks. *The Lancet,* 398**,** 698-708.

EIS, D., HELM, D., LAUßMANN, D. & STARK, K. 2010. *Klimawandel und Gesundheit-Ein Sachstandsbericht,* Berlin, Robert Koch-Institut.

EMMONS, L. K., SCHWANTES, R. H., ORLANDO, J. J., TYNDALL, G., KINNISON, D., LAMARQUE, J. F., MARSH, D., MILLS, M. J., TILMES, S., BARDEEN, C., BUCHHOLZ, R. R., CONLEY, A., GETTELMAN, A., GARCIA, R., SIMPSON, I., BLAKE, D. R., MEINARDI, S. & PÉTRON, G. 2020. The Chemistry Mechanism in the Community Earth System Model Version 2 (CESM2). *Journal of Advances in Modeling Earth Systems,* 12**,** e2019MS001882.

EUROPEAN COMISSION 2021. EU Action Plan: 'Towards Zero Pollution for Air, Water and Soil'. *In:* EUROPEAN COMISSION (ed.) *COM(2021).* Brussels: European Comission.

EUROPEAN ENVIRONMENT AGENCY (EEA). 2014. *AirBase - The European air quality database* [Online]. Available: https://www.eea.europa.eu/data-and-maps/data/airbase-the-european-air-quality-database-8 [Accessed 26.03.2020].

EUROPEAN ENVIRONMENT AGENCY (EEA) 2016. Tropospheric ozone: background information. *In:* EUROPEAN ENVIRONMENT AGENCY (ed.) *Tropospheric Ozone in*

EU - The consolidated report. Copenhagen: Plublications Office of the European Union.

EUROPEAN ENVIRONMENT AGENCY (EEA). 2017. *European Air Quality Portal* [Online]. Available: https://aqportal.discomap.eea.europa.eu/ [Accessed 3 July 2020].

EUROPEAN ENVIRONMENT AGENCY (EEA) 2019. Air quality in Europe — 2019 report. Luxembourg: European Environment Agency.

EUROPEAN ENVIRONMENT AGENCY (EEA) 2020. Air quality in Europe — 2020 report. Luxembourg: European Environment Agency.

EUROPEAN ENVIRONMENT AGENCY (EEA) 2021. Air quality in Europe 2021 - Web Report. Online: European Environment Agency.

EYRING, V., ARBLASTER, J. M., CIONNI, I., SEDLÁČEK, J., PERLWITZ, J., YOUNG, P. J., BEKKI, S., BERGMANN, D., CAMERON-SMITH, P., COLLINS, W. J., FALUVEGI, G., GOTTSCHALDT, K. D., HOROWITZ, L. W., KINNISON, D. E., LAMARQUE, J. F., MARSH, D. R., SAINT-MARTIN, D., SHINDELL, D. T., SUDO, K., SZOPA, S. & WATANABE, S. 2013. Long-term ozone changes and associated climate impacts in CMIP5 simulations. *Journal of Geophysical Research: Atmospheres,* 118**,** 5029-5060.

EYRING, V., BONY, S., MEEHL, G. A., SENIOR, C. A., STEVENS, B., STOUFFER, R. J. & TAYLOR, K. E. 2016. Overview of the Coupled Model Intercomparison Project Phase 6 (CMIP6) experimental design and organization. *Geoscientific Model Development,* 9**,** 1937-1958.

FANG, Y., MAUZERALL, D. L., LIU, J., FIORE, A. M. & HOROWITZ, L. W. 2013. Impacts of 21st century climate change on global air pollution-related premature mortality. *Climatic Change,* 121**,** 239-253.

FIORE, A. M., NAIK, V. & LEIBENSPERGER, E. M. 2015. Air quality and climate connections. *Journal of the Air & Waste Management Association,* 65**,** 645-685.

GARDNER, M. W. & DORLING, S. R. 2000. Statistical surface ozone models: an improved methodology to account for non-linear behaviour. *Atmospheric Environment,* 34**,** 21-34.

GASPARRINI, A. & ARMSTRONG, B. 2011. The impact of heat waves on mortality. *Epidemiology,* 22**,** 68-73.

GASPARRINI, A., GUO, Y., SERA, F., VICEDO-CABRERA, A. M., HUBER, V., TONG, S., COELHO, M. D. S. Z. S., SALDIVA, P. H. N., LAVIGNE, E. & CORREA, P. M. 2017. Projections of temperature-related excess mortality under climate change scenarios. *The Lancet Planetary Health,* 1**,** e360-e367.

GETTELMAN, A., MILLS, M. J., KINNISON, D. E., GARCIA, R. R., SMITH, A. K., MARSH, D. R., TILMES, S., VITT, F., BARDEEN, C. G., MCINERNY, J., LIU, H. L., SOLOMON, S. C., POLVANI, L. M., EMMONS, L. K., LAMARQUE, J. F., RICHTER, J. H., GLANVILLE, A. S., BACMEISTER, J. T., PHILLIPS, A. S., NEALE, R. B., SIMPSON, I. R., DUVIVIER, A. K., HODZIC, A. & RANDEL, W. J. 2019. The Whole Atmosphere Community Climate Model Version 6 (WACCM6). *Journal of Geophysical Research: Atmospheres,* 124**,** 12380-12403.

GIBSON, P. B., PERKINS-KIRKPATRICK, S. E., UOTILA, P., PEPLER, A. S. & ALEXANDER, L. V. 2017. On the use of self-organizing maps for studying climate extremes. *Journal of Geophysical Research: Atmospheres,* 122**,** 3891-3903.

GIDDEN, M. J., RIAHI, K., SMITH, S. J., FUJIMORI, S., LUDERER, G., KRIEGLER, E., VAN VUUREN, D. P., VAN DEN BERG, M., FENG, L., KLEIN, D., CALVIN, K., DOELMAN, J. C., FRANK, S., FRICKO, O., HARMSEN, M., HASEGAWA, T., HAVLIK, P., HILAIRE, J., HOESLY, R., HORING, J., POPP, A., STEHFEST, E. & TAKAHASHI, K. 2019. Global emissions pathways under different socioeconomic scenarios for use in CMIP6: a dataset of harmonized emissions trajectories through the end of the century. *Geoscientific Model Development,* 12**,** 1443-1475.

GOHAR, L. K., LOWE, J. A. & BERNIE, D. 2017. The Impact of Bias Correction and Model Selection on Passing Temperature Thresholds. *Journal of Geophysical Research: Atmospheres,* 122**,** 12045-12061.

GUO, Y., GASPARRINI, A., ARMSTRONG, B. G., TAWATSUPA, B., TOBIAS, A., LAVIGNE, E., COELHO, M., PAN, X., KIM, H., HASHIZUME, M., HONDA, Y., GUO, Y. L., WU,

C. F., ZANOBETTI, A., SCHWARTZ, J. D., BELL, M. L., SCORTICHINI, M., MICHELOZZI, P., PUNNASIRI, K., LI, S., TIAN, L., GARCIA, S. D. O., SEPOSO, X., OVERCENCO, A., ZEKA, A., GOODMAN, P., DANG, T. N., DUNG, D. V., MAYVANEH, F., SALDIVA, P. H. N., WILLIAMS, G. & TONG, S. 2017. Heat Wave and Mortality: A Multicountry, Multicommunity Study. *Environmental Health Perspectives,* 125**,** 087006.

GUTIÉRREZ, J. M., MARAUN, D., WIDMANN, M., HUTH, R., HERTIG, E., BENESTAD, R., ROESSLER, O., WIBIG, J., WILCKE, R., KOTLARSKI, S., SAN MARTÍN, D., HERRERA, S., BEDIA, J., CASANUEVA, A., MANZANAS, R., ITURBIDE, M., VRAC, M., DUBROVSKY, M., RIBALAYGUA, J., PÓRTOLES, J., RÄTY, O., RÄISÄNEN, J., HINGRAY, B., RAYNAUD, D., CASADO, M. J., RAMOS, P., ZERENNER, T., TURCO, M., BOSSHARD, T., ŠTĚPÁNEK, P., BARTHOLY, J., PONGRACZ, R., KELLER, D. E., FISCHER, A. M., CARDOSO, R. M., SOARES, P. M. M., CZERNECKI, B. & PAGÉ, C. 2019. An intercomparison of a large ensemble of statistical downscaling methods over Europe: Results from the VALUE perfect predictor cross-validation experiment. *International Journal of Climatology,* 39**,** 3750-3785.

HAJAT, S. & KOSATKY, T. 2010. Heat-related mortality: a review and exploration of heterogeneity. *Journal of Epidemiology & Community Health,* 64**,** 753-760.

HASTIE, T., TIBSHIRANI, R. & FRIEDMAN, J. 2009. *The elements of statistical learning: data mining, inference, and prediction,* New York, Springer.

HASTIE, T., TIBSHIRANI, R. & WAINWRIGHT, M. 2015. *Statistical learning with sparsity: the lasso and generalizations,* Boca Raton, CRC Press.

HE, H. & MA, Y. 2013. *Imbalanced learning: foundations, algorithms, and applications,* Hoboken, John Wiley & Sons.

HENDRIKS, C., FORSELL, N., KIESEWETTER, G., SCHAAP, M. & SCHOEPP, W. 2016. Ozone concentrations and damage for realistic future European climate and air quality scenarios. *Atmospheric Environment,* 144**,** 208-219.

HERSBACH, H. & DEE, D. 2016. *ERA5 reanalysis is in production* [Online]. Available: https://www.ecmwf.int/en/newsletter/147/news/era5-reanalysis-production [Accessed 27.04.2020].

HERTIG, E. 2020. Health-relevant ground-level ozone and temperature events under future climate change using the example of Bavaria, Southern Germany. *Air Quality, Atmosphere & Health,* 13**,** 435-446.

HERTIG, E., RUSSO, A. & TRIGO, R. M. 2020. Heat and Ozone Pollution Waves in Central and South Europe - Characteristics, Weather Types, and Association with Mortality. *Atmosphere,* 11**,** 1271.

HERTIG, E., SCHNEIDER, A., PETERS, A., VON SCHEIDT, W., KUCH, B. & MEISINGER, C. 2019. Association of ground-level ozone, meteorological factors and weather types with daily myocardial infarction frequencies in Augsburg, Southern Germany. *Atmospheric Environment,* 217**,** 116975.

HUSAR, R. B. & RENARD, W. P. 1998. Ozone as a function of local wind speed and direction: Evidence of local and regional transport. St Louis: Center for Air Pollution Impact and Trend Analysis.

INNESS, A., ADES, M., AGUSTÍ-PANAREDA, A., BARRÉ, J., BENEDICTOW, A., BLECHSCHMIDT, A.-M., DOMINGUEZ, J. J., ENGELEN, R., ESKES, H., FLEMMING, J., HUIJNEN, V., JONES, L., KIPLING, Z., MASSART, S., PARRINGTON, M., PEUCH, V.-H., RAZINGER, M., REMY, S., SCHULZ, M. & SUTTIE, M. 2019. The CAMS reanalysis of atmospheric composition. *Atmospheric Chemistry and Physics,* 19**,** 3515-3556.

INTERGOVERNMENTAL PANEL ON CLIMATE CHANGE (IPCC) 2013. Climate Change 2013: The Physical Science Basis. Contribution of Working Group I to the Fifth Assessment Report of the Intergovernmental Panel on Climate Change. Cambridge, New York: Cambridge University Press.

INTERGOVERNMENTAL PANEL ON CLIMATE CHANGE (IPCC) 2021. Climate Change 2021: The Physical Science Basis. Contribution of Working Group I to the Sixth

Assessment Report of the Intergovernmental Panel on Climate Change. Cambridge, New York: Cambridge University Press.

INTERGOVERNMENTAL PANEL ON CLIMATE CHANGE (IPCC) 2022. Climate Change 2022: Impacts, Adaptation and Vulnerability. Contribution of Working Group II to the Sixth Assessment Report of the Intergovernmental Panel on Climate Change. Cambridge, New York: Cambridge University Press.

JACOB, D., PETERSEN, J., EGGERT, B., ALIAS, A., CHRISTENSEN, O. B., BOUWER, L. M., BRAUN, A., COLETTE, A., DÉQUÉ, M. & GEORGIEVSKI, G. 2014. EURO-CORDEX: new high-resolution climate change projections for European impact research. *Regional Environmental Change,* 14**,** 563-578.

JACOB, D. J. & WINNER, D. A. 2009. Effect of climate change on air quality. *Atmospheric Environment,* 43**,** 51-63.

JAHN, S. & HERTIG, E. 2021. Modeling and projecting health-relevant combined ozone and temperature events in present and future Central European climate. *Air Quality, Atmosphere & Health,* 14**,** 563-580.

JAHN, S. & HERTIG, E. 2022. Using Clustering, Statistical Modeling, and Climate Change Projections to Analyze Recent and Future Region-Specific Compound Ozone and Temperature Burden Over Europe. *GeoHealth,* 6**,** e2021GH000561.

JAMES, G., WITTEN, D., HASTIE, T. & TIBSHIRANI, R. 2013. *An introduction to statistical learning - with Applications in R,* New York, Springer.

KATRAGKOU, E., ZANIS, P., KIOUTSIOUKIS, I., TEGOULIAS, I., MELAS, D., KRÜGER, B. C. & COPPOLA, E. 2011. Future climate change impacts on summer surface ozone from regional climate-air quality simulations over Europe. *Journal of Geophysical Research: Atmospheres,* 116**,** D22307.

KATSOUYANNI, K. & ANALITIS, A. 2009. Investigating the Synergistic Effects Between Meteorological Variables and Air Pollutants: Results from the European PHEWE, EUROHEAT and CIRCE Projects. *Epidemiology,* 20**,** S264.

KEEBLE, J., HASSLER, B., BANERJEE, A., CHECA-GARCIA, R., CHIODO, G., DAVIS, S., EYRING, V., GRIFFITHS, P. T., MORGENSTERN, O., NOWACK, P., ZENG, G., ZHANG, J., BODEKER, G., BURROWS, S., CAMERON-SMITH, P., CUGNET, D., DANEK, C., DEUSHI, M., HOROWITZ, L. W., KUBIN, A., LI, L., LOHMANN, G., MICHOU, M., MILLS, M. J., NABAT, P., OLIVIÉ, D., PARK, S., SELAND, Ø., STOLL, J., WIENERS, K.-H. & WU, T. 2020. Evaluating stratospheric ozone and water vapour changes in CMIP6 models from 1850 to 2100. *Atmospheric Chemistry and Physics,* 21**,** 5015-5061.

KERR, G. H., WAUGH, D. W., STRODE, S. A., STEENROD, S. D., OMAN, L. D. & STRAHAN, S. E. 2019. Disentangling the Drivers of the Summertime Ozone-Temperature Relationship Over the United States. *Journal of Geophysical Research: Atmospheres,* 124**,** 10503-10524.

KLEIN TANK, A. M. G., WIJNGAARD, J. B., KÖNNEN, G. P., BÖHM, R., DEMARÉE, G., GOCHEVA, A., MILETA, M., PASHIARDIS, S., HEJKRLIK, L. & KERN-HANSEN, C. 2002. Daily dataset of 20th-century surface air temperature and precipitation series for the European Climate Assessment. *International Journal of Climatology,* 22**,** 1441-1453.

KRUEGER, O., HEGERL, G. C. & TETT, S. F. B. 2015. Evaluation of mechanisms of hot and cold days in climate models over Central Europe. *Environmental Research Letters,* 10**,** 014002.

LACOUR, S. A., DE MONTE, M., DIOT, P., BROCCA, J., VERON, N., COLIN, P. & LEBLOND, V. 2006. Relationship between ozone and temperature during the 2003 heat wave in France: consequences for health data analysis. *BMC Public Health,* 6**,** 261.

LEHMAN, J., SWINTON, K., BORTNICK, S., HAMILTON, C., BALDRIDGE, E., EDER, B. & COX, B. 2004. Spatio-temporal characterization of tropospheric ozone across the eastern United States. *Atmospheric Environment,* 38**,** 4357-4369.

LIU, X., ZHU, Y., XUE, L., DESAI, A. R. & WANG, H. 2022. Cluster-Enhanced Ensemble Learning for Mapping Global Monthly Surface Ozone From 2003 to 2019. *Geophysical Research Letters,* 49**,** e2022GL097947.

LU, X., ZHANG, L. & SHEN, L. 2019. Meteorology and Climate Influences on Tropospheric Ozone: a Review of Natural Sources, Chemistry, and Transport Patterns. *Current Pollution Reports,* 5**,** 238-260.

LYAPINA, O., SCHULTZ, M. G. & HENSE, A. 2016. Cluster analysis of European surface ozone observations for evaluation of MACC reanalysis data. *Atmospheric Chemistry and Physics,* 16**,** 6863-6881.

MARAUN, D. & WIDMANN, M. 2018. *Statistical Downscaling and Bias Correction for Climate Research,* Cambridge, Cambridge University Press.

MATTHIES, F., BICKLER, G. & MARÍN, N. C. 2008. Heat-Health Action Plans: Guidance. Copenhagen: World Health Organization.

MAYER, M., SCHREIER, S. F., SPANGL, W., STAEHLE, C., TRIMMEL, H. & RIEDER, H. E. 2022. An analysis of 30 years of surface ozone concentrations in Austria: temporal evolution, changes in precursor emissions and chemical regimes, temperature dependence, and lessons for the future. *Environmental Science: Atmospheres,* 2**,** 601-615.

MCGREGOR 2015. Heatwaves and Health: Guidance on Warning-System Development. Geneva: World Meteorological Organization and World Health Organization.

MEEHL, G. A. & TEBALDI, C. 2004. More intense, more frequent, and longer lasting heat waves in the 21st century. *Science,* 305**,** 994-997.

MEEHL, G. A., TEBALDI, C., TILMES, S., LAMARQUE, J.-F., BATES, S., PENDERGRASS, A. & LOMBARDOZZI, D. 2018. Future heat waves and surface ozone. *Environmental Research Letters,* 13**,** 064004.

MIYAZAKI, K., BOWMAN, K., SEKIYA, T., ESKES, H., BOERSMA, F., WORDEN, H., LIVESEY, N., PAYNE, V. H., SUDO, K., KANAYA, Y., TAKIGAWA, M. & OGOCHI, K. 2020. Updated tropospheric chemistry reanalysis and emission estimates, TCR-2, for 2005-2018. *Earth System Science Data,* 12**,** 2223-2259.

MOGHANI, M. & ARCHER, C. L. 2020. The impact of emissions and climate change on future ozone concentrations in the USA. *Air Quality, Atmosphere & Health,* 13**,** 1465–1476

MORGENSTERN, O., HEGGLIN, M. I., ROZANOV, E., O'CONNOR, F. M., ABRAHAM, N. L., AKIYOSHI, H., ARCHIBALD, A. T., BEKKI, S., BUTCHART, N., CHIPPERFIELD, M. P., DEUSHI, M., DHOMSE, S. S., GARCIA, R. R., HARDIMAN, S. C., HOROWITZ, L. W., JÖCKEL, P., JOSSE, B., KINNISON, D., LIN, M., MANCINI, E., MANYIN, M. E., MARCHAND, M., MARÉCAL, V., MICHOU, M., OMAN, L. D., PITARI, G., PLUMMER, D. A., REVELL, L. E., SAINT-MARTIN, D., SCHOFIELD, R., STENKE, A., STONE, K., SUDO, K., TANAKA, T. Y., TILMES, S., YAMASHITA, Y., YOSHIDA, K. & ZENG, G. 2017. Review of the global models used within phase 1 of the Chemistry-Climate Model Initiative (CCMI). *Geoscientific Model Development,* 10**,** 639-671.

NUVOLONE, D., PETRI, D. & VOLLER, F. 2018. The effects of ozone on human health. *Environmental Science and Pollution Research International,* 25**,** 8074-8088.

O'NEILL, B. C., TEBALDI, C., VAN VUUREN, D. P., EYRING, V., FRIEDLINGSTEIN, P., HURTT, G., KNUTTI, R., KRIEGLER, E., LAMARQUE, J.-F., LOWE, J., MEEHL, G. A., MOSS, R., RIAHI, K. & SANDERSON, B. M. 2016. The Scenario Model Intercomparison Project (ScenarioMIP) for CMIP6. *Geoscientific Model Development,* 9**,** 3461-3482.

O'NEILL, B. C., KRIEGLER, E., EBI, K. L., KEMP-BENEDICT, E., RIAHI, K., ROTHMAN, D. S., VAN RUIJVEN, B. J., VAN VUUREN, D. P., BIRKMANN, J., KOK, K., LEVY, M. & SOLECKI, W. 2015. The roads ahead: Narratives for shared socioeconomic pathways describing world futures in the 21st century. *Global Environmental Change,* 42**,** 169-180.

O'NEILL, B. C., KRIEGLER, E., RIAHI, K., EBI, K. L., HALLEGATTE, S., CARTER, T. R., MATHUR, R. & VAN VUUREN, D. P. 2014. A new scenario framework for climate

change research: the concept of shared socioeconomic pathways. *Climatic Change,* 122**,** 387-400.

ODOULAMI, R. C., WOLSKI, P. & NEW, M. 2020. A SOM-based analysis of the drivers of the 2015-2017 Western Cape drought in South Africa. *International Journal of Climatology,* 41**,** E1518-E1530.

ORRU, H., ÅSTRÖM, C., ANDERSSON, C., TAMM, T., EBI, K. L. & FORSBERG, B. 2019. Ozone and heat-related mortality in Europe in 2050 significantly affected by changes in climate, population and greenhouse gas emission. *Environmental Research Letters,* 14**,** 074013.

OSWALD, E. M., DUPIGNY-GIROUX, L.-A., LEIBENSPERGER, E. M., POIROT, R. & MERRELL, J. 2015. Climate controls on air quality in the Northeastern U.S.: An examination of summertime ozone statistics during 1993-2012. *Atmospheric Environment,* 112**,** 278-288.

OTERO, N., JURADO, O. E., BUTLER, T. & RUST, H. W. 2022. The impact of atmospheric blocking on the compounding effect of ozone pollution and temperature: a copula-based approach. *Atmospheric Chemistry and Physics,* 22**,** 1905-1919.

OTERO, N., SILLMANN, J., SCHNELL, J. L., RUST, H. W. & BUTLER, T. 2016. Synoptic and meteorological drivers of extreme ozone concentrations over Europe. *Environmental Research Letters,* 11**,** 024005.

PARK, S., SON, S.-W., JUNG, M.-I., PARK, J. & PARK, S. S. 2020. Evaluation of tropospheric ozone reanalyses with independent ozonesonde observations in East Asia. *Geoscience Letters,* 7**,** 12.

PATTENDEN, S., ARMSTRONG, B., MILOJEVIC, A., HEAL, M. R., CHALABI, Z., DOHERTY, R., BARRATT, B., KOVATS, R. S. & WILKINSON, P. 2010. Ozone, heat and mortality: acute effects in 15 British conurbations. *Occupational and Environmental Medicine,* 67**,** 699-707.

PEDUZZI, P., CONCATO, J., KEMPER, E., HOLFORD, T. R. & FEINSTEIN, A. R. 1996. A simulation study of the number of events per variable in logistic regression analysis. *Journal of Clinical Epidemiology,* 49**,** 1373-1379.

PENG, C.-Y. J., LEE, K. L. & INGERSOLL, G. M. 2010. An Introduction to Logistic Regression Analysis and Reporting. *Journal of Educational Research,* 96**,** 3-14.

PORTER, W. C. & HEALD, C. L. 2019. The mechanisms and meteorological drivers of the summertime ozone-temperature relationship. *Atmospheric Chemistry and Physics,* 19**,** 13367-13381.

PUSEDE, S. E., STEINER, A. L. & COHEN, R. C. 2015. Temperature and recent trends in the chemistry of continental surface ozone. *Chemical Reviews,* 115**,** 3898-918.

RASMUSSEN, D. J., FIORE, A. M., NAIK, V., HOROWITZ, L. W., MCGINNIS, S. J. & SCHULTZ, M. G. 2012. Surface ozone-temperature relationships in the eastern US: A monthly climatology for evaluating chemistry-climate models. *Atmospheric Environment,* 47**,** 142-153.

RASMUSSEN, D. J., HU, J., MAHMUD, A. & KLEEMAN, M. J. 2013. The ozone-climate penalty: past, present, and future. *Environmental Science & Technology,* 47**,** 14258-14266.

REQUIA, W. J., DI, Q., SILVERN, R., KELLY, J. T., KOUTRAKIS, P., MICKLEY, L. J., SULPRIZIO, M. P., AMINI, H., SHI, L. & SCHWARTZ, J. 2020. An Ensemble Learning Approach for Estimating High Spatiotemporal Resolution of Ground-Level Ozone in the Contiguous United States. *Environmental Science & Technology,* 54**,** 11037-11047.

ROBINE, J. M., MICHEL, J. P. & HERRMANN, F. R. 2012. Excess male mortality and age-specific mortality trajectories under different mortality conditions: a lesson from the heat wave of summer 2003. *Mechanisms of Ageing and Development,* 133**,** 378-386.

RUSSO, A., LIND, P. G., RAISCHEL, F., TRIGO, R. & MENDES, M. 2015. Neural network forecast of daily pollution concentration using optimal meteorological data at synoptic and local scales. *Atmospheric Pollution Research,* 6**,** 540-549.

SCHNELL, J. L. & PRATHER, M. J. 2017. Co-occurrence of extremes in surface ozone, particulate matter, and temperature over eastern North America. *Proceedings of the National Academy of Sciences of the United States of America,* 114**,** 2854-2859.

SCHNELL, J. L., PRATHER, M. J., JOSSE, B., NAIK, V., HOROWITZ, L. W., ZENG, G., SHINDELL, D. T. & FALUVEGI, G. 2016. Effect of climate change on surface ozone over North America, Europe, and East Asia. *Geophysical Research Letters,* 43**,** 3509-3518.

SCHOETTER, R., CATTIAUX, J. & DOUVILLE, H. 2014. Changes of western European heat wave characteristics projected by the CMIP5 ensemble. *Climate Dynamics,* 45**,** 1601-1616.

SCOTTO, M. G., BARBOSA, S. M. & ALONSO, A. M. 2011. Extreme value and cluster analysis of European daily temperature series. *Journal of Applied Statistics,* 38**,** 2793-2804.

SELLAR, A. A., JONES, C. G., MULCAHY, J. P., TANG, Y., YOOL, A., WILTSHIRE, A., O'CONNOR, F. M., STRINGER, M., HILL, R., PALMIERI, J., WOODWARD, S., MORA, L., KUHLBRODT, T., RUMBOLD, S. T., KELLEY, D. I., ELLIS, R., JOHNSON, C. E., WALTON, J., ABRAHAM, N. L., ANDREWS, M. B., ANDREWS, T., ARCHIBALD, A. T., BERTHOU, S., BURKE, E., BLOCKLEY, E., CARSLAW, K., DALVI, M., EDWARDS, J., FOLBERTH, G. A., GEDNEY, N., GRIFFITHS, P. T., HARPER, A. B., HENDRY, M. A., HEWITT, A. J., JOHNSON, B., JONES, A., JONES, C. D., KEEBLE, J., LIDDICOAT, S., MORGENSTERN, O., PARKER, R. J., PREDOI, V., ROBERTSON, E., SIAHAAN, A., SMITH, R. S., SWAMINATHAN, R., WOODHOUSE, M. T., ZENG, G. & ZERROUKAT, M. 2019. UKESM1: Description and Evaluation of the U.K. Earth System Model. *Journal of Advances in Modeling Earth Systems,* 11**,** 4513-4558.

SELTZER, K. M., SHINDELL, D. T. & MALLEY, C. S. 2018. Measurement-based assessment of health burdens from long-term ozone exposure in the United States, Europe, and China. *Environmental Research Letters,* 13**,** 104018.

SHEN, L., MICKLEY, L. J. & GILLELAND, E. 2016. Impact of increasing heat waves on U.S. ozone episodes in the 2050s: Results from a multimodel analysis using extreme value theory. *Geophysical Research Letters,* 43**,** 4017-4025.

SHERIDAN, S. C. & LEE, C. C. 2011. The self-organizing map in synoptic climatological research. *Progress in Physical Geography,* 35**,** 109-119.

SILLMAN, S. 1999. The relation between ozone, NO_x and hydrocarbons in urban and polluted rural environments. *Atmospheric Environment,* 33**,** 1821-1845.

SILLMAN, S. 2003. Tropospheric Ozone and Photochemical Smog. *In:* LOLLAR, B. S., HOLLAND, H. D. & TUREKIAN, K. K. (eds.) *Treatise on Geochemistry.* 1 ed. Michigan: Elsevier.

SILLMAN, S. 2014. Tropospheric Ozone and Photochemical Smog. *In:* HOLLAND, H. D. & TUREKIAN, K. K. (eds.) *Treatise on Geochemistry.* 2 ed. Michigan: Elsevier.

SILLMAN, S. & SAMSON, P. J. 1995. Impact of temperature on oxidant photochemistry in urban, polluted rural and remote environments. *Journal of Geophysical Research,* 100**,** 11497-11508.

SONG, X., WANG, S., HU, Y., YUE, M., ZHANG, T., LIU, Y., TIAN, J. & SHANG, K. 2017. Impact of ambient temperature on morbidity and mortality: an overview of reviews. *Science of the Total Environment,* 586**,** 241-254.

SREBOT, V., GIANICOLO, E. A. L., RAINALDI, G., TRIVELLA, M. G. & SICARI, R. 2009. Ozone and cardiovascular injury. *Cardiovascular Ultrasound,* 7**,** 30.

STEINER, A. L., DAVIS, A. J., SILLMAN, S., OWEN, R. C., MICHALAK, A. M. & FIORE, A. M. 2010. Observed suppression of ozone formation at extremely high temperatures due to chemical and biophysical feedbacks. *Proceedings of the National Academy of Sciences of the United States of America,* 107**,** 19685-19690.

SUN, Z. & ARCHIBALD, A. T. 2021. Multi-stage ensemble-learning-based model fusion for surface ozone simulations: A focus on CMIP6 models. *Environmental Science and Ecotechnology,* 8**,** 100124.

TAKAHASHI, K., HONDA, Y. & EMORI, S. 2007. Assessing mortality risk from heat stress due to global warming. *Journal of Risk Research,* 10**,** 339-354.

TAYLOR, K. E., STOUFFER, R. J. & MEEHL, G. A. 2012. An Overview of CMIP5 and the Experiment Design. *Bulletin of the American Meteorological Society,* 93**,** 485-498.

TEUTSCHBEIN, C. & SEIBERT, J. 2012. Bias correction of regional climate model simulations for hydrological climate-change impact studies: Review and evaluation of different methods. *Journal of Hydrology,* 456-457**,** 12-29.

THE EXPERT TEAM ON CLIMATE CHANGE DETECTION AND INDICES (ETCCDI). 2009. *Climate Change Indices* [Online]. Available: http://etccdi.pacificclimate.org/list_27_indices.shtml [Accessed 24.05.2020].

TIAN, J., CASSANO, J. J. & SCHUENEMANN, K. C. 2014. Anomaly Detection Using Self-Organizing Maps-Based K-Nearest Neighbor Algorithm. *Proceedings of the European Conference of the PHM Society 2014.*

TIBSHIRANI, R. 1996. Regression shrinkage and selection via the lasso. *Journal of the Royal Statistical Society: Series B (Methodological),* 58**,** 267-288.

TIBSHIRANI, R. 2011. Regression shrinkage and selection via the lasso: a retrospective. *Journal of the Royal Statistical Society: Series B (Statistical Methodology),* 73**,** 273-282.

TURNOCK, S. T., ALLEN, R. J., ANDREWS, M., BAUER, S. E., DEUSHI, M., EMMONS, L., GOOD, P., HOROWITZ, L., JOHN, J. G., MICHOU, M., NABAT, P., NAIK, V., NEUBAUER, D., O'CONNOR, F. M., OLIVIÉ, D., OSHIMA, N., SCHULZ, M., SELLAR, A., SHIM, S., TAKEMURA, T., TILMES, S., TSIGARIDIS, K., WU, T. & ZHANG, J. 2020. Historical and future changes in air pollutants from CMIP6 models. *Atmospheric Chemistry and Physics,* 20**,** 14547-14579.

VAROTSOS, K. V., GIANNAKOPOULOS, C. & TOMBROU, M. 2019. Ozone-temperature relationship during the 2003 and 2014 heatwaves in Europe. *Regional Environmental Change,* 19**,** 1653-1665.

VAROTSOS, K. V., TOMBROU, M. & GIANNAKOPOULOS, C. 2013. Statistical estimations of the number of future ozone exceedances due to climate change in Europe. *Journal of Geophysical Research: Atmospheres,* 118**,** 6080-6099.

VESANTO, J. & ALHONIEMI, E. 2000. Clustering of the self-organizing map. *IEEE Transactions on Neural Networks,* 11**,** 586-600.

WILKS, D. 2006. *Statistical Methods in the Atmospheric Sciences,* London, Elsevier Academic Press.

WORLD HEALTH ORGANIZATION (WHO) 2006. WHO Air quality guidelines for particulate matter, ozone, nitrogen dioxide and sulfur dioxide. Geneva: World Health Organization.

WORLD HEALTH ORGANIZATION (WHO) 2008. Improving public health responses to extreme weather/heat-waves - EuroHEAT. Copenhagen: World Health Organization.

WORLD HEALTH ORGANIZATION (WHO) 2013. Review of evidence on health aspects of air pollution - REVIHAAP Project. Copenhagen: World Health Orgnaization.

WORLD HEALTH ORGANIZATION (WHO) 2021. WHO global air quality guidelines: particulate matter (PM2.5 and PM10), ozone, nitrogen dioxide, sulfur dioxide and carbon monoxide. Geneva: World Health Organization.

WU, S., MICKLEY, L. J., LEIBENSPERGER, E. M., JACOB, D. J., RIND, D. & STREETS, D. G. 2008. Effects of 2000-2050 global change on ozone air quality in the United States. *Journal of Geophysical Research,* 113**,** D06302.

YOUNG, P. J., NAIK, V., FIORE, A. M., GAUDEL, A., GUO, J., LIN, M. Y., NEU, J. L., PARRISH, D. D., RIEDER, H. E., SCHNELL, J. L., TILMES, S., WILD, O., ZHANG, L., ZIEMKE, J., BRANDT, J., DELCLOO, A., DOHERTY, R. M., GEELS, C., HEGGLIN, M. I., HU, L., IM, U., KUMAR, R., LUHAR, A., MURRAY, L., PLUMMER, D., RODRIGUEZ, J., SAIZ-LOPEZ, A., SCHULTZ, M. G., WOODHOUSE, M. T. & ZENG, G. 2018. Tropospheric Ozone Assessment Report: Assessment of global-scale model performance for global and regional ozone distributions, variability, and trends. *Elementa-Science of the Anthropocene,* 6**,** 10.

YUKIMOTO, S., KAWAI, H., KOSHIRO, T., OSHIMA, N., YOSHIDA, K., URAKAWA, S., TSUJINO, H., DEUSHI, M., TANAKA, T., HOSAKA, M., YABU, S., YOSHIMURA, H., SHINDO, E., MIZUTA, R., OBATA, A., ADACHI, Y. & ISHII, M. 2019. The Meteorological Research Institute Earth System Model Version 2.0, MRI-ESM2.0: Description and Basic Evaluation of the Physical Component. *Journal of the Meteorological Society of Japan. Ser. II,* 97**,** 931-965.

ZHAO, Y., LI, Y., KUMAR, A., YING, Q., VANDENBERGHE, F. & KLEEMAN, M. J. 2022. Separately resolving NO_x and VOC contributions to ozone formation. *Atmospheric Environment,* 285**,** 119224.

ZSCHEISCHLER, J., MARTIUS, O., WESTRA, S., BEVACQUA, E., RAYMOND, C., HORTON, R. M., VAN DEN HURK, B., AGHAKOUCHAK, A., JÉZÉQUEL, A., MAHECHA, M. D., MARAUN, D., RAMOS, A. M., RIDDER, N. N., THIERY, W. & VIGNOTTO, E. 2020. A typology of compound weather and climate events. *Nature Reviews Earth & Environment,* 1**,** 333-347.